

**DEVELOPMENT OF REPORTER GENES FOR USE IN GRAM
POSITIVE BACTERIA**

By

Saara N. A. Qazi (BSc)

**Thesis submitted to the University of Nottingham for the degree of Doctor of
Philosophy, October 1999**



CONTENTS

Contents	i
List of Figures	viii
List of Tables	xiv
Abbreviations	xv
Abstract	xvii
Acknowledgements	xix
Chapter 1: Introduction	1
1.1. Green Fluorescent Protein	2
1.1.1. Background	2
1.1.2. Properties of GFP	3
1.1.3. The GFP Chromophore	4
1.1.4. The three-dimensional structure of GFP	5
1.1.5. Limitations to wild-type GFP	6
1.1.6. GFP Mutants	7
1.1.6.1. Red Shifted GFP Mutants	7
1.1.6.2. Blue Emission GFP Variants	11
1.1.6.3. Yellow-Green Emission Variant (YFP)	12
1.1.7. Potential uses of GFP and GFP Variants	12
1.1.8. Unstable GFP Variants	15
1.1.9. Advantages to Using GFP as a Reporter	18
1.1.10. Disadvantages to using GFP as a reporter	19
1.2. Bacterial Bioluminescence: Organisation, regulation and Application of the <i>lux</i> genes.	21
1.2.1. Introduction	21
1.2.2. Luminescent bacteria	21
1.2.3. Physiological function of Bioluminescence	22
1.2.4. The Genetic Basis of Bioluminescence	22
1.2.5. Applications of <i>lux</i> genes	25

1.3. <i>Listeria monocytogenes</i>	29
1.3.1. Background	29
1.3.2. <i>Listeria monocytogenes</i> as a pathogen	30
1.4. <i>Staphylococcus aureus</i>	35
1.4.1. Background	35
1.4.2. Resistant Isolates of <i>S. aureus</i>	35
1.4.3. The Regulation of <i>S. aureus</i> pathogenicity	36
1.4.3.1. The <i>agr</i> Regulatory System	37
1.4.3.2. The <i>Sar</i> Regulatory System	39
1.4.4. Grouping of <i>S. aureus</i> strains	40
1.4.5. <i>S. aureus</i> as an intracellular pathogen: influence of <i>agr</i>	41
Chapter 2: Materials and Methods	43
2.1. Bacterial Strains and Plasmids used	44
2.2. Solutions utilised	53
2.2.1. Media	53
2.2.2. Antibiotics and Supplements	53
2.3. Growth of bacterial cultures	54
2.4. Monitoring Growth of Bacterial Cultures	54
2.5. Preparation, Manipulation and Analysis of DNA	54
2.5.1. Determination of DNA concentrations	54
2.5.2. Preparation of Plasmid DNA	54
2.5.3. Amplification of DNA using Polymerase Chain Reaction (PCR)	55
2.5.4. Cleavage of DNA with restriction enzymes	55
2.5.5. Agarose gel Electrophoresis	56
2.5.6. Phenol Chloroform extraction of DNA	56
2.5.7. Purification of DNA from a Low melting point agarose gel	57
2.5.8. Ligation of DNA fragments	57
2.5.9. Bacterial Transformation	58
2.6. Microscopy	59
2.6.1. Properties of Fluorescent Signals and Filters Used	59

2.7. Analysis of RNA by Northern Hybridisation	60
2.7.1. mRNA Isolation from <i>Listeria monocytogenes</i>	60
2.7.2. Preparation of a Digoxigenin-labelled hybridisation probe	60
2.7.3. RNA Analysis by Northern Blotting	61
2.7.4. Prehybridisation and hybridisation	62
2.7.5. Stringency Washes and Detection	63
2.8. Colony Hybridisation	63
2.9. SDS PAGE (1 dimensional)	64
2.9.1. Preparation of <i>E. coli</i> Protein Samples	64
2.9.2. Preparation of <i>L. monocytogenes</i> Protein samples	64
2.9.3. Preparation of an SDS-PAGE Gel	65
2.9.4. Detection of Protein Profiles	65
2.10. Western Blotting	66
2.10.1. Transfer of proteins to Nitrocellulose by Electroblothing	66
2.10.2. Immunodetection of proteins	66
2.11. 2-dimensional gel electrophoresis (2-D PAGE)	68
2.11.1. Preparation of <i>L. monocytogenes</i> whole cell extracts	68
2.11.2. First Dimension	68
2.11.3. Second Dimension	69
2.11.4. Staining and destaining	69
2.11.5. Analysis of 2-D profile	69
2.12. Tissue Culture	70
2.12.1. Maintenance of cell line	70
2.12.2. Trypsinisation of Monolayer Cultures	70
2.12.3. Cell Freezing	71
2.12.4. Tissue Culture Cell Invasion Assay	71
2.12.5. Fixation of tissue culture cells using formaldehyde	72
2.13. Monitoring Bioluminescence of Bacterial Cultures	72
2.13.1. Measuring Bioluminescence from colonies on agar plates	72
2.13.2. Measuring bioluminescence from liquid cultures	73

2.14. Monitoring Fluorescence of Bacterial cultures	73
2.14.1. Observing fluorescence of colonies on agar plates	73
2.14.2. Observing GFP fluorescence from a liquid culture	73
2.14.3. Observing degradation of the C-terminal Modified GFP variants	74
Chapter 3: Construction of <i>gfp</i> expression vectors for expression In Gram positive bacteria	75
3.1. Introduction	76
3.2. Construction of a Gram positive GFP expression vector	76
3.3. Investigations of plasmid stability in <i>L. monocytogenes</i>	83
3.4. Cloning a terminator downstream of <i>gfp</i>	85
3.5. Does Overexpression of GFP result in non-Fluorescent Cells?	89
3.5.1. Cloning unstable GFP variants	89
3.5.2. Disrupting translation of GFP at the 5' coding region	91
3.6. Cloning a new promoter upstream of <i>gfp</i>	93
3.7. Expressing GFP from the xylose regulated promoter	97
3.8. Northern Blot Analysis of <i>L. monocytogenes</i> harbouring <i>gfp</i> expression Vectors.	101
3.9. Translational analysis of transformed bacteria harbouring <i>gfp</i> expression vectors	104
3.10. Removal of a Potential Ribosome Stall site from GFP	110
3.11. Codon Usage and secondary mRNA Structure	118
3.11.1. Cloning EGFP	120
3.12. Enhancing translational initiation of <i>gfp</i>	127
3.13. Constructing a constitutive <i>gfp</i> reporter for expression in Gram positive bacteria.	132
3.14. Construction of an Unstable GFP Plasmid for use as a reporter in Gram positive bacteria	135
3.15. Discussion	138

Chapter 4: Evaluation and expression of GFP reporters in Gram positive organisms	143
4.1. Growth characteristics of <i>L. monocytogenes</i> (pSB2018)	144
4.2. Evaluation of fluorescence characteristics of <i>L. monocytogenes</i> cells containing the inducible reporter pSB2018 and the constitutive reporter pSB2019	149
4.3. Fluorescence characteristics of <i>L. monocytogenes</i> cells harbouring the unstable <i>gfp</i> plasmids	155
4.4. Investigating the degradation rate of the unstable <i>gfp</i> variants	165
4.5. Tagging bacterial cells with GFP to monitor bacterial movement in an intracellular environment	169
4.6. Discussion	172
Chapter 5: Construction and evaluation of a lux based reporter for expression in Gram positive bacteria	177
5.1. Expression of the <i>Photobacterium luminescens lux</i> operon from the P _{xy} promoter	178
5.2. Reconstruction of the <i>P. luminescens lux</i> operon	184
5.3. Cloning the <i>luxABCDE</i> operon into the superlinker plasmid pSL1190	191
5.4. Cloning the <i>luxABCDE</i> operon into a Gram positive shuttle vector	192
5.5. Construction of a constitutive <i>lux</i> reporter for expression studies in Gram positive bacteria	197
5.6. Cloning a transcriptional terminator downstream of the <i>lux</i> operon	199
5.7. Growth of <i>L. monocytogenes</i> harbouring the xylose inducible <i>lux</i> plasmid pSB2026	203
5.8. Comparison of growth and bioluminescence of <i>L. monocytogenes</i> (pSB2026) and <i>L. monocytogenes</i> (pSB2027)	208
5.9. Comparison of growth and bioluminescence of <i>L. monocytogenes</i> (pSB2028) and <i>L. monocytogenes</i> (pSB2027)	212

5.10. Two-dimensional gel electrophoresis (2-D PAGE) of <i>L. monocytogenes</i> (pSB2026)	217
5.11. Discussion	223
Chapter 6: Construction of a dual reporter for expression studies in Gram positive bacteria	226
6.1. Creating a dual reporter	227
6.2. Comparison of growth and fluorescence of <i>L. monocytogenes</i> (pSB2019) and <i>L. monocytogenes</i> (pSB2030)	238
6.3. Growth and bioluminescence of <i>L. monocytogenes</i> (pSB2027) and <i>L. monocytogenes</i> (pSB2030)	243
6.4. Discussion	247
Chapter 7: Construction, evaluation and use of reporter systems for the <i>agr</i> P3 promoter system of <i>Staphylococcus aureus</i>	250
7.1. Construction of a <i>gfp</i> reporter for the <i>agr</i> P3 promoter of <i>S. aureus</i>	251
7.2. <i>In vitro</i> evaluation of pSB2031 as a reporter of <i>agr</i> expression	255
7.3. Construction of a <i>luxABCDE</i> reporter for the <i>agr</i> P3 promoter of <i>S. aureus</i>	259
7.4. Construction of a dual reporter for the <i>agr</i> P3 promoter of <i>S. aureus</i>	262
7.5. <i>In vitro</i> Evaluation of pSB2033 and pSB2034 as a reporter of <i>agr</i> expression through the use of bacterial supernatant and <i>lux</i> expression	265
7.5.1. Monitoring <i>luxABCDE</i> expression upon induction of P3	265
7.5.2. Monitoring <i>luxABCDE</i> and <i>gfp3opt</i> expression upon induction of P3	269
7.6. Use of the dual reporter of <i>agr</i> expression to evaluate potential activators and inhibitors of P3 activity	273

7.6.1. Determining the minimum concentration of a synthetic group-1 activator molecule required to induce P3	273
7.6.2. Determining the minimum concentration of a synthetic <i>agr</i> inhibitor from <i>S. lugdunensis</i> required for inhibition of P3	277
7.7. Discussion	281
Chapter 8: Discussion	284
References	294
Appendices	323

List of Figures

- 1.1.2.1. Excitation and Emission spectra of the GFP from *Aequorea*
- 1.1.4.1. The cylindrical β -can structure of GFP
- 1.1.6.1. Excitation and emission spectra of *gfpwt* (black) and red shifted *gfp* variants (green)
- 1.1.7.1a. Excitation (left panel) and Emission (right panel) spectra of EGFP, EBFP and EYFP
- 1.1.7.1b. Schematic representation of FRET
- 1.2.4.1. The bacterial bioluminescence system
- 1.2.4.2. The organisation and function of bacterial *lux* genes
- 1.3.2.1. Schematic representation of the virulence gene cluster activated by PrfA
- 1.3.2.2. *prfA* gene transcription. Arrows indicate *prfA* transcripts produced from the *plcA* promoter and P1 and P2 promoters
- 1.4.3.1. The *agr* system
- 2.7.2. The principal behind random primed labelling
- 3.2.1. Restriction map of pGC4
- 3.2.2. Agarose gel showing presence of *gfp* insert in recombinant colonies
- 3.2.3. Restriction map of pSB2002 and pSB2003
- 3.2.4a and b. *E. coli* (pSB2002) and *E. coli* (pSB2003)
- 3.2.4c and d: *L. monocytogenes* (pSB2002) and *L. monocytogenes* (pSB2003)
- 3.4.1. Restriction map of pSB354
- 3.4.2. Restriction analysis of putative recombinant DNA containing the *rrnBT* fragment
- 3.4.3. Predicted restriction map of pSB2004 and pSB2005
- 3.6.1. Genetic organisation of the xylose-utilisation determinant in *B. megaterium*
- 3.6.2. Restriction map of pSB2010
- 3.7.1. Diagram to show how PCR was used to screen for transformants containing the new xylose promoter
- 3.7.2. Restriction map of pSB2011 and pSB2012
- 3.7.3a and b. *E. coli* (pSB2012) and *E. coli* (pSB2011)
- 3.7.3c and d. *L. monocytogenes* (pSB2012) and *L. monocytogenes* (pSB2011)

- 3.8.1. Northern Blot showing a full length mRNA transcript is generated from transformed bacteria harbouring *gfp* expression vectors
- 3.9.1a. SDS PAGE gel of bacteria harbouring pSB2002
- 3.9.1b. Western blot of bacteria harbouring pSB2002
- 3.9.2a. SDS PAGE gel of bacteria harbouring pSB2003
- 3.9.2b. Western Blot of bacteria harbouring pSB2003
- 3.10.1. Rational behind removal of the potential stall site from *gfp3*
- 3.10.2. Restriction map of pSB2013
- 3.10.3. Gram positive bacteria harbouring pSB2013
- 3.10.5. Agarose gel of PCR products amplified from colonies thought to contain P_{xylA} upstream of *gfp3r/s*
- 3.10.6. Restriction map of pSB2014
- 3.11.1. Restriction analysis of pSB2015
- 3.11.2. Restriction map of pSB2015
- 3.11.3. Expression Characteristics of two Gram positive bacteria harbouring pSB2015
- 3.11.4. Colony hybridisation of Putative colonies thought to express *egfp* from P_{xylA}
- 3.11.5. Restriction Analysis of Putative DNA thought to express *egfp* from P_{xylA}
- 3.11.6. Restriction map of pSB2016
- 3.12.1. Agarose gel showing Putative colonies expressing *gfp3opt* from P_{xylA}
- 3.13.1. Linear diagram representing the promoter fragment of pSB2018
- 3.13.2. Restriction Map of pSB2019
- 3.14.1. Procedure for cloning the unstable *gfp3* variants downstream of P_{xylA}
- 4.1.1. Growth and fluorescence of *L. monocytogenes* (pSB2018)
- 4.1.2. Growth and fluorescence of *L. monocytogenes* (pSB2018)
- 4.2.1. Fluorescence characteristics of *L. monocytogenes* harbouring an inducible and constitutive *gfp* reporter
- 4.2.2. Fluorescence characteristics of *L. monocytogenes* harbouring an inducible and constitutive *gfp* reporter
- 4.3.1. Growth and fluorescence of *L. monocytogenes* harbouring unstable *gfp3opt* plasmids
- 4.3.1a: Growth and fluorescence of *L. monocytogenes* (pSB2018)
- 4.3.1b: Growth and fluorescence of *L. monocytogenes* (pSB2020)
- 4.3.1c: Growth and fluorescence of *L. monocytogenes* (pSB2021)

- 4.3.2. Growth and fluorescence of *L. monocytogenes* harbouring unstable *gfp3opt* plasmids
 - 4.3.2a. Growth and fluorescence of *L. monocytogenes* (pSB2018)
 - 4.3.2b. Growth and fluorescence of *L. monocytogenes* (pSB2020)
 - 4.3.2c. Growth and fluorescence of *L. monocytogenes* (pSB2021)
- 4.4.1. Stability of *gfp* variants in *L. monocytogenes* following a downshift to media without xylose
- 4.5.1. Intracellular GFP tagged *S. aureus*
- 5.1.1. Restriction map of pBluelux
 - 5.1.2a. Restriction Analysis of DNA thought to contain the *lux* operon
 - 5.1.2b. Restriction map of pSB2022
 - 5.1.3. SDS PAGE gel of *L. monocytogenes* (pSB2022)
- 5.2.1. Restriction Map of pHG327
- 5.2.2. Restriction Map of pSB2023
- 5.2.3. Restriction Analysis of pSB2024
- 5.2.4. Restriction Map of pSB2024
- 5.3.1. Restriction map of pSB2025
- 5.4.1. Restriction map of pSB2026
- 5.4.2. *L. monocytogenes* (pSB2026) when grown on media with and without added xylose
 - 5.5.1. Linear restriction map of the *xylR-luxABCDE* fragment from pSB2026
 - 5.5.2. Restriction Map of pSB2027
- 5.6.1. Strategy used for cloning the *rnnB* terminator downstream of the *luxABCDE* operon
- 5.6.2. Restriction Analysis of *lux* recombinant colonies thought to contain the *rnnB* terminator
- 5.7.1. Growth and Bioluminescence of *L. monocytogenes* (pSB2026)
- 5.7.2. Growth and Bioluminescence of *L. monocytogenes* (pSB2026)
- 5.8.1. Growth and bioluminescence of *L. monocytogenes* harbouring constitutive and inducible *lux* plasmids
- 5.8.2. Growth and bioluminescence of *L. monocytogenes* harbouring constitutive and inducible *lux* plasmids
- 5.9.1. Growth and bioluminescence of *L. monocytogenes* harbouring constitutive *lux* plasmids with and without a transcriptional terminator

- 5.9.2. Growth and bioluminescence of *L. monocytogenes* harbouring constitutive *lux* plasmids with and without a transcriptional terminator
- 5.10.1. 2-D analysis of *L. monocytogenes* harbouring pSB2019
- 5.10.2. 2-D gel analysis of *L. monocytogenes* harbouring pSB2027
- 6.1.1. Expression vectors pSB2018 and pSB2025
- 6.1.2. Restriction maps of pSB2029 and pGC4
- 6.1.3. Restriction Analysis of pSB2030
- 6.1.4. Restriction Map of pSB2030
- 6.1.5. *L. monocytogenes* (pSB2030)
- 6.1.6. *S. aureus* RN4220 (pSB2030)
- 6.1.7. *S. aureus* 8325-4 (pSB2030)
- 6.1.8. Haemolytic activity of two different strains of *S. aureus*
- 6.2.1. Growth and fluorescence of *L. monocytogenes* (pSB2019) c.f. *L. monocytogenes* (pSB2030)
- 6.2.2. Growth and fluorescence of *L. monocytogenes* (pSB2019) c.f. *L. monocytogenes* (pSB2030)
- 6.3.1. Growth and bioluminescence of *L. monocytogenes* (pSB2027) c.f. *L. monocytogenes* (pSB2030)
- 6.3.2. Growth and bioluminescence of *L. monocytogenes* (pSB2027) c.f. *L. monocytogenes* (pSB2030)
- 6.4.1. Comparison of bioluminescence and fluorescence of *L. monocytogenes* (pSB2030)
- 6.4.2. Comparison of bioluminescence and fluorescence of *L. monocytogenes* (pSB2030)
- 7.1.1. Restriction Map of pSB2017
- 7.1.2. Basis behind the PCR used to amplify putative DNA thought to contain the P3 promoter
- 7.1.3. Restriction Map of pSB2031
- 7.2.1. *In vitro* induction of the P3 promoter from *S. aureus* 8325-4 (pSB2031) through the addition of spent bacterial supernatant to the culture media
- 7.3.1. Restriction map of pSB2025
- 7.3.2. Restriction Map of pSB2032
- 7.4.1. Restriction map of pSB2033 and pSB2034

- 7.5.1.1. *S. aureus* 8325-4 (pSB2033) grown in the presence of different concentration of spent bacterial supernatant (data represents RFU/OD vs time)
- 7.5.1.2. *S. aureus* 8325-4 (pSB2033) grown in the presence of different concentration of spent bacterial supernatant (data represents RFU/OD and OD vs time)
- 7.5.1.3. *S. aureus* 8325-4 (pSB2034) grown in the presence of different concentrations of spent bacterial supernatant (data represents RLU/OD vs time)
- 7.5.1.4. *S. aureus* 8325-4 (pSB2034) grown in the presence of different concentrations of spent bacterial supernatant (data represents RLU/OD and OD vs time)
- 7.5.2.1. Luminescence data obtained from *S. aureus* 8325-4 (pSB2033) grown in the presence of different concentrations of spent bacterial supernatant
- 7.5.2.2. Fluorescence data obtained from *S. aureus* 8325-4 (pSB2033) grown in the presence of different concentrations of spent bacterial supernatant
- 7.5.2.3. Fluorescence and luminescence data obtained from *S. aureus* 8325-4 (pSB2033) grown in the presence of different concentrations of spent bacterial supernatant
- 7.6.1.1. *S. aureus* 8325-4 (pSB2033) grown with different concentrations of a synthetic activator (data represents RLU/OD vs Time)
- 7.6.1.2. *S. aureus* 8325-4 (pSB2033) grown with different concentrations of a synthetic activator (data represents RLU/OD and OD vs Time)
- 7.6.1.3. *S. aureus* 8325-4 (pSB2034) grown with different concentrations of a synthetic activator (data represents RLU/OD vs Time)
- 7.6.1.4. *S. aureus* 8325-4 (pSB2034) grown with different concentrations of a synthetic activator (data represents RLU/OD and OD vs Time)
- 7.6.2.1. Utilising *S. aureus* 8325-4 (pSB2033) to determine the effective concentration of a synthetic *agr* inhibitor (data represents RLU/OD vs Time)
- 7.6.2.2. Utilising *S. aureus* 8325-4 (pSB2033) to determine the effective concentration of a synthetic *agr* inhibitor (data represents RLU/OD and OD vs Time)

7.6.2.3. Utilising *S. aureus* 8325-4 (pSB2034) to determine the effective concentration of a synthetic *agr* inhibitor (data represents RLU/OD vs Time)

7.6.2.4. Utilising *S. aureus* 8325-4 (pSB2034) to determine the effective concentration of a synthetic *agr* inhibitor (data represents RLU/OD and OD vs Time)

List of Tables

- 1.1.6.1. Excitation and Emission Spectra for GFPwt and Mutant GFPs
- 2.2.1. Bacterial strains used during the course of this study
- 2.1.2. Plasmids used in this study
- 4.1.1. Average Growth rates of *L. monocytogenes* cells harbouring pSB2018
- 4.2.1. Comparative Growth rates of *L. monocytogenes* (pSB2018) and *L. monocytogenes* (pSB2019)
- 4.3.1. Mean Maximum Relative Fluorescent values for *L. monocytogenes* harbouring unstable *gfp3opt* expression vectors
- 4.3.2. Average growth rates of *L. monocytogenes* cells harbouring the unstable *gfp3opt* expression vectors
- 4.4.1. %RFU for *gfp* variants in *L. monocytogenes* following a downshift into media without 0.5% xylose
- 5.2.1. Restriction sites incorporated into the primers for amplification of the *lux* operon
- 5.7.1. Mean Exponential Growth Rates of *L. monocytogenes* harbouring pSB2026 with pMK4 as a control culture
- 5.8.1. Mean exponential growth rates of *L. monocytogenes* (pSB2026) and *L. monocytogenes* (pSB2027)
- 5.9.1. Exponential growth rates of *L. monocytogenes* cells harbouring pSB2027 and pSB2028
- 5.10.1. Comparison of known and calculated properties of the individual Lux proteins
- 6.2.1. Mean exponential growth rates of *L. monocytogenes* (pSB2019) and *L. monocytogenes* (pSB2030)
- 6.3.1. Mean growth rates of *L. monocytogenes* harbouring *lux* expression vectors.
- 7.6.1.1. Concentrations of the GP1 used to induce P3 activity from *S. aureus* 8325-4 (pSB2033) and *S. aureus* 8325-4 (pSB2034)
- 7.6.2.1. Concentrations of the inhibitor used to repress P3 activity from *S. aureus* 8325-4 (pSB2033) and *S. aureus* 8325-4 (pSB2034)

ABBREVIATIONS

GFP:	Green Fluorescent Protein
GFPwt:	Wild Type variant of green fluorescent protein
GFP3:	Red shifted GFP variant
GFP3opt:	Translationally optimised red shifted GFP variant
EYFP:	Eukaryotic Yellow Fluorescent Protein
EBFP:	Eukaryotic Blue Fluorescent Protein
FITC:	Fluorescein isothiocyanate
FRET:	Fluorescence Energy Resonance Transfer
FACS:	Fluorescence Activated Cell Sorter
CCD:	Charged Coupled Device
SCV:	Small Colony Variant
MRSA:	Methicillin Resistant <i>Staphylococcus aureus</i>
VRSA:	Vancomycin Resistant <i>Staphylococcus aureus</i>
Agr:	Accessory Gene Regulator
Sar:	Staphylococcal Accessory Regulator
GP-1:	Synthetic activator of the P3 promoter
HUVEC:	Human Umbilical Veined Endothelial Cells
DNA:	deoxyribonucleic acid
RNA:	ribonucleic acid
RnaseA:	Ribonuclease A
DIG:	digoxigenin
SDS:	sodium dodecyl sulphate
PAGE:	polyacryamide gel electrophoresis
PCR:	Polymerase Chain Reaction
pSB:	Plasmid Sutton Bonington
IPTG:	isopropyl- β -D-thiogalactopyranoside
EDTA:	ethylene diamine tetra acetic acid
NCTC:	National Culture Type Collection
Xyl:	Xylose
Amp:	Ampicillin
Cm:	Chloramphenicol

rpm:	revolutions per minute
g:	Gram
mg:	milligram (1×10^{-3} gram)
μ g:	microgram (1×10^{-6} gram)
ng:	nanogram (1×10^{-9} gram)
L:	litre
ml:	millilitre (1×10^{-3} litre)
μ l:	microlitre (1×10^{-6} litre)
M:	Molar concentration
mM:	millimolar (1×10^{-3} molar)
μ M:	micromolar (1×10^{-6} molar)
cm:	centimetre (1×10^{-2} metre)
mm:	millimetre (1×10^{-3} metre)
μ m:	micrometre (1×10^{-6} metre)
nm:	nanometre (1×10^{-9} metre)
kDa:	kilo Daltons
kb:	Kilo base
b.p:	base pair
mA:	milliamp
kJ:	Kilo Joule
$^{\circ}$ C:	Degrees Celsius
min:	minute
sec:	second
OD:	Optical Density
LB:	Luria-Bertani broth
BHI:	brain heart infusion
FBS:	Foetal Bovine Serum
SDW:	Sterile Distilled Water
PBS:	Phosphate Buffered Saline
HMW:	High Molecular Weight

ABSTRACT

Green fluorescent protein (*gfp*) and bacterial luminescence (*lux*) reporter genes have been used to construct a variety of reporter plasmids for Gram positive bacteria with the aim of using these for bacterial localisation and gene expression studies. The native *gfp* and *luxCDABE* genes were cloned into a shuttle vector and the resulting plasmids used to transform *Listeria monocytogenes*. However, the bacterial populations were found to be weakly fluorescent or luminescent compared to *E. coli* harbouring the same plasmids.

When *L. monocytogenes* expressing *gfp* were examined by fluorescence microscopy, only a small proportion of the population was seen to fluoresce. This phenomenon was observed regardless of the *gfp* variant used in the cloning procedure. However, when *gfp3* was placed downstream of P_{xyIA} , slightly more individual fluorescent cells were observed compared to when *gfp3* was expressed from P_{xyB} , but the majority of the population was still non-fluorescent. Northern blot analysis and subsequent analysis by SDS PAGE and immunoblotting lead to the supposition that translation of GFP was limiting in *L. monocytogenes*. A variety of factors could potentially lead to poor translation of the protein, for example poor codon usage, the presence of a ribosome stall site, or poor initiation of translation by the ribosomes. These were all investigated in turn to determine why translation of *gfp3* was limiting. Modification of the translational initiation region of *gfp3*, resulted in a homogeneously fluorescent *L. monocytogenes* population when the modified gene was expressed from P_{xyIA} . Individual *lux* genes, *luxA*, *luxC* and *luxE* were also translationally enhanced in a similar way to *gfp3*, and reorganised into an operon where the luciferase genes were adjacent to, but separate from the aldehyde genes. This engineered *luxABCDE* operon was also expressed from P_{xyIA} and highly luminescent populations of *L. monocytogenes* and *Staphylococcus aureus* obtained.

Having optimised translation for expression in Gram positive bacteria, these reporters were used to construct a variety of reporter plasmids that were successfully

employed to observe the intracellular invasion and to monitor *agr* expression in *S. aureus*.

ACKNOWLEDGEMENTS

I would like to thank Dr P. J. Hill and Dr C. E. D. Rees for their invaluable support, advice and encouragement throughout the course of this project and the BBSRC for their financial support.

I would also like to thank Dave Fowler for his technical assistance and Wendy Fielder, for all the advice they have provided throughout the last three years. I would also like to say a big thank-you to the other staff and students in the laboratory for their help, especially Tania Perehenic who provided technical assistance at the start of this project.

Finally I wish to thank all my family and friends for all their support, understanding, and encouragement.

Aims of the Project

The aims of this project were to clone and efficiently express the two reporter genes, *gfp* and *lux*, in Gram positive bacteria with particular reference to *L. monocytogenes* and *S. aureus*. After demonstrating these genes could be expressed at high levels in these organisms they could be used to observed expression of particular genes, for example *agr* in *S. aureus*, and also to track the organisms during the infectious process within eukaryotic cell lines.

CHAPTER 1

INTRODUCTION

CHAPTER 1: INTRODUCTION

1.1. Green Fluorescent Protein

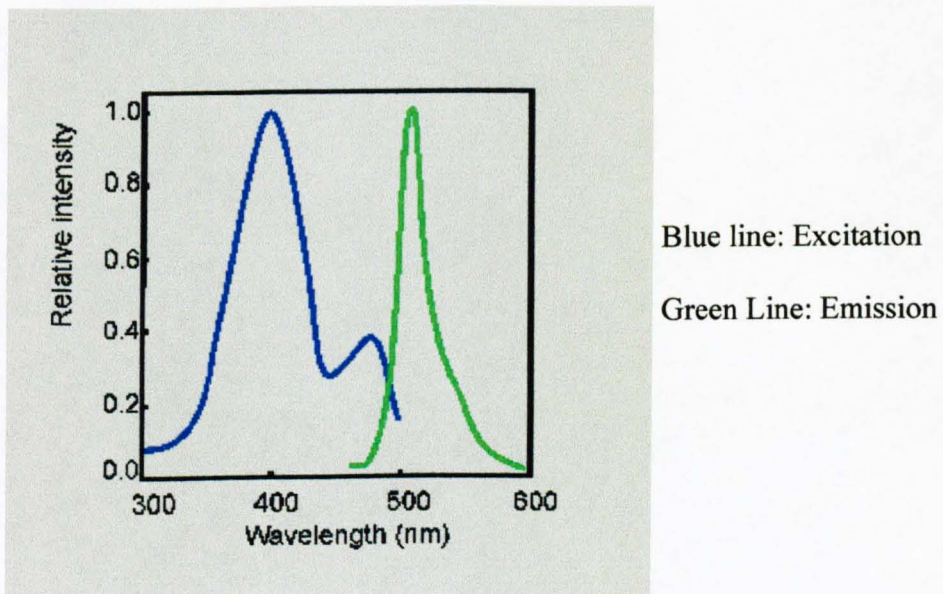
1.1.1. Background

Green fluorescent proteins (GFP) are spontaneously fluorescent proteins originally isolated from coelenterates. Several bioluminescent coelenterates, such as the jellyfish *Aequorea victoria* emit green light from a green fluorescent protein (Morin and Hastings, 1971). In *Aequorea*, the green fluorescence is due to the action of two closely associated proteins, a Ca^{2+} activated photoprotein (aequorin) and GFP. Aequorin is a 21.4kDa complex consisting of a Ca^{2+} binding apoprotein (apoaquorin), molecular oxygen and coelenterazine (Johnson and Shimomura, 1978; Charbonneau *et al.*, 1985; Inouye *et al.*, 1985). Purified aequorin, isolated from *A. victoria* photocytes was found to generate blue rather than green light (Shimomura *et al.*, 1962). When aequorin is activated by Ca^{2+} , it catalyses the oxidation of coelenterazine to coelenteramide, which is in an excited state. Coelenteramide returns to its ground state by emitting light at 470nm, which is the blue light generated by purified aequorin. *In vivo*, an energy transfer occurs from the excited state of the coelenteramide (complexed with aequorin and Ca^{2+}) to GFP, which is the green fluorescence observed. However, aequorin is not an essential part of the green-light reaction, purified GFP can be induced to emit green light by excitation directly with blue light (Ward, 1979).

1.1.2. Properties of GFP

The GFP of the jellyfish *A. victoria* is a 27kDa polypeptide comprised of 238 amino acid residues (Ward, 1979). The *Aequorea* GFP absorbs blue light maximally at 395nm and exhibits a minor excitation peak at 470nm, and emits green light at 508nm with a shoulder at 540nm (Morise *et al.*, 1974; Ward *et al.*, 1980), this is illustrated in Figure 1.1.2.1. Excitation with 395nm UV light results in rapid photobleaching of GFP fluorescence, whereas excitation with 470nm light results in relatively stable fluorescence.

Figure 1.1.2.1: Excitation and Emission spectra of the GFP from *Aequorea*.



1.1.3. The GFP Chromophore

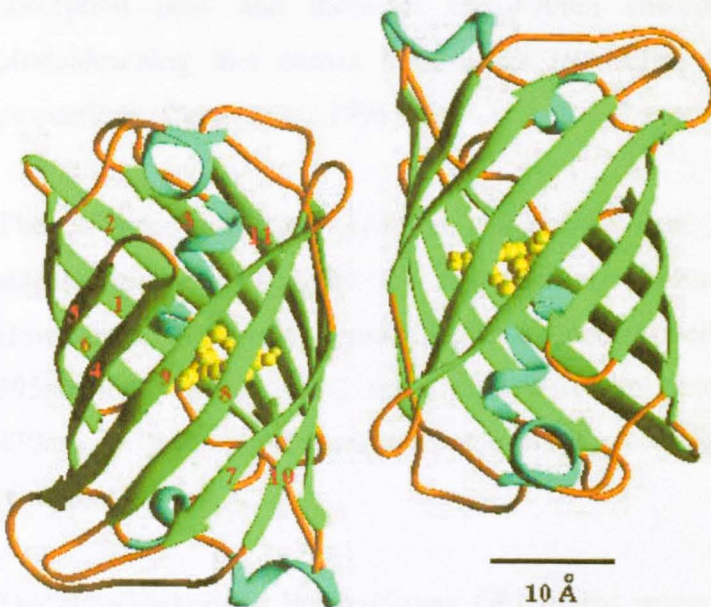
The intense fluorescence of GFP can be attributed to a chromophore, which is composed of modified amino acids within the polypeptide. Unlike other bioluminescent reporters this chromophore is intrinsic to the primary structure of the protein. Before GFP is able to fluoresce, the newly synthesised GFP molecules need to be processed into the mature fluorescent form (Inouye and Tsuji, 1994; Cubbit *et al.*, 1995). The fluorescent chromophore is generated by post-translational modification from the primary amino acid sequence, by cyclisation and oxidation of the serine-tyrosine-glycine sequence at residues 65-67 within the polypeptide (Cody *et al.*, 1993). Chromophore formation is oxygen dependent, occurs gradually after translation (Inouye and Tsuji, 1994), and does not appear to be enzymatic (Heim *et al.*, 1994). Since fluorescent GFP forms in a wide range of organisms, the steps for chromophore formation are either autocatalytic or use factors that are ubiquitous.

The fluorescent chromophore is stable to a variety of harsh conditions, including heat, extreme pH and chemical denaturants. If GFP is subjected to base or acid treatment or addition of guanidine hydrochloride, fluorescence is lost. However upon neutralisation of the pH or removal of the denaturant, fluorescence returns with an identical emission spectrum (Bokman and Ward, 1981; Ward and Bokman, 1982). Data obtained from the renaturation experiments suggests that the chromophore remains intact when GFP is denatured, upon proper protein refolding, the chromophore returns to a suitable environment and fluorescence is restored. The stability of GFP appears to be due to its unique three-dimensional structure (Yang *et al.*, 1996) which provides the correct environment required for the fluorescent chromophore.

1.1.4. The three-dimensional structure of GFP

The crystal structure of the wild-type GFP protein was determined by Yang *et al.* (1996). The structure of GFP revealed a regular β -barrel with 11 strands on the outside of the cylinder. These cylinders have a diameter of approximately 30 Å and a length of about 40 Å (Yang *et al.*, 1996). Inside the β -barrel, near the geometric centre, is an α -helix, which contains the chromophore (Yang *et al.*, 1996). Short helical segments cap the top and bottom of the β -can and also provide a scaffold for the chromophore. This structure is illustrated in Figure 1.1.4.1 and provides the proper environment for the chromophore to fluoresce by excluding solvent and oxygen. This folding motif, with sheet outside and helix inside, represents a new class of proteins, which has been named the β -can (Yang *et al.*, 1996).

Figure 1.1.4.1: The cylindrical β -can structure of GFP (taken from Yang *et al.*, 1996)



The regularity of the β -can is unique, with the 11 strands of the sheet forming an almost seamless structure. The tightly constructed β -barrel appears to have two roles,

protecting the chromophore and providing overall stability and resistance to unfolding by heat and denaturants.

1.1.5. Limitations of wild-type GFP

The wild-type GFP has several unfavourable properties that limit it as a reporter of gene expression and as a fluorescent tag, and these will be discussed in turn.

1. The wild-type GFP excitation spectra is not optimal for use with commonly used filter sets. The presence of GFP can be monitored in cells using standard fluorescein isothiocyanate (FITC) excitation emission filter sets, which make use of the minor absorption peak at 470nm. This absorption peak can also be utilised by argon lasers commonly found in flow-cytometers and laser scanning microscopes, which emit with a wavelength of 488nm. Irradiation of wild-type GFP with 395nm light can cause two spectral changes over time, photoisomerisation (Cubitt *et al.*, 1995) that progressively decreases the 395nm absorption peak and increases the 470nm absorption peak, as well as photobleaching that causes both peaks to decline by approximately equal proportions (Cubitt *et al.*, 1995).
2. The 470nm absorption peak is subject to less photoisomerisation and autofluorescence compared to excitation at 395nm (Cubitt *et al.*, 1995). However, the protein has a much higher extinction coefficient when excited with 395nm light, that is to say that the fluorescence generated from excitation at 470nm is much lower than when the protein was excited with 395nm light (Cubitt *et al.*, 1995).
3. The chromophore in the wild-type GFP forms rather slowly, this potentially limits its use to detect fast transcriptional events and changes in promoter activity. (Heim *et al.*, 1994; Heim *et al.*, 1995). Another limitation is the high stability of the protein, which again would limit *gfp* as a reporter to detect changes in gene expression (Cubitt *et al.*, 1995).

In order to overcome some of these problems a large variety of GFP mutants have been created.

1.1.6. GFP Mutants

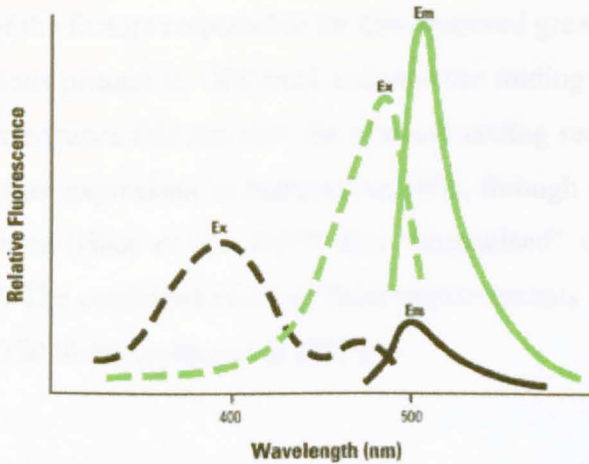
In order to create GFP mutants a wide variety of different strategies have been performed, for example site directed mutagenesis (Heim *et al.*, 1995; Ormö *et al.*, 1996) and randomisation of a pre-determined stretch of residues (Delagrave *et al.*, 1995; Cormack *et al.*, 1996). As there are numerous GFP mutants available only a few will be discussed, particularly those used in the course of this study. Mutagenesis of wild type (*gfpwt*) revealed two broad classes of mutants (Heim *et al.*, 1994), those that fluoresce blue (emission wavelength 458nm) when excited by UV light, and those where the excitation wavelength has been shifted (to a maximum of 490nm).

1.1.6.1. Red Shifted GFP Mutants

Red shifted *gfp* variants contain mutations in their chromophore which shift the maximal excitation peak to around 490nm. The major excitation peak of all the red shifted *gfp* variants encompasses the excitation wavelength of many commonly used FITC filter sets, similarly the argon laser used in many fluorescence activated cell sorters (FACS) and confocal scanning laser microscopes emit at 488nm, so the excitation of the red shifted *gfp* variants is more efficient than that of *gfpwt*. This means that the limits of detection in microscopy and FACS are lower with the red shifted *gfp* variants compared with *gfpwt*. Whilst the excitation peak of the red shifted *gfp* variants has been shifted by approximately 100nm, the emission spectra are virtually identical to that of *gfpwt*, as illustrated in Figure 1.1.6.1. Through the use of selective excitation, co-expression of *gfpwt* and the red shifted *gfp* will enable the analysis of two proteins or two promoters in one cell or organism. The possible uses of *gfp* variants will be discussed in a later section.

Figure 1.1.6.1: Excitation and emission spectra of *gfpwt* (black) and red shifted *gfp* variants (green). Taken from Clontech Living Colours User Manual

Excitation: dashed lines. Emission: solid lines. The emission for *gfpwt* was obtained with excitation at 475nm. (The emission peak for *gfpwt* is several fold higher when illuminated at 395nm).



Cormack *et al.* (1996) constructed a library of mutant GFP molecules through the use of an oligo-directed codon-based mutagenesis method (Glaser *et al.*, 1992; Cormack and Struhl, 1993). Through this method, random amino acid substitutions, NNK (where N is any base and K is G or T), were introduced in the 20 amino acid region (54-74) surrounding the chromophore (65-67) with a 10% probability of substituting NNK for each wild type codon. The resulting mutants were then screened by FACS, to select for variants of GFP that fluoresced more intensely than GFPwt when excited at 488nm. The differences in fluorescence intensity between GFPwt and the mutant GFPs could have been due to a number of factors, for example, increased expression of the protein, more efficient protein folding, increased absorption at 488nm, faster chromophore formation or greater solubility of the protein. Several classes of mutants were identified, all of which were shown to have markedly shifted excitation

spectra compared to that of GFPwt. Two of the mutants have been used in this study and are described in more detail below.

One mutant, designated GFPmut1 (Cormack *et al.*, 1996) was found to contain a double amino acid substitution, F64L and S65T. This variant was selected on its increased fluorescence in FACS assays relative to GFPwt, this is primarily due to an approximately 35-fold increase in its extinction coefficient (E_m) relative to GFPwt. One of the factors responsible for this observed greater fluorescence output is that the mutations present in GFPmut1 enhance the folding and solubility of the protein. To further enhance this reporter, the *gfp*mut1 coding sequence has been codon optimised for higher expression in mammalian cells, through the virtue of 190 silent base pair mutations (Haas *et al.*, 1996), this "humanised" variant of GFPmut1 was termed EGFP. The combined effect of these improvements increases the sensitivity of EGFP up to 350 times compared to GFPwt.

Cormack *et al.* (1996) isolated another GFP mutant, this was termed GFPmut3b. This too has a double amino acid substitution, this being S65G and S72A, and was isolated on its ability to fluoresce with a greater intensity upon excitation at 488nm compared to GFPwt.

The mutations isolated in these two *gfp* variants were found to have a significant effect on protein folding. Heim *et al.* (1994) observed that much of the GFPwt was found in the cell as non-fluorescent insoluble protein enclosed in inclusion bodies. When the mutant *gfp* variants were expressed, GFPmut1 was found to be 90% soluble, with virtually all GFPmut3 being soluble (Cormack *et al.*, 1996), this in part contributes to the increase fluorescence observed from bacteria expressing these mutant GFP proteins. When the mutant proteins were analysed by fluorescence spectroscopy, the excitation spectra was found to be different compared to that of GFPwt, ranging between 480-501nm, whilst the emission spectra was essentially unchanged, ranging from 507-511nm. This major shift in the absorption spectra is responsible for most of the increased fluorescence. Measurements obtained from

spectral analysis of equal amounts of soluble GFP have shown that when excited at 488nm, fluorescence per soluble unit of GFP is between 19 and 35-fold higher for the GFP mutants compared to GFPwt. This is illustrated in Table 1.1.6.1.

Table 1.1.6.1: Excitation and Emission Spectra for GFPwt and Mutant GFPs

Protein	Emission maxima (nm)	Excitation maxima (nm)	Fluorescence Intensity (relative to wild type)
GFPwt	395	508	1
GFPmut1	488	507	35
GFPmut3	501	511	21

Although the fluorescence data from analysis per unit soluble protein suggests that GFPmut1 has the highest fluorescence intensity, it is interesting to note that bacteria expressing GFPmut3 fluoresce with more than twice the intensity than those expressing GFPmut1 (Cormack *et al.*, 1996). This difference is most likely to be due to the folding characteristics of the protein. This is consistent with the fact to some GFPmut1 is found in inclusion bodies in an insoluble form, whereas virtually all GFPmut3 is soluble (Cormack *et al.*, 1996). So the increase in fluorescence of bacteria expressing GFPmut1 and GFPmut3 is due to a shift in the absorption spectra and also due to an increase in soluble protein as a result of more efficient protein folding (Cormack *et al.*, 1996). The enhanced protein folding or chromophore formation may be due to the second mutation in the protein. Heim *et al.* (1994) showed that the mutation S65T resulted in a six-fold increase in fluorescence intensity of the mutant protein. The GFP mutants of Cormack *et al.* (1996) whilst having a mutation at position 65, (S65T and S65G), the protein also contains a second mutation (F64L and S72A respectively). As these mutants fluoresce with a much greater intensity than those having a single mutation (Heim *et al.*, 1994) it appears as though this second mutation is critical for maximal fluorescence. It is possible that this second mutation may be necessary for protein folding or

chromophore formation, alternatively it may have a direct effect on the absorption efficiency (Cormack *et al.*, 1996).

1.1.6.2. Blue Emission GFP Variants

Heim *et al.* (1994) performed random mutagenesis on the *gfp* cDNA by hydroxylamine treatment and error prone PCR. The resulting bacterial colonies were screened using illumination with alternating 395nm and 475nm excitation, and screened for altered excitation and emission properties. The mutants isolated fell into two distinct groups, those where the excitation maxima had been altered as described in Section 1.1.6.1 and those that emitted light with a different wavelength compared to GFPwt. Heim *et al.* (1994) isolated a mutant that was excitable with shorter wavelength UV light, and fluoresced bright blue, in contrast to the green emission of GFPwt. The emission and excitation spectra of this blue mutant are similar to those observed by other blue emission variants (Heim and Tsien, 1996; Mitra *et al.*, 1996). The mutated DNA was found to contain five mutations, but only one of these was shown to be critical, this being Y66H (Tyr66His). As the blue emission variants are excited by UV light, photobleaching of the signal occurs quite rapidly (within seconds), so these mutants may not be of great use in microscopic studies. This problem has been overcome to some extent by the virtue of a new blue variant (Yang *et al.*, 1998) supplied by Clontech as EBFP. The rate of photobleaching from this variant has been reported to be one-half to one-third that of other blue variants, making this protein more stable EBFP contains the substitution Y66H as well as three others, F64L, S65T Y145F. It is thought that these other three substitutions enhance the brightness and solubility of the protein, probably due to improved folding properties of the protein and increased efficiency of chromophore formation (Cormack *et al.*, 1996; Heim and Tsien, 1996; Yang *et al.*, 1998).

1.1.6.3. Yellow-Green Emission Variant (YFP)

One other GFP variant with many potential applications was described by Ormö *et al.* (1996). This variant was termed clone 10C (available as EYFP, Clontech) and it contains four different amino acid substitutions, S65G, V68L, S72A, T203Y. These mutations shift the fluorescence from green (508nm) to yellow-green (527nm). The excitation maxima of this protein is 513nm, however it can be efficiently excited at 488nm, thus allowing excitation by standard lasers.

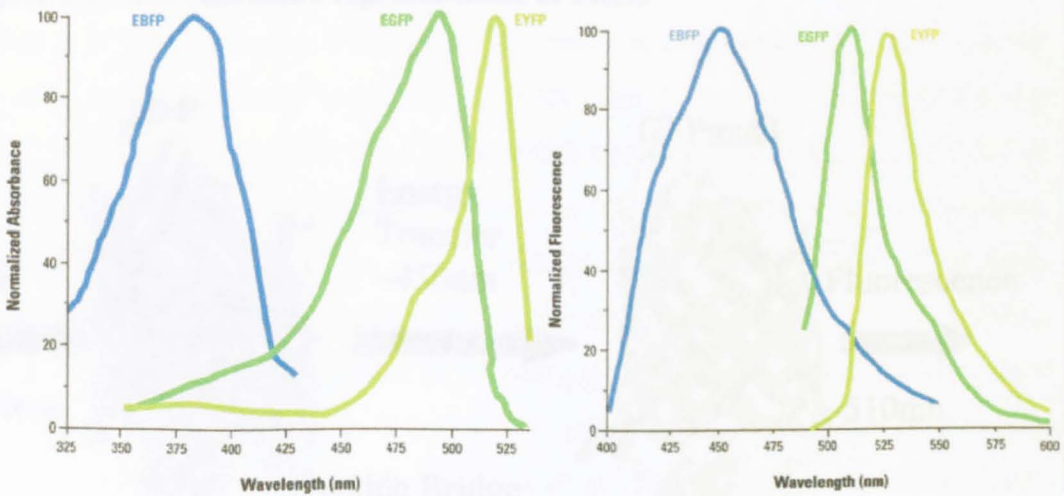
1.1.7. Potential uses of GFP and GFP Variants

The green fluorescent protein of *A. victoria* can be used as an *in vivo* reporter for monitoring dynamic processes in cells or organisms (Gerdes and Kaether, 1996). GFPwt has been shown to produce green fluorescence in a wide variety of diverse organisms, such as bacteria, plants and mammals (Cubitt *et al.*, 1995). It has numerous applications, including using GFP as a reporter for gene expression (Chalfie *et al.*, 1994), as a marker to study cell lineage during development (Tannahill *et al.*, 1995) and as a tag to study protein localisation, function and dynamics in living cells (Wang and Hazelrigg, 1994). The development of a wide range of GFP variants has opened up a wide range of applications that were not possible with GFPwt alone.

The red shifted GFP variants generate a brighter signal compared to that of GFPwt, so by using these it is possible to increase the sensitivity and decrease the lag time of detection of fluorescent activity. In bacteria growing in log phase at 37°C, GFPwt is not detectable until 1-2 hours after induction, whereas the signal generated from the red shifted GFP variants was reported to occur four times faster than that from GFPwt under identical conditions (Heim *et al.*, 1994; Cormack *et al.*, 1996).

The different excitation and emission spectra shown by the GFP variants makes it possible to perform dual labelling experiments. The GFP variants can all be separated by the wavelength of light needed for excitation or the resulting emission wavelength of light generated, this is illustrated in Figure 1.1.7.1a.

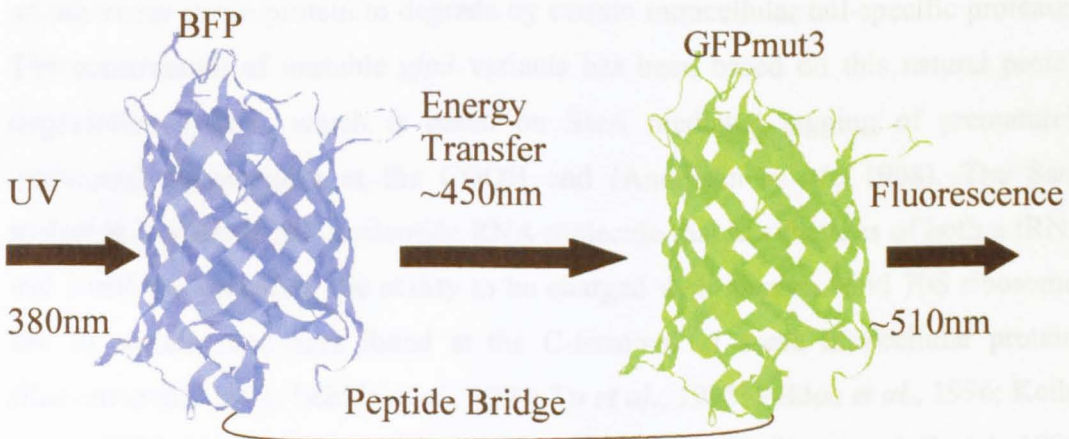
Figure 1.1.7.1a: Excitation (left panel) and Emission (right panel) spectra of EGFP, EBFP and EYFP. (Adapted from Clontech Living Colours User Manual) The emission data were obtained with excitation at 488nm (390nm for EBFP) These spectra show that, for microscopy, it is easier to distinguish between EBFP and EYFP or EGFP than between EGFP and EYFP.



Double labelling experiments with GFPwt and other GFP variants has several promising applications. These include microscopy of multiple cell populations in a mixed consortia; monitoring gene expression from two different promoters in the same cell, tissue or organism; monitoring the localisation of multiple proteins in the same cell, tissue or organism (Kain *et al.*, 1995; Rizzuto *et al.*, 1996); the monitoring of different cell lineages in a single tissue or organism; FACS analysis of mixed cell populations e.g. a mixture of cells expressing EGFP/ EBFP (Yang *et al.*, 1998), EGFP / EYFP (Lybarger *et al.*, 1998). The GFP variants could also be used to give real time analysis, by fluorescence resonance energy transfer (FRET), of protein-protein interactions of two distinct protein fusions (Heim and Tsien, 1996; Mitra *et al.*, 1996). FRET involves labelling one protein with a donor fluorophore and the

other protein with an acceptor fluorophore. The emission spectrum of the donor must overlap significantly with the excitation spectrum of the acceptor, however, the overlap between the two excitation and emission spectra should be minimised. For example, a blue GFP variant could be the donor (excitation maximum 382nm, emission maximum ~450nm), whilst red shifted mutants could be the acceptor (excitation maximum 488nm, emission 510nm). This is illustrated schematically in Figure 1.1.7.1b. Wild type GFP would not be a favourable acceptor, because UV excitation of the blue variant near its 382nm absorption peak would also directly excite wild type GFP at its 395nm absorption peak without any energy transfer.

Figure 1.1.7.1b: Schematic representation of FRET



1.1.8. Unstable GFP Variants

A major drawback of GFP is its stability once formed (Tombolini *et al.*, 1997), this makes the protein less valuable for real time gene expression studies. Properly matured GFP is a very stable protein and as such may be unable to reflect dynamic bi-directional changes in gene expression within the cell, thus a real time representation of gene expression would not be obtained. Based on a natural protein degradation system (Keiler *et al.*, 1996), Anderson *et al.* (1998) constructed variants of *gfp3* which were shown to have different functional half lives in *E. coli*.

Keiler *et al.* (1996) showed that a specific C-terminal oligopeptide extension caused an otherwise stable protein to degrade by certain intracellular tail-specific proteases. The construction of unstable *gfp3* variants has been based on this natural protein degradation system, which is based on SsrA mediated tagging of prematurely terminated polypeptides at the COOH end (Anderson *et al.*, 1998). The SsrA molecule is a stable 362 nucleotide RNA molecule that has features of both a tRNA and a mRNA, including the ability to be charged with alanine, bind 70S ribosomes and to encode sequences found at the C-terminal of some intracellular proteins (Komine *et al.*, 1994; Ushida *et al.*, 1994; Tu *et al.*, 1995; Felden *et al.*, 1996; Keiler *et al.*, 1996; Muto *et al.*, 1996; Tadaki *et al.*, 1996; Williams and Bartel, 1996; Feldon *et al.*, 1997; Muto *et al.*, 1998; Williams and Bartel, 1998). Genes homologous to *ssrA* have been identified in Gram positive (Ushida *et al.*, 1994) and Gram negative (Brown *et al.*, 1990, Tyagi and Klinger, 1992) bacteria, implying this peptide tagging system mediated by SsrA may be conserved in all bacteria (Williams and Bartel, 1996).

Keiler *et al.* (1996) proposed that in *E. coli*, the alanine charged SsrA RNA binds in the A site of ribosomes stalled on damaged mRNA or mRNA that lacks a termination codon. Through cotranslational switching of the ribosome, the ribosome donates the charged alanine to the nascent polypeptide chain and then replaces the damaged message as a surrogate mRNA (Keiler *et al.*, 1996). The resultant translation product

carries an 11-residue C-terminal peptide tag (AANDENYALAA), which is recognised and rapidly degraded by intracellular proteolytic systems. The Tsp protease specifically recognises these tagged polypeptides both *in vitro* and for periplasmic proteins *in vivo* (Keiler and Sauer, 1996), but Tsp does not degrade tagged cytoplasmic proteins *in vivo* (Silber and Sauer, 1994). In the cytoplasm, the addition of this C-terminal peptide tag makes the tagged protein a substrate for proteolysis by C-terminal specific proteases (Tu *et al.*, 1995; Keiler *et al.*, 1996; Gottesman *et al.*, 1998).

Unstable GFP mutants have been constructed with minor alterations in the Tsp consensus sequence. This has resulted in *gfp3* variants with an additional C-terminal peptide tag (Anderson *et al.*, 1998). As GFP accumulates within the cytoplasm, it is thought that the addition of this C-terminal tag causes this tagged protein to become a substrate for intracellular proteases (Tu *et al.*, 1995; Keiler *et al.*, 1996; Gottesman *et al.*, 1998). Gottesman *et al.* (1998) suggested that ClpAP and ClpXP proteases were responsible for degrading proteins carrying a carboxy-terminal peptide tail added by the SsrA tagging system.

The Clp family of proteins constitutes a large family of closely related peptides that are found in both prokaryotic and eukaryotic cells (Schirmer *et al.*, 1996). Several members of the Clp family are chaperones that are also able to target specific proteins for degradation by association with ClpP (Squires and Squires, 1992; Wawrzynow *et al.*, 1996; Gottesman *et al.*, 1997). By itself ClpP has only peptidase activity, however upon association with other members of the Clp family, ClpA or ClpX (Gottesman *et al.*, 1993; Katayama *et al.*, 1998), the resulting Clp complex has serine protease activity (Maurizi *et al.*, 1990). Several *E. coli* proteins have been shown to be degraded *in vivo* by either ClpAP or ClpXP protease, including those that have a C-terminal peptide tail that was added by the SsrA-tagging system (Gottesman *et al.*, 1998).

As previously mentioned, in order for full proteolytic activity to occur ClpP has to associate with one of two related ATPase subunits, ClpA or ClpX, both of which are members of the Hsp/Clp family of molecular chaperones (Schirmer *et al.*, 1996). Of the two ATPase subunits in *E. coli*, ClpA was the first identified (Katayama *et al.*, 1988) and is thus best characterised. The proteolytic complex is composed of two central heptameric rings of ClpP flanked by one or two rings of ClpA. ClpA has approximately twice the binding affinity for ClpP than ClpX (Grimaud *et al.*, 1998).

The ClpAP protease complex is able to degrade large proteins to short peptides comprised of approximately seven to ten amino acids without any apparent sequence specificity (Thompson and Maurizi, 1994; Thompson *et al.*, 1994), but the process does require both Mg^{2+} and ATP hydrolysis (Katayama *et al.*, 1988). ATP binds to two distinct sites on the ClpA protein, and ATP hydrolysis at one is sufficient to allow protein degradation by the ClpAP complex. The ATP molecule bound to the other domain is primarily required for ClpA oligomerization (Singh and Maurizi, 1994; Seol *et al.*, 1995). ClpA also binds the protein that has been targeted for degradation, and in steps that require ATP, is able to unfold the protein in order to increase its accessibility to the ClpP proteolytic active sites (Wang *et al.*, 1997).

ClpP is also able to form an active protease with ClpX, a smaller protein than ClpA, which has only one ATP binding domain (Gottesman *et al.*, 1993). As *E. coli* possesses only one type of ClpP protein, association of ClpA and ClpX simultaneously may increase the proteolytic efficiency and the range of the resulting enzyme (Porankiewicz *et al.*, 1999).

The unstable GFP variants are degraded intracellularly by Clp proteases. These proteins are based on cell proteins in *E. coli* that have been co-translationally modified by the addition of the peptide sequence ANDENYALAA at the C-terminal end (Anderson *et al.*, 1998). It is these C-terminally tagged proteins that are targeted for degradation by both the ClpAP and ClpXP proteases (Gottesman *et al.*, 1998).

1.1.9. Advantages to Using GFP as a Reporter

GFP is a non-invasive marker, which allows gene expression or protein localisation to be followed *in vivo*. Wild type GFP when expressed in both prokaryotes and eukaryotic cells yields bright green fluorescence upon excitation with UV or blue light. It requires no other substrates, co-factors or additional gene products from *A. victoria* for detection and fluorescence occurs in a species independent fashion. That the GFP fluorescence is generated in the absence of other factors was conclusively demonstrated when the GFP cDNA was heterologously expressed in bacteria and *Caenorhabditis elegans*, giving rise to bright green organisms when excited with blue light (Chalfie *et al.*, 1994). The fluorescence of GFP can be detected and measured non-invasively in living tissues. GFP is an extremely stable protein, and the purified protein retains its fluorescence under many different harsh conditions, both when expressed *in vivo* and *in vitro*. For example fluorescence is retained even after samples have been fixed in gluteraldehyde or formaldehyde. GFP is also resistant to heat, temperatures up to around 70°C, alkaline pH (greater than pH12), detergents, organic solvents and most common proteases, except pronase (Bokman and Ward, 1981; Ward, 1981; Roth, 1985; Robart and Ward, 1990). Upon exposure of GFP to high temperature, extreme pH or guanidinium chloride the GFP is denatured and fluorescence is lost, however this can be partially recovered if the protein is allowed to renature (Bokman and Ward, 1981; Ward and Bokman, 1982). In order to aid renaturation of the protein into a fluorescent form a thiol compound may need to be added (Surpin and Ward, 1989). Whilst strong reducing agents, such as 2mM FeSO₄ convert GFP into a non-fluorescent form, fluorescence is fully recovered after exposure to atmospheric oxygen (Inouye and Tsuji, 1994). As well as GFP being extremely stable, it is also a sensitive marker. Although GFP has a lower extinction coefficient than fluorescein, Wang and Hazelrigg (1994) found that using fluorescence microscopy, GFP fusion proteins gave greater sensitivity and resolution compared to staining with fluorescently labelled antibodies (Wang and Hazelrigg, 1994). GFP fusions have the advantage of being more resistant to photobleaching and of avoiding background caused by the non-specific binding of primary and secondary antibodies to targets other than the antigen (Wang and Hazelrigg, 1994).

1.1.10. Disadvantages to using GFP as a reporter

Although GFP has a number of advantages for use as a reporter gene there are also some problems associated with using it, as GFPwt has many non-optimal properties. These include low signal output, a significant delay between protein synthesis and fluorescence development (Heim *et al.*, 1994) and the complex process of photoisomerisation. Although many of the weaknesses of GFPwt have been ameliorated through the development of GFP variants, GFP fundamentally lacks one stage of amplification built into a true enzymatic reporter system in which each protein molecule can generate thousands of chromophore or fluorophore molecules. Each GFP molecule represents one fluorophore, thus relatively high levels of GFP expression, as much as 10^6 molecules per cell (Rizzuto *et al.*, 1995) may be necessary to generate bright signals.

Aequorea GFP owes its visible absorbance and fluorescence to a chromophore (Prasher *et al.*, 1992; Cody *et al.*, 1993) which is formed by cyclisation of Ser65, Tyr66, and Gly67 and 1,2-dehydrogenation of the tyrosine. This modification of the protein occurs post-translationally and is a crucial constraint with which GFP can report changes in gene expression. The process of chromophore formation is oxygen dependent, therefore if oxygen is limiting in the environment this may be the rate-limiting step in chromophore formation. Expression of GFP in anaerobic environments is therefore not possible. However, a red shifted GFP mutant has been expressed in *L. lactis*, *Enterococcus faecalis* and *Streptococcus gordonii* (Scott *et al.*, 1998). When grown anaerobically these colonies were able to fluoresce following subsequent exposure to air (Scott *et al.*, 1998). Thus it was determined that highly anaerobic environments will prevent GFP fluorescence but not GFP synthesis. This suggests that even obligate anaerobes marked with GFP should be able to be detected upon exposure to oxygen.

The slow rate of chromophore formation and the apparent stability of GFPwt may preclude the use of GFPwt as a reporter to monitor fast changes in promoter activity.

This has been reduced to some extent through the use of GFP variants, where modification to the coding sequence has resulted in proteins, e.g. EGFP, which acquire fluorescence at a faster rate compared to GFPwt. In order to overcome the problem of stability of GFPwt, protease recognition sequences have been placed at the C-terminal of GFPmut3 to reduce the half-life of the protein (Anderson *et al.*, 1998). GFPmut3, a red shifted GFP variant, fluoresces with a greater intensity compared to GFPwt, is more soluble and if the unstable variants are turned over in Gram positive bacteria then these variants will be improve the ability of GFP to report on changes in gene expression. In addition to the unstable GFP variants of Anderson *et al.* (1998), Clonotech produce vectors that contain an unstable variant of EGFP, which has been shown to have a half-life of approximately 2 hours when expressed in mammalian cells.

Although fluorescent GFP is highly thermostable, formation of the GFP chromophore appears to be temperature sensitive. It has been noticed that *E. coli* expressing GFP showed stronger fluorescence when grown at 24°C or 30°C compared to 37°C (Heim *et al.*, 1994). Mammalian cells expressing GFP have also been shown to exhibit stronger fluorescence at 30°C compared to higher temperature of approximately 37°C (Pines, 1995; Ogawa *et al.*, 1995). This would limit GFP in intracellular environments, possibly with weaker fluorescence levels being observed.

1.2. Bacterial Bioluminescence: Organisation, regulation and Application of the *lux* genes.

1.2.1. Introduction

Bioluminescence refers to the ability of living organisms to produce light through the action of an enzyme catalyst. The enzymes that catalyse the bioluminescent reactions in these organisms are called luciferases and the substrates are often referred to as luciferins. Bioluminescent organisms are ubiquitous in nature and are comprised of many different species, including bacteria, dinoflagellates, fungi, fish, insects and algae. However, whilst all these organisms emit light, significant differences occur between the light emitting reactions, structure of the luciferases and luciferins from different organisms. The only common component between all the bioluminescent systems so far studied is the requirement for oxygen.

1.2.2. Luminescent bacteria

Luminescent bacteria are the most common light emitting organisms. They are found in a wide variety of environments, including marine, freshwater and terrestrial habitats. Although their primary habitat is in the ocean as free-living species they are also found in saprophytic or parasitic habitats (on the surface of fish, crustacea and mollusca), commensal (as gut bacteria of fish), or symbiotic habitats (specialised light organs of fish). Almost all the luminescent bacteria have been classified into three genera, *Vibrio*, *Photobacterium*, which are marine in nature, and *Photorhabdus* (previously known as *Xenorhabdus*) (Baumann *et al.*, 1983; Hastings *et al.*, 1985; Campbell, 1989; Meighen, 1988). Only the *Photorhabdus* genus contains terrestrial species (Colepiccolo *et al.*, 1989; Farmer *et al.*, 1989).

1.2.3. Physiological function of Bioluminescence

The mechanism of bacterial bioluminescence has many implications in terms of survival, physiology and metabolism (Hastings *et al.*, 1985). For example, luminescence observed by bacteria living in symbiosis with marine organisms may be advantageous for the organism by serving as system for communication, defence, and/or attraction. The host in turn provides a constant source of nutrients for the bacteria.

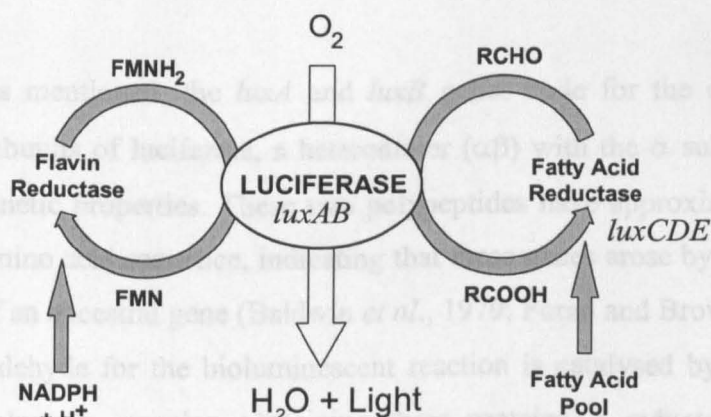
1.2.4. The Genetic Basis of Bioluminescence

The light emitting reaction in bacteria requires relatively simple compounds as substrates from a biochemical point of view, these being a source of energy in the form of reduced flavin mononucleotide (FMNH₂), molecular oxygen (O₂), and a long chain fatty aldehyde molecule (tetradecanal *in vivo*). In bacteria the light emitting reaction involves the oxidation of the FMNH₂ and a long-chain fatty aldehyde with the emission of blue-green light. The reaction is summarised in Figure 1.2.4.1.



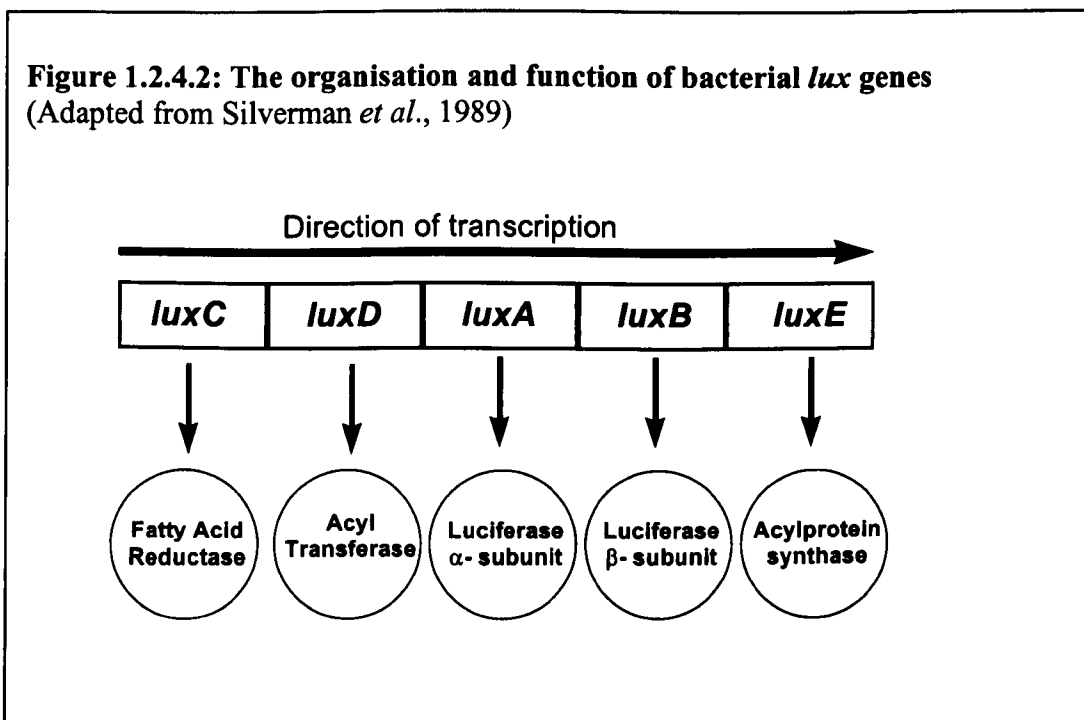
Figure 1.2.4.1: The bacterial bioluminescence system

Adapted from Meighen (1993)



Genes of the *lux* operon code for the luciferase and for the fatty acid reductase complex responsible for synthesis and recycling of aldehyde substrate (RCHO). Also required for the reaction is oxygen and reduced flavin (FMNH₂) obtained from the bacterium's electron transport chain.

The structural genes that encode the proteins necessary for the bioluminescent reaction are all found on one single operon, the *lux* operon. This single transcriptional unit contains genes that code for the α and β subunits of the bacterial luciferase, *luxA* and *luxB*, and also *luxC*, *luxD* and *luxE* which encode the fatty acid reductase complex which is required for biosynthesis of the long chain fatty acid substrate (tetradecanal). These five genes appear to be universally conserved and associated in all *lux* systems of bioluminescent bacteria, and the order of these genes is conserved. The *luxCDE* genes flank the *luxAB* genes in the different luminescent species, with transcription always occurring in the order of *luxCDABE*. The order of these structural genes of the *lux* operon is shown schematically in Figure 1.2.4.2.



As mentioned, the *luxA* and *luxB* genes code for the α (40kDa) and β (36kDa) subunits of luciferase, a heterodimer ($\alpha\beta$) with the α subunit dictating the primary kinetic properties. These two polypeptides have approximately 30% identity in the amino acid sequence, indicating that these genes arose by a tandem gene duplication of an ancestral gene (Baldwin *et al.*, 1979; Foran and Brown, 1988). The synthesis of aldehyde for the bioluminescent reaction is catalysed by a multienzyme fatty acid reductase complex containing three proteins, a reductase (54kDa), a transferase

(33kDa) and a synthetase (42kDa) (Riendeau *et al.*, 1982; Rodriguez *et al.*, 1983a; Rodriguez *et al.*, 1983b). These three polypeptides are encoded by *luxC*, *luxD* and *luxE* respectively. The *luxCDE* genes code for the polypeptides that are required for the conversion of fatty acids into the long chain aldehyde required for the bioluminescence reaction.

Although the luciferase and fatty acid reductase genes are the only common *lux* genes in luminescent bacteria, new *lux* genes are continually being discovered which adds to the complexity and diversity. The discovery of such genes and their subsequent identification of their roles helps in understanding how the luminescence system is connected with other metabolic pathways and related to the overall physiology of the different bacteria. For example, in *Vibrio* the order of the operon is *luxCDABE*, but in the case of *Photobacterium* the order is *luxCDABFE* (Engebrecht and Silverman, 1984; Mancini *et al.*, 1988; Meighen, 1988, Soly *et al.*, 1988)), where *luxF* encodes a flavoprotein related in sequence to the luciferase genes. This gene only appears to be found in *Photobacterium* strains. However, LuxF protein is not necessary for bioluminescence, it may play a specific role in the luminescence of *Photobacterium* species found in mid or deep water, but was found to be absent in a *P. leiognathi* species that is a symbiont of a shallow water fish (Lee *et al.*, 1991).

1.2.5. Applications of *lux* genes

The bioluminescence phenomenon provides a real time, non-invasive reporter for measuring gene expression, marking bacteria so their progression and movement can be monitored and also it can be used as a measure of intracellular biochemical function, i.e. as a measure of cell viability. When the *lux* genes are placed after a suitable promoter and transferred into non-luminous organisms, they can be used as a sensor for a wide variety of processes or substances and are limited only by the properties of the expression system or the organism.

The strength and regulation of transcription from various promoters can be monitored by using *lux* genes as reporters of gene expression. For example bioluminescence has been used to detect and measure the strength of promoters under temporal and morphological or spatial regulation during sporulation, mycelium development, and/or germination of *Bacillus* (Carmi *et al.*, 1987, Stewart *et al.*, 1989; Cook *et al.*, 1993). Carmi *et al.* (1987) were the first to use luciferase as a marker for gene expression in *Bacillus* spp. The use of a non-disruptive reporter, such as bacterial luciferase, is particularly valuable in developmental systems such as sporulation where the integrity of the mother cell is directly dependent on spore development. The results of Cook *et al.* (1993) demonstrated that *B. subtilis* strains expressing *lux* genes from *V. fischeri* and *V. harveyi* could be detected against a high background of non-luminescent indigenous soil microbial colonies on agar plates using a CCD camera. Expression of the *lux* genes would allow environmental detection of bacteria and also allow the metabolic activity of the released bacteria to be monitored, thus information on the survival and spread of the genetically modified organisms could be gathered.

As the production of light from recombinant bacteria containing the *lux* genes depends upon cells being biochemically active, it can be assumed that any substance in the environment that impairs the biochemistry, and thus compromises the cellular viability will lead to a reduction in luminescent emission. Thus there is the potential

to use the *lux* genes as environmental biosensors, for example to assess levels of soil pollution by different metals (Paton *et al.*, 1997). The *lux* tagged bacteria were demonstrated to be sensitive to a variety of metals, such as cadmium, nickel, zinc and copper, highlighting the potential use of *lux* genes as a sensitive indicator of soil pollution.

Other factors that may decrease cell viability can also be monitored through the application of *lux* genes. For example, the effect of antimicrobial agents or other inimical process on industrial relevant bacteria may be studied in real time. This could also be applied within the medical environment to observe the effects of bactericidal regimes upon bacteria, for example those involved in biofilms, where the organism may be more resistant to disinfection (Costerton, 1984).

One of the most important reasons for using *lux* genes to mark expression, noted in the work of Shaw and Kado (1986) and O’Kane *et al.* (1988) is to monitor bacteria during host-pathogen interactions or host-symbiont interactions. Shaw and Kado (1986) demonstrated that the distribution and viability of bacteria in plants could be followed through the use of *lux* genes. O’Kane *et al.* (1988) demonstrated that *lux*-containing *Bradyrhizobium* lead to the luminescence of soybean root nodules, this ultimately gave the location of the bacteria. This would seem particularly important in clinical diseases where the pathogenicity studies cannot be completed without reference to the host-microbe interactions.

In order to advance our understanding of host-pathogen interactions and gene regulation, non-invasive assays for monitoring the progression of infectious agents and other biological processes in the living animal are extremely valuable. For more than 100 years, researchers have used *in vitro* conditions that mimic host environments to study virulence factors expressed by pathogens. Tissue culture cells have also been used as a model system of infection, giving important information on host pathogen interactions. However, *in vivo* there are complex and dynamic interactions that occur which can never be replicated by *in vitro* model systems,

which are deficient in reproducing much in not all the host immune system with which pathogens have co-evolved. Therefore the intact animal remains the ultimate model of choice.

The experiments of Contag *et al.* (1995) allowed bacterial movement to be viewed non-invasively within the living animal. The researchers used three different strains of *Salmonella*, which had been modified with genes from *Photobacterium luminescens* to produce bioluminescence, and inoculated these into mice. By using an intensified CCD camera the bacteria were imaged and the course of each infection followed. The intensity of light produced by the bacteria was enough to visualise some infected tissues, particularly the caecum, and if the infection was not controlled by the immune system of the animal, the bacteria appeared to spread out from this reservoir. Also, by monitoring the mice over a fixed 8-day period it was possible to distinguish between the different *Salmonella* strains. With the least virulent strain, bioluminescence vanished, as the mice were able to eliminate it. Contag *et al.* (1995) were also able to monitor a rapid decrease of fully virulent strains by naturally occurring resistant mouse strains (Contag *et al.*, 1995).

The results of Contag *et al.* (1995) could have a significant impact upon the development of novel drugs, understanding gene regulation during development and during infectious processes, as well as many other biological events. Optical methods for assessing the efficacy of drugs would greatly impact development of new antibacterial and antiviral agents, by both accelerating the process and utilising fewer animals. In principal, the activity of any gene fusion to *lux* can be followed in live animal tissues. However, luciferase activity is highly sensitive to the concentration of molecular oxygen (Contag *et al.*, 1995), thus making it difficult to draw correlation's between photon emission and the level of gene transcription, especially in oxygen deficient tissues. Nevertheless, gene fusion to *lux* should provide reliable measurements of gene expression providing the substrates are not limiting.

As *lux* genes in Gram negative bacteria have proved to be so useful, we have decided to try and engineer similar constructs for use in Gram positive bacteria. *Lux* reporters are useful in the fact that they permit monitoring of gene expression over time, as the short half-life of the luciferases guarantees that photon emission observed represents expression of the gene of interest. In addition, sensitive photon counting equipment and cameras allows *lux* expression to be visualised with single cell resolution.

1.3. *Listeria monocytogenes*

1.3.1. Background

Listeria monocytogenes is a Gram positive non-sporing bacillus, which is an intracellular pathogen of animals, and it is able to cause food-borne infections, listeriosis, in a wide range of animals and humans (Gray and Klinger, 1966). *L. monocytogenes* is widely distributed in animals (fish, birds, mammals and insects), plants and soil, from these reservoirs it is transmitted to humans by contact with animals or their faeces, by unpasteurised milk and by contaminated vegetables. As the consumption of refrigerated ready-to-eat foods, salads and ready to serve fresh packed vegetables has significantly increased in recent years, these products might cause concern as potential sources of *L. monocytogenes*. This bacterium has several important properties that makes it an important food borne pathogen: its ability to grow at refrigeration temperatures; its resistance to changes in pH and relative resistance to other unfavourable conditions used for food preservation, for example low water activity. The ability of the organism to survive refrigeration and freezing temperatures has important implications within the food industry, as it permits the slow multiplication of the organism to high infectious doses. For example, if bacteria were introduced into food at the time of manufacture, an initial low inoculum could give rise to a substantial dose of listeriae for the consumer, depending on the shelf life and handling of the product. The most likely source of infections that arise endogenously are *via* the gastrointestinal tract, i.e. through ingestion of contaminated food. Whilst *Listeria* infections are not a major health issue for the majority of healthy individuals, in some cases they may be responsible for a variety of health problems, including severe encephalitis, meningitis, flu-like symptoms, low grade septicaemia, pneumonia, urethritis and abortion. *L. monocytogenes* is an opportunistic pathogen, particularly causing serious disease or possibly fatality in immunocompromised persons, pregnant women and newborns (Gray and Killinger, 1966; Seeliger, 1988).

1.3.2. *Listeria monocytogenes* as a pathogen

L. monocytogenes are able to invade and replicate *in vitro* in both phagocytic and normally non-phagocytic mammalian host cells (Gaillard *et al.*, 1987; Kuhn *et al.*, 1988; Tilney and Portnoy, 1989). Once the bacterium has been internalised, it escapes from the phagosome into the cytoplasm through the action of a secreted hemolysin (reviewed by Cossart and Mengaud, 1989) where it grows intracellularly. Having grown in the host cytoplasm, the bacteria uses a host system of actin based motility to mediate movement both within one cell and from cell to cell without leaving the cytoplasm (Beradini *et al.*, 1989; Tilney and Portnoy, 1989; Dabiri *et al.*, 1990; Mounier *et al.*, 1990, Theriot *et al.*, 1992). Once the bacteria have entered the cell cytoplasm they are surrounded by filamentous F-actin. This is arranged into a 'comet tail' which protrudes from the bacterial cell end opposite to the direction of movement (Beradini *et al.*, 1989; Tilney and Portnoy, 1989; Dabiri *et al.*, 1990; Mounier *et al.*, 1990; Theriot *et al.*, 1992). The bacteria when they move leave trails of F-actin behind them, some of these bacteria then become incorporated into the tip of pseudopod-like structures, which in turn are internalised by adjacent cells. So ultimately cell to cell spread is *via* a double membraned vacuole. The two membranes then surrounding the bacteria are lysed and the infection cycle begins again in the new host (Tilney and Portnoy, 1989).

Several *L. monocytogenes* genes that are involved in cellular invasion and intracellular parasitism have been identified and their function and products studied in detail (reviewed in Portnoy *et al.*, 1992). These include the pleiotropic regulator of the virulence gene cluster *prfA*, members of the virulence gene cluster (*plcA*, *hlyA*, *mpl*, *actA* and *plcB*), and the *inl* family of invasion genes (Gaillard *et al.*, 1991; Chakraborty *et al.*, 1992).

The entry of *L. monocytogenes* into eukaryotic cells is mediated by a number of proteins belonging to the internalin family. Analysis of transposon-induced non-invasive mutants led to the identification of the genetic locus involved in the entry of

L. monocytogenes into mammalian cells (Gaillard *et al.*, 1991; Dramsi *et al.*, 1993; Dramsi *et al.*, 1995). This locus is comprised of two genes, *inlA* and *inlB* (Dramsi *et al.*, 1993). *inlA* encodes internalin, a protein comprised of 800 amino acids and expression of this protein can confer invasiveness to *L. innocua* which is related to *L. monocytogenes* but is non-invasive (Gaillard *et al.*, 1991). InlA is required for entry of *L. monocytogenes* into the intestinal epithelial cell line Caco-2 (Gaillard *et al.*, 1991) and other cell lines expressing its receptor, the cell adhesion molecule E-cadherin (Mengaud *et al.*, 1996). Although a proportion of InlA is secreted into the culture medium, the surface associated form of this protein can mediate entry into cells (Lebrun *et al.*, 1996). The carboxy-terminal of InlA contains an LPXTG motif, a sequence necessary for sorting and cell anchoring of many surface proteins of Gram positive bacteria, for example protein A of *Staphylococcus aureus* (Gaillard *et al.*, 1991; Schneewind *et al.*, 1992). The second gene, *inlB*, encodes a 630 amino acid protein, this protein is homologous to InlA and is required for entry into cultured hepatocytes (Dramsi *et al.*, 1995; Gaillard *et al.*, 1996; Gregory *et al.*, 1996). InlB has no LPXTG motif at its carboxy-terminal, but it does contain repeated sequences of approximately 80 amino acids beginning with the dipeptide GW. These GW repeats are sufficient to anchor InlB to the bacterial surface, even when the protein is added externally (Braun *et al.*, 1997). A third gene has been identified that codes for a protein of 297 amino acids. This protein was found to have high homology to InlA and InlB and was termed InlC (Engelbrecht *et al.*, 1996), and in fact the gene sequence is related to the other internalins. It was suggested that InlC may play a role in a late stage of *L. monocytogenes* infection rather than in the uptake of *L. monocytogenes* by non-professional phagocytes, as *inlC* is strongly transcribed in the cytoplasm of phagocytic cells (Engelbrecht *et al.*, 1996), but its precise function is still unknown.

Once the bacteria have become internalised, several genes are responsible for the virulent phenotype observed by *L. monocytogenes*. The recognised virulence genes of *L. monocytogenes* are localised in a single chromosomal cluster (Portnoy *et al.*, 1992) which is flanked by two housekeeping genes, *prs* (phosphoribosyl synthetase) and *ldh* (lactate dehydrogenase) (Gouin *et al.*, 1994; Lampidis *et al.*, 1994). This gene cluster has been identified in all clinical isolates of *L. monocytogenes* tested,

and consists of six genes in the order, *prfA* (positive regulation factor A), *plcA* (phosphatidylinositol-specific phospholipase C), *hly* (listeriolysin), *mpl* (metalloproteases), *actA* (nucleator for polymerisation of F-actin) and *plcB* (phosphatidylcholine-specific phospholipase C) (for reviews see Portnoy *et al.*, 1992; Sheehan *et al.*, 1994; Kuhn and Goebel, 1995).

Upon uptake by epithelial cells the bacteria are located within a phagosomal vacuole and thus have to be released into the cytoplasm. Lysis of this phagosomal vacuole is essential for intracellular bacterial growth and virulence. It is mediated by a haemolysin, listeriolysin O (LLO), encoded by *hly*, and also involves a phosphatidylinositol-specific phospholipase C (PI-PLC) encoded by *plcA* (Camilli *et al.*, 1993). Once in the cytoplasm the bacteria divide. They are able to move within the cell and also spread to adjacent cells through a processes involving polymerisation of host cellular actin (reviewed by Tilney and Tilney, 1993; Cossart and Kocks, 1994). Another intracellular infection cycle then begins in the second infected cell. This direct cell to cell spread requires the *actA* gene product, a protein necessary for actin-based bacterial propulsion through the cell cytoplasm (Domann *et al.*, 1992; Kocks *et al.*, 1992), and a phosphatidylcholine-specific phospholipase C (PC-PLC), also called lecithinase (Vazquez-Boland *et al.*, 1992). The PC-PLC is encoded by the *plcB* gene, and this product lyses the double cell membrane which forms a barrier in cell to cell spread (Vazques-Boland *et al.*, 1992). The *mpl* gene encodes a metalloprotease that processes the immature form of PC-PLC into a mature form (Dorman *et al.*, 1991; Poyart *et al.*, 1993).

The transcription of these virulence genes is under the control of the transcriptional activator PrfA, illustrated in Figure 1.3.2.1. PrfA also activates the expression of other genes, including the *inlAB* locus (Leimeister-Wächter *et al.*, 1990; Mengaud *et al.*, 1991; Chakraborty *et al.*, 1992; Dramsi *et al.*, 1993) and the *inlC* gene (Engelbrecht *et al.*, 1996). PrfA mediated activation requires binding of PrfA at a conserved 14bp dyad-symmetric site in PrfA target promoters (PrfA box) (Freitag *et al.*, 1993; Sheehan *et al.*, 1995). It has been shown that activation by PrfA is more efficient at promoters that possess a perfectly symmetrical PrfA box than at

promoters which have one or two base pair substitutions in the PrfA box (Sheehan *et al.*, 1995). For examples, the activation of transcription by PrfA is most efficient at the divergently transcribed *hly* and *plcA* promoters, and is less efficient at the virulence gene promoters which have one (*actA*, *mpl*) or two (*inlA*) base pair substitutions relative to the consensus PrfA site (Sheehan *et al.*, 1996). It has been shown that PrfA can be transcribed from three different promoters, the *plcA* promoter and the P1 and P2 *prfA* specific promoters. Since PrfA activates transcription from the *plcA* promoter, it can positively regulate its own expression. This is illustrated in Figure 1.3.2.2.

Figure 1.3.2.1: Schematic representation of the virulence gene cluster activated by PrfA. Adapted from Renzoni *et al.*, 1997.

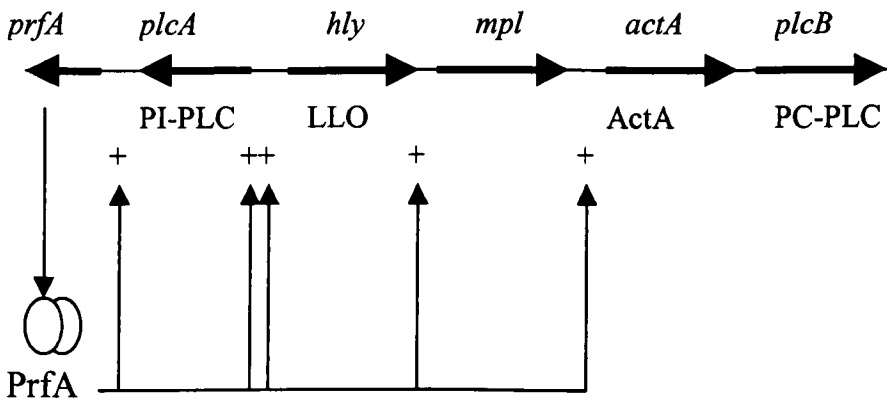
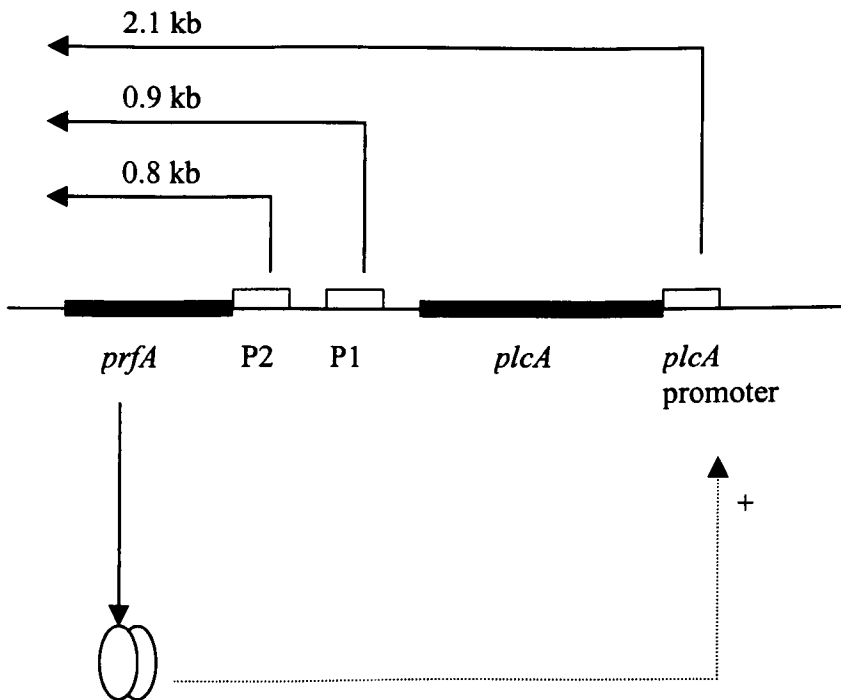


Figure 1.3.2.2: *prfA* gene transcription. Arrows indicate *prfA* transcripts produced from the *plcA* promoter and P1 and P2 promoters. Adapted from Renzoni *et al.*, 1997.



1.4. *Staphylococcus aureus*

1.4.1. Background

Members of the genus *Staphylococcus* are Gram positive cocci, approximately 0.5-1.5µm, that occur singly, in pairs, tetrads, short chains and irregular 'grape-like' clusters. They are non-motile and non-spore forming, and most species are facultative anaerobes, growing better under aerobic rather than anaerobic conditions.

Staphylococcus aureus is a pathogen with a broad host range and is a leading cause of infections in humans and domesticated animals worldwide. *S. aureus* has been implicated in a wide range of diseases ranging from superficial skin abscesses to a number of more serious diseases, including septicaemia, meningitis, endocarditis, osteomyelitis, septic arthritis, toxic-shock syndrome (TSS) and food poisoning (reviewed by Projan and Novick, 1997). The infections associated with this organism are extremely common and can be life threatening, therefore there is the potential for *S. aureus* to cause increased morbidity and mortality. *S. aureus* is also the leading cause of intramammary infections in ruminants, with approximately half the dairy cows in the United States affected with some form of mastitis. This accounts for around 70% of the total expenses for dairy farmers (Ferrow, 1980) and results in the loss of billions of dollars each year (Blosser, 1979).

1.4.2. Resistant Isolates of *S. aureus*

Staphylococci have a record of developing resistance quickly and successfully to antibiotics. This defensive response is a consequence of the acquisition and transfer of antibiotic resistant plasmids and the possession of intrinsic resistance mechanisms, which may have evolved. The acquired defence systems by staphylococci may have originated from antibiotic-producing organisms, where they may have been

developed and then passed on to other genera. It is presumed that the genus *Staphylococcus* has been one of the recipient genera as a consequence of coming into contact with antibiotic producing bacteria and fungi in their natural habitat (Kloos *et al.*, 1981).

As *S. aureus* is able to cause a wide range of often fatal diseases, the increasing emergence of antibiotic resistant isolates is causing considerable alarm within the medical community (Bayles *et al.*, 1998). The appearance of methicillin-resistant *S. aureus* (MRSA) strains and also the recent emergence of *S. aureus* isolates that show an intermediate level of resistance to vancomycin (VRSA) compound this threat.

The recent increase in antibiotic resistance and a lack of potential vaccine candidates have highlighted the importance of finding new approaches to control this pathogen and prevent staphylococcal disease. In order to develop novel antimicrobial agents that are based on global regulatory networks it is necessary to understand the genetic basis behind expression of virulence factors in *S. aureus*. Such an agent would help preclude the use of antibiotics, which may decrease the rate of development of drug resistant strains of bacteria.

1.4.3. The Regulation of *S. aureus* pathogenicity

In *S. aureus*, many exoproteins are synthesised and secreted at the end of exponential growth under the control of several global regulatory loci, one of which is known as the accessory gene regulator, *agr* (Recsei *et al.*, 1986; Morfeldt *et al.*, 1988; Peng *et al.*, 1988). The importance of the *agr* system is supported by *in vivo* studies, which show that *agr* mutants are greatly attenuated with regards to virulence in several animal models tested, including mammary infections (Foster *et al.*, 1990), arthritis (Abdelinour *et al.*, 1993), subcutaneous abscesses in mice (Brag *et al.*, 1992) and endocarditis in rabbits (Cheung *et al.*, 1994). The proposed function of this regulatory system is to enhance the production of cell wall associated attachment and

potential defensive factors during attachment during the early stages of infection, followed by the expression of invasive factors (hemolysins, proteases etc) once the infection has become established. Another important regulator of virulence determinant production in *S. aureus* is the staphylococcal accessory regulator, encoded by *sarA* and will be discussed further on.

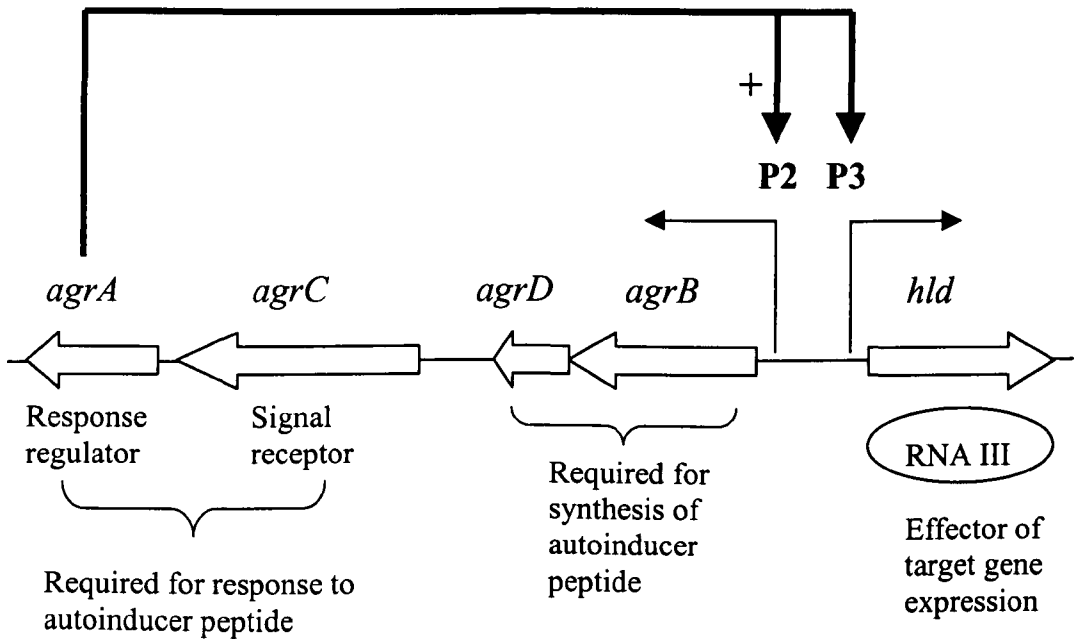
1.4.3.1. The *agr* Regulatory System

The *agr* locus is complex and consists of two divergent transcriptional units using two promoters, P2 and P3. The P2 operon contains four genes, *agrB*, *agrD*, *agrC* and *agrA*, all of which are required for the activation of the *agr* system (Novick *et al.*, 1995). The primary function of this operon is to activate the two major *agr* promoters, P2 and P3 (Lofdahl *et al.*, 1988; Peng *et al.*, 1988; Kornblum *et al.*, 1990). However, the actual effector of *agr*-dependent exoprotein gene regulation is the P3 transcript RNA III (Janzon and Arvidson, 1990; Kornblum *et al.*, 1990; Novick *et al.*, 1993). RNA III up-regulates transcription of the secretory protein genes and down-regulates transcription of the surface protein genes by an unknown mechanism that possibly involves proteins encoded by genes outside the *agr* locus (Novick and Muir, 1999). The *agr* locus is shown schematically in Figure 1.4.3.1.

The genes *agrC* and *agrA* code for a classical two-component signal transduction pathway (Nixon *et al.*, 1986), where AgrC corresponds to the signal receptor and AgrA to the response regulator (Kornblum *et al.*, 1990, Novick *et al.*, 1995; Morfeldt *et al.*, 1996a). The other two genes *agrB* and *agrD* combine to produce an autoinducer peptide. It was demonstrated that addition of this peptide to early exponential cultures of the producing strain caused the immediate activation of transcription from the two *agr* promoters (Ji *et al.*, 1995). Both *agrB* and *agrD* are necessary to form functional autoinducer peptide, it is thought that *agrB* encodes a protein that is necessary for processing of the autoinducer (Ji *et al.*, 1995).

Before bacteria enter stationary phase, the P2 operon is transcribed at low levels and the autoinducer peptide is produced by modification of the agrD peptide by the membrane protein AgrB. The mature autoinducer peptides contain a thiolactone structure and this feature is necessary for full biological activity (Ji *et al.*, 1997; Mayville *et al.*, 1999). At this point in the bacteria the production of cell wall associated pheromone proteins (fibronectin and collagen binding proteins) and of potential defensive factors (protein A) is maximal *in vitro* (Novick *et al.*, 1993). Under undefined environmental conditions such as high cell density, the resultant autoinducer peptide is thought to bind to the transmembrane receptor AgrC. AgrC is a transmembrane histidine protein kinase with five transmembrane helices (Ji *et al.*, 1995; Lina *et al.*, 1998). The ligand binding site is known to be located in the 16-18 aminoacyl residues of the final extracellular loop of AgrC (Lina *et al.*, 1998). Binding of the autoinducing peptide triggers a two-component signal transduction event in which the AgrC receptor becomes autophosphorylated on a histidine residue (Lina *et al.* 1998). This phosphate residue is then transferred to an aspartate residue in the N-terminal region of the AgrA response regulator (Morfeldt *et al.*, 1996a), this leads to an allosteric shift in its C-terminal domain. The phosphorylated AgrA is assumed to then activate transcription from both P2 and P3 *agr* promoters (Lina *et al.*, 1998). Therefore the primary role of the *AgrAC* signalling pathway is to upregulate both major *agr* promoters, P2 and P3, which is done in conjunction with a second transcription factor SarA (Cheung *et al.*, 1992; Morfeldt *et al.*, 1996b). The subsequent RNA III transcript from the P3 promoter acts as the effector of the *agr* system and is responsible for the upregulation of secreted virulence factors as well as the down regulation of surface proteins (Novick *et al.*, 1993; Morfeldt *et al.*, 1995). RNA III also encodes the *agr*-regulated δ -hemolysin (*hld*) (Janzon *et al.*, 1989) which has no significant role in the regulation of other *S. aureus* virulence genes (Arvidson *et al.*, 1989). AgrA also activates P2 which leads to the synthesis of more autoinducer peptide and hence further activation of the *AgrAC* signalling pathway, this causes a rapid burst of autoinducer peptide synthesis as well as a rapid response of RNA III (Ji *et al.*, 1995).

Figure 1.4.3.1: Genetic regulation of the *agr* system (adapted from Novick and Muir, 1999). Diagram illustrates the autoinduction of the P3 regulon



1.4.3.2. The *Sar* Regulatory System

The *sar* operon was first identified by Cheung *et al.* (1992) in a Tn917 screen for fibrinogen binding protein deficient mutants (Cheung *et al.*, 1992). The inactivated locus was found to affect exoprotein and surface protein expression (Cheung *et al.*, 1992). The *sar* operon consists of three overlapping transcripts initiated from a triple promoter system, P1, P2 and P3 (Projan and Novick, 1997). Transcriptional and binding studies have shown that the SarA protein binds to both P2 and P3 of the *agr* locus, increasing levels of both RNA II and RNA III, hence altering the synthesis of virulence factors (Heinrichs *et al.*, 1996; Morfeldt *et al.*, 1996; Cheung *et al.*, 1997).

The mechanism by which *S. aureus* controls virulence determinant gene expression is therefore complex, involving an interactive, hierarchical regulatory cascade between the products of the *sar* and *agr* loci and possibly other components.

1.4.4. Grouping of *S. aureus* strains

S. aureus uses a global regulator, *agr*, which is activated by secreted autoinducer peptides, to control expression of most virulence genes. The majority of *S. aureus* and other staphylococci produce and secrete a soluble inducer of RNA III transcription, however between *S. aureus* strains and staphylococcal species the interaction is inhibitory. That is to say that the autoinducer peptide produced by one strain or species inhibits the activation of RNA III transcription in most others (Ji *et al.*, 1997). This inhibition constitutes a novel form of bacterial interference, as it involves inhibition of a specific group of genes rather than inhibiting bacterial growth (Ji *et al.*, 1997). On this basis *S. aureus* strains have been divided into three major groups, named I to III. Each of the secreted autoinducer peptide molecules can activate the *agr* response in members within the same group and inhibit the *agr* response in strains belonging to other groups (Ji *et al.*, 1997). The structure of the autoinducer peptides from *S. aureus* groups I to III are show in Figure 1.4.4a and b.

Figure 1.4.4a: The sequence of *agrD* (Taken from Novick, 1999). Diagram illustrates an amino acid sequence alignment of *agrD* from different *S. aureus* groups

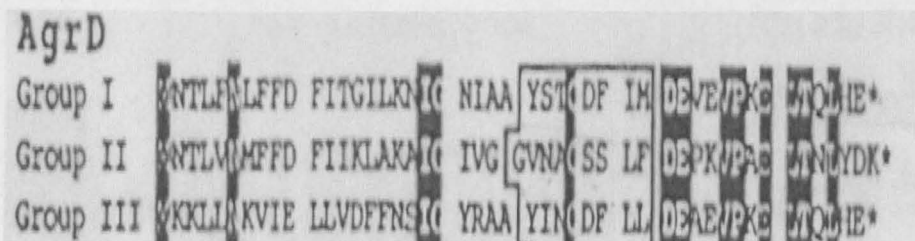
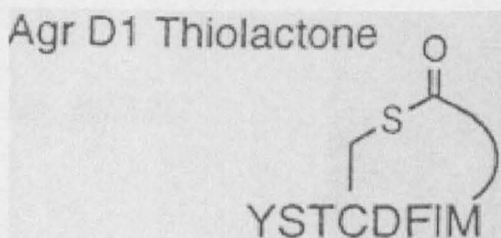


Figure 1.4.4.b: The chemical structure of the group I autoinducer peptide (Taken from Mayville *et al.*, 1999)



Mayville *et al.* (1999) showed that synthetic group II autoinducer peptides were able to inhibit the *agr* response from other groups. The experiments also revealed a dose-dependent relationship between the amount of autoinducer added to the bacterial culture supernatant and the degree of activation or inhibition of the *agr* response (Mayville *et al.*, 1999). This critical threshold concentration of autoinducer which was required for activation of the *agr* response, was consistent with the autoinduction mechanism previously proposed (Novick *et al.*, 1995). It has also been demonstrated that a reactive thiol ester bond was necessary for activation of the *agr* response but not for inhibition, and a cyclic structure present within the autoinducer peptides was necessary for all biological activity (Mayville *et al.*, 1999). The fact that it is possible to inhibit but not activate the *agr* response is very significant in terms of exploiting the *agr* response as a route to novel therapeutics for *S. aureus* infections.

1.4.5. *S. aureus* as an intracellular pathogen: influence of *agr*

S. aureus is primarily known as an extracellular pathogen, however Hamill *et al.* (1986) showed that *S. aureus* was able to internalise and survive within non-professional phagocytes such as bovine aortic endothelial cells (Hamill *et al.*, 1986). Subsequent to this, several other reports confirmed that *S. aureus* was able to internalise and survive in a wide variety of mammalian cells (Vann and Proctor, 1987; Hudson *et al.*, 1995; Almeida *et al.*, 1996; Bayles *et al.*, 1998). From these results it was proposed that the intracellular survival of *S. aureus* plays an important role in staphylococcal persistence and chronic staphylococcal disease (Vann and Proctor, 1987; Hudson *et al.*, 1995; Bayles *et al.*, 1998).

Wesson *et al.* (1998) proposed a model for the function of *agr*-mediated quorum sensing in staphylococcal disease. In that model extracellular *S. aureus* express cell surface-associated proteins, such as fibronectin- or collagen binding protein, due to the dilution of the autoinducer peptide molecule in the surrounding fluids. This results in the bacteria being in a physical state which is optimal for binding to cell surfaces and subsequent internalisation. Once the bacteria become internalised they

are quickly surrounded by an endosomal membrane (Hudson *et al.*, 1995; Bayles *et al.*, 1998). The presence of this endosomal membrane means that the bacteria are now confined in a small space, the autoinducer peptide can now rapidly accumulate and triggers expression of *agr* and its up-regulated exoproteins. Some of the exoproteins (particularly the hemolysins) could play a role in escape from the endosome. Bayles *et al.* (1998) showed that shortly after internalisation, *S. aureus* was able to escape from the endosome *via* a process that resulted in lysis of the endosomal membrane. Once the bacteria have escaped from the endosome, the autoinducer peptide would become diluted resulting in a shift away from exoprotein expression. This would lead to bacteria that were adapted to survive and grow within the cytoplasm.

Once the bacteria are in the cytoplasm, Wesson *et al.* (1998) have proposed three possible outcomes. The first pathway would lead to the production of an Agr-regulated factor that triggers the induction of apoptosis, and the resulting apoptotic bodies would then be engulfed by macrophages. The engulfment of these membrane bound bacteria could provide a protective environment for *S. aureus* against host defence systems and also drugs, which would allow the bacteria to persist and spread to adjacent cells. Another alternative is that metabolically inactive small colony variant (SCVs) would be formed (Proctor *et al.*, 1994). These SCVs cause little damage to the host cell but lead to a more chronic and persistent disease (Proctor *et al.*, 1994). The final outcome is that if the bacteria can accumulate to a high concentration within the cytoplasm, autoinducer peptide levels could reach a level sufficient to promote expression of exoproteins through the *agr*-response. The production of exoproteins, such as hemolysin, would result in lysis of the host cell. This would provide a route for dissemination to distant sites where potential metastatic infections may occur, for example abscess formation or a more progressive and invasive disease. Entry into this final pathway depends on the ability of *S. aureus* to replicate in the host. According to this model, any inhibition of growth in the cytoplasm reduced the accumulation of the autoinducer peptide and hence delays lysis of the host cell. Thus the commitment to advance towards a more progressive infection is made within the cytoplasm and could be based on the immunological status of the host.

CHAPTER 2

MATERIALS AND METHODS

CHAPTER 2: MATERIALS AND METHODS

2.1. Bacterial Strains and Plasmids used.

The bacterial strains and plasmids used or constructed in this study are listed in Table 2.1.1 and Table 2.1.2.

Table 2.1.1: Bacterial strains used during the course of this study

STRAIN	GENOTYPE	REFERENCE / SOURCE
<i>E. coli</i> JM109	$\Delta(lac-proAB)$, <i>recA1</i> , <i>endA1</i> , <i>gyrA9b</i> , <i>thi</i> , <i>hsdR17</i> , <i>supE44</i> , <i>relA1</i> , F' [<i>traD36</i> , <i>proAB</i> , <i>lacI^f</i> , <i>lacZ</i> $\Delta M15$]	Culture Collection Yanisch-Perron (1985)
<i>E. coli</i> JM110	<i>rpsL</i> , <i>thr</i> , <i>leu</i> , <i>thi</i> , <i>lacY</i> , <i>galK</i> , <i>galT</i> , <i>dam</i> , <i>dcm</i> , <i>ara</i> , <i>tonA</i> , <i>relA1</i> , λ^- , (<i>lac-</i> <i>proAB</i>), [F' <i>traD36</i> , <i>proAB</i> , <i>lacI^fZ</i> $\Delta M15$]	Culture Collection Yanisch-Perron (1985)
<i>L. monocytogenes</i> NCTC 7973	Wild type Serotype1/ 2a	NCTC
<i>B. megaterium</i> NCTC 10342	Wild type	Culture Collection at Sutton Bonington
<i>B. subtilis</i> 168	<i>trpC2</i> mutant	Bron and Venema (1972)
<i>S. aureus</i> RN4220	restriction deficient <i>agr</i> mutant, derivative of 8325-4	Kreiswirth <i>et al.</i> (1983)
<i>S. aureus</i> 8325-4	Derivative of the prototypic NCTC 8325 laboratory strain, cured of prophages and plasmids	Novick (1967)

Table 2.1.1: cont.

<i>S. epidermidis</i> 570	Wild type	Clinical isolate provided by Roger Finch, City Hospital, Nottingham
---------------------------	-----------	---

NCTC = National Culture Type Collection

Table 2.1.2: Plasmids used in this study

Plasmid	Relevant Features	Source or Reference
pMK4	Gram positive shuttle vector, Ap ^R , Cm ^R	Sullivan <i>et al.</i> (1984)
pGC4	pMK4 derivative; 8.2kb plasmid, contains <i>luxAB</i> fusion from <i>V. harveyi</i> expressed from P _{<i>xyn</i>} , Ap ^R and Cm ^R	Dr. C. Rees unpublished
pSL1190	Superlinker plasmid, contains 64 restriction sites, Amp ^R	Pharmacia
pBluelux	<i>luxCDABE</i> inserted into <i>Sma</i> I site of pBluescript IKS, Amp ^R	Dr. J. Throup Unpublished data
pHG327	Based on pHG165, contains pUC18 multi cloning site, Amp ^R	Stewart <i>et al.</i> (1986)
pSB354	Based on pHPS9, contains <i>luxAB</i> fusion with <i>rrnB</i> terminator inserted downstream, Em ^R , Cm ^R	Hill <i>et al.</i> (1994)
pJBA33	Contains the red shifted <i>gfp</i> variant <i>gfp3</i> , Amp ^R , Km ^R	Kindly provided by Dr. J. Anderson (Denmark)
pJBA41	pUC19-Not1 based expression plasmid, contains <i>gfp3</i> (LAA)	Kindly provided by Dr. J. Anderson (Denmark)
pJBA46	pUC19-Not1 based expression plasmid, contains <i>gfp3</i> (ASV)	Kindly provided by Dr. J. Anderson (Denmark)
pJBA47	pUC19-Not1 based expression plasmid, contains <i>gfp3</i> (AGA)	Kindly provided by Dr. J. Anderson (Denmark)

Table 2.1.2: cont.

pGFP	Contains wild type <i>gfp</i> from <i>A. victoria</i>	Clontech
pEGFP	Contains <i>gfp3</i> gene modified for expression in eukaryotes (EGFP)	Clontech
pSB2002	pGC4 carrying <i>gfp3</i> , amplified by PCR from pJBA33, inserted into <i>SmaI</i> / <i>SaII</i> restriction sites, Ap ^R , Cm ^R	This study
pSB2003	pGC4 derivative containing <i>gfp</i> wild type, amplified by PCR from pGFP1 (Clontech) inserted into <i>SmaI</i> / <i>SaII</i> restriction sites, Ap ^R , Cm ^R	This study
pSB2004	<i>rrnB</i> terminator excised from pSB354, inserted downstream of <i>gfp3</i> into <i>SaII</i> site of pSB2002	This study
pSB2005	<i>rrnB</i> terminator excised from pSB354, inserted downstream of <i>gfp3</i> into <i>SaII</i> site of pSB2003, Ap ^R , Cm ^R	This study
pSB2006	<i>gfp3</i> (LAA) amplified by PCR and inserted into <i>SmaI</i> / <i>SaII</i> restriction sites of pGC4, Ap ^R , Cm ^R	This study
pSB2007	<i>gfp3</i> (ASV) amplified by PCR and inserted into <i>SmaI</i> / <i>SaII</i> restriction sites of pGC4, Ap ^R , Cm ^R	This study

Table 2.1.2: cont.

pSB2008	<i>gfp3</i> (AGA) amplified by PCR and inserted into <i>SmaI</i> / <i>SaII</i> restriction sites of pGC4, Ap ^R , Cm ^R	This study
pSB2009	<i>gfp3</i> amplified by PCR from pJBA33, protein engineered to contain a poor Gram positive RBS, Ap ^R , Cm ^R	This study
pSB2010	<i>xylR</i> P _{<i>xylA</i>} fragment amplified by PCR from <i>B. megaterium</i> NCTC 10342, restricted <i>MunI</i> / <i>SmaI</i> and inserted into <i>EcoRI</i> / <i>SmaI</i> site of pGC4	This study
pSB2011	<i>luxAB</i> excised from pSB2010 and replaced with <i>gfpwt</i> gene from pSB2003, Ap ^R , Cm ^R	This study
pSB2012	<i>luxAB</i> excised from pSB2010 and replaced with <i>gfp3</i> gene from pSB2002, Ap ^R , Cm ^R	This study
pSB2013	Potential stall site removed from the 5' coding region of <i>gfp3</i> and replaced with corresponding sequence from <i>egfp</i> , PCR product cloned into <i>SmaI</i> / <i>SaII</i> sites of pGC4, Ap ^R , Cm ^R	This study

Table 2.1.2: cont.

pSB2014	<i>P_{xyn}</i> promoter excised from pSB2013 as <i>EcoRI/ SmaI</i> fragment and replaced with <i>xylR P_{xylA}</i> from <i>B. megaterium</i> <i>MunI/ SmaI</i> , Ap ^R , Cm ^R	This study
pSB2015	<i>egfp</i> amplified from pEGFP by PCR, cloned into pGC4 <i>SmaI/ SalI</i> , Ap ^R , Cm ^R	This study
pSB2016	<i>P_{xyn}</i> promoter excised from pSB2015 as <i>EcoRI/ SmaI</i> fragment and replaced with <i>xylR P_{xylA}</i> from <i>B. megaterium</i> <i>MunI/ SmaI</i> , Ap ^R , Cm ^R	This study
pSB2017	Translationally enhanced <i>gfp3</i> amplified by PCR from pJBA33, inserted <i>SmaI/ SalI</i> sites of pGC4, Ap ^R , Cm ^R	This study
pSB2018	Translationally enhanced <i>gfp3</i> amplified by PCR from pJBA33, inserted into <i>SmaI/ SalI</i> sites of pSB2010 following excision of <i>luxAB</i> , Ap ^R , Cm ^R	This study
pSB2019	<i>P_{xylA}-gfp3opt</i> fragment excised from pSB2018 <i>EcoRI/ SalI</i> , and inserted into pGC4 restricted with <i>EcoRI/ SalI</i> , Ap ^R , Cm ^R	This study

Table 2.1.2: cont.

pSB2020	Translationally enhanced <i>gfp3</i> AGA amplified by PCR from pJBA47, inserted into <i>SmaI/ SalI</i> restriction sites of pSB2010, Ap ^R , Cm ^R	This study
pSB2021	Translationally enhanced <i>gfp3</i> ASV amplified by PCR from pJBA46, inserted into <i>SmaI/ SalI</i> restriction sites of pSB2010, Ap ^R , Cm ^R	This study
pSB2022	<i>luxCDABE</i> fragment excised from pBluelux and inserted into <i>SmaI/ SalI</i> sites of pGC4, Ap ^R , Cm ^R	This study
pSB2023	Translationally enhanced <i>luxAB</i> inserted into MCS of pHG327 Ap ^R	This study
pSB2024	Translationally enhanced <i>luxCDE</i> inserted downstream of <i>luxAB</i> in pSB2023 Ap ^R	This study
pSB2025	<i>luxABCDE</i> operon excised from pSB2024 and ligated with pSL1190 Ap ^R	This study

Table 2.1.2: cont.

pSB2026	<i>luxABCDE</i> excised from pSB2025 and inserted into <i>SmaI/ SalI</i> restriction sites of pSB210, Ap ^R , Cm ^R	This study
pSB2027	P _{<i>xyIA</i>} - <i>luxABCDE</i> inserted into <i>SmaI/ SalI</i> sites of pGC4, Ap ^R , Cm ^R	This study
pSB2028	<i>rrnB</i> terminator amplified from JM109, restricted <i>NsiI/ PstI</i> and inserted into <i>PstI</i> site in pSB2027, Ap ^R , Cm ^R	This study
pSB2029	P _{<i>xyIA</i>} - <i>gfp3opt</i> excised from pSB2018 with <i>SalI</i> and inserted into <i>SalI</i> site of pSL1190, Ap ^R	
pSB2030	P _{<i>xyIA</i>} - <i>gfp3opt-luxABCDE</i> excised from pSB2029 <i>EcoRI/ PstI</i> and inserted into <i>EcoRI/ PstI</i> of pGC4, Ap ^R , Cm ^R	This study
pSB2031	P _{<i>xyA</i>} excised from pSB2017 and replaced with P3 promoter amplified by PCR from <i>S. aureus</i> 8325-4, Ap ^R , Cm ^R	This study (Neil Dickinson performed cloning)
pSB2032	<i>gfp3opt</i> gene excised from pSB2031 with <i>SmaI/ PstI</i> and replaced with <i>luxABCDE</i> from pSB2025, Ap ^R , Cm ^R	This study

Table 2.1.2: cont.

pSB2033	<i>gfp3opt</i> excised from pSB2033 <i>SmaI</i> / <i>SalI</i> and replaced with translationally optimised <i>gfp3</i> LAA amplified by PCR from pJBA41, Ap ^R , Cm ^R	This study (Emillie Council performed cloning)
pSB2034	<i>gfp3opt</i> excised from pSB2033 <i>SmaI</i> / <i>SalI</i> and replaced with translationally optimised <i>gfp3</i> ASV amplified by PCR from pJBA46, Ap ^R , Cm ^R	This study (Emillie Council performed cloning)

2.2. Solutions utilised

2.2.1. Media

The media used, their abbreviations and reference/source are shown below:

LB : Luria-Bertani Medium, modified to 4g l^{-1} NaCl, Sambrook *et al.* (1989)

LA : LB plus 15g l^{-1} agar number 1 (Oxoid)

BHI : Brain Heart Infusion (Oxoid)

BHI agar : BHI plus 15g l^{-1} agar number 1 (Oxoid)

Blood agar : BHI + 5% defibrinated sheep blood (Oxoid)

BM : Basic Medium, 10g l^{-1} Peptone, 5g l^{-1} Yeast extract, 1g l^{-1} Glucose, 5g l^{-1} NaCl, 1g l^{-1} K_2HPO_4

BM agar : BM plus 15g l^{-1} agar number 1 (Oxoid)

All media was sterilised by autoclaving at 15 psi for 20 min.

2.2.2. Antibiotics and Supplements

Any supplements used, their abbreviations, source and working concentrations are given below:

Ampicillin (Amp); (Sigma): $50\mu\text{g ml}^{-1}$

Chloramphenicol (Cm); (Sigma): $30\mu\text{g ml}^{-1}$ for Gram negative organisms
 $7\mu\text{g ml}^{-1}$ for Gram positive organisms

Xylose (Xyl); (Sigma): added to media at a concentration of 0.5%

IPTG (Isopropyl- β -D-thiogalactopyranoside) 0.5mM

2.3. Growth of bacterial cultures

Cultures were grown aerobically at 37°C; liquid cultures were shaken at 200rpm. Liquid *E. coli* cultures were grown in LB and plated cultures on LA, *B. subtilis* 168 and *B. megaterium* NCTC 10342 were grown in the same manner. *L. monocytogenes* strains were grown in BHI broth or on BHI agar plates. *S. aureus* and *S. epidermidis* 570 were grown routinely in BM media or on BM agar plates. Stock strains were kept as 15% (v/v) glycerol in LB or BHI, depending on the organism, at -20°C and -80°C.

2.4. Monitoring Growth of Bacterial Cultures

Growth of aerobically grown cultures was monitored by optical density readings at 600nm (unless otherwise stated) on a Cecil 2000 series spectrophotometer.

2.5. Preparation, Manipulation and Analysis of DNA

2.5.1. Determination of DNA concentrations

The concentration of DNA in samples was determined using a GeneQuant (Pharmacia Biotech).

2.5.2. Preparation of Plasmid DNA

Plasmid DNA was prepared by plasmid miniprep using the alkaline lysis method as described in Sambrook *et al.* (1989). Large scale preparation of plasmid DNA was carried out using Qiagen 500 maxiprep kits or Qiagen 100 midi kits according to the manufactures instructions (Qiagen GmbH).

2.5.3. Amplification of DNA using Polymerase Chain Reaction (PCR)

Polymerase chain reaction (PCR) originally described by Saiki *et al.* (1988) was used for the amplification of specific regions of DNA. PCR was performed using 1U per 50 μ l reaction of *Taq* DNA Polymerase (Advanced Biotechnologies Ltd), 2mM MgCl₂, 1xBufferIV (200mM (NH₄)₂SO₄, 750mM Tris-HCl pH9.0, 0.1% Tween), each dNTP (Pharmacia) was added at a final concentration of 200 μ M (16 μ l of 625 μ M stock dNTP solution). Oligonucleotides were supplied by Genosys Biotechnologies (Europe) Ltd. The dried oligonucleotides were resuspended in sterile water to a final concentration of 1 μ g μ l⁻¹, 1 μ g primers were then added to each reaction. *Taq* DNA polymerase was added to the reaction after a 5 min hot start at 95°C. A typical run involved 30 cycles of template denaturation at 95°C for 30 sec, followed by annealing of primers to template at the required temperature for the specified time (generally 1 min per kb DNA), followed by extension at 72°C (again 1 min per kb DNA). The run was finished with an extension at 72°C for 5 min to ensure all strands were completed. The temperatures and primers used are detailed in the relevant Results sections.

2.5.4. Cleavage of DNA with restriction enzymes

Plasmid DNA was digested with restriction enzymes obtained from Pharmacia and Boehringer Mannheim and used according to the manufactures instructions. RnaseA (1mgml⁻¹; Sigma) was prepared according to details described in Sambrook *et al.* (1989) and used in digestions when necessary. Typically, 1 μ l of the RnaseA stock was used in a total digest of 20 μ l, and incubated with the DNA for the duration of the digest.

2.5.5. Agarose gel Electrophoresis

Plasmids, DNA restriction fragments and PCR products were analysed by agarose gel electrophoresis according to Sambrook *et al.* (1989). Molecular weight markers were loaded onto the gel in order to determine fragment length. Markers used were $0.5\mu\text{gml}^{-1}$ of λ *Hind*III (MBI Fermentas) and 100 base pair ladder (Pharmacia). All samples and markers were loaded onto the gel using 5xDNA loading buffer (10xTAE, 20% (w/v) Glycerol, 0.05% Bromophenol Blue). Depending on size of fragment expected, agarose gels between 0.8-1.5% were prepared in 1xTAE buffer (80mM Tris-acetate pH 7.8, 19mM EDTA) plus $0.5\mu\text{gml}^{-1}$ ethidium bromide (Sigma), and electrophoresis performed using 1xTAE buffer in horizontal tanks (Anachem) at 50-90V for the required length of time. DNA fragments then visualised using a UV transilluminator (UVP).

2.5.6. Phenol Chloroform extraction of DNA

This procedure was performed in order to purify restricted DNA prior to cloning. The restriction digest was made up to a 200 μl volume using sterile distilled water. An equal volume of Phenol: Chloroform: Isoamylalcohol (mixed in the ratio 25:24:1) was added to the DNA and mixed by inversion. This was centrifuged at 13,000 rpm for 5min in a Biofuge 13 microcentrifuge (Heraeus Sepatech). The upper aqueous phase was removed into a clean eppendorf, an equal volume of Chloroform : Isoamylalcohol (ratio 24:1) was then added to this. This was then mixed and centrifuged as before. Following the removal of the upper aqueous phase into a new eppendorf, 1/10 volume 3M sodium acetate and 2 volumes absolute ethanol were added, this was then incubated at -20°C for at least 1 hour in order to precipitate the DNA. DNA was recovered by centrifugation at 13,000 rpm for 20 min in a Biofuge 13 microcentrifuge (Heraeus Sepatech). The DNA pellet was washed in 70% ethanol, dried and resuspended in an appropriate volume TE buffer.

2.5.7. Purification of DNA from a Low melting point agarose gel

If a DNA fragment was to be purified, e.g. restricted DNA or PCR products, electrophoresis was performed using SeaPlaque low melting point agarose (FMC Bioproducts) at 50V. DNA was isolated *via* the freeze-thaw extraction method described by Qian and Wilkinson (1991). This involved excision of the fragment from the gel into an eppendorf, followed by the addition of three volumes of 1xTE buffer (10mM Tris-HCl pH7.9, 1mM EDTA) to the gel slice. This was heated to 70°C for 10 min in an Intelligent Heating Block (Hybaid), frozen in liquid nitrogen for 10 min, defrosted and then centrifuged in a Biofuge 13 microcentrifuge (Heraeus Sepatech) at 13,000rpm for 10 min and the agarose free supernatant removed. DNA was precipitated by the addition of 1/10th volume 3M Na-acetate pH 4.8 and 2 volumes of 100% ethanol. After incubation at -20°C for at least one hour the DNA was recovered by centrifugation at 13,000rpm for 20 min in a Biofuge 13 microcentrifuge (Heraeus Sepatech). The resulting pellet was washed in 70% ethanol and then dried at 37°C. DNA was then resuspended in 10µl 1xTE buffer.

2.5.8. Ligation of DNA fragments

T4 DNA ligase was used to catalyse the ligation of DNA ends by forming a phosphodiester bond between the 3'-OH group and one of the 5'-phosphate groups of another end (Weiss *et al.*, 1968). Ligations of DNA into a suitable vector were performed essentially as described in the Promega Protocols and Applications Guide (Promega). Ligations were set up in a reaction volume of 10µl. The molar ratio of fragment: vector used was typically 7: 1, using 1U T4 DNA ligase (1Uµl⁻¹, Promega) and 1x ligase buffer (Promega). Ligations were incubated at 18°C overnight.

2.5.9. Bacterial Transformation

Competent *E. coli* electroporation cells were prepared according to the protocol described by Ausubel *et al.* (1994); *Listeria monocytogenes* cells were transformed as described by Park *et al.* (1990). Competent *Bacillus subtilis* 168 were transformed by the method of by the method of Boylan *et al.* (1972). Competent *S. aureus* and *S. epidermidis* strains were made and transformed according the method of Augustin and Gotz (1990).

Prior to electroporation of all bacterial strains, the DNA that was to be introduced into the cells was dialysed to remove excess salt. Dialysis was achieved by pipetting the DNA onto a 0.025 μ m dialysis filter (Millipore), which was floating on distilled water, for 15 min at room temperature. The DNA was added to a 40 μ l aliquot of competent cells. The cell solution was mixed and then transferred to a 0.2cm electroporation cuvette (BioRad). The cuvette was then placed in an ice cold safety chamber slide and for *E. coli*, *S. aureus* and *S. epidermidis*, a pulse of 2.5 μ F, 2.5kV + 200 Ω was delivered using a BioRad gene pulsar™ electroporator. After the pulse 1ml of sterile LB was added to *E. coli* cells, for staphylococcal species 1ml of SMMP50 (SMM buffer [1M sucrose, 0.4M Maleic acid, 0.04M MgCl, final pH 6.5], 7% Penassay broth (Antibiotic Media number 1, Oxoid) 10% BSA in the ratio 55:40:5) was added to the transformed cells. Following the addition of 1ml fresh medium, *E. coli* cells were incubated at 37°C (static) for 1 hour before being plated onto antibiotic selective agar plates to isolate cells containing recombinant DNA. Transformed staphylococci were incubated with 1ml SMMP50 at 37°C, shaking at 200rpm for 90 minutes. Cells were then plated onto selective agar plates in order to isolated cells containing recombinant DNA.

For *L. monocytogenes* cells the voltage was changed to 2.0kV and competent cells electroporated in the same way. After the pulse, 1ml of sterile broth, BHI+0.5% sucrose was added to the transformed *L. monocytogenes* in the cuvette, the contents

were mixed by gentle pipetting and then incubated at 37°C (static) for 1 hour. Cells were then plated onto antibiotic selective agar to isolate cells containing recombinant DNA.

Recombinant colonies of both *E. coli* and *B.subtilis* were obtained using selective LA plates, *L. monocytogenes* transformants were isolated using selective BHI agar plates. Recombinant staphylococcal species were isolated following selection on antibiotic selective BM agar plates. All plates were incubated at 37°C for 1-2 days depending on the cells that had been transformed.

2.6. Microscopy

Bacterial cells harbouring GFP expression vectors were examined by epifluorescent microscopy using a Zeiss TV100 inverted microscope (Carl Zeiss Ltd).

2.6.1. Properties of Fluorescent Signals and Filters Used

GFP wild type:	Excitation maximum	395nm
	Emission maximum	509nm
	Filter block used	#2 (Carl Zeiss Ltd)
EGFP / GFP mut3	excitation maximum	~488nm
	Emission maximum	509nm
	Filter block used	#9 (Carl Zeiss Ltd)

2.7. Analysis of RNA by Northern Hybridisation

2.7.1. mRNA Isolation from *Listeria monocytogenes*

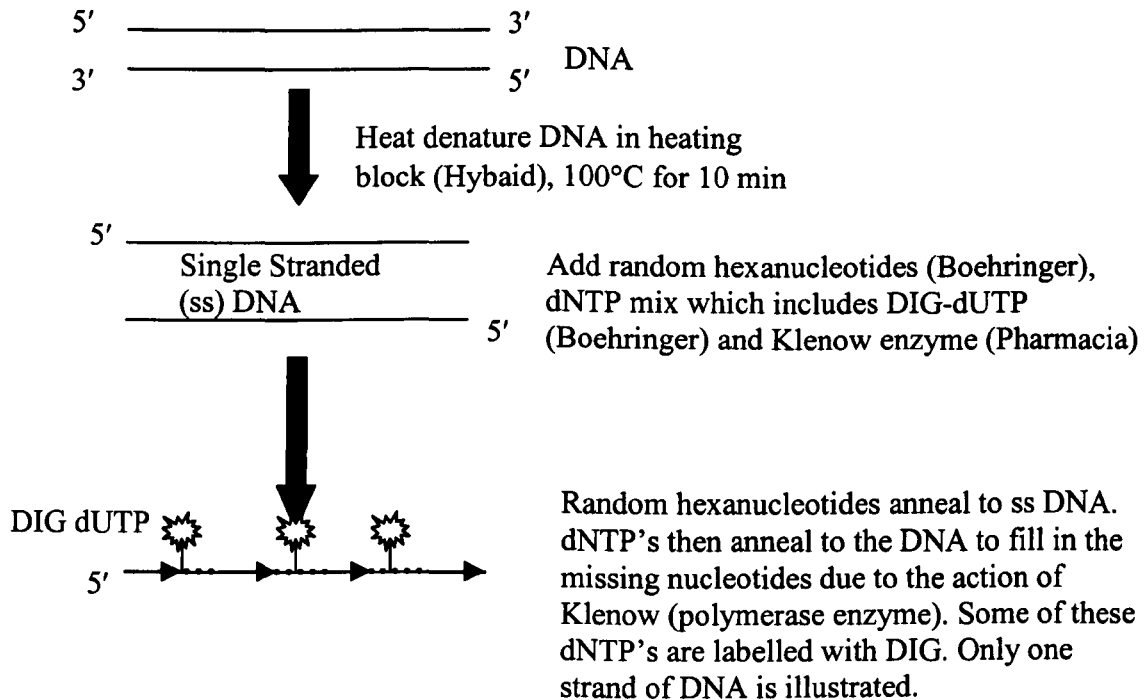
Bacterial RNA was isolated by the method described with Trizol LS Reagent (Gibco BRL). 10ml BHI was inoculated with *L. monocytogenes* culture, incubated overnight at 37°C in a shaking incubator. The culture was then diluted 1: 50 in 100ml fresh pre-warmed media and incubated at 37°C in a shaking incubator until OD₆₀₀ = 0.5-0.6. 10ml samples were taken and rifampicin added to a final concentration of 150µgml⁻¹. Samples were then centrifuged at 1560g for 10 min at room temperature and the supernatant was then removed. The bacterial pellet was resuspended in 1ml Trizol LS Reagent (Gibco BRL) and incubated for 5 min at room temperature. After adding 260µl chloroform, the sample was shaken vigorously for 15 seconds and then incubated at room temperature for 2-15 min, prior to centrifugation at 12,000g for 15 min at 4°C. The upper aqueous layer was then transferred to a fresh eppendorf containing 660µl of isopropanol, mixed and incubated at room temperature to precipitate RNA. RNA was recovered by centrifugation at 12,000g for 10 min at 4°C, the supernatant was poured off and the RNA pellet washed in 1ml 75% ethanol in DEPC treated water (0.01% (v/v) diethylpyrocarbonate (DEPC); Sigma). After removal of the ethanol, the RNA was vacuum dried for 5-10 min, redissolved in 10-20µl of DEPC-treated water and stored at -70°C.

2.7.2. Preparation of a Digoxigenin-labelled hybridisation probe

Probes were generated using random primed labelling of DNA fragments in low melting point agarose as described in the DIG Systems user's guide for filter hybridisation (Boehringer Mannheim), illustrated in Figure 2.7.2. The band of interest was excised from a gel and heated to 95°C for 10 min to denature the DNA. After rapidly cooling on ice, 2µl random hexanucleotides (Boehringer Mannheim),

2µl DIG-labelled dNTP's and 1µl Klenow (Pharmacia) was added to the heat-treated DNA.

Figure 2.7.2: The principal behind random primed labelling



2.7.3. RNA Analysis by Northern Blotting

Total cellular RNA was analysed on 1% submerged agarose gel containing 2.2M formaldehyde according to Ausubel *et al.* (1994) with electrophoresis in 1xMOPS buffer. Prior to loading, samples were mixed with 25µl sample buffer (129µl 10x MOPS, 226µl formaldehyde, 645µl formamide, 0.5µl Ethidium Bromide if required) and heated at 65°C in a heating block (Hybaid) for 10 min in order to remove secondary RNA structure. 4µl of loading buffer (1mM EDTA, 0.25% Bromophenol Blue, 0.25% Xylene cyanol, 50% glycerol) was then added to the samples, which were then centrifuged at 13,000 rpm for 20 sec in a Biofuge 13 microcentrifuge (Heraeus Sepatech). RNA samples were then loaded onto the gel, which was then

electrophoresed at 100V until the bromophenol blue had migrated 1/2 to 2/3, the length of the gel.

Following electrophoresis the gel was washed 2x in DEPC-water in an RNase free container. The gel was then placed on 3MM Whatman paper with the wicks dipped into 20x SSC (3M NaCl, 300mM Sodium Citrate pH7.0). Hybond N⁺ Nylon membrane (Amersham) was cut to the size of the gel, dampened with 20x SSC and placed on top of the gel excluding air bubbles. This was followed by 2-3 pieces 3MM Whatman paper pre-wetted with 20x SSC, a stack of paper towels and a 1.5Kg weight. The blot was left overnight at room temperature to achieve RNA transfer. After transfer, the RNA was fixed to the membrane using a UV stratalinker (Stratagene) using 12.5kJ of ultraviolet irradiation for 30 seconds. Both sides of the membrane were fixed in this manner. In order to check that transfer to the membrane had been successful, the membrane was stained for 2-3 min in a solution of methylene blue (0.3M Na-acetate, 0.02% methylene blue, DEPC-treated), and then destained using DEPC-water. The membrane was then probed or stored at -20°C until required.

2.7.4. Prehybridisation and hybridisation

The membrane was incubated with 20ml DIG Easy-Hyb (Boehringer Mannheim) for 1 hour at 42°C. After removal of this pre-hybridisation solution, the probe was denatured at 100°C for 10 min and then added to 15ml DIG Easy-Hyb, this solution was then added to the membrane. Hybridisation was carried out at 42°C overnight for *L. monocytogenes* samples.

2.7.5. Stringency Washes and Detection

Following hybridisation the membrane was washed 2x15min at room temperature to remove excess probe in 2x wash solution (2x SSC, 0.1%SDS), this was followed by two 15min stringency washes at 68°C in 0.1x wash solution (0.1%SSC, 0.1%SDS).

Prior to detection the membrane was blocked by gentle agitation in 1x blocking solution (Boehringer Mannheim) for 30 min at room temperature. This was followed by incubation with a 1:20,000 dilution of Anti-Digoxigenin Fab fragments (Boehringer Mannheim) diluted in 1x blocking solution for 30 min at room temperature. After washing the membrane to remove excess antibody for 2x15 min in washing buffer (0.1M maleic acid, 0.15M NaCl, 0.3% (w/v) Tween 20; pH7), the membrane was then equilibrated at room temperature in detection buffer (100mM Tris-HCl, pH9.5; 100mM NaCl) for 2 min. CDP-Star (Boehringer Mannheim) was then diluted 1:100 in detection buffer and applied to the membrane between two acetate sheets. This was incubated for 5 min at room temperature and the membrane then observed under a Berthold luminograph camera (E, G+G Berthold). Alternatively, the membrane was placed on Lumi-film (Chemiluminescent detection film, Boehringer Mannheim) and exposed for 5-30 min according to the signal strength. The chemiluminescent film was then developed by incubation in developer (Ilford 2000 RT) for 2min, following a wash with water the membrane was placed in fixer (Ilford 2000 RT) for 1min and washed again with water.

2.8. Colony Hybridisation

E. coli transformants were picked onto gridded Hybond N⁺ membrane, and a replica plate was also made. The membrane was then incubated on LA selective agar at 37°C for 3-4 hours until growth was visible. Cell lysis was achieved by placing the membrane on Whatman 3MM filter paper soaked in 0.4M NaOH for 15 min and the membrane was then neutralised by washing for 2x1min in 2xSSC. After 1 hour

incubation in Pre-hybridisation solution (DIG Easy-Hyb) at 42°C, the membrane was incubated with the probe overnight at the same temperature. Post hybridisation washes and detection was performed in the same way as for Northern Blots (Section 2.7.5).

2.9. SDS PAGE (1 dimensional)

2.9.1. Preparation of *E. coli* Protein Samples

E. coli cells were grown overnight at 37°C in a shaking incubator. 1ml of the overnight culture was removed and centrifuged for 2 min at 13,000 rpm in a Biofuge 13 microcentrifuge (Heraeus Sepatech). The pellet was then washed twice in PBS, in order to remove peptides left behind from the medium, and resuspended in 1ml PBS. 10µl of cell suspension was placed into an eppendorf tube and mixed with an equal volume of 2x sample buffer (0.25M Tris-HCl pH6.8, 4% SDS, 20% Glycerol, 0.001% Bromophenol Blue, 100mM DTT). Samples were then boiled at 100°C for 5 min, followed by centrifugation at 13,000 rpm in a Biofuge 13 Microcentrifuge (Heraeus Sepatech) for 1 min. The samples were then ready for loading onto an SDS-PAGE gel. Low range pre-stained molecular weight markers (Bio-Rad) were also loaded onto the gel.

2.9.2. Preparation of *L. monocytogenes* Protein samples

Cell lysis cannot be achieved from *L. monocytogenes* by boiling alone. *L. monocytogenes* samples were grown up overnight. 50ml of each culture was then centrifuged at 6,000g in order to pellet the bacterial cells. The resulting bacterial pellet re-suspended in 0.5ml freshly made sonication buffer (20mM Tris-HCl pH8, 1mM EDTA, 1mM PMSF). Samples were then subjected to 3x30sec-burst sonication (Soniprep 150, MSE) at an amplitude of 5 microns. Between each round of sonication the sample was kept on ice for an interval of 30sec. Sonicated samples

were then centrifuged at 13,000rpm (Biofuge 13 microcentrifuge, Heraeus Sepatech) for 10 min. The removed supernatant was then mixed with an equal volume of 2x Sample buffer and boiled at 100°C for 10 min. Protein extracts were then run on an SDS-PAGE gel.

2.9.3. Preparation of an SDS-PAGE Gel

Protein profiles were visualised using 12.5% discontinuous SDS-PAGE gel electrophoresis. A mini-gel was prepared using the following procedure: 2.9 ml of Acrylamide/Bisacrylamide (37.5:1) solution (Boehringer Mannheim), 3.75ml Buffer A (0.75M Tris-HCl pH8.8, 0.2% SDS), 0.825µl water, 30µl 10% APS (BDH), 2.5µl TEMED (Sigma). The solution was mixed gently and then poured between two ethanol cleaned glass support plates separated by 1mm spacers. The top of the gel was then overlaid with 200µl sterile water and left to polymerise at room temperature. After polymerisation the water was poured off and the top of the gel dried with 3MM Whatman paper. The 7% stacking gel was then prepared as follows: 1.15ml of Acrylamide/Bisacrylamide (37.5:1) solution, 2.5ml Buffer B (0.25M Tris-HCl pH6.8, 0.2% SDS), 1.3ml water, 25µl 10% APS, 5µl TEMED were mixed gently, and then poured on top of the stacking gel. A comb was inserted and the gel left to polymerise at room temperature. Running buffer (5mM Tris-HCl, 0.19% SDS, 0.192M Glycine) was then added to both chambers of the electrophoresis tank (Bio-Rad), just before use the comb was removed and the resulting wells flushed out with running buffer. The cell extracts that had been mixed with 2x sample buffer and then heat treated (as in section 2.9.1) were then loaded into the wells. The gel was then run at 150V using Bio-Rad Mini-Protean II apparatus, until the dye front had reached the bottom of the separating gel (~2hours).

2.9.4. Detection of Protein Profiles

Following electrophoresis, the gel was removed from its support plates and stained in Coomassie blue staining solution (0.25% (w/v) Coomassie blue R, 25% (v/v)

Propan-2-ol, 10% (v/v) Glacial Acetic Acid) for at least 20 min. The gel was then destained in a 10% (v/v) Propan-2-ol / 10% (v/v) 10% Glacial acetic acid solution until the peptide bands were visible and the background colour minimal.

2.10. Western Blotting

2.10.1. Transfer of proteins to Nitrocellulose by Electroblothing

In order to determine if GFP was being translated in Gram positive bacteria two 12.5% SDS-PAGE gels were loaded in duplicate. One was stained using Coomassie blue, the proteins on the other were transferred to BioTrace Nitrocellulose blotting membrane (Gelman Sciences) and subjected to immunoblotting analysis. In order to achieve this Nitrocellulose and six pieces of Whatman 3MM filter paper were cut to the same size as the gel. Both the nitrocellulose and gel were then incubated in semi-dry transfer buffer (Glycine, Tris-HCl, SDS, 20% (v/v) Methanol) for 10-15min. A sandwich was then built on a Multiphore II electroblotter (Pharmacia Biotech) using three pieces of Whatman paper saturated with transfer buffer, nitrocellulose membrane, gel and the three remaining pieces of Whatman paper. Care was taken to ensure no bubbles were present in the stack. Proteins were transferred to membrane by electrotransfer for 30min at 100mA. In order to check transfer had been successful, the membrane was stained for 1 min with Ponceau S (Sigma), and then destained using several changes of water.

2.10.2. Immunodetection of proteins

For immunodetection of GFP the membrane was first incubated overnight at 4°C in blocking solution (5% milk, PBS, 0.05% (v/v) Tween-20). Primary antibody (Polyclonal GFP, Clontech) was then diluted 1:2000 in blocking buffer and the membrane incubated for 1 hour at room temperature gently shaking. This solution was removed and the membrane washed 1x5 min in a solution of 5%-milk, PBS,

0.05% (v/v) Tween-20. This was followed by a further 2x 5 min washes in PBS, 0.05% (v/v) Tween-20). Secondary antibody (alkaline-phosphatase conjugated anti-rabbit IgG; Sigma) was diluted to 1:10,000 in blocking buffer and the membrane incubated at room temperature, gently shaking, for a further hour. The membrane was then washed as before, and a further 2x1 min washes in PBS carried out. The immunoblot was then equilibrated in Tris-buffered saline (100mM Tris-HCl pH9.5, 100mM NaCl, 5mM MgCl) for 1min at room temperature.

For colorimetric detection 50ml colour reagent was made up using 125µl of both BCIP (Boehringer Mannheim) and NBT (Boehringer Mannheim) diluted in Tris-buffered Saline pH9.5. The blot was then incubated in the dark until the signal was visible (usually about 1 hour).

Alternatively for chemiluminescent detection CDP-Star was then diluted 1:100 in 1ml detection buffer, applied to the membrane between 2 acetate sheets incubated at room temperature for 5min. The chemiluminescent signal was then visualised using a Berthold Luminograph 980 (E, G+G Berthold). The chemiluminescent signal could also be visualised after exposure to Lumi film (chemiluminescent detection film, Boehringer Mannheim), or HyperfilmTMECLTM (hyper performance chemiluminescent film, Amersham Life Science). Exposures of 5-30 min were used, and the chemiluminescent film was then developed using the same protocol as described for chemiluminescent detection of an RNA signal.

2.11. 2-dimensional gel electrophoresis (2-D PAGE)

Proteins were resolved on 2-D gels by the Method of O'Farrell (1975) with modifications as recommended by the manufacturer (Pharmacia Biotech).

2.11.1. Preparation of *L. monocytogenes* whole cell extracts

L. monocytogenes harbouring *lux* expression vectors were grown to a point where the luminescence reached a maximum. Cells were then washed in an equal volume of Tris-EDTA buffer (0.1M Tris-HCl pH7.5, 1mM EDTA), concentrated 10-fold in sonication buffer (10mM Tris-HCl pH7.5, 5mM MgCl₂, 2mM PMSF) and then disrupted using a mini-bead beater (Biospec products). Ten 30 sec bursts in the bead beater were performed, with a 30 sec interval on ice. Samples were then centrifuged for 10min at 13,000 rpm in a Biofuge 13 Microcentrifuge (Heraeus Sepatech) in order to remove the beads. Samples were stored at -80°C until required.

2.11.2. First Dimension

The proteins were resolved by isoelectric-focussing in the first dimension using a Multiphore II electrophoresis unit (Pharmacia Biotech). The first dimension involved using pre-cast Immobiline DryStrips (Pharmacia Biotech) with a linear pH gradient of pH4-7 according to the protocol supplied by Pharmacia Amersham. This enabled the cellular proteins to be separated according to charge.

2.11.3. Second Dimension

The proteins were separated according to size by horizontal gel electrophoresis using ExcelGel SDS (Pharmacia Biotech). With a 8 to 18% (wt/vol) polyacrylamide gradient. Gels were run on a multiphore II electrophoresis unit (Pharmacia Biotech), according to the protocol of Pharmacia Amersham.

2.11.4. Staining and destaining

Gels were stained with coomasie blue and destained as previously described in Section 2.9.4.

2.11.5. Analysis of 2-D profile

Images of the gels were captured with a Sharp JX-330 scanner linked to an image analysis software package (Image Master 2D Elite, Amersham Pharmacia Biotech)

2.12. Tissue Culture

2.12.1. Maintenance of cell line

Human Umbilical Veined Endothelial Cells (HUVEC) were obtained from Queen's Medical Centre (Nottingham). Cells were cultured in RPMI-1640 (Sigma), supplemented with 2mM glutamine (Sigma), 100 units ml⁻¹ penicillin (Sigma), 0.1 mgml⁻¹ streptomycin (Sigma) and 10% heat inactivated foetal bovine serum (FBS; Sigma) and grown at 37°C in 5% CO₂. Cells were maintained by changing the medium every 48-72 hours until a monolayer was obtained.

2.12.2. Trypsinisation of Monolayer Cultures

When cells reached confluence the medium was removed. Cells were then washed twice with 5-10ml of phosphate buffered saline (PBS; Oxoid). 1ml/50cm² trypsin EDTA (0.5g porcine trypsin, 0.2g EDTA; Sigma) was added to the flask, which was then incubated at 37°C for 5min. On the addition of 5ml fresh pre-warmed RPMI-1640 (Sigma) cells were removed by gentle tapping of the culture vessel, or by flushing with a sterile pipette. The resuspended cells were then plated out at the required cell density in fresh culture vessels. Cells were used to inoculate fresh flasks in roughly 1 flask: 4-6 flasks or, cells were counted on a haemocytometer and then re-seeded at a density of 10⁵ cells ml⁻¹. The maximum volume of medium used to plate out cells is indicated:

25cm² flask: 10ml

75cm² flask: 20ml

10% Foetal Bovine Serum (Bibco BRL) was added to each flask which was then incubated at 37°C in 5% CO₂.

2.12.3. Cell Freezing

For long term storage of cell lines, cells were harvested by trypsinisation and centrifugation at 1200rpm (MSE bench-top centrifuge) for 5-10 min. The freezing mixture was then made up containing 90% foetal bovine serum + 10% DMSO (Sigma). As DMSO is toxic at room temperature, cells and freezing mixture were placed on ice in order to reach a temperature of 4°C. 1ml of freezing mixture was transferred to the vessel containing the pre-chilled cell pellet, and the cells were resuspended using a Pasteur pipette. The cell suspension was then transferred to a cryovial, which was then stored at -80°C.

2.12.4. Tissue Culture Cell Invasion Assay

The invasion of HUVEC cells with *S. aureus* was carried out using a minor modification of the procedure described by Yao *et al.* (1995). Tissue culture cells were harvested and seeded into 35mm glass bottom Microwell dishes (MatTek Corporation, USA) or onto glass coverslips. These were left at 37°C in 5% CO₂ for 48 hours in order for cells to re-attach and to cover 80-90% of the surface. Medium was removed from the cells and replaced with medium that did not contain antibiotics and left for a further hour at 37°C. During this time the bacterial inoculum was prepared. An overnight culture was centrifuged for 15 min, 4500 rpm, at 4°C. The pellet was washed twice in fresh medium (BM) and then resuspended in 1 volume of fresh antibiotic medium (BM Cm7) This was then diluted 1:20 into fresh medium and grown for a further 1 hour period at 37°C. This culture was then diluted 1:20 into fresh BM Cm7 which was the incubated for a further 3 hour period. Following this, 1ml samples were taken, centrifuged at 13,000 rpm in a Biofuge 13 microcentrifuge (Heraeus Sepatech), washed twice in PBS and resuspended in 9ml of fresh unsupplemented RPMI-1640 medium (Sigma). Media was then removed from the tissue culture cells and replaced with the prepared bacterial culture. This was then incubated at varying times at 37°C for two hours. After this period, the tissue culture cells were fixed with formaldehyde.

2.12.5. Fixation of tissue culture cell using formaldehyde

The method was originally described by Knutton *et al.* (1989) and has been modified slightly. After incubation with *S. aureus*, tissue culture cells were washed 3x with PBS to remove non-adhering bacteria. Cells were then fixed for 20 min with 3% Formalin (Sigma). Cells were then washed 3x in PBS and mounted in glycerol-PBS (Citifluor). Specimens were then examined by epifluorescence microscopy using the appropriate filter sets (Section 2.6). Microscopy was performed using an Axiovert 135TV fluorescence microscope linked to an Improvisions® Openlab™ image manager which controlled a Hamamatsu ORCA-2 cooled CCD camera.

2.13. Monitoring Bioluminescence of Bacterial Cultures

2.13.1. Measuring Bioluminescence from colonies on agar plates

Bioluminescent colonies expressing *luxAB*, grown on agar plates, were examined under a Hamamatsu VIM3 camera after the addition of exogenous aldehyde.

Bacterial colonies expressing *luxCDABE* or *luxABCDE* were examined under a Hamamatsu VIM3 camera. No exogenous substrate needed to be added to these cultures.

2.13.2. Measuring bioluminescence from liquid cultures

Bacterial cultures harbouring *lux* plasmids were grown overnight. This was diluted 1/100 into pre-warmed fresh culture media containing the necessary supplements. Cultures were grown at 37°C in a shaking waterbath. Bioluminescence from 1ml samples was measured using a Turner luminometer (Septech).

Alternatively, bioluminescent cultures were grown overnight at 37°C. These were then diluted 1:100 and grown for 1 hour at 37°C. This was then diluted at different concentrations into fresh antibiotic containing media. 200µl samples of each dilution were loaded into a clear-bottomed 96-well microtitre plate, which was then placed into an Anthos Lucy 1 photoluminometer. This was set to 37°C and was programmed to measure OD at approximately 600nm and also to measure bioluminescence every 30 minutes after shaking.

2.14. Monitoring Fluorescence of Bacterial cultures

2.14.1. Observing fluorescence of colonies on agar plates

Colonies expressing GFP were examined under either UV light (UVP) or blue light excitation. Those colonies expressing GFP were seen to fluoresce under the correct excitation conditions.

2.14.2. Observing GFP fluorescence from a liquid culture

Bacterial cultures expressing GFP were grown overnight at 37°C, shaking. The overnight culture was diluted 1/100 into fresh pre-warmed broth containing the

necessary antibiotics and supplements. A 1.5ml sample was removed from the culture vessel, centrifuged at 13,000 rpm in a Biofuge 13 Microcentrifuge (Heraeus Sepatech) for 2 min, washed twice in an equal volume of PBS, resuspended in 1/10th volume of PBS and loaded into a microtitre plate. Fluorescence was then observed using a excitation wavelength of 488nm and an emission wavelength of 510nm in a Victor 1420 multilabel counter (Wallac, E G & G).

2.14.3. Observing degradation of the C-terminal Modified GFP variants

Bacterial cultures were grown overnight and diluted as previously described in section 2.15.2. *L. monocytogenes* cells were then grown for a period of 8 hours, in the presence of 0.5% xylose, it was known that as this point fluorescence had reached a detectable level. Bacterial cultures were then washed in an equal volume of PBS and diluted 1/5 in fresh pre-warmed media without added xylose. Fluorescence measurements were then taken at hourly interval as previously described.

CHAPTER 3

CONSTRUCTION OF GFP EXPRESSION VECTORS FOR EXPRESSION IN GRAM POSITIVE ORGANISMS

CHAPTER 3: CONSTRUCTION OF GFP EXPRESSION VECTORS FOR EXPRESSION IN GRAM POSITIVE ORGANISMS

3.1. Introduction

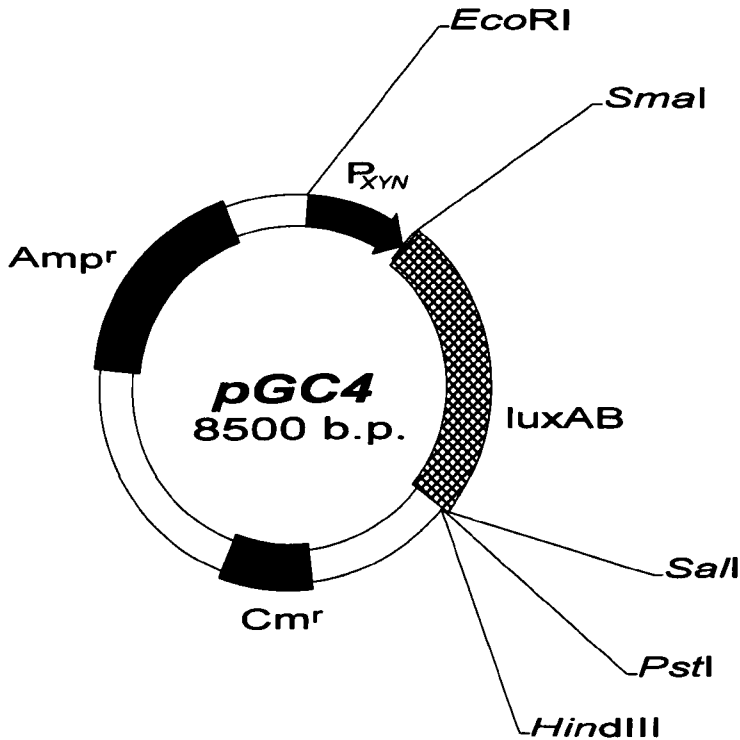
In order to express *gfp* in Gram positive organisms, the gene has to be stably maintained within the organism. For this study the shuttle vector pMK4 has been utilised as the basic cloning vector. pMK4 was generated from the fusion of pUC9 and pC194, and hence contains both a Gram negative and Gram positive origin of replication (Sullivan *et al.*, 1984)). The main advantage of using such a vector is that all the initial cloning and screening can be carried out in *E. coli*, to facilitate the process due to higher transformation efficiencies, and ease with which plasmid DNA extractions can be performed. Once the correct plasmid construct has been identified the DNA can be amplified and used to transform the Gram positive organisms of choice. Initially it was decided to perform all the initial gene expression studies in *L. monocytogenes*.

3.2. Construction of a Gram positive GFP expression vector

As stated previously, the basic shuttle vector used for all construction work was based on pMK4. The plasmid used was pGC4 (C. Rees, unpublished) and is illustrated in Figure 3.2.1, this contains the P_{xyn} promoter from *Bacillus pumilus* and a *luxAB* fusion from *Vibrio harveyi*. This promoter has previously been shown to be active in *L. monocytogenes* and *B. subtilis* (Jacobs *et al.*, 1991). In order to confirm that P_{xyn} was functional in *E. coli* and *L. monocytogenes*, plasmid DNA was introduced into both bacteria by electroporation of competent cells. Upon the addition of exogenous aldehyde to recombinant colonies on agar plates, as described in the Materials and Methods, individual colonies were seen to bioluminescence under a Hamamatsu VIM3 camera, due to the expression of the *luxAB* fusion within

pGC4. All colonies showed a highly bioluminescent phenotype, indicating that the P_{xyt} promoter was functional within *E. coli* and *L. monocytogenes*.

Figure 3.2.1: Restriction map of pGC4



In order to construct the *gfp* expression vectors it was necessary to excise the *luxAB* fusion from pGC4 and replace it with the *gfp* coding sequence. Initially it was decided to use two *gfp* variants, *gfp* wild type (*gfp_wt*) and a red shifted *gfp* variant, *gfp* mutant3 (*gfp₃*) originally described by Cormack *et al.* (1996).

PCR was used to generate restriction sites at both the 5' and 3' ends of the coding sequence of each variant. A *SmaI* site was introduced at the 5' region and a *SalI* site

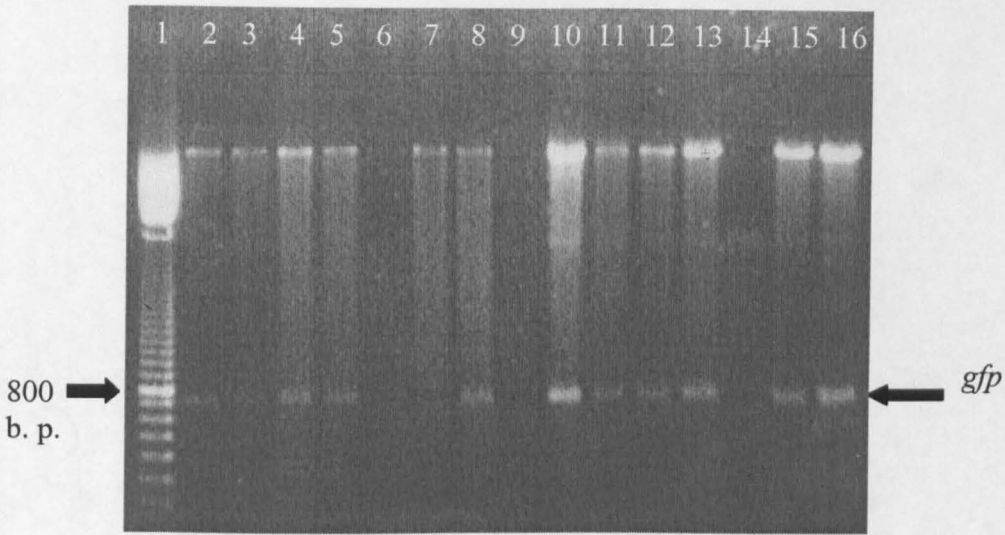
at the 3' region to facilitate the cloning process. Primers utilised were designated primers 1 and 2 and are shown in Appendix 1. Primers were designed to homologous regions of both *gfpwt* and *gfp3*, so the same sets of primers could be used to amplify the DNA of the individual variants.

In order to amplify the *gfp* gene by PCR a DNA template was necessary in the reaction. For *gfpwt* the gene template was derived from pGFP-1, a plasmid supplied by Clontech, J. Anderson, Denmark, supplied the *gfp3* (pJBA33, Anderson *et al.* (1998). For the PCR, an annealing temperature at 50°C for one minute was used followed by a period of DNA extension at 72°C, again for one minute. This resulted in the production of a PCR product of approximately 800bp, which contained the fore-mentioned restriction enzyme recognition sequences.

The PCR products containing the two *gfp* genes were restricted with *SmaI* and *SalI*, pGC4 was also digested with the same enzymes. The *luxAB* fragment was excised from pGC4 and the remaining vector DNA, and restricted PCR products purified from a low melting point agarose gel. Following recovery of all DNA fragments, the two *gfp* variants were ligated with pGC4, prior to introduction into *E. coli* JM109 competent cells by electroporation. The resulting transformants were screened for *gfp* expression using either blue or UV excitation to identify positive clones.

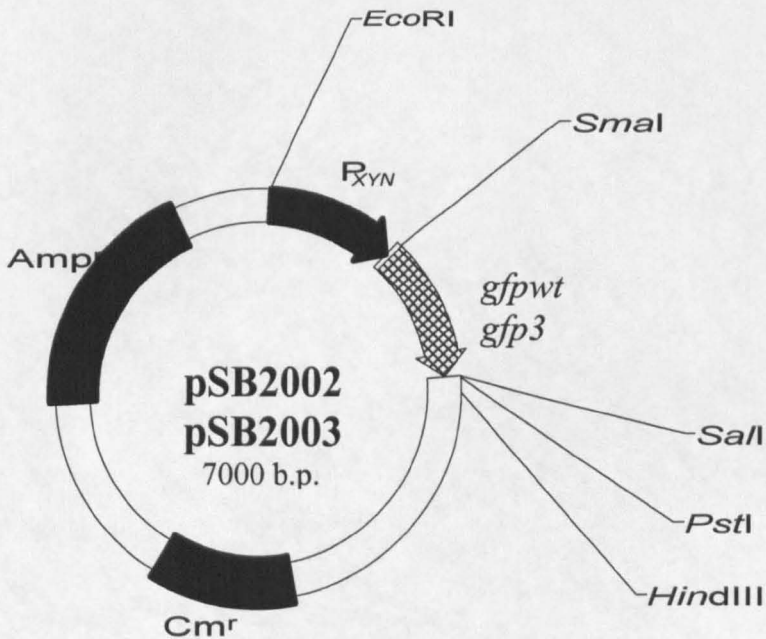
Having isolated fluorescent colonies, these were inoculated into 5ml LB amp⁵⁰ and grown overnight at 37°C. Plasmid DNA was extracted by plasmid miniprep, and the resulting DNA was examined following restriction with *SmaI* and *SalI*. From the restriction analysis, a clear band of approximately 800bp could be seen on a 1% agarose gel, shown in Figure 3.2.2. These data showed that both *gfpwt* and *gfp3* have both successfully been cloned into the vector pGC4. The new *gfp3* and *gfpwt* expression vectors were designated pSB2002 and pSB2003 respectively and are illustrated in Figure 3.2.3.

Figure 3.2.2: Agarose gel showing presence of *gfp* insert in recombinant colonies



- Lane 1: 100 base pair ladder (Pharmacia)
- Lane 2-8: Putative *gfp3* constructs restricted with *SmaI* / *SaII*
- Lane 9-16: Putative *gfpwt* constructs restricted with *SmaI* / *SaII*

Figure 3.2.3: Restriction map of pSB2002 and pSB2003



The recombinant plasmids pSB2002 and pSB2003 were prepared on a large scale by plasmid maxi prep. This DNA was then used to transform electrocompetent *L. monocytogenes*, however the resulting recombinant colonies were not seen to fluoresce under the correct excitation wavelength. All individual *E. coli* cells harbouring these constructs were seen to emit green light when subjected to fluorescence microscopy. However, when the plasmids pSB2002 and pSB2003 were introduced into *L. monocytogenes*, the population was found to be heterogeneous with regard to its fluorescence characteristics. Only a small proportion of the population was seen to fluoresce upon excitation. This is different to observations noted from *E. coli* cells expressing *gfp*, where every individual cell fluoresces. The differences in the fluorescent characteristics of the two populations are indicated in Figure 3.2.4 a, b, c, d.

It can be seen from Figure 3.2.4 that only a small proportion of cells within the *L. monocytogenes* population are fluorescing compared to that of *E. coli*. It should also be noted that the fluorescent signal generated from the wild type protein was of a lower intensity than that from GFP3, the latter of which appeared to generate a much brighter signal in accordance with Cormack *et al.* (1996). But, it is known that prolonged excitation of the GFPwt protein with UV light causes photobleaching of the signal. Also, those *L. monocytogenes* cells that do show a fluorescent phenotype appear to fluoresce with a lower intensity than *E. coli* cells expressing the same protein, regardless of the *gfp* variant that they are expressing. However, this in part is probably due to the fact that the plasmid has a lower copy number in Gram positive organisms such as *L. monocytogenes* compared to that seen in Gram negative organisms. If copy number is an issue then Gram positive cells may show lower levels of fluorescence compared to Gram negative cells harbouring the same constructs, the differences in plasmid copy number does not explain why all the *L. monocytogenes* cells are not fluorescent.

There are many issues that may be responsible for the heterogeneous phenotype exhibited by *L. monocytogenes* expressing *gfp*. One possibility is that the plasmid is unstable within the Gram positive bacteria and those cells that are not fluorescent

have actually lost the plasmid. Another possible explanation is that transcription of *gfp* is being terminated prematurely resulting in a partial transcript and this has led to incomplete synthesis of GFP in most cells. It may be that translation of *gfp* is poorly initiated or prematurely terminated within *L. monocytogenes*, again leading to truncated non-functional protein. Another possibility is that *L. monocytogenes* are over producing the protein and this has caused protein aggregation and non-fluorescent inclusion body formation prior to chromophore formation within the cells.

Figure 3.2.4a and b: *E. coli* (pSB2002) and *E. coli* (pSB2003). The data illustrates the higher fluorescent output seen when *E. coli* express *gfpwt*

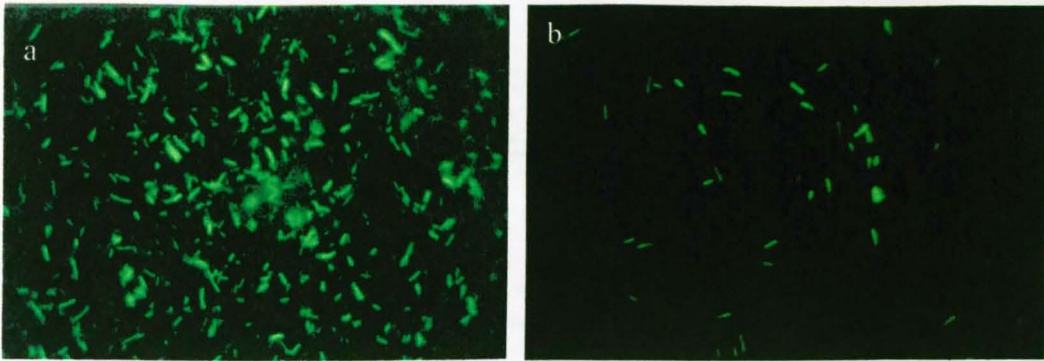
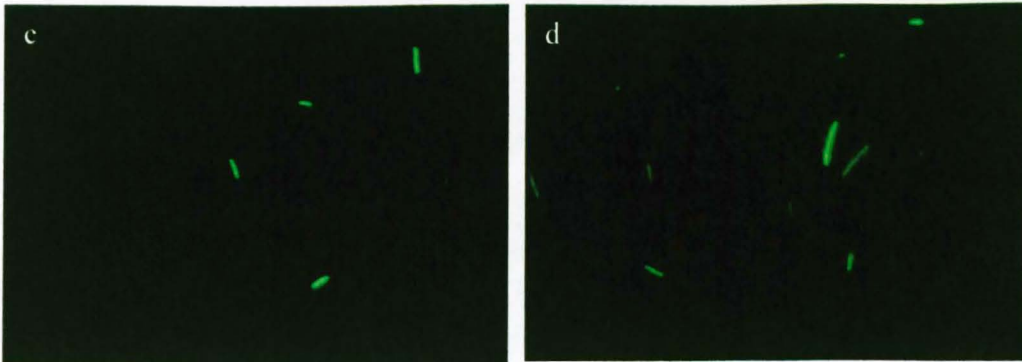


Figure 3.2.4c and d: *L. monocytogenes* (pSB2002) and *L. monocytogenes* (pSB2003). Note the lower percentage of fluorescent cells compared to *E. coli* harbouring identical constructs.



3.3. Investigations of plasmid stability in *L. monocytogenes*

One possibility for the lack of fluorescent *L. monocytogenes* cells could be due to plasmid instability. Do the non-fluorescent cells still contain the *gfp* expression vectors, pSB2002 and pSB2003, or have they lost them due to the plasmid being unstable? In order to investigate this, *L. monocytogenes* cells harbouring pSB2002 and SB2003 were grown overnight at 37°C in BHI broth both with and without chloramphenicol selection present. Ten fold serial dilutions of the overnight cultures were then prepared and these then plated onto BHI agar plates, again both with and without chloramphenicol selection. As controls, *L. monocytogenes* cells containing pMK4 and pGC4 were also subjected to the same analytical treatment.

From the data obtained (shown in Appendix 2) several things were apparent. In all cases it is clear that antibiotic selection helped maintain the plasmid within the cells, as when *L. monocytogenes* harbouring the plasmids were grown overnight with chloramphenicol, the percentage loss of plasmid from the cells was reduced. It also seems apparent that the expression of reporter genes within pMK4 also increased plasmid instability. The expression vectors pGC4, pSB2002 and pSB2003 all show greater instability than pMK4, this degree of instability was greater when cells were grown without chloramphenicol selection. As pMK4 was stable when grown with chloramphenicol selection, it appears as though the expression of the reporter genes, either *luxAB* or *gfp* places a significant stress upon the cells resulting in plasmid instability.

The plasmid pMK4 was originally constructed from pUC9 and pC194 (Sullivan *et al.*, 1984). Plasmid pC194 shows several properties unfavourable for cloning and stability. It generates considerable amounts of single stranded DNA (ssDNA) in *B. subtilis*, approximately 20% of the total plasmid DNA (te Riele *et al.*, 1986), and it also generates large amounts of high molecular weight (HMW) DNA when carrying heterologous inserts (Gruss and Ehrlich, 1998). HMW DNA consists of linear head-to-tail multimers in which five or more plasmid copies are tandemly arranged. In

general the levels of HMW DNA production is related to plasmid size, it also depends on the insert of DNA. However, as much as 90% of the plasmid DNA may be present as HMW products. If this is occurring when the reporter genes are cloned into pMK4, then this may explain why the plasmid stability is reduced compared to that of pMK4 which contains no heterologous inserts.

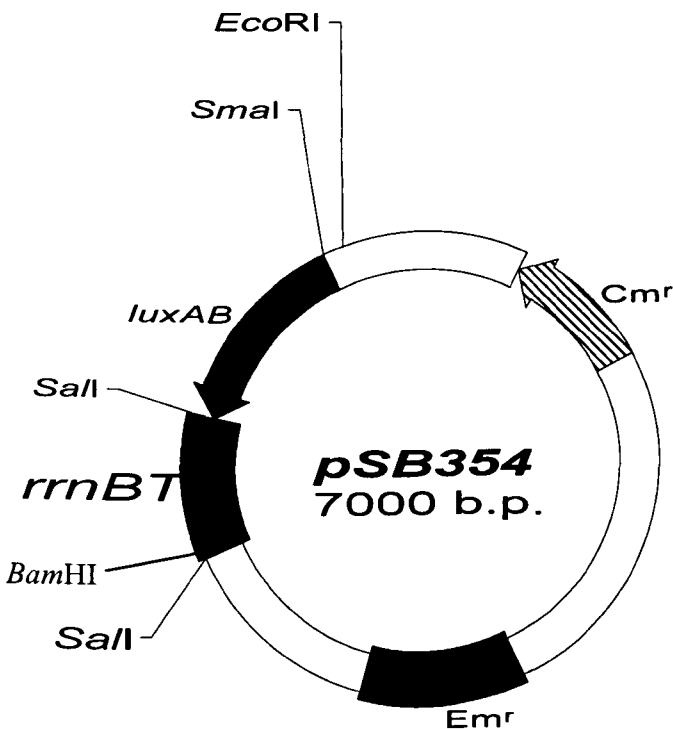
When *L. monocytogenes* express *gfp3* from pSB2002 approximately 30% of the cells are seen to lose the plasmid when grown with chloramphenicol. Thus it might be expected that around 70% of the cells would be fluorescent, however only a small proportion of the cells are seen to fluoresce, perhaps 5%. So whilst the plasmid is known to be unstable in *L. monocytogenes*, plasmid instability does not appear to be the sole factor responsible for the lack of fluorescence observed when *L. monocytogenes* express *gfp*. Some other factor appears to have a major factor on the lack of fluorescence observed by *L. monocytogenes* expressing *gfp*.

3.4. Cloning a terminator downstream of *gfp*

The apparent instability of the reporter plasmids may be due to the fact that there is no transcriptional terminator downstream of the reporter gene. As there is no terminator, transcription has no defined region at which to stop and readthrough into the plasmid structure may be responsible for the observed heterogeneity of *gfp* expression by the *L. monocytogenes* cells. It was decided to clone a terminator fragment downstream of the *gfp* variants to see if this had any effect of the fluorescent characteristics of the population.

The terminator that was cloned was the *rrnBT* terminator originally isolated from *E. coli* (Orosz *et al.*, 1991). This terminator had previously been cloned into the plasmid pSB354 (Hill *et al.*, 1994), which is illustrated in Figure 3.4.1.

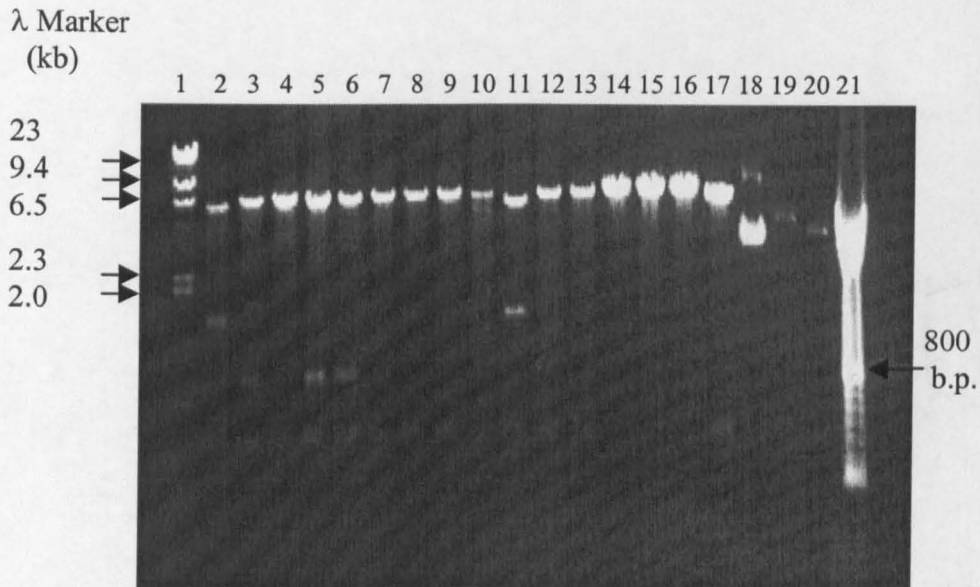
Figure 3.4.1: Restriction map of pSB354



The terminator was excised from pSB354 using *Sa*II and then inserted downstream of *gfp* in both pSB2002 and pSB2003, which had also been linearised with *Sa*II. The ligated DNA was used to transform *E. coli* JM109 competent cells, and recombinant colonies were isolated following selection on ampicillin selective agar plates. DNA was prepared from recombinant colonies by plasmid miniprep, this was then restricted using *Bam*HI and *Sma*I to confirm whether the terminator had successfully inserted downstream of the *gfp* and if so, which orientation the fragment was in. If the terminator had been inserted into pSB2002 and pSB2003 in the correct orientation then the resulting plasmid, when restricted with *Bam*HI and *Sma*I should drop out a fragment of approximately 1.6kb. The restriction analysis of DNA isolated from recombinant colonies thought to contain *rrnBT* downstream of *gfp3* is illustrated in Figure 3.4.2. It can be clearly seen that lanes 2 and 11 show the presence of a 1.6kb insert, as this can only be obtained if *rrnBT* had inserted in the correct orientation downstream of *gfp*, then it was assumed that these colonies contained the correct recombinant DNA. Similar analysis was carried out for the equivalent wild type construct based on pSB2003.

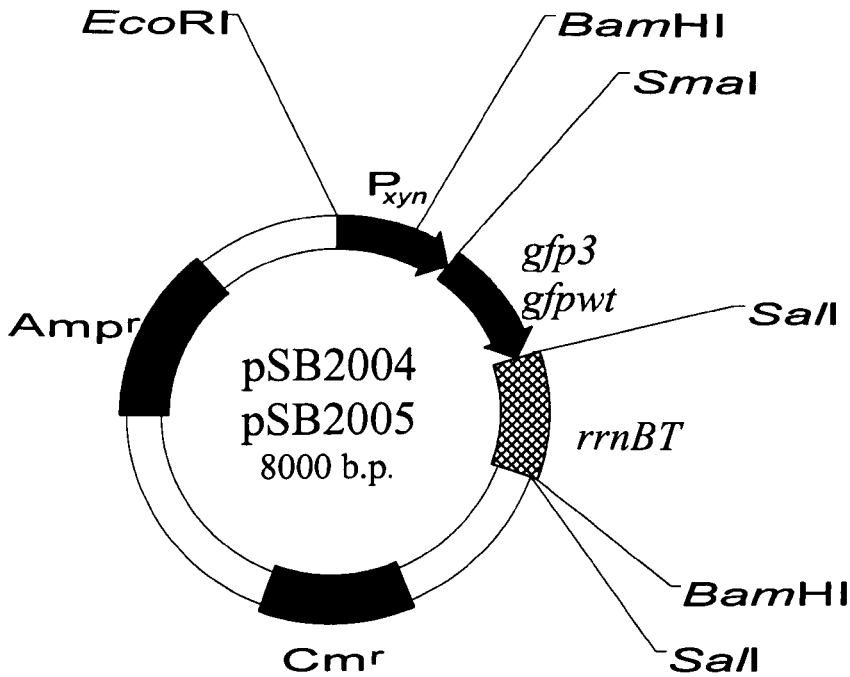
The resulting *gfp3* and *gfpwt* expression vectors that contained a transcriptional terminator downstream of the reporter gene were designated pSB2004 and pSB2005 respectively, and are illustrated in Figure 3.4.3. Having isolated the correct clones, DNA was prepared by plasmid maxiprep. This was then used to transform electrocompetent *L. monocytogenes*. Recombinant colonies were isolated following selection on chloramphenicol selective agar plates, they were subsequently screened for *gfp* expression using either blue or UV excitation, depending on the *gfp* variant.

Figure 3.4.2: Restriction analysis of putative recombinant DNA containing the *rrnBT* fragment



- Lane 1: Lambda *Hind*III (MBI)
- Lane 2-13: Putative recombinant DNA restricted with *Sma*I/*Bam*HI
- Lane 14: pSB2002 restricted with *Sma*I
- Lane 15: pSB2002 restricted with *Sal*I
- Lane 16: pSB2002 restricted with *Bam*HI
- Lane 17: pSB2002 restricted with *Sma*I/*Bam*HI
- Lane 18: pSB2002 uncut DNA
- Lane 19-20: Uncut recombinant DNA
- Lane 21: 100 base pair ladder (Pharmacia)

Figure 3.4.3: Predicted restriction map of pSB2004 and pSB2005



E. coli cells expressing *gfp* from pSB2004 and pSB2005 all showed a highly fluorescent phenotype when subjected to examination by fluorescence microscopy. However, the same constructs in *L. monocytogenes* did not appear to improve the fluorescence characteristics of the cells. Only a small percentage of the total number of the Gram positive cells fluoresced under excitation conditions, again the signal of those fluorescing was much lower than that seen in *E. coli*.

So it appears that the *gfp* containing plasmid is not being made unstable by transcriptional readthrough into the plasmid further downstream of the *gfp* coding sequence, as the addition of a transcriptional terminator into the *gfp* constructs makes no difference to the fluorescence characteristics of the *L. monocytogenes* population.

3.5. Does Overexpression of GFP result in non-Fluorescent Cells?

One possible explanation for the small percentage of *L. monocytogenes* cells that were expressing the GFP protein was that the peptide was actually synthesised, but was then being packaged into non-fluorescent inclusion bodies prior to folding. Another hypothesis was that GFP was being synthesised in large amounts, but the levels made were toxic to the cells. In order to investigate both these possibilities simultaneously, it was decided to reduce the levels of fluorescent protein *within L. monocytogenes*. This was done using two different approaches.

3.5.1. Cloning unstable GFP variants

In order to investigate these hypotheses, it was decided to utilise the unstable *gfp3* variants of Anderson *et al.* (1998). Keiler *et al.* (1996) demonstrated that specific C-terminal oligopeptide extensions could render otherwise stable proteins to degradation by certain intracellular tail-specific proteases. Anderson *et al.* (1998) exploited this natural protein degradation system and created variants of *gfp3* which were degraded at different rates within the cell. This was achieved by the addition of short peptide sequences to the C-terminal of the intact GFP protein, which rendered the GFP susceptible to the action of indigenous house-keeping proteases. This resulted in protein variants with half-lives ranging from 30 minutes to a few hours when synthesised in *E. coli* and *Pseudomonas putida* (Anderson *et al.*, 1998). So if GFP is having an adverse effect on *L. monocytogenes*, then by using these variants the overall concentration of protein within a cell will be decreased compared to the stable GFP3 due to the rapid turnover of the protein. These lower levels of GFP protein may be more favourable to allow efficient expression within *L. monocytogenes* and may prevent aggregation of excess protein, which can result in the formation of inclusion bodies.

Three unstable *gfp3* variants were available for use, these being *gfp3* (LAA), *gfp3* (ASV) and *gfp3* (AGA). These had reported half-lives of approximately 30, 60 and 300 minutes respectively in *E. coli* (Anderson *et al.*, 1998). A new primer to the 3' region of each of these variants was constructed, the primer was designed to a homologous area downstream of the protease recognition tag, thus the same primer could be used to amplify each unstable *gfp3*, and it also contained a *SalI* restriction site to facilitate cloning. This primer was used in conjunction with the *gfp* forward primer that has been used previously, details of the primers used, primers 1 and 3 are given in Appendix 1. The PCR was performed as previously described in Section 3.2.

The resulting PCR products were restricted with *SmaI* and *SalI*. Following purification these were ligated with pGC4 that had been restricted with the same endonucleases and the *luxAB* fusion excised from it. The ligated DNA was then used to transform *E. coli* JM109 competent cells, colonies containing recombinant DNA were isolated following selection on ampicillin selective agar plates. Resulting transformants were screened for *gfp* expression under blue light excitation (~488nm) in order to identify possible clones. No individual colonies were seen to fluoresce, it is probable that the protein was being turned over too rapidly within the cell to allow accumulation.

In order to screen recombinant colonies, DNA was prepared from the cells by plasmid miniprep. This was then restricted with *SmaI* and *SalI* to excise the *gfp* gene that had been cloned in place of the *luxAB*. In some cases, when the DNA was electrophoresed on an agarose gel, a band of 800bp was seen, indicating that the DNA did contain the *gfp* downstream of P_{lyn}. These new unstable *gfp* expression vectors were designated pSB2006 (*gfp3* LAA), pSB2007 (*gfp3* ASV) and pSB2008 (*gfp3* AGA). Large scale DNA preparations were performed from *E. coli* cells containing these expression vectors by plasmid maxi prep.

Electrocompetent *L. monocytogenes* cells were transformed with pSB2006, pSB2007 and pSB2008. Cells containing recombinant DNA were isolated following selection on chloramphenicol selective agar plates. Again, using fluorescence microscopy, transformants were observed under blue light excitation to observe fluorescence characteristics. With *L. monocytogenes* (pSB2006) no fluorescent cells were seen in the population. This however is the protein with the shortest half-life and it is possible that the protein was degrading before the chromophore could fold and generate a fluorescent signal. Another possibility is that the level of fluorescence was too low to be detected by eye, more sensitive equipment or a longer acquisition period may have located a signal from *L. monocytogenes* harbouring this plasmid. With *L. monocytogenes* (pSB2007) and *L. monocytogenes* (pSB2008) only a few cells within the population exhibited a fluorescent phenotype upon excitation. It is a possibility that in *L. monocytogenes* the proteins have different half-lives than those observed in *E. coli*, resulting in the degradation of the protein before the chromophore has been able to fold and generate a fluorescent signal.

The results of this experiment appear to suggest that the lack of fluorescence within *L. monocytogenes* is not due to the protein being toxic to the cells and having an adverse effect on their growth. It also suggests that the *gfp* is not being overexpressed within the cells resulting in inclusion body formation, as lower levels of GFP production within *L. monocytogenes* does not increase the overall fluorescence of the population, heterogeneity is observed with only a small proportion of the cells fluorescing. However, it may be possible that these variants simply turnover too rapidly for a visible signal to be detected. All the cells may be producing GFP but at levels the eye cannot detect.

3.5.2. Disrupting translation of GFP at the 5' coding region

Another method was employed to try and lower the levels of *gfp* expression within the bacteria. Using PCR, the Gram positive ribosome binding site (RBS) at the 5' coding region of the stable *gfp3* was changed to one that would be poorly recognised

by the bacteria. This was achieved by replacing the Gram positive RBS in the forward PCR primer with one which would be poorly recognised, details of the primers used, primers 2 and 4, are given in Appendix 1. It was predicted that this approach would restrict the number of ribosomes attaching and initiation translation, thus reducing total expression of the protein within the bacteria. Hence if over-expression of the protein within the bacteria was an issue, then this procedure should alleviate the problem.

The new primer, that would allow the protein to be poorly translated, was used to amplify *gfp3* by PCR, using a 30 cycle reaction with an annealing temperature of 50°C for one minute followed by a 1 minute period of DNA extension at 72°C. This generated a PCR product of 800bp, named *gfp3p/t*.

The *gfp3p/t* PCR product contained *SmaI* and *SalI* restriction sites at the 5' and 3' ends of the coding sequence respectively. These enzymes were used to restrict the *gfp3p/t*, which was then ligated with pGC4 that had been digested with the same restriction enzymes. The ligated DNA was used to transform *E. coli* JM109 competent cells by electroporation, colonies containing recombinant DNA were isolated following selection on ampicillin selective agar. The resulting transformants were examined under blue light and any colonies that fluoresced green were isolated for further investigation. DNA was prepared from some of the fluorescent colonies by plasmid miniprep. This DNA was then restricted with *SmaI* and *SalI* in an attempt to drop out the cloned *gfp3p/t*, electrophoresed on an agarose gel, which was then examined for the presence of an 800bp fragment. Such a band was obtained from all the fluorescent colonies investigated, suggesting that the *gfp3p/t* had successfully integrated downstream of P_{xyn} , the resulting construct was termed pSB2009. This *gfp* expression vector was prepared on a large scale from recombinant *E. coli* cells by plasmid maxi prep.

pSB2009 was then introduced into *L. monocytogenes* by electroporation, cells containing recombinant DNA were isolated following selection on chloramphenicol

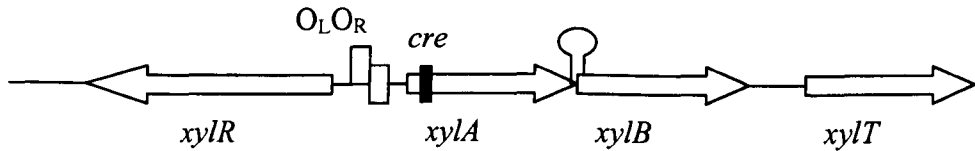
selective agar plates. Those colonies obtained were not seen to fluoresce under blue light excitation, so a single colony was mounted in PBS on a glass slide and observed by fluorescence microscopy, but no fluorescent cells could be seen under blue light excitation. This showed that lower levels of *gfp3* expression did not produce homogeneous fluorescent *L. monocytogenes* populations. This suggests that the protein was not being packaged into non-fluorescent inclusion bodies as lower expression does not increase the fluorescence of the population. Inclusion bodies tend to form when the GFP is produced in excess, this can result in the chromophore being unable to fold or folding incorrectly and the native protein aggregates and occludes in the cell. However, it is possible that translation within the cell has been disrupted to such an extent that the bacteria are no longer translating any *gfp* within the cell.

3.6. Cloning a new promoter upstream of *gfp*

In order to try and increase the fluorescence characteristics of *L. monocytogenes* expressing *gfp*, it was decided to express the reporter from a different promoter. The promoter that was chosen was the xylose regulatable promoter from *Bacillus megaterium*. This system is illustrated in Figure 3.6.1.

D-xylose is an abundant carbon source in nature, and many bacteria are able to utilise it. The xylose utilisation genes *xyIA* (encoding xylose isomerase) and *xyIB* (encoding xylooligase) are clustered and co transcribed in a number of organisms, including *E. coli* (Lawlis *et al.*, 1984) and *Bacillus megaterium* (Rygus *et al.*, 1991). Nevertheless, despite the uniformity in the xylose utilisation genes, there are large differences in xylose uptake depending on the species concerned.

Figure 3.6.1: Genetic organisation of the xylose-utilisation determinant in *B. megaterium*, adapted from Schmiedel *et al.* (1997). The genes involved in xylose utilisation are indicated by arrows. *xylR* encodes the Xyl repressor, *xylA*, *xylB* and *xylT* are co-transcribed from the *xyl* promoter. The *xyl* operator is denoted by O_LO_R indicating the fact that two overlapping binding sites for the Xyl repressor are present (Dahl *et al.*, 1994). *cre* indicates the catabolite responsive element (Hueck *et al.*, 1994; Hueck and Hillen, 1995).



The *xyl* operon in *B. megaterium* is negatively regulated by the xylose inducible Xyl repressor (XylR) (Rygu and Hillen, 1992; Dahl *et al.*, 1995). The operon is also subject to carbon catabolite repression mediated by the *trans* factor CcpA (Hueck *et al.*, 1995) which binds to the catabolite responsive element (*cre*) located in the coding sequence of *xylA*.

It was decided to clone the *xylR* repressor and the *xylA* promoter (P_{xylA}) from *B. megaterium*, and then use the resulting promoter fragment in order to direct expression *gfp*. PCR was used to amplify the promoter and generate restriction sites at both the 5' and 3' sequence of *xylR*- P_{xylA} . At the 5' end, a *MunI* site was incorporated into the sequence, and at the 3' end, a *SmaI* site was introduced. The sequences of primers 5 and 6 utilised in the reaction are given in Appendix 1.

The PCR was carried out as described earlier in section 2.5.3. *Bacillus megaterium* genomic DNA was prepared from the strain NCTC 10342, this was then utilised as a DNA template in the PCR. In order to amplify the DNA an annealing temperature of 52°C for 1½ minutes was employed in the reaction, followed by a period of DNA

extension at 72°C for 2 minutes. The resulting PCR products were analysed by agarose gel electrophoresis and were seen to be approximately 1.4kb.

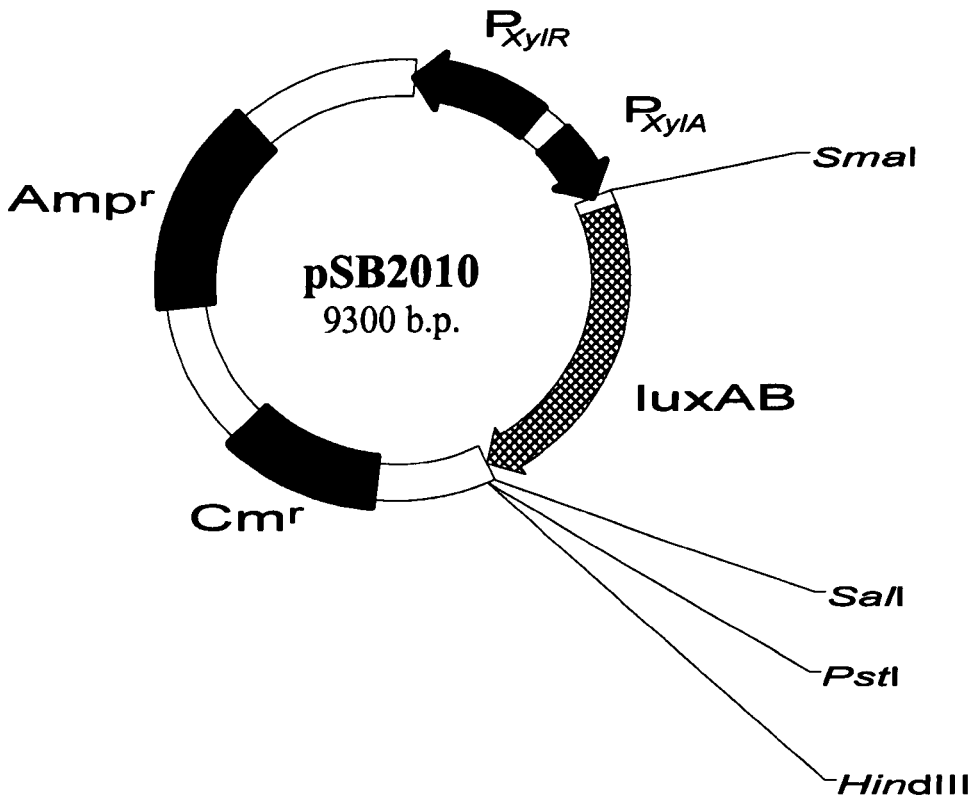
Following electrophoresis of the PCR product on a low melting point agarose gel, the DNA band was excised and purified by freeze thaw extraction. After re-precipitation, the DNA was restricted using *MunI* and *SmaI*, restriction enzymes were then inactivated by phenol chloroform extraction. This digested PCR product was ligated with pGC4 which had had the P_{*xyn*} promoter excised by restriction with *EcoRI* and *SmaI*. The ligated DNA was used to transform *E. coli* JM109 competent cells by electroporation, cells containing recombinant DNA were isolated following selection on ampicillin agar plates with D-xylose added at a final concentration of 0.5%. The resulting transformants were screened in the presence of exogenous aldehyde under a Hamamatsu VIM3 camera and some highly luminescent colonies were observed.

From the phenotypic data, it was unclear as to which promoter the recombinant plasmid contained upstream of *luxAB*. PCR was used to re-amplify the *xyIR*-P_{*xyIA*} fragment which had been cloned upstream of the reporter gene. The reaction was performed as before using the primers designed to this xylose regulatable gene, the sequences of primers 5 and 6 which were utilised in the reaction are given in Appendix 1. Agarose gel electrophoresis of the ensuing PCR products showed that some of the cells contained this new promoter upstream of *luxAB*, as bands of approximately 1.4kb were seen on the gel and these correspond to the size of the new promoter.

Analysis of the recombinant plasmid showed it to be approximately 9.3kb, this construct was designated pSB2010. DNA was prepared on a large scale by plasmid maxiprep, further restriction analysis of the plasmid DNA confirmed the validity of pSB2010, which is illustrated in Figure 3.6.2

On introduction of pSB2010 into electro-competent *L. monocytogenes*, recombinant colonies isolated on BHI agar plates containing chloramphenicol with 0.5% xylose, were seen to be highly luminescent upon the addition of exogenous aldehyde. However, when cells were grown in the absence of xylose, almost no luminescence was seen when exogenous aldehyde was present. This shows that P_{xyIA} gives high, well regulated, expression of genes downstream of the promoter in *L. monocytogenes*.

Figure 3.6.2: Restriction map of pSB2010



3.7. Expressing GFP from the xylose regulated promoter

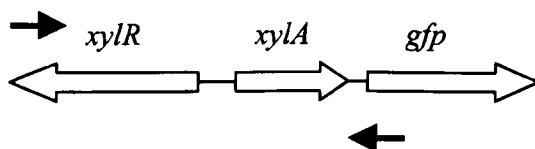
Having isolated a regulated promoter that appeared to strongly express genes in Gram positive bacteria, the next step was to determine whether this promoter would give high expression of the *gfp* variants in *L. monocytogenes*. The aim of the experiment was to excise the *luxAB* fragment from pSB2010 and replace it with the *gfp* variants from pSB2002 and pSB2003. However, the presence of a second *SaII* site downstream of the *xyIR* regulator made a direct exchange difficult. Instead a different cloning strategy was employed to replace the promoter in pSB2002 and pSB2003.

Both pSB2002 and pSB2003 were restricted with *EcoRI* and *SmaI* and the P_{xyn} promoter fragment excised from the DNA by purification from a low melting point agarose gel. P_{xylA} and its regulator *xyIR* were amplified by PCR from *B. megaterium* NCTC 10342 as described earlier in Section 3.6. Again, the ensuing PCR product was restricted with *MunI* and *SmaI*, following phenol chloroform extraction to inactivate the restriction enzymes, this was ligated with the digested *gfp* expression vectors, pSB2002 and pSB2003. Competent *E. coli* JM109 cells were electroporated with the ligated DNA and recombinant colonies were isolated following selection on ampicillin selective agar plates with 0.5% xylose. The resulting transformants were screened under UV or blue light, depending on the *gfp* variant used, any fluorescent colonies were isolated and further investigations carried out to verify whether these plasmids contained the new xylose regulated promoter.

Those colonies that exhibited fluorescence characteristics under excitation conditions were screened using PCR. The reaction was performed using primers 5 and 7 listed in Appendix 1, these were the 5' primer to P_{xylA} and a *gfp* reverse sequencing primer which reads out from the 5' end of the coding sequence of *gfp*, this is illustrated in Figure 3.7.1. It can be seen that the only way a PCR product could be generated was if P_{xylA} had correctly ligated upstream of *gfp*. If the original P_{xyn} promoter has not

been excised fully from pSB2002 and pSB2003 then no PCR product will be generated.

Figure 3.7.1: Diagram to show how PCR was used to screen for transformants containing the new xylose promoter. Filled black arrows depict PCR primers and their location with regards to the DNA sequence.



In order to carry out this reaction new PCR parameters had to be established. Again 30 cycles were utilised, these contained an annealing temperature of 50°C for 1½ minutes, followed by a period of DNA extension for 3 minutes at 72°C. Upon analysis of the PCR products by agarose gel electrophoresis, it was apparent which of the recombinant colonies contained the new promoter fragment, as bands of around 1.4kb were present on the gel. The only way that a band of this size can be generated is if P_{xylA} has inserted upstream of the *gfp* variant. The construct containing *gfp_{wt}* downstream of P_{xylA} was designated pSB2011, and the equivalent one housing *gfp₃* was named pSB2012. These *gfp* expression vectors were then prepared on a large scale from recombinant *E. coli* cells by plasmid maxiprep. Both these plasmids were been mapped and are essentially the same, except for the *gfp* variant that they contain, and are illustrated in Figure 3.7.2.

Both pSB2011 and pSB2012 were introduced into *L. monocytogenes* by electroporation of competent cells. Cells containing recombinant DNA were isolated following selection on chloramphenicol selective agar plates containing 0.5% xylose, however, these recombinant colonies were not seen to fluoresce under the correct

excitation wavelength. The recombinant colonies were then examined by fluorescence microscopy to determine the fluorescence characteristics of individual cells. Once more, it was seen that when cells were grown in the presence of 0.5% xylose, only a proportion of the cells fluoresced green upon excitation. However, the number of fluorescent cells appeared greater when the *gfp* was expressed from P_{xylA} compared with expression from P_{xyn} , so the overall fluorescence of the population had been increased, but the population as a whole was still not homogeneously fluorescent. When cells were grown on chloramphenicol agar plate with no added xylose, a small percentage of the cells fluoresced green under excitation conditions, but numbers were very small. This shows that the promoter does indeed appear to be well regulated in *L. monocytogenes* although it cannot be completely inhibited. The fluorescence characteristics of the cells are depicted in Figures 3.7.3a, b, c, d.

Figure 3.7.2: Restriction map of pSB2011 and pSB2012

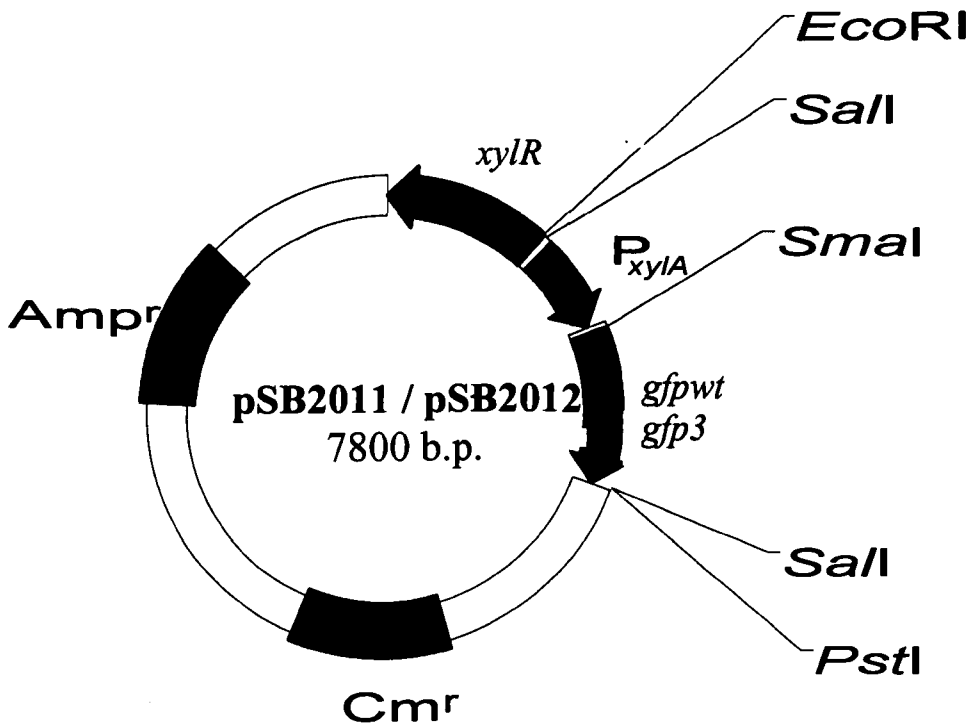


Figure 3.7.3a and b: *E. coli* (pSB2012) and *E. coli* (pSB2011) Cells were grown in the presence of 0.5% xylose

Comparison of fluorescence characteristics of *E. coli* expressing *gfpwt* and *gfp3*, note the brighter signal from *gfp3*

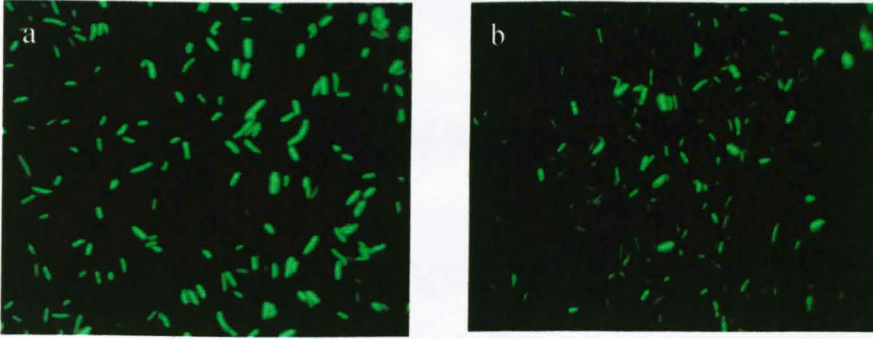
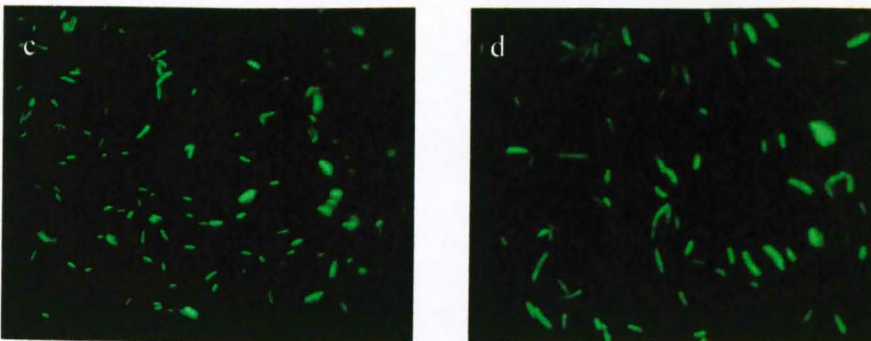


Figure 3.7.3c and d: *L. monocytogenes* (pSB2012) and *L. monocytogenes* (pSB2011) Cells were grown in the presence of 0.5% xylose

Note the brighter signal from cells expressing *gfp3* compared to those expressing *gfpwt*, also total number of fluorescent cells is lower compared to *E. coli* harbouring the same constructs



It could be seen that cells harbouring pSB2011, the wild type GFP construct, fluoresced with a much lower intensity than cells expressing *gfp3* from pSB2011. The signal generated from cells expressing pSB2012 was also more stable than its wild type counterpart, which tended to lose signal brightness upon excitation for prolonged periods. These observations are in accordance with Cormack *et al.* (1996) and prove that the signal generated from *gfp3* is of a greater intensity than the fluorescent signal generated from the wild type protein.

From the data gathered so far, it appears that fluorescence of GFP in *L. monocytogenes* is partially limited by the strength of the promoter that is being used, as P_{xylA} appears to give a better signal compared to that generated from P_{xyn} . Some other factor is limiting production of fluorescent protein within the cells.

A number of factors may be responsible for poor expression of *gfp* in the recombinant organisms; 1. Transcription of the *gfp* gene may be truncated, resulting in partial synthesis of the GFP protein; 2. Translation of the *gfp* could be poorly initiated or prematurely terminated resulting in a truncated, non-fluorescent protein within the cells; 3. The *gfp* may be translated but the chromophore is unable to fold properly resulting in non-fluorescent protein.

3.8. Northern Blot Analysis of *L. monocytogenes* harbouring GFP expression Vectors.

In order to determine whether a full length mRNA transcript was being transcribed from *gfp*, RNA was extracted from *L. monocytogenes* cells harbouring the *gfp* expression vectors, pSB2002 and pSB2003, and also *E. coli* JM109 cells containing the same plasmids. RNA was taken from the *E. coli* cells in order to provide a positive control for the Northern blot, as it is clear in these cells a full length transcript is being generated as all individual cells were seen to fluoresce under examination by fluorescence microscopy. These plasmids were chosen as *L.*

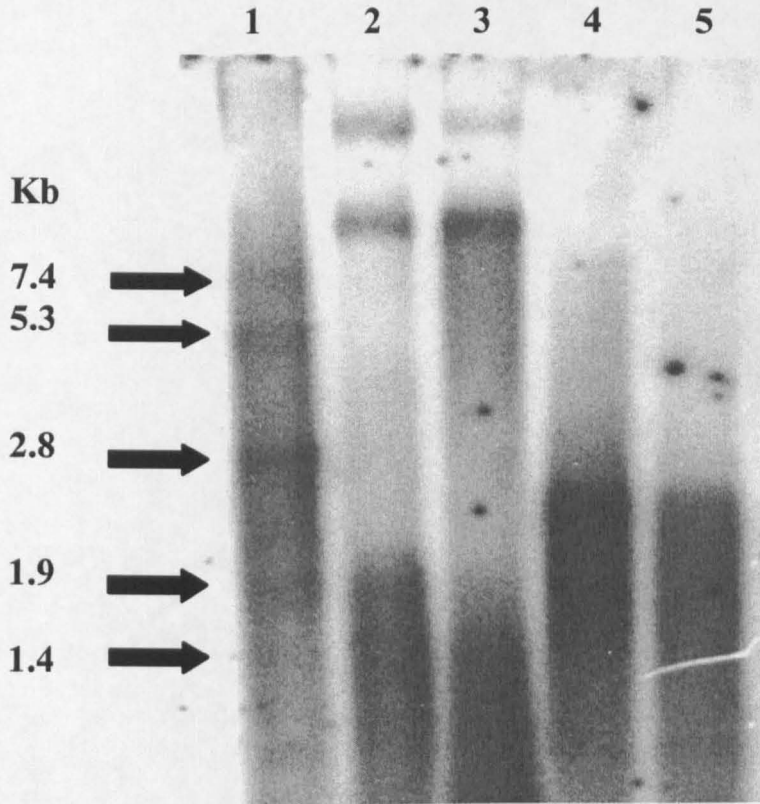
monocytogenes harbouring these constructs were the least fluorescent of all those obtained so far.

After transfer to nylon membrane, the blot was probed with a random primed DIG-labelled *gfp* probe, made from the whole gene. In order to determine if any transcript was present, CDP-Star was used as the chemiluminescent substrate to detect the probe and the blot then exposed to film as described in the methods section.

Following development of the film, it could be seen that in samples taken from both *E. coli* and *L. monocytogenes* a large amount of full length transcript was seen from the transformed bacteria. This is illustrated in Figure 3.8.1.

The *gfp* gene is approximately 800bp and thus it would be expected that an RNA transcript of at least the same length would be produced. It can be seen from the blot that a transcript of around 2kb is produced, this is much greater than that expected. However, it should be noted that these *gfp* expression vectors do not contain a transcriptional terminator, thus there is no defined stop region for RNA transcription to cease. This would explain the fact that the transcript is much larger than that expected, also as there is no defined area for transcription to cease, it could also explain why a smear is seen down the blot rather than a defined band although this could also be attributed to degradation of the RNA. As there is no transcriptional terminator, the RNA polymerase could have generated transcripts of many different sizes, and hence the apparent smear down the blot. Nevertheless, these results indicate that it is not transcription that is inhibiting to GFP production within Gram positive cells, and it may be a translational problem. It is a possibility that the cells are not translating the mRNA into GFP protein, or maybe only part of the mRNA is being translated, resulting in a truncated non-fluorescent GFP protein.

Figure 3.8.1: Northern Blot showing a full length mRNA transcript is generated from transformed bacteria harbouring *gfp* expression vectors.



Lane1: Dig labelled Markers (Boehringer Mannheim)

Lane2: *E. coli* (pSB2002)

Lane3: *E. coli* (pSB2003)

Lane4: *L. monocytogenes* (pSB2002)

Lane5: *L. monocytogenes* (pSB2003)

3.9. Translational Analysis of Transformed Bacteria Harboured *gfp* Expression vectors

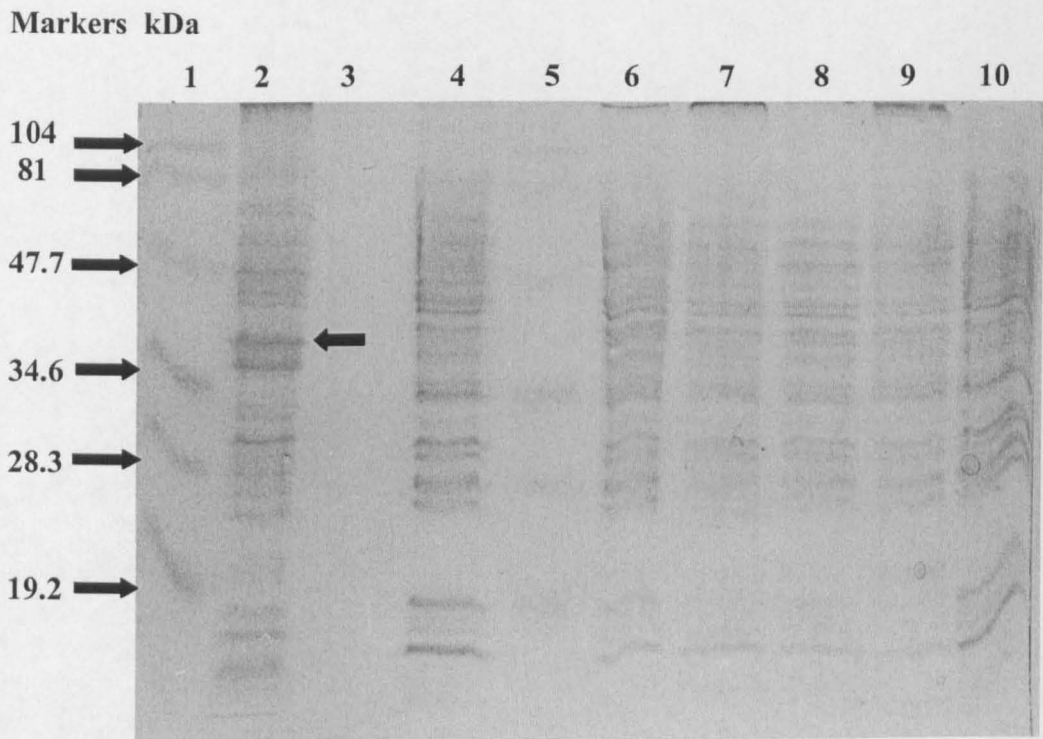
The results of the transcript analysis suggested that a full length mRNA was being produced in *L. monocytogenes* harbouring *gfp* expression vectors. It appears that there is some problem with translation of this mRNA into protein in these Gram positive cells.

In order to investigate translation of mRNA into protein, whole cell extracts were prepared of *L. monocytogenes* cells harbouring the *gfp* expression vectors pSB2002 and pSB2003. As control samples, protein was extracted from non-recombinant *L. monocytogenes* cells, and also from *L. monocytogenes* (pGC4). In addition to the *L. monocytogenes* cell extracts, whole cell protein extracts were prepared from *E. coli* harbouring the same *gfp* expression vectors. As these cells are green under excitation conditions they are producing full length functional protein, and would thus act as a positive control on the Western blot.

Protein samples were run on a 14% SDS PAGE gel and then transferred to nitrocellulose membrane by semi-dry blotting. A polyclonal antibody to GFP, (Clontech), was used to detect whether the bacteria were producing any GFP peptide. The GFP primary antibody was used at a dilution of 1:2000. After removal of excess primary antibody, the membrane was then incubated with an anti-rabbit alkaline phosphatase secondary antibody conjugate. Upon incubation with substrate, in this case CDP-Star, if protein was present on the membrane, the substrate would react with the bound secondary antibody, thus causing the production of a chemiluminescent signal. The results of the immunoblots from cells harbouring pSB2002 and pSB2003 are shown in Figure 3.9.1. and 3.9.2. respectively.

Figure 3.9.1a: SDS PAGE gel of bacteria harbouring pSB2002.

All samples are whole cell extracts taken from overnight bacterial cultures



Layout of Samples on SDS Page gel:

Lane 1: low range molecular weight markers (Biorad)

Lane 2: *E. coli* (pSB2002), GFP indicated by arrow on gel

Lane 3: Blank

Lane 4: *L. monocytogenes* (pSB2002)

Lane 5: Low range molecular weight markers

Lane 6: *L. monocytogenes* (pSB2002)

Lane 7: *L. monocytogenes* (pGC4)

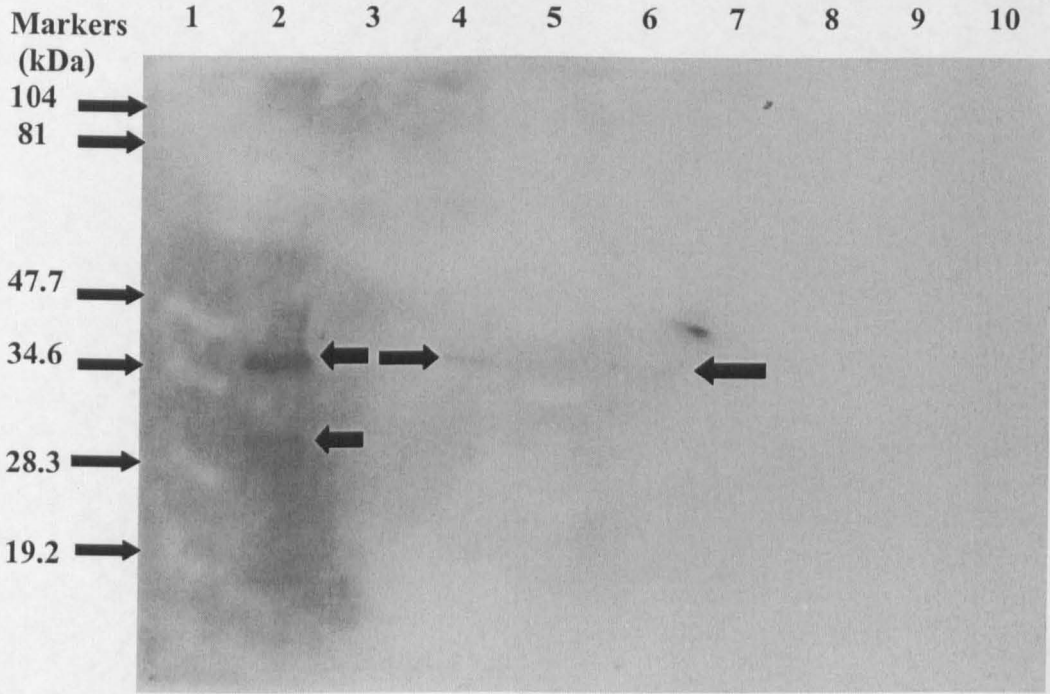
Lane 8: *L. monocytogenes* (pSB2002)

Lane 9: *L. monocytogenes* (non-recombinant cells)

Lane 10: *L. monocytogenes* (pSB2002)

Figure 3.9.1b: Western blot of bacteria harbouring pSB2002

All samples are whole cell extracts taken from overnight bacterial cultures



Layout of Samples on Western Blot:

Lane1: low range molecular weight markers (Biorad)

Lane 2: *E. coli* (pSB2002) GFP indicated by arrow on blot

Lane 3: Blank

Lane 4: *L. monocytogenes* (pSB2002) GFP indicated by arrow on blot

Lane 5: Low range molecular weight markers

Lane 6: *L. monocytogenes* (pSB2002) GFP indicated by arrow on blot

Lane 7: *L. monocytogenes* (pGC4)

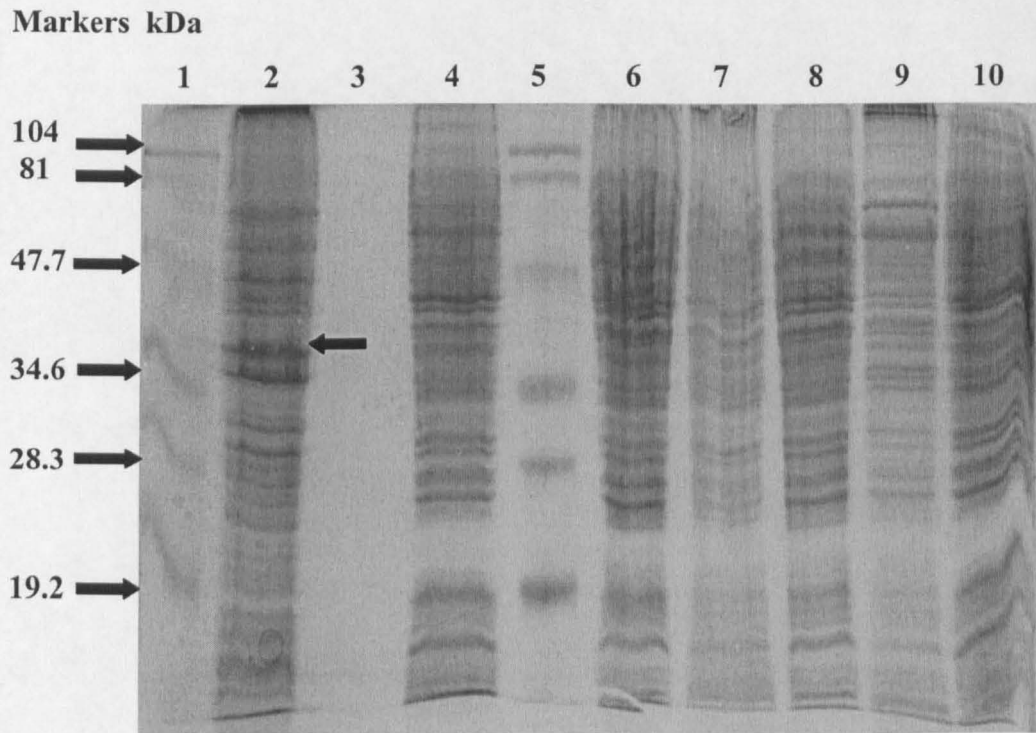
Lane 8: *L. monocytogenes* (pSB2002)

Lane 9: *L. monocytogenes* (non-recombinant cells)

Lane10: *L. monocytogenes* (pSB2002)

Figure 3.9.2a: SDS PAGE gel of bacteria harbouring pSB2003.

All samples are whole cell extracts taken from overnight bacterial cultures

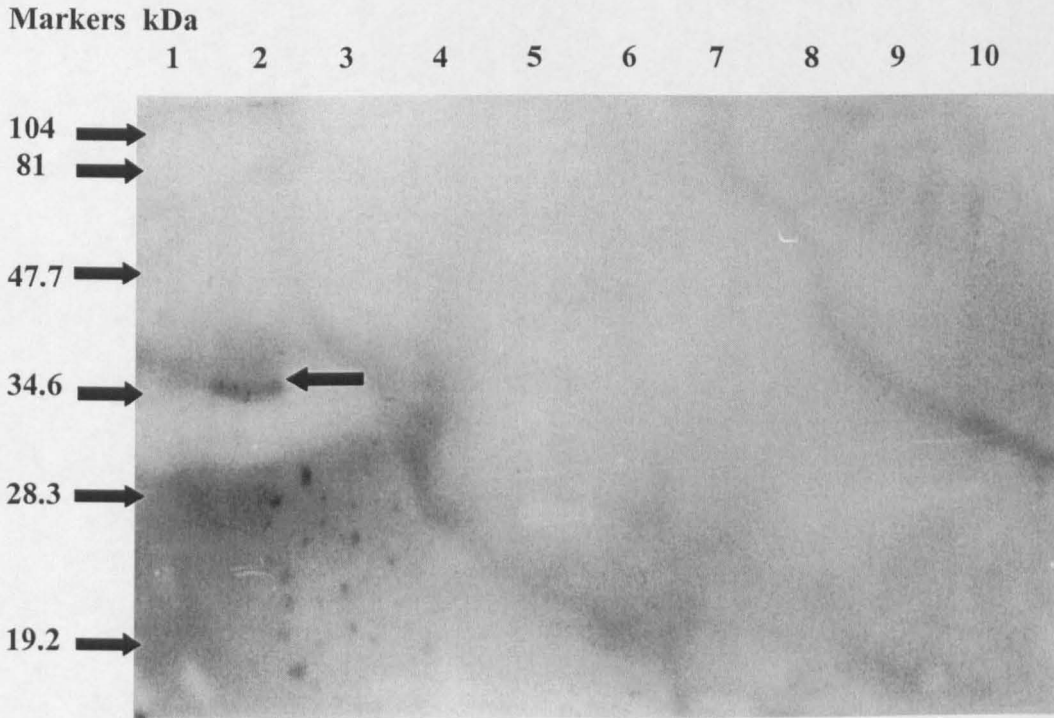


Layout of Samples on SDS Page gel:

- Lane 1: low range molecular weight markers (Biorad)
- Lane 2: *E. coli* (pSB2003) GFP indicated by arrow on gel
- Lane 3: Blank
- Lane 4: *L. monocytogenes* (pSB2003)
- Lane 5: Low range molecular weight markers
- Lane 6: *L. monocytogenes* (pSB2003)
- Lane 7: *L. monocytogenes* (pGC4)
- Lane 8: *L. monocytogenes* (pSB2003)
- Lane 9: *L. monocytogenes* (non-recombinant cells)
- Lane 10: *L. monocytogenes* (pSB2003)

Figure 3.9.2b: Western Blot of bacteria harbouring pSB2003

All samples are whole cell extracts taken from overnight bacterial cultures



Layout of Samples on Western Blot:

- Lane 1: low range molecular weight markers (Biorad)
- Lane 2: *E. coli* (pSB2003) GFP indicated by arrow on blot
- Lane 3: Blank
- Lane 4: *L. monocytogenes* (pSB2003)
- Lane 5: Low range molecular weight markers
- Lane 6: *L. monocytogenes* (pSB2003)
- Lane 7: *L. monocytogenes* (pGC4)
- Lane 8: *L. monocytogenes* (pSB2003)
- Lane 9: *L. monocytogenes* (non-recombinant cells)
- Lane 10: *L. monocytogenes* (pSB2003)

It can be seen from Figures 3.9.1 that the *E. coli* cells harbouring pSB2002 produce a large amount of full length protein. It is known that this is functional protein as cells expressing *gfp* from this plasmid are all green. However, as well the full length protein, there is also a large amount of a smaller peptide which also cross reacts with the antibody. This may be a truncated GFP so is non-fluorescent, as the whole GFP protein is needed to provide the correct environment for the chromophore. Another possibility for the appearance of these smaller products is that an *E. coli* protein has cross reacted with the antibody.

When *L. monocytogenes* cells express *gfp* from pSB2002, a faint band around 30kDa can be seen on the membrane after the detection process has been carried out, shown in Figure 3.9.1b. However, levels of protein appear to be much lower than comparable samples from *E. coli*. This suggests that translation within the *L. monocytogenes* cells is not as efficient as that in *E. coli*. In the *L. monocytogenes* samples, no truncates or evidence of a degraded GFP protein can be seen on the membrane.

Similar results were observed from bacteria harbouring pSB2003, the *gfpwt* expression vector, illustrated in Figure 3.9.2. Again, with the whole cell extracts prepared from *E. coli*, a large amount of protein was seen at around 30kDa on the immunoblot, in this case almost no protein of the predicted size was detected from equivalent samples of *L. monocytogenes*.

The data gained from analysis of mRNA by Northern blot, illustrated in Figure 3.8.1, showed that a large amount of full length mRNA was produced by *L. monocytogenes* harbouring the *gfp* expression vectors. As no truncated GFP was seen from protein samples of *L. monocytogenes* cells harbouring the *gfp* expression vectors, it appeared unlikely that translation of the *gfp* was terminated prematurely. Nevertheless, it is known from the Western blots that translation of the protein is poor within the *L. monocytogenes* cells, as almost no protein was detected from the immunoassays. There are several possible explanations for the lack of GFP protein in the *L.*

monocytogenes cells and these will be discussed in detail throughout the rest of the chapter.

It may be that poor codon usage within the bacteria or secondary mRNA structure is responsible for lack of fluorescent protein. The Western blots suggested the translation was not prematurely terminated, however, if a hungry codon (Kurland and Gallant, 1996) was nearer the start of the gene, then this would result in a partial GFP protein that would be too small to resolve on a 14% gel. Another possible explanation for the lack of fluorescent protein within the *L. monocytogenes* cells could be poor initiation of translation by the ribosomes within the cells. Perhaps the Shine-Dalgarno sequence is not strong enough for translation to initiate efficiently in Gram positive organisms.

3.10. Removal of a Potential Ribosome Stall site from GFP

A sequence with high similarity to a Gram positive ribosome binding site (RBS) was identified five base pairs downstream of the start codon of both GFPwt and GFP3. In Gram positive bacteria such sequences can function as ribosomal stall sites thus leading to an overall decrease in the protein yield (Spanjaard and Van Duin, 1988). The sequence of a strong Gram positive RBS is AGGAGG, and there is a homologous sequence at the start of *gfp*. At such sites, the ribosome may cease its progression along the mRNA and as a consequence of this translation would cease. If in Gram positive organisms the majority of ribosomes were stalling at this RBS at the start of *gfp*, this may explain why only low levels of protein can be isolated from *L. monocytogenes*. As this potential stall is close to the start, this may explain why no truncated GFP was isolated from whole cell extracts of *L. monocytogenes*, translation may be terminating prematurely, but the resulting truncate may be too small to resolve on an SDS-PAGE gel. It was therefore decided to remove this sequence, from the GFP3 protein, and replace it with the corresponding sequence from *egfp* (Clontech) which does not contain a potential stall site. *gfp3* was chosen as this

variant of *gfp* produces a much brighter signal upon excitation compared to that of the wild type protein (Cormack *et al.*, 1996)

PCR was used to generate a new protein where the potential stall site had been replaced with the equivalent sequence from *egfp*, another red shifted *gfp* variant which has been codon optimised for maximal expression in mammalian systems (Hass *et al.*, 1996). The primer to the 5' end of the gene incorporated a *SmaI* restriction site and seven bases of the *gfp3* gene were exchanged for equivalent bases from the *egfp* sequence. The bases that were replaced corresponded to the potential stall site that was five base pairs downstream from the ATG start. The rationale for the primer design is illustrated in Figure 3.10.1, and a more detailed description of the primers used, primers 2 and 8, is given in Appendix 1. The 3' end of the gene was amplified so as to contain a *SalI* restriction site. The same PCR conditions that have been described previously were used to amplify the altered *gfp3* gene.

Figure 3.10.1: Rational behind removal of the potential stall site from *gfp3*

gfp3 Sequence:

Potential Stall Site

5' ATG AGT AAA GGA GAA GAA CTT TTC ACT GGA G
 Proteins: M S K G E E L F T G

egfp Sequence:

5' ATG GTG AGC AAG GGC GAG GAG CTG
 Proteins: M V S K G E E L

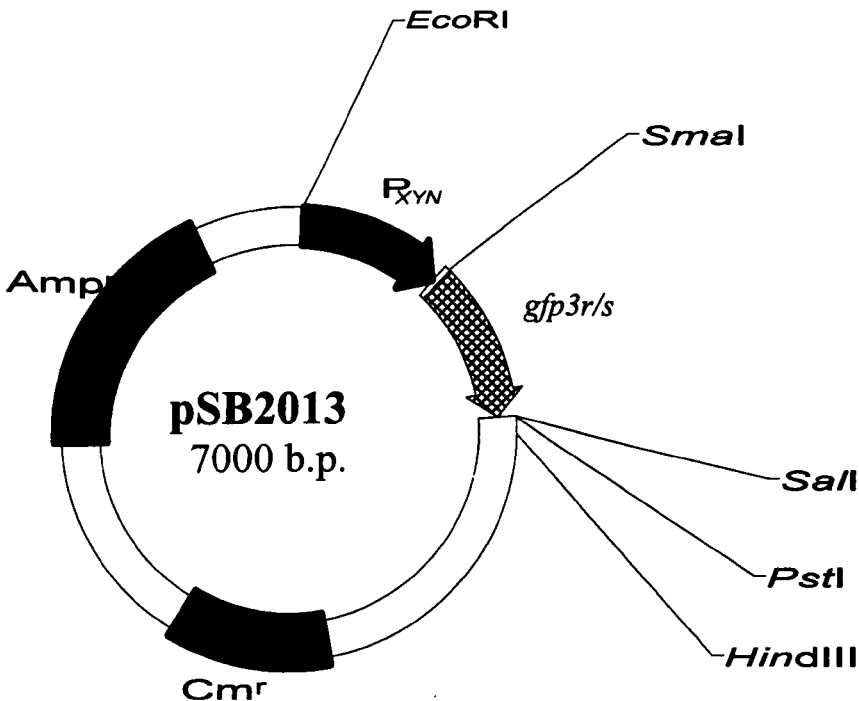
gfp3 sequence where potential stall site has been replaced with corresponding sequence from *egfp*:

exchanged bases

5' ATG AGT AAC AAG GGC GAA CTT TTC ACT GGA GTT G
 Proteins: M S N K E E L F T G V

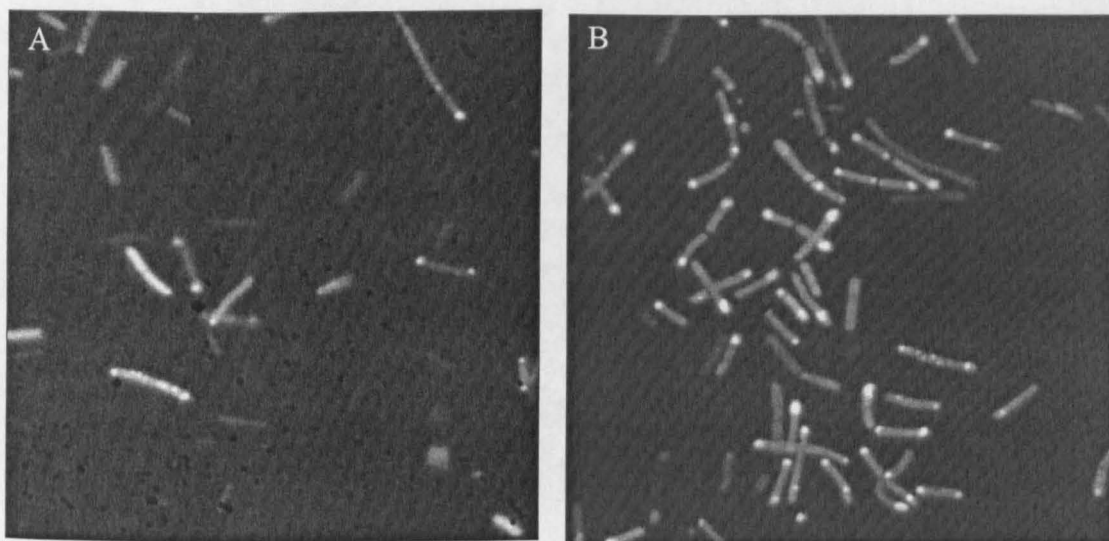
Following amplification of this altered *gfp3* gene (*gfp3r/s*), the PCR product was restricted with *SmaI* and *SalI*. This was then ligated with pGC4 that had been restricted with the same enzymes and the *luxAB* fusion excised from it. The ligated DNA fragments were then used to transform competent *E. coli* JM109 cells. Recombinant colonies were isolated following selection on antibiotic agar plates. The resulting transformants were screened for *gfp* expression using blue light in order to identify positive clones. Fluorescent colonies were isolated and DNA extracted from the cells by plasmid miniprep. The resulting DNA was restricted with *SmaI* and *SalI* to excise the 800bp *gfp3r/s* fragment that had been cloned into the plasmid vector. A few of the DNA samples did map correctly, one was chosen and a large-scale preparation of the DNA was made by plasmid maxiprep. This plasmid was designated pSB2013.

Figure 3 10.2: Restriction map of pSB2013.



Further restriction analysis was then carried out on the plasmid pSB2013 to verify the validity of the construct. Analysis with a number of restriction endonucleases confirmed that the *gfp3r/s* had successfully integrated into the plasmid downstream of P_{xyM} , pSB2013 is illustrated in Figure 3.10.2. This plasmid, pSB2013, was then introduced into *L. monocytogenes* cells by electroporation of competent cells, recombinant cells were isolated following selection on chloramphenicol selective agar, however when subjected to excitation conditions these were not seen to be fluorescent. Individual recombinant colonies were examined by fluorescence microscopy. It was noticed that the *L. monocytogenes* were not uniform in their fluorescence characteristics, the GFP protein appeared to be localised at the bacterial poles and fluorescence was not regular along the length of the cell. The same plasmid was also introduced into *B. subtilis* 168 cells to see if this phenomenon was seen in other Gram positive bacteria or whether it was specific to *L. monocytogenes* cells. Upon examination under fluorescence microscopy, the *B. subtilis* also showed localisation of GFP at the bacterial poles. This is illustrated in Figure 3.10.3.

Figure 3.10.3: Gram positive bacteria harbouring pSB2013. Figure A: shows *L. monocytogenes* (pSB2013), Figure B: shows *B. subtilis* (pSB2013). Note the localisation of fluorescent GFP at the bacterial poles.



It was not understood why fluorescent protein was seen at specific locations along the length of the cell. Several explanations have been proposed. The work of Neelson and Escher (1998), suggests that the aggregation of GFP within the bacterial cells is due to expression of chaperonins. Through the use of a 104kDa luciferase-GFP fusion protein, they postulated that overexpression of both *groES* and *groEL* genes caused an increase in both soluble and aggregated luciferase-GFP fusion protein amounts, with an overall increase in GFP fluorescence. When cells expressing this fusion protein alone also overexpressed *groEL* only, lower levels of soluble and aggregated luciferase-GFP protein amounts were seen. The fact the GFP was functional in both the soluble and aggregated forms suggested that the aggregation and solubility of the fluorescent protein was dependent on its luciferase moiety, as no foci could be observed when *gfp* alone was expressed. Their results indicated that the GFP protein could be used to visualise chaperonin-mediated folding *in situ*. However, this *gfp3r/s* only contains 3 changed amino acids compared to that of *gfp3* and so this theory seems unlikely as the same event does not occur when other GFP vectors have been expressed in Gram positive bacteria.

In order to investigate why this was occurring, a reverse sequencing primer was made to the start of the *gfp* in order to sequence back out into the plasmid, primer 7 in Appendix 1. Examination of the sequence data suggested that a fusion protein was being made to the start of *gfp*. This sequence was then compared with other sequences in the 'owl' database, and the fusion protein was found to have a 94% identity to XynB *Bacillus pumilus* beta-xylosidase. It appears that *gfp3r/s* is translationally fused to the *Bacillus pumilus* XynB' peptide downstream of P_{xyn}. The construction of this fusion has caused the localisation of GFP3r/s at the bacterial poles, perhaps indicating the localisation properties of XynB.

As cloning *gfp3r/s* downstream of P_{xyn} appeared to have caused the production of a fusion protein that targeted specific areas of the bacteria, it was decided to express *gfp3r/s* from P_{xylA} from *B. megaterium*. This was done to see if the fusion protein was responsible for the aggregation of GFP or whether changing the 3 amino acids near the start of the coding sequence had created a targeting motif, which was responsible

for the localisation of the protein. If this was the case, then the protein would be expected to localise regardless of which promoter it was expressed from.

P_{xylA} and its regulator *xylR* were amplified by PCR from genomic *B. megaterium* DNA as previously described in Section 3.6. The resulting PCR product was restricted with *MunI* and *SmaI* and ligated with pSB2013 which had had P_{xyn} excised from it following digestion with *EcoRI* and *SmaI*. Following ligation of the two purified DNA fragments, the DNA was introduced into *E. coli* JM109 competent cells by electroporation. Recombinant colonies were isolated following selection on ampicillin selective agar plates. The resulting transformants were screened with blue light excitation in order to identify positive clones. However, as one promoter had been exchanged for another, it was impossible to determine from phenotypic analysis of the transformants whether the new promoter had been successfully cloned into the plasmid. Colonies that were seen to fluoresce under excitation conditions were examined by restriction analysis of plasmid DNA. DNA was prepared from cells by plasmid miniprep, this was digested with *EcoRI* and *SaII* in an attempt to excise P_{xylA} and *gfp3r/s*, a fragment of 1.3kb. One DNA sample appeared to contain the new promoter upstream of *gfp3r/s*, but in order to confirm this another PCR was carried out using those colonies thought to contain the new promoter. This time, the *xylR* forward primer was used in conjunction with the *gfp* reverse sequencing primer that was available, primers 5 and 7 respectively in Appendix 1, the reaction was performed as described in section 3.6. The resulting PCR products were electrophoresed on an agarose gel, some were seen to contain a product of approximately 1.3kb. This was assumed to be the promoter fragment and a small segment of the 5' coding region of *gfp3r/s*. This PCR proved that some of the recombinant colonies did indeed contain the new promoter upstream of *gfp3r/s*. This can be seen in Figure 3.10.5.

After positive identification of recombinant colonies containing the new plasmid, designated pSB2014, DNA was prepared on a large scale by plasmid maxiprep, this was then examined further by restriction analysis. The restriction map of pSB2014 is illustrated in Figure 3.10.6.

Figure 3.10.5: Agarose gel of PCR products amplified from colonies thought to contain P_{xyIA} upstream of *gfp3r/s*.

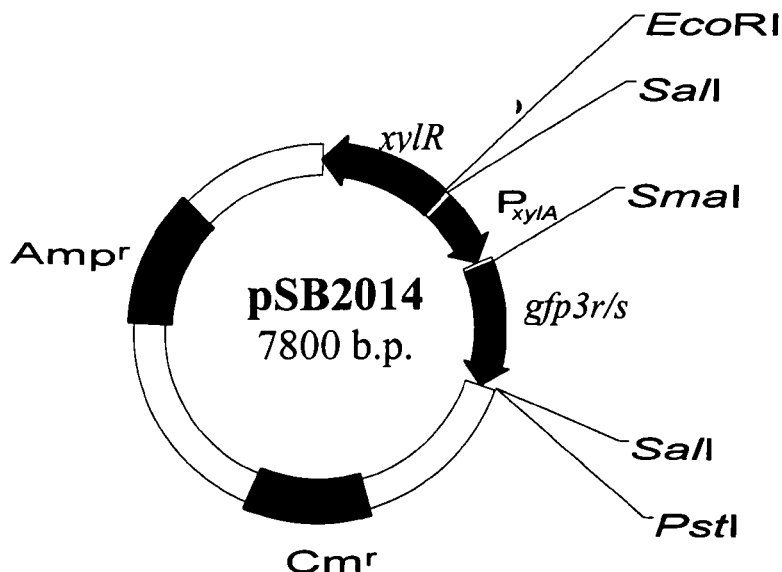


Lane 1: Lambda *Hind*III (MBI)

Lane 2-16: PCR product from colonies thought to contain P_{xyIA} upstream of *gfp3r/s*

Lane 17: Negative Control (no DNA template in PCR reaction)

Figure 3.10.6: Restriction map of pSB2014.



The *gfp* expression vector, pSB2014 was then introduced into *L. monocytogenes* by electroporation of electrocompetent cells, recombinant cells were isolated following selection on chloramphenicol agar plates. In order to de-repress *P_{xylA}*, xylose was added to the BHI agar plates at a concentration of 0.5%. Individual *L. monocytogenes* colonies were not seen to fluoresce under excitation conditions, when individual cells were observed by fluorescence microscopy, not all cells showed a fluorescent phenotype, a large percentage of the cells were non-fluorescent. However, with those cells that were fluorescent the fluorescence was uniform along the length of the cell and not localised at specific areas along the cell.

These data suggest that it is the fusion of *gfp3r/s* to the XynB' peptide that is causing the protein to localise within the bacteria. The XynB' peptide itself may localise within the bacteria. It seems unlikely that replacing three amino acids near the start of the gene has created a protein-targeting motif, as when the *gfp3r/s* is expressed

from a different promoter that does not have *xynB* downstream from it then these localisation patterns are abolished. The results of this experiment also suggest that the RBS at the start of *gfp* is not acting as a stall site, as removal of this site from the sequence does not affect the fluorescence characteristics of *L. monocytogenes* cells harbouring the plasmid, that is to say a homogenous fluorescent population has not been achieved.

3.11. Codon Usage and secondary mRNA Structure.

Another possible cause for a lack of functional GFP within all *L. monocytogenes* cells may be codon usage. If the *gfp* contains a number of codons that are found rarely in *L. monocytogenes*, then this may explain why only a small amount of full length GFP can be isolated from the cells. All species have their own set of biases in the use of the 61 amino acid codons. They also have a tRNA population that is closely matched to the overall codon bias of the resident mRNA population (Ikemura, 1981; Dong *et al.*, 1996). The cell only contains a limited number of tRNAs for each amino acid, but there is at least one tRNA present for each amino acid. Within the organism some amino acids are used more frequently than other rarer ones. The set of tRNAs responding to the various codons for each amino acid is distinctive for each organism, and multiple tRNAs may respond to a particular codon. A tRNA has two crucial properties; it is able to represent only one amino acid to which it is covalently linked and it contains a tri-nucleotide sequence, the anticodon, which is complementary to the codon representing the amino acid. The anticodon enables the tRNA to recognise the codon *via* complementary base pairing. So, if the cloned gene, in this case *gfp*, is markedly different in its codon bias to that of its host, the translation of the gene may not proceed to completion or translational errors may be incorporated into the protein. This is due to the fact that high level expression of the *gfp* may place demands on the host protein synthetic apparatus that is not matched to its normal tRNA population.

Study of codon utilisation tables did not show any apparent rare codons within *L. monocytogenes* compared to the sequence of *gfpwt* or *gfp3*, but by using a different *gfp* variant, namely *egfp*, it was possible to determine whether codon usage was affecting translation of *gfp*.

egfp is a red shifted *gfp* variant, which has been codon optimised for maximal translational efficiency in mammalian systems (Cormack *et al.*, 1996). This was achieved by virtue of approximately 190 silent base pair mutations along the length of the gene (Hass *et al.* 1996). Due to the presence of these numerous changes, the codon usage within *L. monocytogenes* is very different to that of *gfpwt* and *gfp3*. Thus if expression of *gfpwt* or *gfp3* places a demand on the tRNA population of *L. monocytogenes*, then expression of *egfp* should result in an entirely different set of tRNAs being used to synthesis protein within the host.

Another possible explanation for the lack of full length GFP produced by *L. monocytogenes* is inhibition of translation by secondary mRNA structure. Normally, a ribosome attaches to mRNA at or near the 5' end of the coding region. As it moves towards the 3' end of the RNA it translates each triplet code into an amino acid. As the ribosome proceeds, the appropriate aminoacyl-tRNAs associate with it, donating their amino acids to the polypeptide chain. At any given moment, the ribosome accommodates the two aminoacyl-tRNAs corresponding to successive codons, which makes it possible for a peptide bond to form between the two corresponding amino acids. If the mRNA has a large amount of secondary structure associated with it, this may prevent, or limit ribosome progression along the mRNA, which may result in little or no full length GFP produced by the *L. monocytogenes* cells.

egfp can also be used to investigate whether mRNA secondary structure is responsible for lack of full-length GFP protein in *L. monocytogenes* cells. Due to the number of differences that *egfp* contains within its coding sequence, its mRNA secondary structure will be altered compared to that of both *gfpwt* and *gfp3* and thus any premature translational termination should be overcome.

Therefore, in order to investigate whether codon usage or mRNA secondary structure were responsible for low levels of active GFP protein in *L. monocytogenes*, *egfp* was expressed from the xylose inducible promoter P_{xylA} .

3.11.1. Cloning EGFP

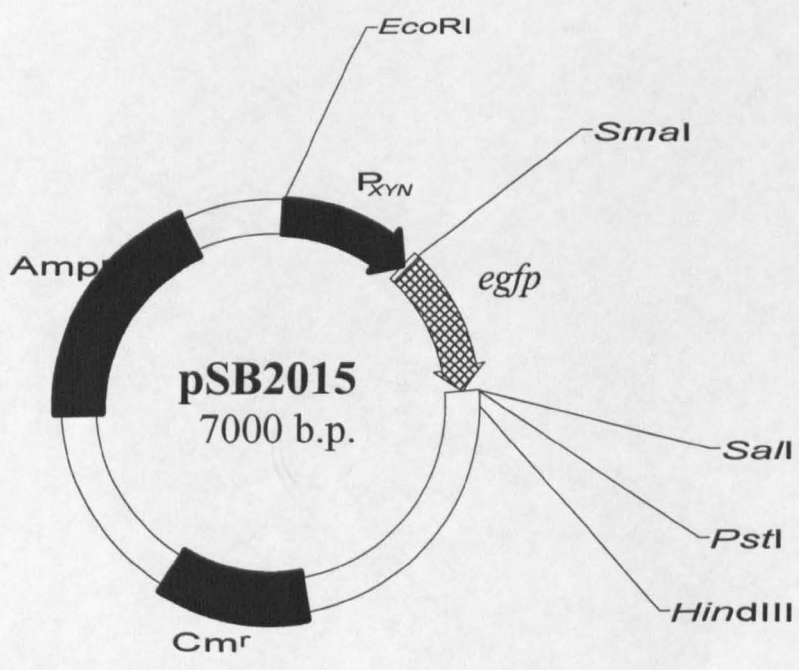
egfp was amplified *via* PCR using plasmid EGFP-1 (Clontech) as template DNA. Primers were designed to the N and C terminal region of the gene, these were designated primers 9 and 10 respectively, and are listed in Appendix 1. The PCR primers incorporated *Sma*I and *Sal*I restriction sites at the 5' and 3' ends of the coding region respectively to facilitate the cloning process. A 30 cycle PCR was carried out that utilised a 1 minute period at 56°C to allow primer annealing and a 1½ minute interval of DNA extension at 72°C. This resulted in the amplification of the 800bp *egfp* gene, that was flanked by the fore-mentioned restriction sites.

The *egfp* PCR product was restricted with *Sma*I and *Sal*I. Following inactivation of the restriction enzymes by phenol chloroform extraction, the restricted PCR product was ligated with pGC4 which had also been restricted with the same enzymes and subsequently purified from a low melting point agarose gel in order to excise the *luxAB* fusion. Following ligation of the purified DNA fragments, the DNA was introduced into competent *E. coli* JM109 cells by electroporation, recombinant colonies were then isolated by plating onto agar plates containing ampicillin. Following incubation at 37°C, resulting transformants were then screened using blue light in order to identify any positive clones. DNA was prepared from fluorescent colonies by plasmid miniprep, this was then subjected to restriction analysis to confirm that the *egfp* had correctly inserted downstream of P_{xyn} . Having isolated a colony that appeared to contain the *egfp* insert, DNA was prepared on a large scale by plasmid maxiprep. Restriction mapping was performed to verify that this new expression vector was correct, this is illustrated in Figure 3.11.1. This plasmid was designated pSB2015 and is illustrated in Figure 3.11.2.

Figure 3.11.1: Restriction analysis of pSB2015

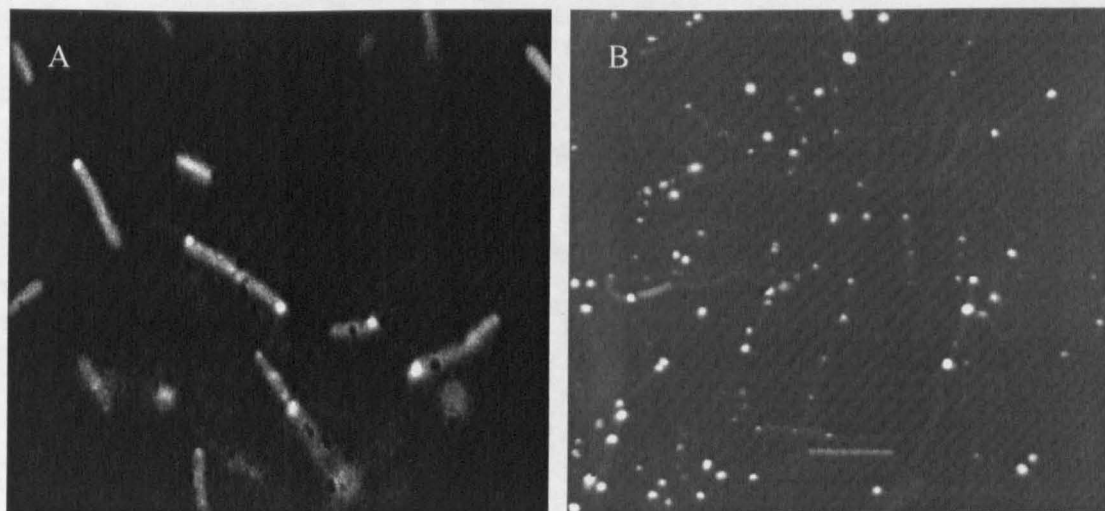


Figure 3.11.2: Restriction map of pSB2015



This *egfp* vector, pSB2015 was then introduced into *L. monocytogenes* competent cells by electroporation. Following isolation of recombinant colonies on chloramphenicol selective agar plates, individual colonies were examined by fluorescence microscopy, this revealed a very strange feature. A high proportion of the population was seen to be fluorescent, but the fluorescence characteristics were not uniform along the length of the cell. The brightest areas of fluorescence were at either one or both of the bacterial poles, with weak fluorescence sometimes seen across the rest of the cell. It was decided to see if this strange phenomenon was a feature of expression of the protein in *L. monocytogenes* or whether the same thing could be observed in other Gram positive bacteria. The plasmid pSB2015 was used to transform *B. subtilis* 168 and transformants were examined under blue light excitation. Again it was noticed that the fluorescence was not uniform and the protein appeared to be localising at specific points, namely the bacterial poles. This can be seen in Figure 3.11.3.

Figure 3.11.3: Expression Characteristics of two Gram positive bacteria harbouring pSB2015. Figure A: *B. subtilis* 168 (pSB2015), Figure B: *L. monocytogenes* (pSB2015).



There are several possible explanations for this occurrence of GFP localisation, but it is still not known what is occurring within the cell. The most likely explanation is that a translational fusion has occurred with *egfp* to the *Bacillus pumilus* XynB' peptide downstream of P_{xyn}. The same localisation patterns of GFP were observed when a similar translational fusion was created between *gfp3r/s* and the XynB' peptide, this was described in Section 3.10. It appears as though it is the construction of this translationally fused protein which is responsible for the localisation of EGFP at the bacterial poles, perhaps indicating where XynB' is localised within the bacterial cell.

In order to determine whether a fusion protein was being made to the XynB' peptide, and to also create a regulatable expression system, it was decided to excise P_{xyn} from pSB2015 using *EcoRI* / *SalI* and replace it with the xylose regulatable promoter P_{xylA} from *B. megaterium*, allowing *egfp* expression from a different promoter. Amplification of this promoter has been described earlier in Section 3.6. The resulting PCR fragment contained *MunI* and *SmaI* restriction sites at the 5' and 3' ends respectively. The PCR fragment was restricted using these enzymes, purified by phenol chloroform extraction and ligated with pSB2015, which had previously had P_{xyn} excised from it following restriction with *EcoRI* and *SmaI* and subsequent purification from a low melting point agarose gel. Ligated DNA was used to transform *E. coli* JM109 competent cells and recombinant colonies were selected on their ability to confirm ampicillin resistance on the bacteria that housed them. The resulting transformants were then observed under blue light in order to screen for positive clones.

As one promoter has been exchanged for another, there was no phenotypic variations between recombinant cells to confirm whether the new promoter had been successfully inserted upstream of *egfp*. It was unsure at this stage if those colonies that fluoresced green under excitation conditions contained P_{xylA} or if carry through of P_{xyn} had occurred.

In order to investigate this the recombinant colonies were checked by colony hybridisation using a Dig-labelled P_{xyIA} promoter fragment as a probe. Both positive (P_{xyIA}) and negative (pSB2015) control samples were included on the blot. Once the colony blot was developed it could be seen that several samples were homologous to the probe as they gave a positive signal. This suggested that these colonies contained P_{xyIA} and its regulator upstream of *egfp*. Results from the colony blot are depicted in Figure 3.11.4.

Although the results of the colony hybridisation suggested that these colonies contained P_{xyIA} , plasmid DNA was prepared by plasmid miniprep from some colonies thought to contain the new expression vector. The resulting DNA was then restricted with *EcoRI* / *SaII*, as a control pSB2015 was restricted in the same manner. If the plasmid contains the new promoter upstream of *egfp*, the restriction analysis would reveal an excised band approximately 400bp smaller than if P_{xyn} was upstream of *egfp*. Results of the restriction analysis are illustrated in Figure 3.11.5.

Figure 3.11.4: Colony hybridisation of Putative colonies thought to express *egfp* from P_{xyIA}

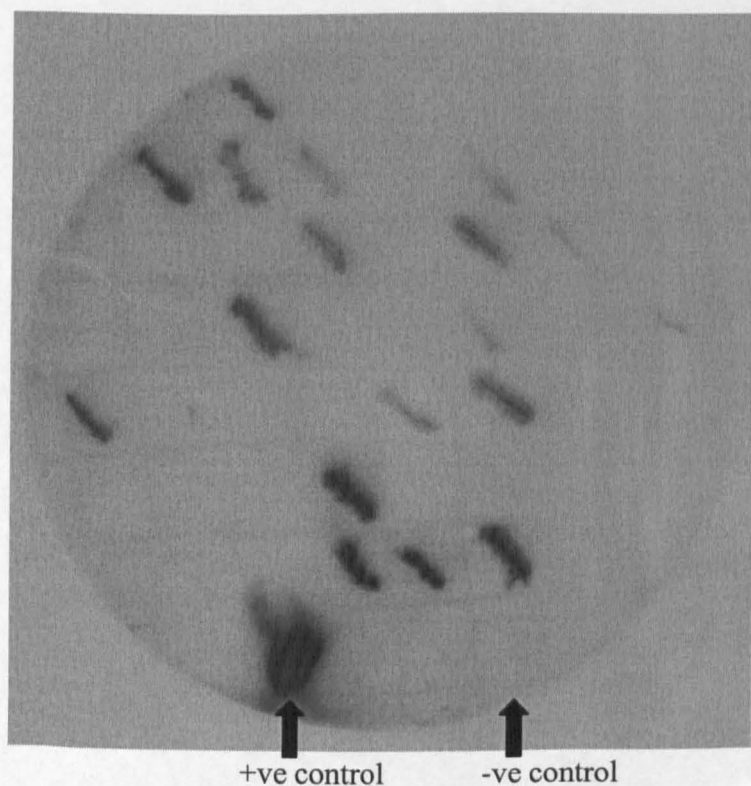
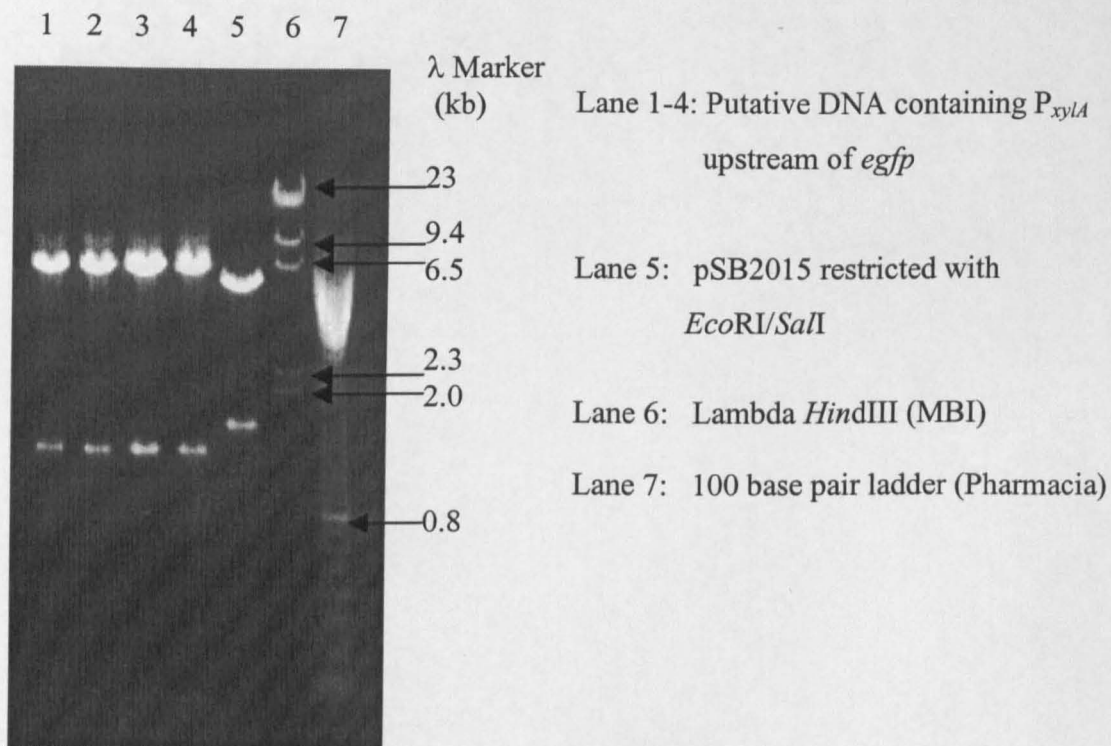


Figure 3.11.5: Restriction Analysis of Putative DNA thought to express *egfp* from P_{xyIA}

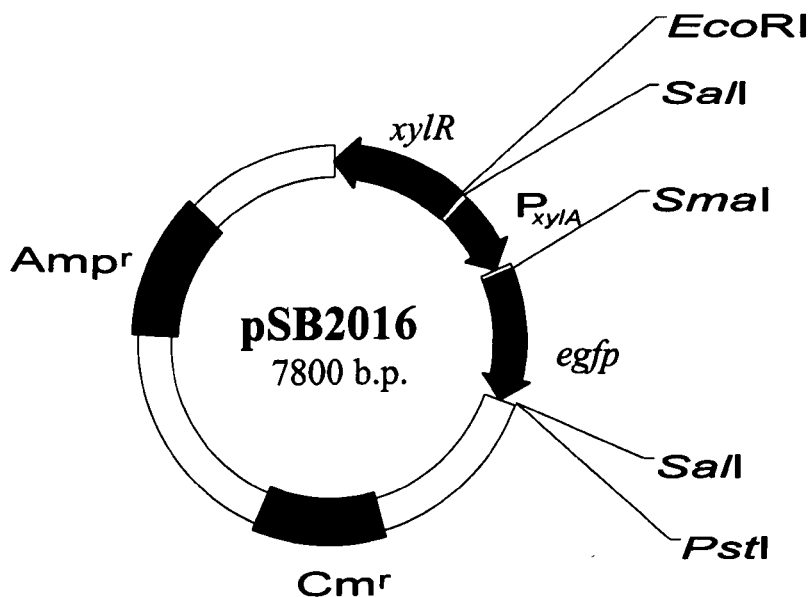


It can be clearly seen from the gel that all recombinant colonies when restricted with *EcoRI* and *SalI* yield a band of approximately 1.3kb, this is a smaller band than that excised from pSB2015 restricted with the same restriction enzymes, suggesting that these colonies contain P_{xyIA} upstream of *egfp*. So the restriction analysis of plasmid DNA confirms the results obtained from the colony hybridisation, this new expression vector was designated pSB2016.

Following isolation of cells containing the correct construct, DNA was prepared on a large scale by plasmid maxiprep. This plasmid, pSB2016, was then used to transform *L. monocytogenes* competent cells by electroporation. Recombinant colonies were isolated following selection on chloramphenicol selective agar, the resulting colonies were screened under blue light but no fluorescence was observed. Individual colonies were then examined by fluorescence microscopy using blue light excitation. Under these conditions only a few cells exhibited a green phenotype, but the fluorescence

along these cells was uniform, no localisation of EGFP was observed in the bacteria. Due to the fact that all the *L. monocytogenes* cells were not fluorescent, the plasmid pSB2016 was checked by restriction mapping to confirm plasmid structure. The results obtained matched those predicted and are illustrated in Figure 3.11.6.

Figure 3.11.6: Restriction map of pSB2016



When *egfp* was expressed from *P_{xylA}* no localisation of *egfp* was observed. As the XynB' peptide is not present in pSB2016, the data gathered does suggest that when *egfp* was cloned downstream of *P_{xyn}*, a translational fusion was created with the XynB' peptide that caused the protein to localise within the bacterial cell. It is not *egfp* itself that is localising within the cell, but the *egfp* may mark the position of XynB' within the cells.

Since only a small number of individual *L. monocytogenes* cells expressing *egfp* exhibited a fluorescent phenotype under excitation conditions, it may be concluded that codon usage and mRNA secondary structure are not responsible for the lack of translated protein. However, this is not conclusive as the use of *egfp* may still result in codon usage problems within *L. monocytogenes* cells, although studies of codon usage tables suggest that *egfp* places no demand on the host protein synthetic apparatus, i.e. although *egfp* has different codon usage to *gfp3*, like *gfp3* it does not appear to be markedly different in its codon bias to that of *L. monocytogenes*.

3.12. Enhancing translational initiation of *gfp*

From the plasmid constructs generated so far, very little fluorescent protein has been generated when *gfp* is expressed in Gram positive cells. Previous experiments appear to suggest that the problem is one of translation and not transcription within the cells as full length mRNA is produced from cells harbouring the *gfp* plasmids. The protein does not appear to be truncated and use of a different variant of *gfp* with altered codon usage and secondary mRNA structure appears to have no effect on the fluorescence characteristics of the population.

One factor that has not been considered as yet is the initiation of translation. Is translation actually being initiated effectively within Gram positives? If the ribosomes are not recognising the Shine-Dalgarno sequence on the mRNA near the 5' end of the coding sequence, then they will not be able to translate each codon into an amino acid. If the Shine-Dalgarno sequence is weak, it is possible that only a few of the ribosomes are able to initiate translation, this would explain why in Gram positive bacteria only low levels of fluorescence are seen under excitation conditions.

Vellanoweth has previously described all the individual elements that are required for efficient initiation of translation in *B. subtilis* (Vellanoweth, 1993). He postulated that in *B. subtilis* a strong Shine-Dalgarno sequence was necessary for efficient

translation, this was determined to be AAGGAGG. The spacing between the Shine-Dalgarno sequence and the initiation codon was also found to be critical, with the optimum being between 7-9 base spacings. It was suggested that the bases between the Shine-Dalgarno sequence and the initiation codon should be either A's or T's, preferably A's, with no C's or G's between the spacer region. All these factors make up the optimal *B. subtilis* translational initiation sequence.

Taking all this into account a new forward PCR primer to *gfp* was designed, that incorporated all factors necessary for efficient initiation of translation in Gram positives as well as *SmaI* and *HpaI* restriction sites to facilitate cloning of the gene into the shuttle vector pGC4. The details of this new primer, primer 11, and the reverse primer, primer 2, which incorporated a *SalI* site, are given in Appendix 1. The *gfp3* gene was amplified using these primers as previously described in Section 3.2. The resulting translationally optimised *gfp3* gene, *gfp3opt*, was restricted with *SmaI* and *SalI*, the DNA was then purified by phenol chloroform extraction. This restricted PCR product was then ligated with pCG4 that had previously been digested with the same restriction enzymes and the *luxAB* excised from it following purification from a low melting point agarose gel. The ligated DNA was used to transform *E. coli* JM109 competent cells, and the resulting transformants were screened under blue light excitation to identify any positive clones.

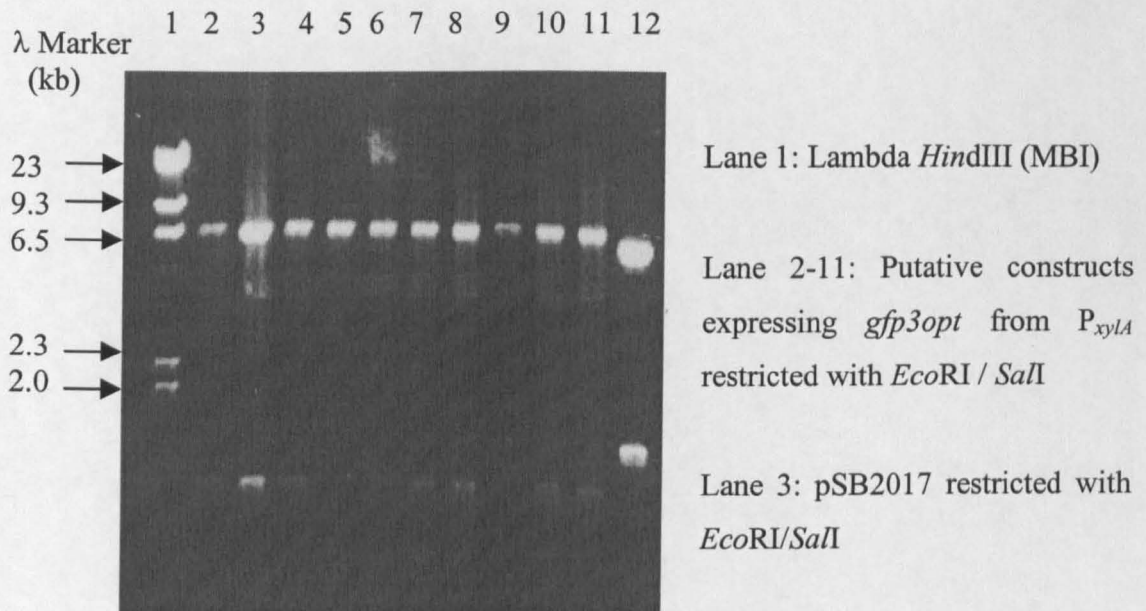
To confirm that these fluorescent colonies did contain *gfp3opt*, DNA was prepared by plasmid miniprep. The resulting DNA was restricted with *SmaI* and *SalI* in order to excise the cloned *gfp3opt*. All the fluorescent colonies were seen to contain this insert, suggesting that the cloning had been successful and *gfp3opt* had been inserted downstream of P_{xyn} , the resulting plasmid was named pSB2017 and was introduced into *L. monocytogenes* by electroporation of competent cells. The resulting recombinant colonies were screened with blue light but individual colonies were not seen to fluoresce. Upon examination by fluorescence microscopy, some individual cells were seen to fluoresce but the population was still not 100% fluorescent. The proportion of fluorescent *L. monocytogenes* (pSB2017) appeared to be greater than *L. monocytogenes* (pSB2002) indicating that translation of *gfp3* was more efficient in

these cells. Previous work, described in Section 3.7, had suggested that the use of a different promoter increased the fluorescence characteristics of cells expressing *gfp*. Thus it was decided to express the translationally optimised *gfp3* from P_{xylA} to see if a combination of factors would increase translation of *gfp3* in *L. monocytogenes*.

PCR was used to amplify P_{xylA} from the *B. megaterium* genome, as described previously in Section 3.6. After purification from a low melting point agarose gel, the promoter fragment was restricted with *MunI* and *SmaI*. The restricted PCR product was then purified by phenol chloroform extraction and ligated with pSB2017 which had already undergone restriction with *EcoRI* and *SmaI* and had been purified from a low melting point agarose gel in order to excise P_{xyn} .

Following ligation of the two fragments the DNA was introduced into competent *E. coli* JM109 cells by electroporation, recombinant colonies were isolated following selection on ampicillin selective agar plates. Once again, resulting recombinants were screened under blue light excitation to see if any of the colonies fluoresced green. As one promoter was being exchanged for another, plasmid DNA was prepared from fluorescent cells by plasmid miniprep and then subjected to restriction analysis using *EcoRI* and *SaI* to ascertain which promoter was in the plasmid construct. As a control, pSB2017 was restricted with the same enzymes. As the P_{xylA} -*gfp3opt* fragment is smaller than that of P_{xyn} -*gfp3opt*, analysis of restricted DNA was fairly straightforward. The restricted DNA was electrophoresed on an agarose gel and the ensuing banding patterns are depicted in Figure 3.12.1.

Figure 3.12.1: Agarose gel showing Putative colonies expressing *gfp3opt* from P_{xyIA}



As can be seen from Figure 3.12.1, several of the recombinant colonies contain the new promoter, these being those run in Lanes 2, 3, 4, 7, 8, 10, 11. The excised fragment in these colonies is approximately 400bp smaller than the restricted control plasmid pSB2017. The only way a smaller band can be excised is if P_{xyIA} is upstream of *gfp3opt*.

The act of optimising *gfp3* translational initiation and then expressing the gene from P_{xyIA} resulted in *E. coli* colonies that were highly fluorescent upon excitation. In fact the gene was being translated so efficiently that colonies harbouring recombinant DNA were yellow in appearance compared to non-recombinant colonies. However, it should be noted that in the *E. coli* this promoter is not regulated by xylose. No difference in fluorescence was observed when cells were grown on media without xylose compared to when 0.5% xylose was present. It appears that the regulation of this promoter is poor in *E. coli* and growth without xylose cannot repress P_{xyIA} .

This translationally enhanced *gfp* expression vector was designated pSB2018, DNA was then prepared from recombinant colonies by plasmid maxiprep. This was then investigated by further restriction analysis in order to confirm the validity of the new construct pSB2018. pSB2018 was introduced into electrocompetent *L. monocytogenes* cells, recombinant colonies were isolated following selection on chloramphenicol agar plates containing 0.5% xylose. Recombinant colonies were then examined using fluorescence microscopy. When cells were grown in the presence of 0.5% xylose in order to induce P_{xylA} , the majority of the population was seen to fluoresce, although some cells showed much brighter fluorescence characteristics than others. When cells grown in the absence of xylose were viewed under excitation conditions, only a small proportion of the population was seen to fluoresce. This suggests that the promoter is not completely repressed in all the cells of the population. Nevertheless, the main aim seemed to have been achieved and almost all the *L. monocytogenes* population exhibit a fluorescent phenotype upon excitation with blue light. Thus it appears that in order to express *gfp* in *L. monocytogenes*, the reporter has to be placed downstream of a strong promoter and translation of the reporter has to be efficiently initiated.

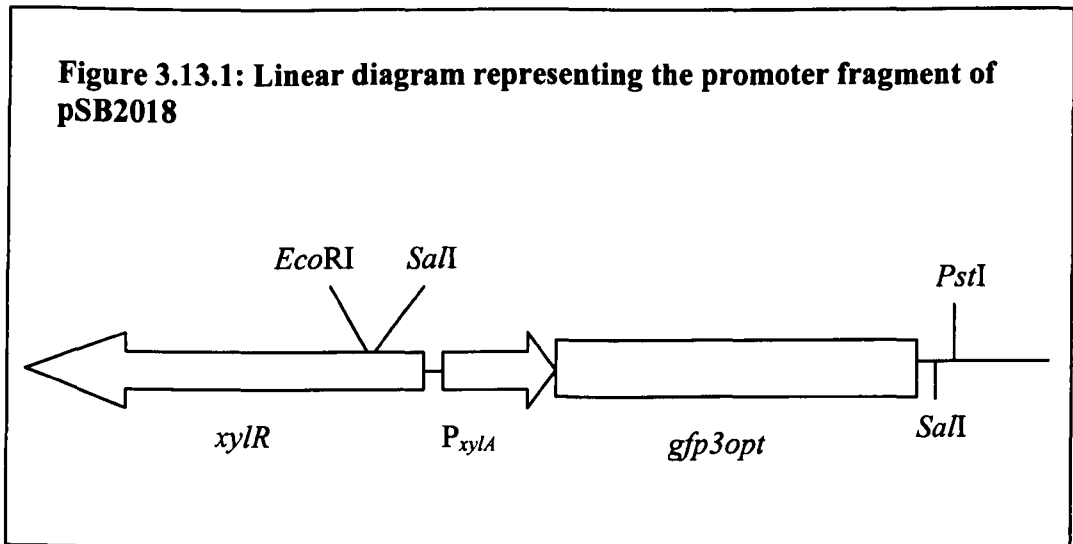
Having expressed *gfp3* in *L. monocytogenes* effectively, it was decided to see if the translationally enhanced vector pSB2018 could be expressed in other Gram positive bacteria. The plasmid was introduced into two other Gram positive bacteria, these being *Staphylococcus aureus* RN4220 and *Bacillus subtilis* 168. *S. aureus* RN4220 were transformed by electroporation as described by Augustin and Gotz (1990); the *Bacillus* are naturally competent bacteria and are able to take up DNA in exponential growth and were transformed by the method of Boylan *et al.* (1972). After transformation of both bacteria with pSB2018, recombinant colonies were selected on agar plates containing chloramphenicol. Any colonies obtained were then screened under blue light excitation and the fluorescence properties observed. Both sets of colonies harbouring the plasmid were seen to fluoresce under blue light when P_{xylA} was induced by the addition of 0.5% xylose. The *B. subtilis* cells were the most fluorescent, and these colonies were yellow compared to non-recombinant colonies under white light. It might be expected that the *B. subtilis* fluoresced with the greatest intensity compared to the other Gram positive bacteria tested, as

enhancement of the translation process was based on observations originally made in *B. subtilis*.

3.13. Constructing a constitutive *gfp* reporter for expression in Gram positive bacteria.

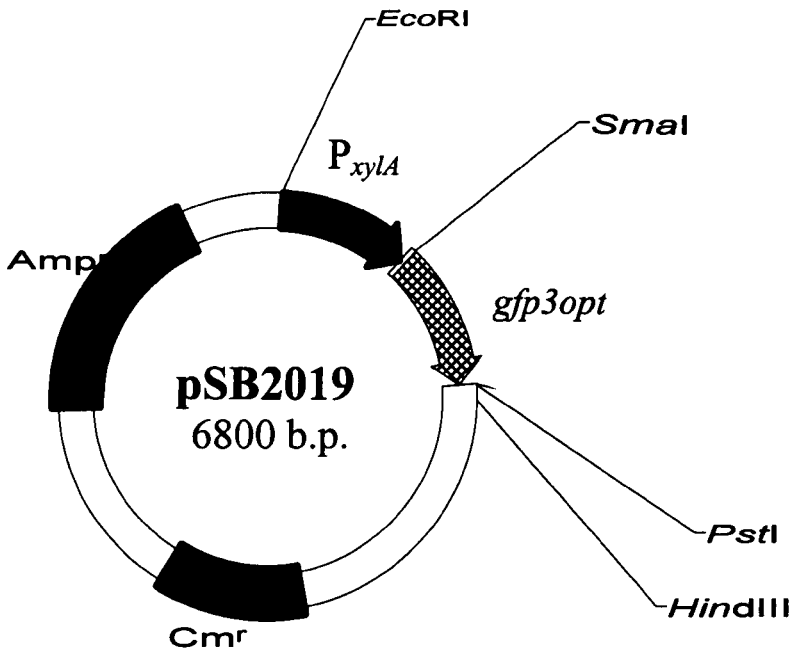
Having optimised the translation of *gfp* for expression in Gram positive bacteria, it was decided to construct a vector with a constitutive promoter for *gfp3opt*, as cells containing pSB2018 require the addition of xylose to de-repress P_{xylA} and allow expression of *gfp3opt*.

The *xylR* gene contains an *EcoRI* site approximately 350bp from its 5' end. This is about 400bp before the start of P_{xylA} . The plasmid pSB2018 was restricted with *EcoRI* and *PstI*, which generated a fragment of approximately 1.3kb, which contained P_{xylA} and *gfp3opt*. This is shown in Figure 3.13.1.



Following restriction of pSB2018, the DNA was electrophoresed on a low melting point agarose gel, this was then purified by freeze thaw extraction. This purified fragment was then ligated with pGC4 which had also been restricted with *EcoRI* / *PstI* and then purified from a low melting point agarose gel in order to excise the P_{xyt} -*luxAB* fragment from the plasmid. The ligated DNA was used to transform *E. coli* JM109 competent cells by electroporation and recombinant colonies isolated following selection on ampicillin selective agar plates. The resulting transformants were screened under blue light excitation and green fluorescent colonies isolated for further investigation. DNA was prepared from a few of the colonies that were seen to fluoresce upon excitation by plasmid miniprep. The resultant DNA was restricted with *SaII* to identify the correct recombinants. The digests were analysed on an agarose gel and a band of approximately 1.3kb identified. This corresponded to the P_{xyt} -*gfp3opt* fragment, suggesting that the recombinant colonies contained the correct construct, this plasmid was designated pSB2019. Using the recombinant colonies, DNA was prepared on a large scale by plasmid maxiprep, this was subjected to further restriction mapping and is illustrated in Figure 3.13.2.

Figure 3.13.2: Restriction Map of pSB2019



Following the introduction of pSB2019 into *L. monocytogenes* competent cells by electroporation, the resulting transformants were mounted onto glass slides and observed using fluorescence microscopy. All individual cells presented a fluorescent phenotype upon excitation with the correct wavelength of light, indicating that *gfp3opt* was being efficiently expressed in all the bacterial cells.

The construction of a constitutive Gram positive *gfp* expression vector has been accomplished. All cells harbouring this plasmid display a fluorescent phenotype upon excitation. When bacteria containing pSB2019 are grown on media both with and without xylose there is no apparent difference in the fluorescence intensity. Xylose appears to have no effect on the action of the promoter in this plasmid, this is to be expected as the xylose regulator is not present in this construct.

3.14. Construction of an Unstable GFP Plasmid for use as a reporter in Gram positive bacteria

As GFP is such a stable protein, none of the *gfp* vectors built so far for use in Gram positive bacteria will give an accurate representation of promoter kinetics or gene expression studies within the cell. Anderson *et al.* (1998), have developed a set of unstable *gfp* variants. As described earlier, these are all based on *gfp3*, but the last 3 amino acids have been changed to an *E. coli* protease recognition sequence which enables the protein to be turned over within the cell at different rates depending on the protease recognition sequence utilised. Thus protein is generated and is turned over within the cell and therefore does not accumulate. So if a promoter was active in the cell a fluorescent signal would be generated, if that promoter was switched off, no more GFP would be made and that already existing within the cell would be degraded and this would indicate that the promoter was no longer active. If the stable protein was used, no idea of the promoter kinetics could be obtained as the half-life for *gfp3* is greater than one day (Anderson *et al.*, 1998).

In order to determine whether these unstable *gfp* variants were active in Gram positive bacteria, it was decided to clone translationally optimised unstable *gfp* variants downstream of the xylose regulatable promoter P_{xy1A}. As this is a regulatable promoter it would allow expression of the *gfp3* unstables and when the promoter is repressed by the removal of xylose from the medium, any accumulated protein would degrade. This would allow determination of the half-lives in Gram positive bacteria, which could then be compared to observed rates determined in Gram negative bacteria.

Previously in Section 3.5.1, details of the construction of non-translationally optimised unstable *gfp3* variants has been described. Sequence analysis of both *gfp3* and pMK4 revealed the presence of a unique *NcoI* restriction site. In *gfp3* this was approximately half way through the gene and in pMK4 this site was found to be within the chloramphenicol resistance gene. In order to construct unstable *gfp3*

variants that were optimised for translation in Gram positive bacteria, it was decided to excise the *NcoI* fragment from the P_{xyn} -*gfp3* unstable vectors, pSB2007 and pSB2008 and purify the fragment from a low melting point agarose gel. These were then ligated with pSB2018, which had also been restricted with the same enzymes, the *NcoI* fragment excised and the remaining DNA purified from a low melting point agarose gel. This would mean that the 3' end of the translationally optimised *gfp3opt* would be replaced with an equivalent sequence that contained the protease recognition sequence, thus creating translationally enhanced unstable *gfp3* expression vectors that could be regulated by xylose. Only two of the unstable *gfp3* genes were chosen, *gfp3* (ASV) and *gfp3*(AGA), as these were the two where only a few fluorescent cells had been observed when the gene was expressed from P_{xyn} . It was thought that *gfp3* (LAA) had a half-life that was too short to be able to observe fluorescence by eye, and so this variant was not used.

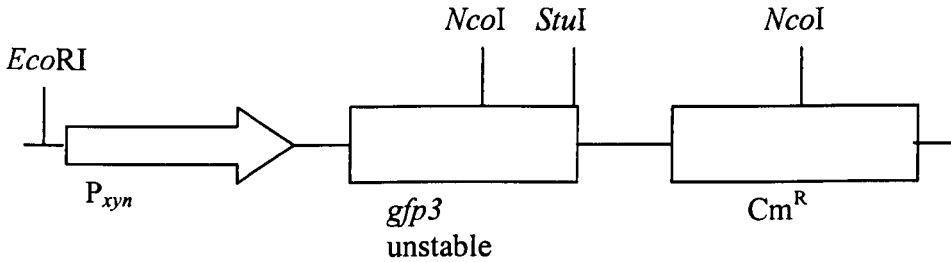
Following ligation of these two DNA fragments the DNA was introduced into *E. coli* JM109 competent cells by electroporation and recombinant colonies were selected by plating cells onto media containing chloramphenicol. Although cloning of this *NcoI* fragment was not directional, only colonies containing the unstable *gfp3* could be obtained, because if the insert was to go in the wrong orientation the chloramphenicol resistance gene would be disrupted, so colonies would not grow on media containing chloramphenicol. The recombinant colonies were screened under blue light excitation and DNA prepared by plasmid miniprep from any that showed a fluorescent phenotype. This DNA was then restricted using *EcoRI* and *StuI* to confirm if these colonies contained the correct construct. The unstable GFP vector that expressed *gfp3* (AGA) from P_{xylA} was designated pSB2020, the equivalent expression vector containing *gfp3* (ASV) was named pSB2021. The basis behind the cloning procedure resulting in construction of pSB2020 and pSB2021 is illustrated in Figure 3.14.1.

Figure 3.14.1: Procedure for cloning the unstable *gfp3* variants downstream of

P_{xylA}

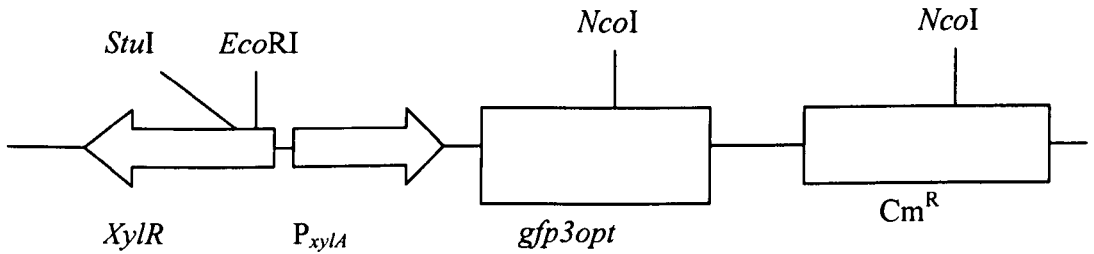
Vectors:
pSB2007 (*gfp3* ASV)
pSB2008 (*gfp3* AGA)

Step 1: Excise and purify *NcoI* fragment from pSB2007 and pSB2008



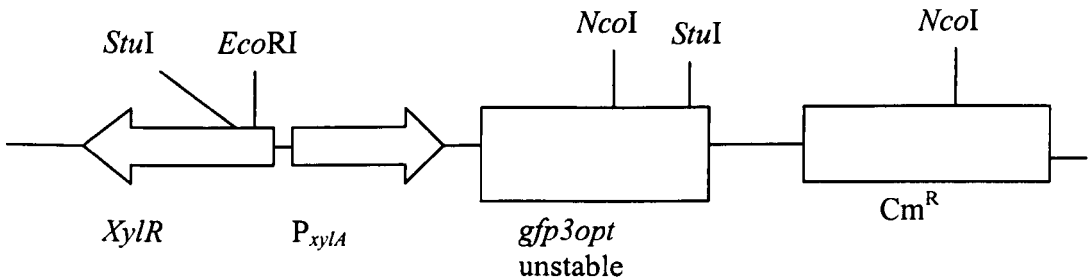
Vector:
pSB2018

Step 2: Excise *NcoI* fragment from pSB2018, purify the large fragment of DNA



New unstable *gfp3opt* cloning vectors:
pSB2020 and pSB2021

Step 3: Ligate the two resulting *NcoI* fragments. This generates translationally enhanced unstable *gfp3* cloning vectors



The plasmids pSB2020 and pSB2021 were introduced into *L. monocytogenes* by electroporation of competent cells, recombinant colonies were isolated following selection on chloramphenicol selective agar plates. The resulting transformants were grown on media containing 0.5% xylose in order to induce P_{xylA} and cells were observed under blue light excitation. *L. monocytogenes* harbouring pSB2021 (*gfp3opt* ASV) appeared to be less fluorescent than equivalent cells harbouring pSB2020 (*gfp3opt* AGA). This may be due to the fact that in *E. coli* *gfp3* ASV has a reported shorter half-life compared to that of *gfp3* AGA (Anderson *et al.*, 1998), so it would not be surprising if the same effects were noticed in *L. monocytogenes*. However, the half-lives of the proteins cannot be assumed to be the same as those observed in *E. coli* due to the possible differences in the protease recognition systems. If the same trends in protein instability, originally observed by Anderson *et al.* (1998), can be demonstrated in *L. monocytogenes*, then cells harbouring pSB2021 will probably have less protein in them at any one time as the protein has a shorter half-life compared to that in pSB2020, thus it would be expected that cells would be less fluorescent.

3.15. Discussion

PCR was used to generate restriction sites at both the 5' and 3' ends of the coding sequence of two *gfp* variants, wildtype *gfp* (*gfpwt*) and a red shifted variant (*gfp3*). These products were then cloned into the shuttle vector pGC4, which contains the P_{xyn} promoter (Boylan *et al.*, 1972). When these constructs, pSB2002 and pSB2003, were introduced into *L. monocytogenes* by electroporation of competent cells, recombinant colonies were not seen to fluoresce and only a small percentage of the total population was seen to fluoresce using fluorescence microscopy. It was noticed that from the cells that were fluorescent a much stronger signal was generated from cells expressing *gfp3* compared to those expressing *gfpwt*. This was expected however, as Cormack *et al.* (1996) reported that *gfp3* fluoresced with an intensity 21 times greater than that of *gfpwt* when excited at 488nm. In part, this was found to be due to the fact that much of the GFPwt was found in inclusion bodies as non-fluorescent insoluble protein. In contrast, Cormack *et al.* (1996) showed that when

gfp3 was expressed under identical conditions, virtually all GFP3 was soluble. This in part contributes to the increased fluorescence of GFP3. So the increase in fluorescence observed by cells expressing *gfp3* is due to a shift in absorption spectra and also due to an increase in the amount of soluble protein due to more efficient protein folding.

One reason suggested for the lack of fluorescent *L. monocytogenes* cells was that read-through into the plasmid, due to the lack of a transcriptional terminator downstream of the reporter gene was causing plasmid instability and therefore loss of the plasmid from the bacteria. The addition of the *rrnB* transcriptional terminator downstream of *gfp3* did not result in a homogeneous fluorescent population, suggesting that this was probably not the problem and some other factor was responsible for the poor fluorescence shown by *L. monocytogenes* expressing *gfp*.

As P_{xyn} had previously been shown to be constitutively active at a high level in *L. monocytogenes* and *B. subtilis* it was possible that the lack of fluorescent cells was due to the production of too much protein resulting in the formation of non fluorescent inclusion bodies within the cells. The other hypothesis was that GFP was being synthesised in large amounts, but the levels made were toxic to the cells. These issues were addressed in two ways, by using the unstable *gfp3* variants available, and making a GFP protein that contained a poor RBS at the 5' coding region. The unstable *gfp3* variants are modified at the C-terminal in such a way that they have become susceptible to indigenous house keeping proteases within the cell. In using these variants, the overall concentration of the protein within a cell will be decreased compared to the stable *gfp3* due to the rapid turnover of the protein. It was hoped that these lower levels of protein would be more favourable to allow efficient expression of *gfp3* within *L. monocytogenes* and may prevent aggregation of excess protein prior to chromophore formation, resulting in the formation of non-fluorescent inclusion bodies. GFP was also modified in such a way, so it would be translated inefficiently by the bacterial cell. This was achieved by creating a poor ribosome binding site, through the incorporation of a poor Shine-Dalgarno recognition sequence and the use of a non-optimal spacer region between the Shine-Dalgarno sequence and the

initiation codon. Again it was hoped that this would lower the translational efficiency of *gfp* within *L. monocytogenes*, thus reducing the total amount of protein within the cell hopefully attaining more favourable conditions for efficient expression of *gfp*. However, neither of these new vectors made a difference to the fluorescence characteristics of *L. monocytogenes*, where only a small proportion of the total population was seen to fluoresce under excitation conditions.

All *gfp* expression vectors constructed to date had been based on the shuttle vector pGC4 and contained P_{xyt}. To confirm that the poor expression of *gfp* was not due to non-homogenous promoter activity, an alternative promoter was cloned upstream of *luxAB* in pGC4. This was P_{xytA} from *B. megaterium*, which is regulated by the repressor *xytR*, which can be de-repressed by the addition of xylose to the culture media. Addition of exogenous aldehyde to recombinant *L. monocytogenes* colonies, grown in the presence of 0.5% xylose, resulted in a high luminescent output, indicating that this was a strong promoter that was constitutive in its action. When *gfp* was cloned downstream of this promoter, again recombinant colonies did not show a fluorescent phenotype under excitation. Upon examination by fluorescence microscopy, individual cells were seen to fluoresce, but these were only a small percentage of the overall population.

Northern blot analysis of *L. monocytogenes* harbouring the *gfp* expression vectors pSB2002 and pSB2003 confirmed that the transformed bacteria generated a large amount of full length *gfp* transcript. This indicated that fluorescence was either limited by the efficiency of translation or poor post-translational modification within the cell.

To address these issues, whole cell extracts of *L. monocytogenes* bearing the *gfp* expression vectors, pSB2002 and pSB2003 were subjected to SDS PAGE and immunoblotting using a polyclonal anti-GFP antibody. These results showed that only small amounts of full length GFP peptide were present in *L. monocytogenes* cell

extracts. No evidence was seen of a truncated or degraded protein by Western blot analysis. These data suggest that translation of *gfp* was the limiting factor.

A number of molecular techniques were employed in an attempt to optimise translation of *gfp* in Gram positive bacteria. These included the removal of a potential stall site from the start of the *gfp* coding sequence (*gfp3r/s*) and the use of *egfp* to investigate whether codon usage or secondary mRNA structure was responsible for the lack of fluorescence in *L. monocytogenes*. These altered *gfp* genes were placed downstream of P_{*xyn*} and upon introduction of these new vectors into *L. monocytogenes*, highly fluorescent cells were observed but the fluorescence characteristics of these was surprising, as fluorescence was not uniform along the length of the cell. In each case areas of fluorescence occurred towards one or both poles of the bacterial cell with weak fluorescence sometimes seen across the rest of the cell. Sequence analysis of *gfp3r/s* showed that a translational fusion had been made to the XynB' peptide. It is not certain if this peptide accumulates naturally within bacterial poles or whether this translational fusion has created an intrinsic protein targeting motif causing protein aggregation towards the bacterial poles. In order to check that this altered *gfp* sequence did not contain a targeting motif, it was placed downstream of P_{*xylA*}. In this case fluorescence was uniform along the length of the bacteria, but these cells still only represented a proportion of the population. The same was observed when *egfp* was cloned downstream of P_{*xylA*}. This led to the supposition that altering the *gfp* sequence was not responsible for protein aggregation, but that fusion of the protein to the XynB' peptide either caused the GFP to follow the natural aggregation patterns of the peptide, or generated a protein targeting motif causing the protein to localise in a polar manner.

Another technique employed to overcome limitations in translation was to make *gfp* expression constructs in which all the elements required for efficient initiation of translation in *B. subtilis* were present, as identified by Vellanoweth, (1993). He postulated that in *B. subtilis* a strong Shine-Dalgarno sequence was necessary for efficient translation, this was determined to be AAGGAGG. The spacing between the Shine-Dalgarno sequence and the initiation codon was also found to be critical, with

the optimum being between 7-9 base spacings, it was preferable that these bases be either A's or T's, preferably A's, with no C's or G's between the spacer region (Vellanoweth, 1993). This translationally enhanced *gfp* gene, *gfp3opt*, was placed downstream of P_{*xylA*} and introduced into *L. monocytogenes*. Recombinant colonies harbouring this translationally enhance plasmid pSB2018, when grown in the presence of 0.5% xylose showed a fluorescent phenotype upon excitation. All individual cells were also seen to fluoresce by fluorescence microscopy, although some were much brighter than others were. pSB2018 was also introduced into *S. aureus* RN4220 and *B. subtilis* 168, again all individual cells were shown to be fluorescent by fluorescence microscopy, suggesting that a *gfp* expression vector had been constructed which gave efficient translation of *gfp*. This construct, pSB2018, was then used to generate a constitutive *gfp* plasmid by removal of the *xylR* gene from upstream of P_{*xylA*}, here no xylose was needed to generate fluorescent colonies indicating that the repressor gene had been successfully removed from the plasmid.

Having solved the problem of *gfp* translation in Gram positive bacteria, the unstable *gfp3* genes (Anderson *et al.*, 1998) were amplified by PCR so as to contain this enhanced translation region for expression in Gram positive bacteria. These were then expressed from the xylose regulated promoter P_{*xylA*} and recombinant cells showed a fluorescent phenotype upon excitation. The cells appeared to generate a weaker signal compared to cells expressing *gfp3opt*. This may be expected as the unstable *gfp3* have been shown to be rapidly turned over in Gram negative bacteria (Anderson *et al.*, 1998) due to the protease recognition tag at the C-terminal end, therefore protein does not accumulate within the bacteria. Anderson *et al.* (1998) reported *gfp3* ASV to have a half-life of 60 minutes while *gfp3* AGA had a half-life of approximately 300 minutes in *E. coli* so it is not unexpected that *L. monocytogenes* expressing *gfp3* AGA from pSB2020 appeared to generate a greater fluorescent signal than *L. monocytogenes* expressing *gfp3* ASV from pSB2021. It is hoped that these constructs will be of more use in gene expression studies due to their unstable nature, so will more readily reflect any bi-directional changes in gene expression.

CHAPTER 4

EVALUATION AND EXPRESSION OF GFP REPORTERS IN GRAM POSITIVE ORGANISMS

CHAPTER 4: EVALUATION AND EXPRESSION OF GFP REPORTERS IN GRAM POSITIVE ORGANISMS

4.1. Growth characteristics of *L. monocytogenes* (pSB2018)

The construction of pSB2018 has been described previously in Section 3.12. This plasmid contains *xylR* and P_{xylA} . On addition of xylose P_{xylA} is de-repressed and the translationally enhanced *gfp3* gene (*gfp3opt*) downstream of the promoter is expressed.

In order to confirm that the promoter could be regulated by xylose, two overnight cultures of *L. monocytogenes* harbouring pSB2018 were grown overnight at 37°C in BHI broth. Both were grown with chloramphenicol selection, but only one culture was grown in the presence of 0.5% xylose. From the overnight cultures, cells were diluted 1/100 into pre-warmed medium containing chloramphenicol, one flask also contained 0.5% xylose. All cultures were incubated at 37°C and the OD₆₀₀ and fluorescence measured every hour. In-order to determine whether expression of *gfp3opt* affected bacterial growth rate, a culture of non-recombinant *L. monocytogenes* 7973 cells were grown in BHI overnight and measurements made in the same way.

In order to measure bacterial GFP fluorescence a sample of the bacterial culture was washed and resuspended in PBS. This was then loaded into a microtitre plate and fluorescence measured using a Victor 1420 multilabel counter (Wallac, E G & G) as described in the Material and Methods, section 2.14.2. Both optical density and fluorescence measurements were made during the experiment over a period of 10 hours. The measured values of green fluorescence of *L. monocytogenes* expressing *gfp3opt* from pSB2018 were corrected for background fluorescence by subtracting the corresponding measured values of fluorescence from the control culture of *L.*

monocytogenes, this gave the relative fluorescence (RFU) for each test culture. The corresponding OD values were then divided into the background-corrected values of fluorescence (RFU) values in order to take into account the effect of dilution on bacterial fluorescence (RFU/OD). As the cells grow, if no new protein is being made then the amount of fluorescence relative to the number of cells in the culture will decrease. The RFU/OD were then plotted as a function of time on an arithmetic plot, in addition to this, the OD values were also plotted on the same graph as a function of time on a log scale. This was done so the amount of fluorescence relative to the growth rate of the cells could be compared. A representation of the data obtained is shown in Figure 4.1.1 and Figure 4.1.2.

Figure 4.1.1: Growth and Fluorescence of *L. monocytogenes* (pSB2018)

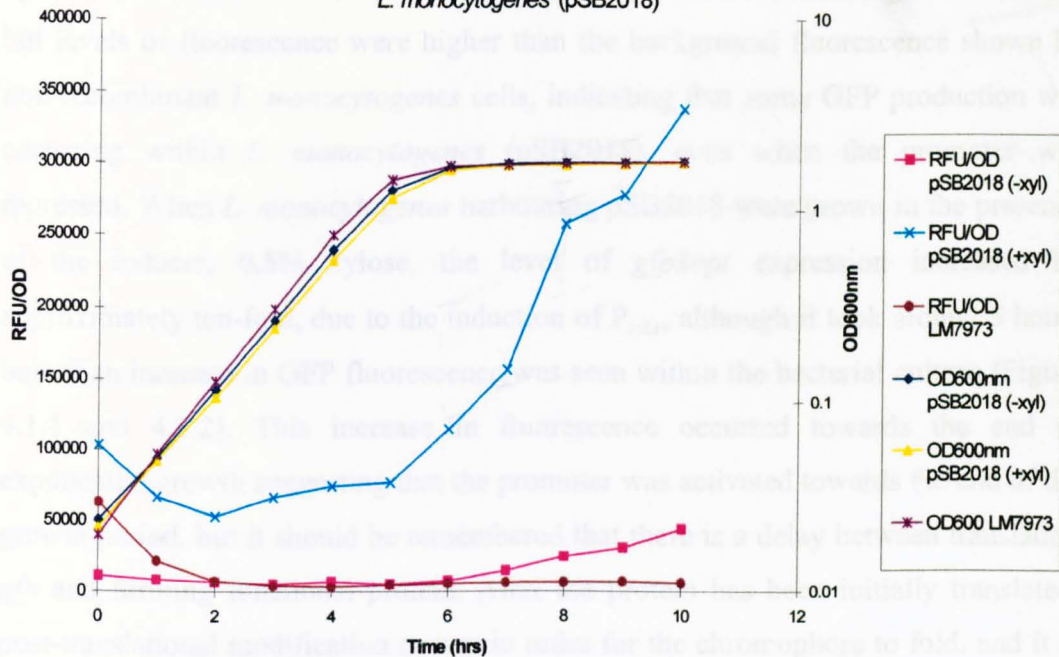
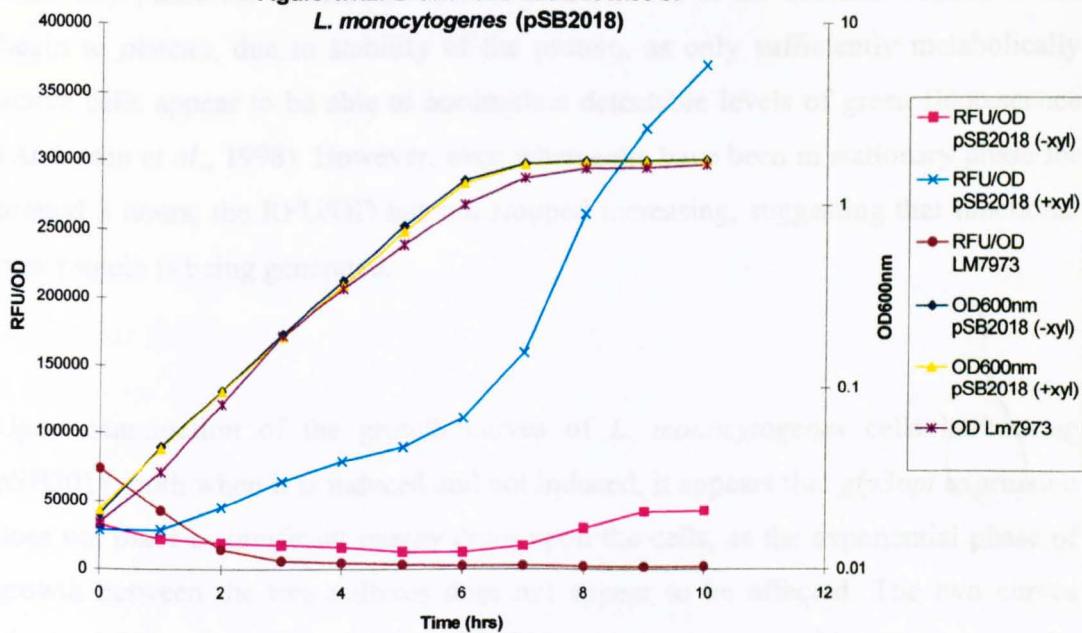


Figure 4.1.2: Growth and fluorescence of *L. monocytogenes* (pSB2018)



The results of the experiment reveal that P_{xyIA} was not completely repressed when xylose was absent from the culture medium. Expression was reduced considerably, but levels of fluorescence were higher than the background fluorescence shown by non-recombinant *L. monocytogenes* cells, indicating that some GFP production was occurring within *L. monocytogenes* (pSB2018), even when the promoter was repressed. When *L. monocytogenes* harbouring pSB2018 were grown in the presence of the inducer, 0.5% xylose, the level of *gfp3opt* expression increased by approximately ten-fold, due to the induction of P_{xyIA} , although it took around 5 hours before an increase in GFP fluorescence was seen within the bacterial culture (Figure 4.1.1 and 4.1.2). This increase in fluorescence occurred towards the end of exponential growth suggesting that the promoter was activated towards the end of the growth period, but it should be remembered that there is a delay between translating *gfp* and forming functional protein. After the protein has been initially translated, post-translational modification occurs in order for the chromophore to fold, and it is this chromophore that is responsible for fluorescence. In prokaryotes it has been reported that the post-translational formation of functional chromophore occurs approximately two hours after synthesis of GFP (Heim *et al.*, 1995), although this again varies according to the variant of *gfp* used. It was thought that as cells entered stationary phase the increase in relative fluorescence of the bacterial culture would begin to plateau, due to stability of the protein, as only sufficiently metabolically active cells appear to be able to accumulate detectable levels of green fluorescence (Anderson *et al.*, 1998). However, even when cells have been in stationary phase for around 3 hours, the RFU/OD has not stopped increasing, suggesting that functional new protein is being generated.

Upon examination of the growth curves of *L. monocytogenes* cells harbouring pSB2018, both when it is induced and not induced, it appears that *gfp3opt* expression does not place a significant energy drain upon the cells, as the exponential phase of growth between the two cultures does not appear to be affected. The two curves obtained from *L. monocytogenes* (pSB2018) grown with and without xylose can be almost superimposed on each other, indicating that expression of *gfp3opt* within *L. monocytogenes* places no extra metabolic load upon the cell resulting in a decreased growth rate. The mean exponential growth rates of bacteria harbouring the *gfp3opt*

expression vector are shown in Table 4.1.1. The growth rate of the culture was determined by the gradient of the line in exponential phase.

The exponential growth rate of non-recombinant *L. monocytogenes* 7973 cells, i.e. cells harbouring no plasmids, was slightly increased compared to *L. monocytogenes* (pSB2018) although this increase is only very slight. This again suggests that expression of *gfp3opt* does not significantly affect the exponential growth rate of *L. monocytogenes* (pSB2018).

Table 4.1.1: Average Growth rates of *L. monocytogenes* cells harbouring pSB2018

Growth rates are shown as an increase in OD per hour

t-test performed, using non-recombinant *L. monocytogenes* 7973 as a control

<i>L. monocytogenes</i> cells	Mean Growth Rate	Standard Deviation	P
pSB2018 (-xyl)	0.186	7.07×10^{-3}	> 0.05
pSB2018 (+xyl)	0.168	1.44×10^{-3}	>0.05
non-recombinant	0.196	4.95×10^{-3}	

The data obtained suggests that expression of *gfp3opt* by *L. monocytogenes* places no significant energy drain upon the cells as the exponential growth rate does not dramatically change between cells expressing *gfp3opt* and those that don't. Any slight differences observed between the cultures can be attributed to the initial inoculum size and not due to an increased load upon the cells. Although the overnight cultures were diluted to approximately the same starting OD, due to the small number of cells within the culture, the spectrophotometer is unable to provide very accurate readings. At this level, only an estimate of cell density can be obtained.

4.2. Evaluation of Fluorescence Characteristics of *L. monocytogenes* cells containing the inducible reporter pSB2018 and the constitutive reporter pSB2019

This experiment was performed to check the promoter kinetics of both pSB2018 and pSB2019 and the fluorescence characteristics of *L. monocytogenes* cells harbouring both expression vectors. When pSB2019 was constructed, as described in Section 3.13, P_{xyIA} , a small segment of the *xyIR* gene and the translationally optimised *gfp3* gene (*gfp3opt*) were excised from pSB2018 and inserted into pGC4. These growth experiments were performed in order to confirm that the construct pSB2019 was constitutive in its expression and that xylose was not needed in order to obtain expression of the *gfp3opt* gene, also to check that the level of expression from both plasmids was the same.

L. monocytogenes (pSB2018) and *L. monocytogenes* (pSB2019) were grown in BHI broth with chloramphenicol selection to maintain the plasmid, *L. monocytogenes* (pSB2018) was also grown in the same conditions but with the addition of 0.5% xylose. As a control non-recombinant *L. monocytogenes* 7973 cells were cultured in BHI. The experiments were performed as previously described in Section 4.1, with both optical density and relative fluorescence being measured every hour. The obtained from the non-recombinant *L. monocytogenes* strain were classed as background fluorescence, and were subtracted from the equivalent data points from the other cultures expressing green fluorescence. Thus any autofluorescence of the bacterial cultures was accounted for.

In order to compensate for the effect of cell number on the fluorescence readings, the background corrected fluorescence values (RFU) were divided by the corresponding optical density values. Both the RFU/OD and OD values were plotted as a function of time, in order to see how bacterial fluorescence changed during the growth cycle. Figures 4.2.1 and Figures 4.2.2 illustrate a representation of the data obtained.

Figure 4.2.1: Growth and Fluorescence Characteristics of *L. monocytogenes* harbouring an inducible and constitutive *gfp* reporter

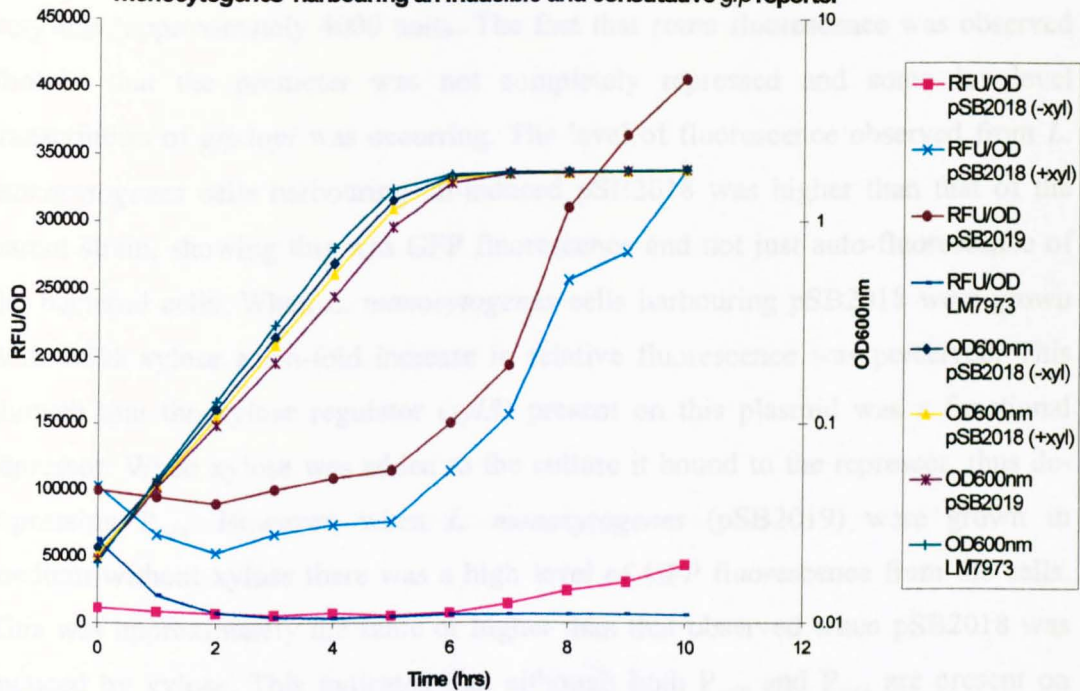
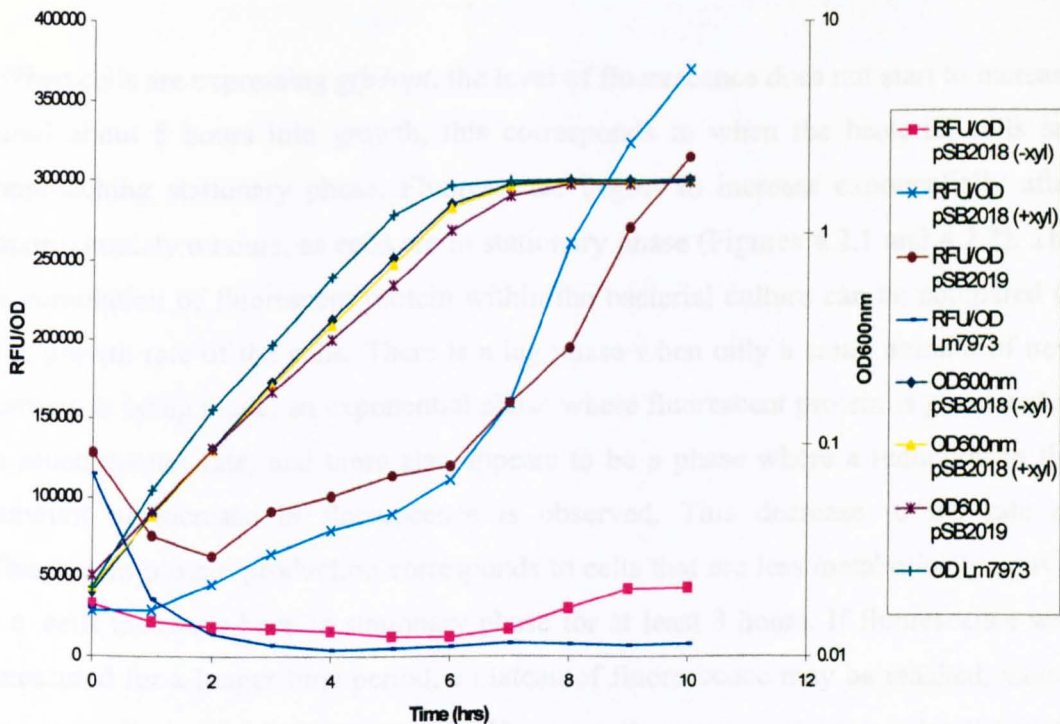


Figure 4.2.2: Growth and Fluorescence Characteristics of *L. monocytogenes* harbouring an inducible and a constitutive *gfp* reporter



The data presented in Figures 4.2.1 and 4.2.2 demonstrates a number of points. When pSB2018 was not induced by xylose the levels of observed green fluorescence were very low, approximately 4000 units. The fact that some fluorescence was observed showed that the promoter was not completely repressed and some low-level transcription of *gfp3opt* was occurring. The level of fluorescence observed from *L. monocytogenes* cells harbouring un-induced pSB2018 was higher than that of the parent strain, showing this was GFP fluorescence and not just auto-fluorescence of the bacterial cells. When *L. monocytogenes* cells harbouring pSB2018 were grown with 0.5% xylose a ten-fold increase in relative fluorescence was perceived. This showed that the xylose regulator (*xyIR*) present on this plasmid was a functional repressor. When xylose was added to the culture it bound to the repressor, thus de-repressing P_{*xyIA*}. However, when *L. monocytogenes* (pSB2019) were grown in medium without xylose there was a high level of GFP fluorescence from the cells. This was approximately the same or higher than that observed when pSB2018 was induced by xylose. This indicated that although both P_{*xyIR*} and P_{*xyIA*} are present on pSB2019, the xylose repressor has been successfully removed from the plasmid, as xylose is not needed to induce *gfp3opt* expression and the level of fluorescence observed was equivalent to that seen when pSB2018 was induced by xylose.

When cells are expressing *gfp3opt*, the level of fluorescence does not start to increase until about 5 hours into growth, this corresponds to when the bacterial cells are approaching stationary phase. Fluorescence begins to increase exponentially after approximately 6 hours, as cells are in stationary phase (Figures 4.2.1 and 4.2.2). The accumulation of fluorescent protein within the bacterial culture can be compared to the growth rate of the cells. There is a lag phase when only a small amount of new protein is being made, an exponential phase where fluorescent protein is generated at a much greater rate, and there also appears to be a phase where a reduction in the amount of increase in fluorescence is observed. This decrease in the rate of fluorescent protein production corresponds to cells that are less metabolically active, i.e. cells that have been in stationary phase for at least 3 hours. If fluorescence was measured for a longer time period, a plateau of fluorescence may be reached, where no new cells or protein is being made. However, fluorescence does not directly relate to the number of cells present, as there is a delay (Heim *et al.*, 1995) between

translating *gfp* and forming functional fluorescent protein. So the protein that is translated from cells in mid-exponential phase may not be seen as fluorescent protein until 2-3 hours later due to the cyclisation and oxidation reactions that have to occur in order for the chromophore to fold.

In order to assess whether expression of *gfp3opt* affects the rate of bacterial growth, the exponential growth rates were determined empirically from the gradient of each line and are represented in Table 4.2.1.

Table 4.2.1: Comparative Growth rates of *L. monocytogenes* (pSB2018) and *L. monocytogenes* (pSB2019)

Growth Rates are shown as an increase in OD per hour
t-test performed, using non-recombinant *L. monocytogenes* 7973 as a control

Bacterial culture	Mean Growth Rate	Standard Deviation	P
pSB2018 (-xyl) (BHI cm7)	0.186	7.07×10^{-3}	> 0.05
pSB2018 (+xyl) (BHI cm7)	0.168	0	> 0.05
pSB2019 (BHI cm7)	0.129	2.12×10^{-3}	> 0.05
Non-recombinant <i>L. monocytogenes</i>	0.259	0.040	

From the data in Table 4.2.1, it appears as though expression of *gfp3opt* does slow down the bacterial growth rate, as all cells harbouring *gfp3opt* expression vectors

have lower growth rates compared to non-recombinant cells. However, expression of *gfp3opt* cannot be solely responsible for the lowered growth rates, as *L. monocytogenes* (pSB2018) when grown without xylose also exhibit a slower growth rate even though P_{xyIA} has been repressed, although this may in part be due to poor regulation of P_{xyIA} .

The data suggests that it is not expression of *gfp3opt per se* that is responsible for the decreased rate of exponential growth, but the presence of the actual plasmid in the cells. Gruss and Ehrlich (1988), suggested that the insertion of heterologous DNA into pMK4 can cause the production of high molecular weight DNA (HMW DNA), it is possible that this is the factor responsible for decreased growth rate. The production of HMW DNA tends to depend on the nature of the inserted fragment and the size of the plasmid (Gruss and Ehrlich, 1988), this will be discussed further in Chapter 8.

As mentioned previously, another explanation for the slight differences in growth rate may be due to inoculum size. It is difficult to inoculate all cultures with the same starting number of bacteria due to limitations of the spectrophotometer, which is unable to accurately measure low cell densities. As viable counts were not recorded at each stage it is difficult to say whether this increased lag phase is due to inoculum size, but this seems unlikely as the same trends were seen during each repetition of the experiment.

One other salient feature that can be observed from the data represented in Figures 4.2.1 and 4.2.2 is that initially lower fluorescence is observed from *L. monocytogenes* (pSB2018) when grown with xylose. This could possibly be attributed to incomplete activation of P_{xyIA} by xylose. It might be considered that if P_{xyIA} was not completely de-repressed then the overall level of fluorescence of *L. monocytogenes* (pSB2018) would be lower than from *L. monocytogenes* (pSB2019). This however is not the case and cells harbouring the different expression vectors reach approximately the same level of fluorescence towards the end of the growth period. This may be due to

the fact that only a specific threshold level of fluorescence can be reached. It is possible that at higher levels the GFP aggregates within the cytoplasm prior to chromophore formation to form non-fluorescent inclusion bodies. If this were the case then no difference in the overall level of fluorescence would be seen between *L. monocytogenes* harbouring the two expression vectors.

4.3. Fluorescence Characteristics of *L. monocytogenes* cells harbouring the unstable *gfp* plasmids

The construction of the unstable *gfp3opt* plasmids, pSB2020 and pSB2021, has previously been described (in Section 3.14). These translationally optimised *gfp3* variants are downstream of the xylose regulatable promoter $P_{xy/A}$, and hence the promoter can be de-repressed by the addition of xylose to the culture media. These experiments were performed to see if GFP fluorescence could be seen with *L. monocytogenes* harbouring these constructs and also to determine if these variants were indeed unstable by comparing the overall fluorescence characteristics of *L. monocytogenes* expressing *gfp3opt* (ASV) and *gfp3opt* (AGA) to *gfp3opt* encoded by pSB2018 which is stable.

In order to examine the growth and fluorescence characteristics of the bacterial population experiments were performed as previously described in Section 4.1 with optical density and relative fluorescence measurements being taken at hourly intervals. To compensate for any auto fluorescence by the *L. monocytogenes* population, fluorescence measurements were taken of non-recombinant *L. monocytogenes* 7973 at each sampling period. These values were then subtracted from the test samples to give a value of relative fluorescence (RFU) for cells harbouring the different *gfp* constructs. Also, to compensate for the effect of optical density (OD) on fluorescence, the RFU were divided by OD to give RFU/OD. In order to observe the fluorescence characteristics of the bacteria through the growth period, both OD and RFU/OD were plotted as a function of time on the same graph. Each set of data was plotted on one graph to give an overall picture of fluorescence of *L. monocytogenes* harbouring the C-terminal modified *gfp* plasmids; this is shown in Figures 4.3.1 and 4.3.2, however these graphs are quite difficult to interpret due to the number of data sets that have been plotted. To ease interpretation of the results, each data set has been split into three groups and then plotted as described earlier. Each graph represents the growth and fluorescence of *L. monocytogenes* cells harbouring pSB2018 (*gfp3opt*), pSB2021 (*gfp3opt* ASV) and pSB2020 (*gfp3opt* AGA) grown both with and without xylose in the culture media. To determine

whether growth rate was affected by expression of *gfp*, the OD₆₀₀ values of the non-recombinant *L. monocytogenes* strain were also plotted on all graphs. These graphs are illustrated in Figures 4.3.1a, b, c and Figures 4.3.2a, b, c.

Figure 4.3.1: Growth and Fluorescence of *L. monocytogenes* harbouring unstable *gfp3opt* plasmids

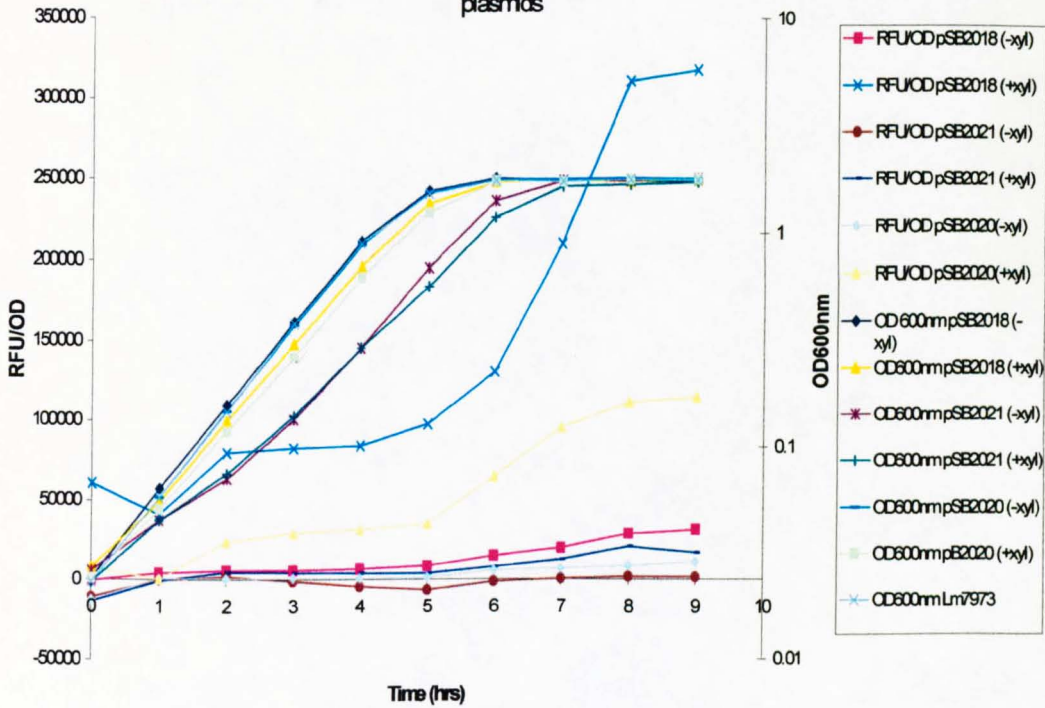


Figure 4.3.1a: Growth and Fluorescence of *L. monocytogenes* (pSB2018)

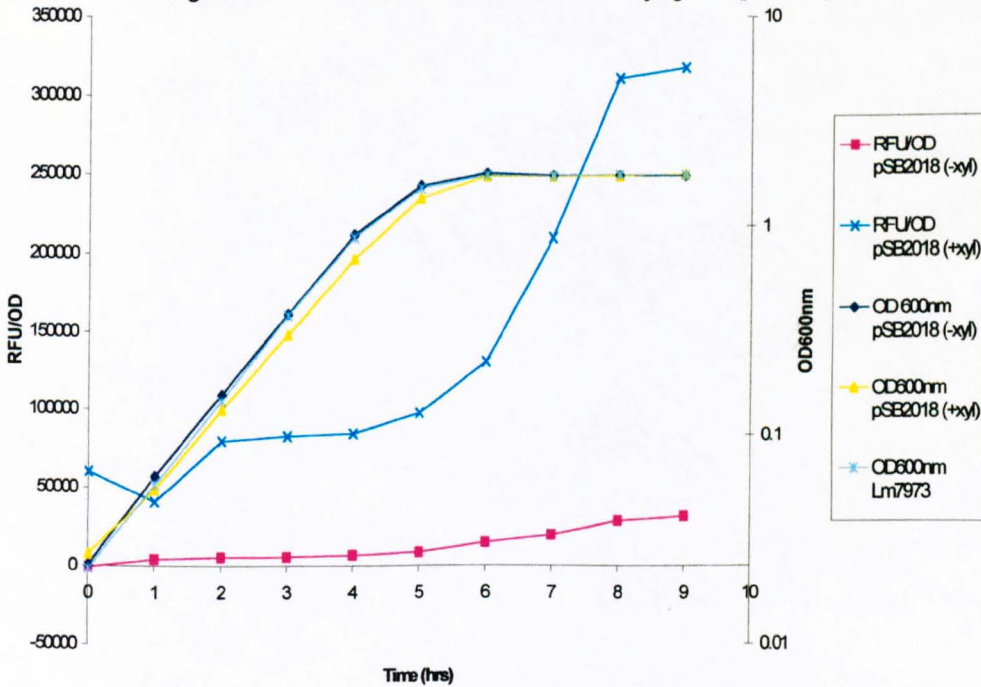


Figure 4.3.1b: Growth and Fluorescence of *L. monocytogenes* (pSB2020)

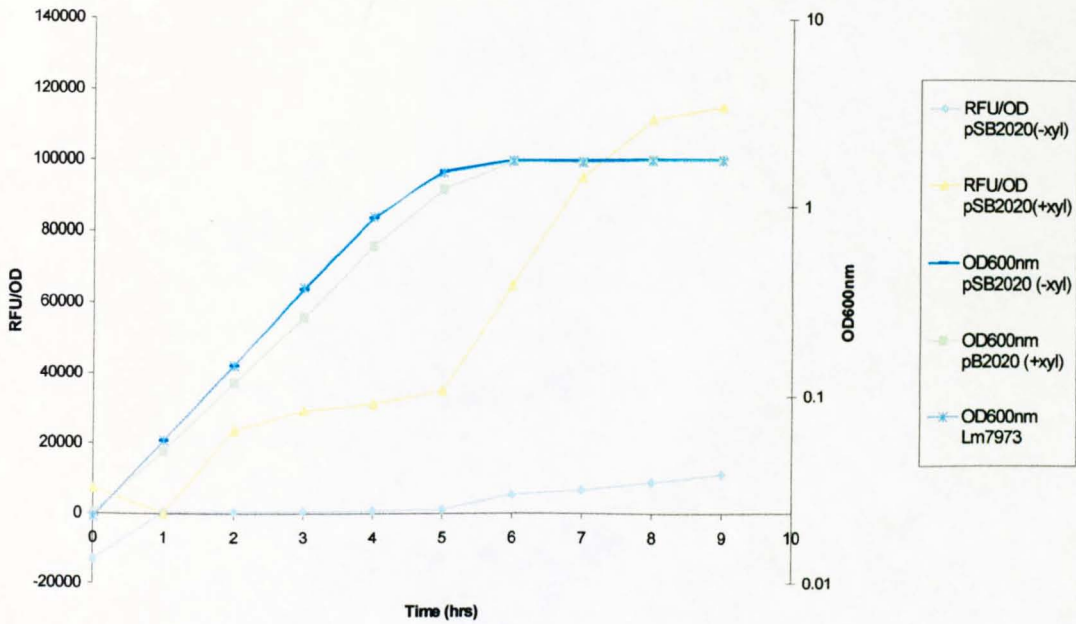


Figure 4.3.1c: Growth and Fluorescence of *L. monocytogenes* (pSB2021)

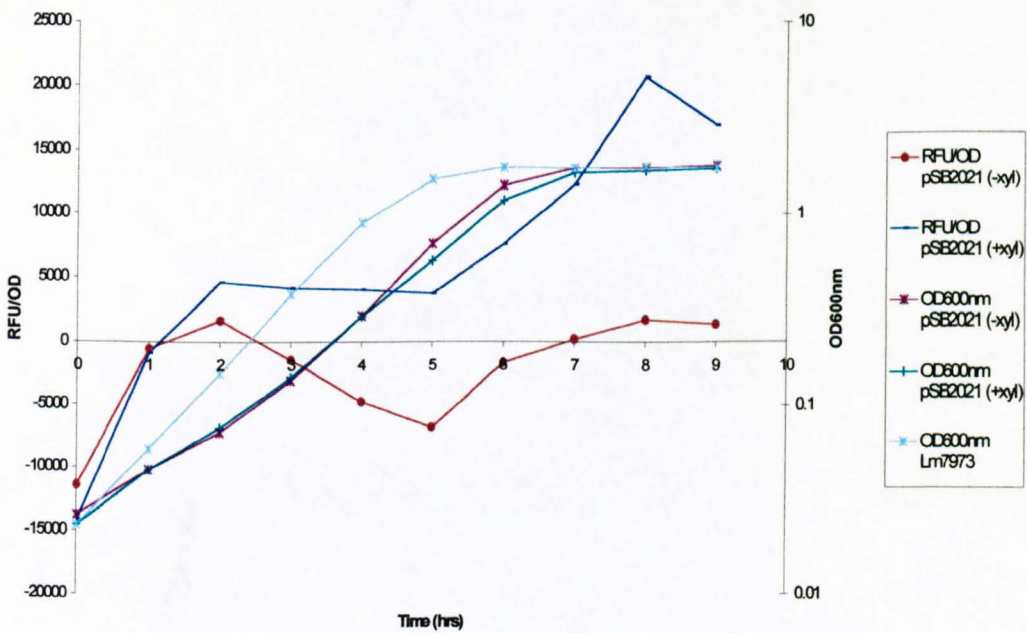


Figure 4.3.2: Growth and Fluorescence of *L. monocytogenes* harbouring unstable *gfp3opt* plasmids

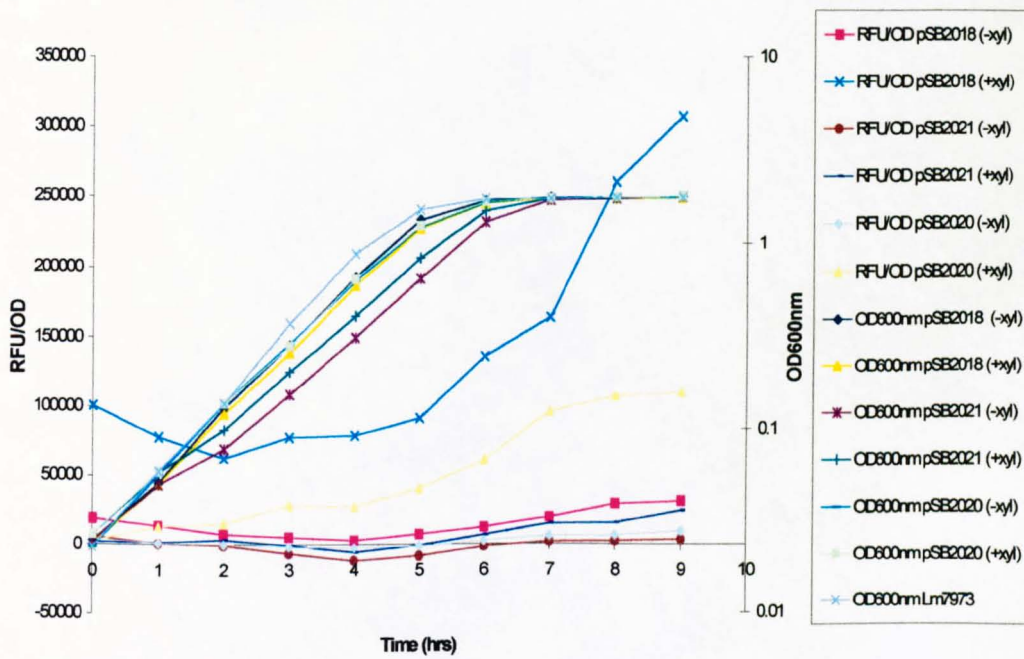


Figure 4.3.2a: Growth and Fluorescence of *L. monocytogenes* (pSB2018)

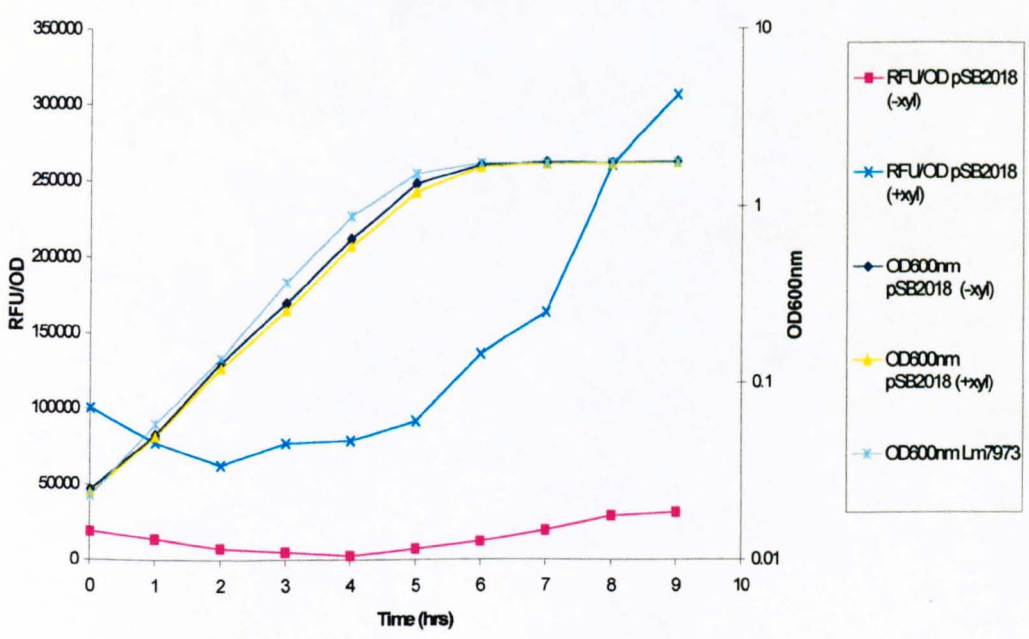


Figure 4.3.2b: Growth and Fluorescence of *L. monocytogenes* (pSB2020)

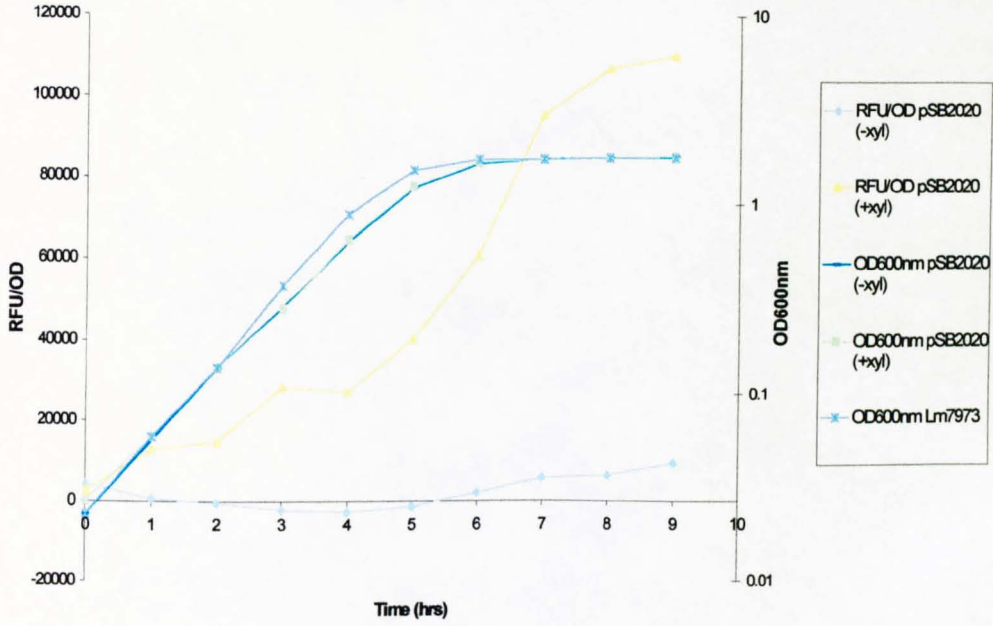
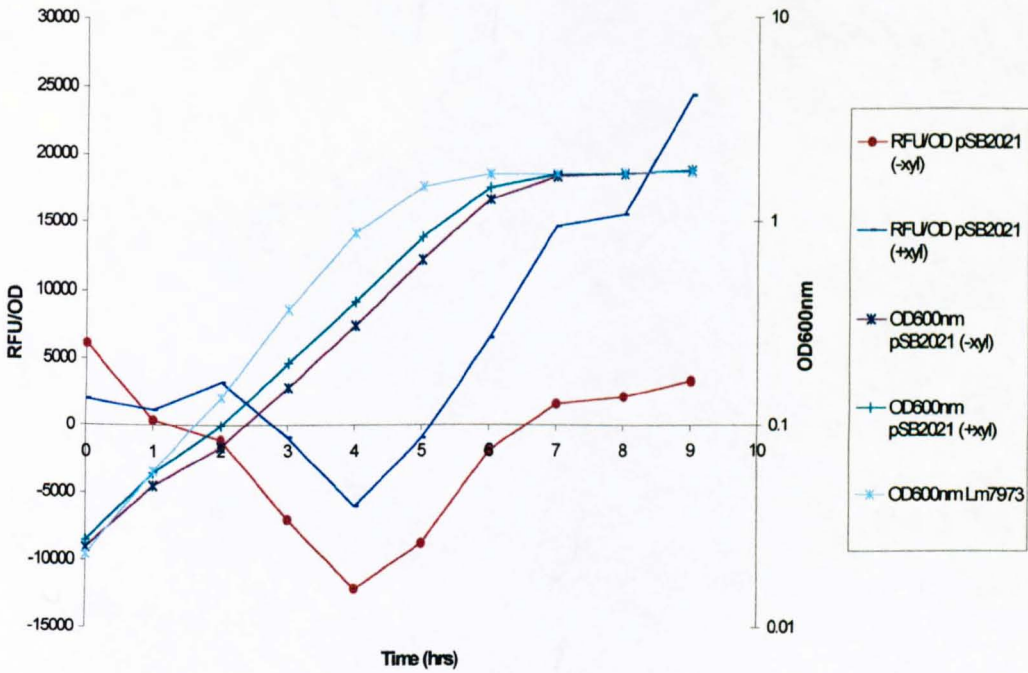


Figure 4.3.2c: Growth and Fluorescence of *L. monocytogenes* (pSB2021)



From the representative graphs that have been drawn using data obtained from these experiments, the overall fluorescence characteristics of the bacterial populations harbouring different *gfp* plasmids were the same on all occasions. The maximum relative fluorescence output for cells grown with and without xylose is shown in Table 4.3.1.

Table 4.3.1: Mean maximum relative fluorescence values for *L. monocytogenes* harbouring stable and unstable *gfp3opt* expression vectors

Plasmid	Maximum RFU/OD + xylose	Maximum RFU/OD - xylose
pSB2018	312473	31387
pSB2020	112450	10237
pSB2021	22513	2323

The *L. monocytogenes* cells that show the highest level of fluorescence are those containing pSB2018. This is a stable variant of *gfp3* that has been translationally optimised for efficient expression in Gram positive organisms (*gfp3opt*). When xylose is not added to the culture media the level of fluorescence observed is approximately ten-fold lower than when P_{xylA} is induced. This shows that P_{xylA} is regulated by xylose and in its absence only a low level of expression of genes downstream of the promoter is observed, indicating that P_{xylA} cannot be completely repressed.

L. monocytogenes (pSB2020) and *L. monocytogenes* (pSB2021) show lower levels of fluorescence compared to *L. monocytogenes* (pSB2018). These plasmids encode

translationally optimised *gfp3* AGA and *gfp3* ASV respectively. This suggests that the *gfp3* variants on these plasmids are indeed unstable. The fact that the GFP3 protein is turned over and cannot accumulate within the bacterial cells is reflected in the overall fluorescence levels. Cells expressing *gfp3opt* AGA show approximately a three-fold reduction in fluorescence compared to cells expressing *gfp3opt*; this is increased to a seven-fold reduction when *gfp3opt* ASV is expressed. There is also a difference in fluorescence between cells that are expressing the different unstable *gfp3* variants. Cells harbouring pSB2021 show much lower levels of fluorescence, about four-fold lower, compared to cells containing pSB2020. This result is not surprising, as it is known that in *E. coli* the unstable GFP variant (*gfp3* ASV) used in the construction of pSB2021 has a shorter half-life (60 minutes) than the equivalent unstable *gfp3* AGA in pSB2020 (300 minutes) (Anderson *et al.*, 1998). The data obtained from the growth experiments with pSB2020 and pSB2021 also showed that fluorescence is increased by a factor of ten when cells are grown with xylose added to the media to induce P_{xyIA} . The fact that some low level fluorescence was detected with all cultures when no xylose is added to the cells, shows the promoter is not fully repressed and some read-through of *gfp* genes downstream of the promoter occurs.

One phenomenon that can be noticed from the graphs (Figures 4.3.1 and 4.3.2) is that the increase in overall fluorescence appears to decrease in all cases approximately three hours after entering stationary phase. With the unstable variants the fluorescence does not appear to increase any further and a plateau has been reached. This suggests that an equilibrium has been attained between synthesis and degradation. It is clear that protein is still being synthesised within the cells due to the fact that levels of fluorescence are not seen to decrease. If cells were to proceed further into stationary phase the activity of P_{xyIA} may be down regulated, if this was to occur a decrease in fluorescence should be observed due to degradation occurring at a faster rate than synthesis of new fluorescent protein.

Examination of the growth rates of *L. monocytogenes* harbouring these *gfp3opt* expression vectors suggests that growth rate is affected slightly by expression of the

unstable *gfp3opt* variants. The mean growth rates of *L. monocytogenes* cells harbouring these xylose induced plasmids are shown in Table 4.3.2.

Table 4.3.2: Average growth rates of *L. monocytogenes* cells harbouring stable and unstable *gfp3opt* expression vectors

Growth rates are shown as an increase in OD per hour

t-test performed, using non-recombinant *L. monocytogenes* 7973 as a control

Plasmid	Mean Growth Rate +xylose	Standard Deviation	P
pSB2018	0.262	5.66×10^{-3}	> 0.05
pSB2020	0.251	2.82×10^{-3}	> 0.05
pSB2021	0.229	8.48×10^{-3}	> 0.05
Non-recombinant <i>L. monocytogenes</i>	0.277 (BHI only)	2.12×10^{-3}	

When xylose was added to the bacterial cultures it could be seen that *L. monocytogenes* expressing the unstable *gfp3opt* variants had a lower rate of growth compared to those expressing the stable *gfp3opt* or non-recombinant cells. This is not unexpected as it is known that these C-terminal modified proteins are degraded by Clp proteases which are ATP dependent, thus the more unstable the protein the greater the energy drain upon the cell which is reflected in the decreased growth rate.

One other point can be noted from examining the growth curves depicted in Figures 4.3.1 and 4.3.2, this is the fact that the more unstable the protein the slower the growth rate at the beginning of the growth cycle. This is unlikely to be due to expression of *gfp3* placing a large energy drain upon the cells, as initially levels of GFP within the cell are very low. *L. monocytogenes* (pSB2021), the protein with the shortest half-life, appears to have the slowest rate of growth initially. It is possible that at the start of growth, energy is directed into degrading any existing protein that is present within the cells, thus there may be a large initial ATP requirement by the

cells and this could be responsible for the initial slower growth rate. The more unstable the protein the higher the ATP requirement by the cell to degrade the protein via Clp proteases thus the slower the initial growth rate. The levels of fluorescent protein are seen to decrease in the first four hours of growth with cells harbouring pSB2021, with cells harbouring pSB2020 and pSB2018 the level of fluorescence within the first four hours does not change dramatically and remains fairly stable. This may explain why the growth rates of cells harbouring pSB2020 and pSB2018 are approximately the same, whereas a much slower initial growth rate is noticed when cells express *gfp3opt* ASV from pSB2021.

The possible ATP requirement by the cells harbouring the unstable *gfp3opt* vectors may explain this slower initial growth, but *L. monocytogenes* (pSB2018) also have a slightly decreased overall growth rate compared to that of non-recombinant *L. monocytogenes* cells whether *gfp3* expression is induced or not. This suggests that some other factor contributes to the decreased growth rate and it cannot not all be attributed to an ATP requirement by the cell to degrade the C- terminal modified GFP proteins as *gfp3opt* encoded by pSB2018 is stable. It appears as though the presence of the *gfp3* expression vectors decreases the growth rate of bacteria harbouring them, especially at the beginning of the growth cycle, this will be discussed further in Chapter 8.

From these experiments it is clear that both pSB2020 and pSB2021 are plasmids that encode unstable *gfp3* variants, as the level of fluorescent protein acquired *L. monocytogenes* harbouring these vectors is much lower than cells that harbour pSB2018, the stable *gfp3* variant. However, the protein is not seen to degrade within the cells, the levels of fluorescence reaches a plateau, which suggests a point is achieved where rate of synthesis equals that of degradation, but as the promoter is constantly synthesising new protein the level of degradation does not exceed that of synthesis.

4.4. Investigating the Degradation Rate of the unstable *gfp* Variants

In order to estimate the degradation rates of the unstable GFP proteins, *L. monocytogenes* harbouring pSB2018, pSB2020 and pSB2021 were grown for a period of 8 hours in xylose. Previous experiments (Section 4.3) showed that at this time levels of fluorescence within the cell were approaching a maximum. The bacterial cultures were washed in an equal volume of PBS, and then concentrated 10-fold in fresh media. These were then used to inoculate fresh media, both with and without 0.5% xylose, at a 1/5 dilution. All cultures were then incubated at 37°C and optical density and fluorescence measured at intervals after the shift.

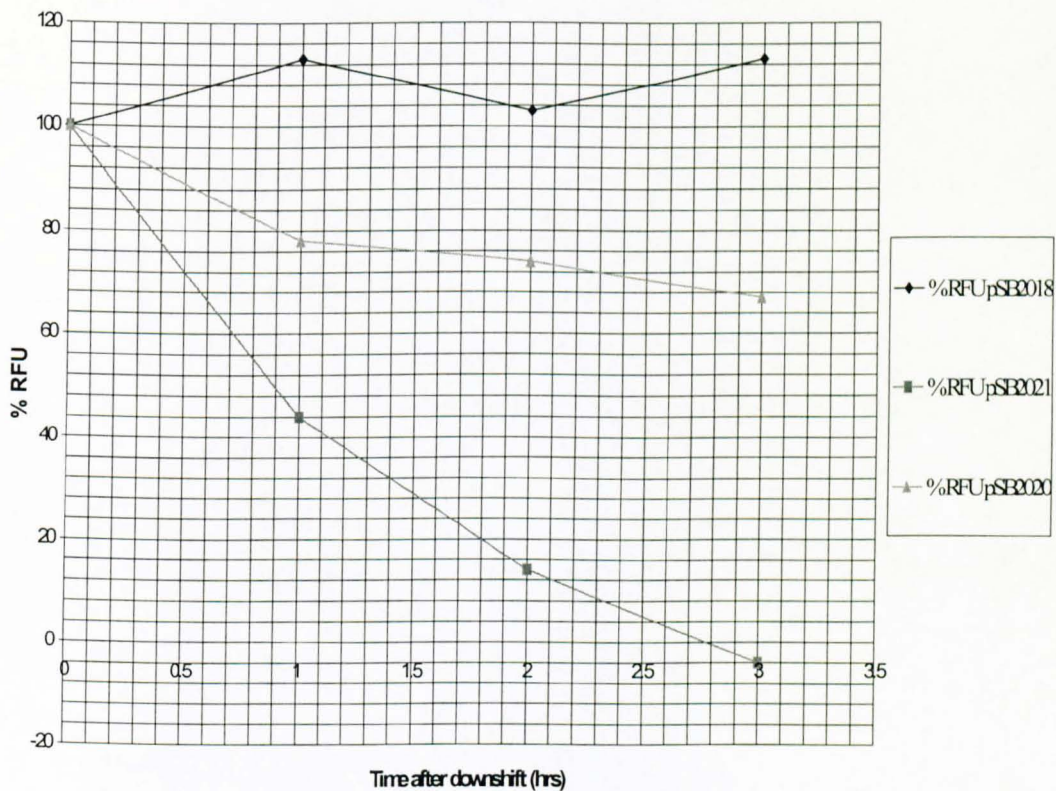
The measured values of green fluorescence of *L. monocytogenes* expressing *gfp3* or the C-terminal modified *gfp3* genes were corrected for background fluorescence by subtracting the corresponding measured fluorescence values of non-recombinant *L. monocytogenes* 7973 cells. When *L. monocytogenes* harbouring the unstable *gfp3* variants were downshifted to media that did not contain the inducer (0.5% xylose), the background corrected values of fluorescence (RFU) were seen to decrease with time. As it is known that only low levels of protein are produced when the promoter is repressed, this suggested that protein previously accumulated within the cells, prior to the downshift, had been degraded within the cells. When *L. monocytogenes* cells expressed the stable *gfp3opt* from pSB2018, no overall loss in RFU was seen, indicating that this protein was stable.

In order to estimate the kinetics of fluorescence and degradation rates of the C-terminal modified GFP proteins, the background corrected RFU were examined. The RFU at time zero was arbitrarily set to 100% and the RFUs at later intervals were calculated as a percentage of this (%RFU). The resulting values are shown in Table 4.4.1. The % RFU was then plotted as a function of postshift time on an arithmetic plot illustrated in Figure 4.4.1.

Table 4.4.1: %RFU for *gfp3* variants in *L. monocytogenes* following a downshift into medium without 0.5% xylose

Time After downshift (hrs)	%RFU pSB2018 (-xyl)	%RFU pSB2021 (-xyl)	%RFU pSB2020 (-xyl)
0	100	100	100
1	113	44	78
2	103	14	74
3	113	-4	67

Figure 4.4.1: Stability of *gfp3* variants in *L. monocytogenes* following a downshift to medium without xylose



From Figure 4.4.1 it could be seen that the fluorescence of *L. monocytogenes* (pSB2018) did not decrease below the starting level. Levels of fluorescence were seen to increase slightly, probably due to poor regulation of P_{xyIA} by xylose. This indicated that the *gfp3* variant in pSB2018 was stable and the protein did not degrade within cells expressing it. This was as expected as *gfp3opt* contains no C-terminal modification, and therefore contains no SsrA protease recognition sequences. This is in accordance with observations by Anderson *et al.* (1998), who demonstrated that colonies and liquid cultures, derived from *E. coli* MV1190 (λ -*pir*), encoding the stable *gfp3* variant, remained fluorescent after several weeks of incubation. The *in vivo* half-life of GFP3 was therefore estimated to be greater than one day.

The fluorescence characteristics of *L. monocytogenes* cells expressing *gfp3opt* ASV from pSB2021 and *gfp3opt* AGA from pSB2020 are also shown in Figure 4.4.1. It could be seen that the cells exhibited a significant decrease in green fluorescence after the shift into new media, due to repression of P_{xyIA} . The gradients of the curves suggested that GFP3 ASV was a more unstable GFP protein than GFP3 AGA. This data backs up the total fluorescence data acquired from these proteins, with cells producing GFP3opt ASV having a lower fluorescent output than GFP3opt AGA. These data suggest that *gfp3* ASV is a more unstable variant than *gfp3* AGA. From the data shown in Figure 4.4.1, the half-lives of the proteins can be determined. The half-life has been estimated as the time taken for a 50% loss to be seen in fluorescence output. The half-life of GFP3 ASV, encoded by pSB2021, was determined to be approximately 54 minutes, the half life for GFP3 AGA, encoded by pSB2020, could not be determined accurately from the graph as it can not be assumed that a linear relationship exists between degradation of the protein with respect to time, but it can be said that the half life is greater than 3 hours. In *E. coli* Anderson *et al.* (1998) reported half-lives of approximately 60 and 300 minutes respectively for GFP3 ASV and GFP3 AGA. In *P. putida* the *in vivo* half-life of GFP3 ASV was reported to be approximately 190 minutes (Anderson *et al.*, 1998). The half-lives generated from *L. monocytogenes* cells encoding pSB2021 (GFP3 ASV) corresponds well with the reported half-life of the same protein in *E. coli* by Anderson *et al.* (1998). However, *P. putida* expressing the same *gfp3* variant (ASV)

was reported to have a much longer half-life compared to expression in *E. coli* (Anderson *et al.*, 1998). These data suggest that there is species independent instability of the C-terminal modified peptides, nevertheless, all C-terminal modified peptides have to shown to be more unstable than the wild type equivalent (GFP3).

These results suggest that the C-terminal modified *gfp3* genes may be more useful as reporter genes than *gfp3*. These reporters could be used to reflect bi-directional changes in gene expression, as such an event would lead to a decrease in fluorescent output from the cells. However, the fluorescence generated by the C-terminal modified proteins is much weaker than that generated from the stable GFP3 protein, so there is likely to be more problems with background fluorescence and sensitivity of the reporters. For example, it is possible that in an intracellular environment, the fluorescent signal generated from the unstable GFP3 proteins may be too weak to see through any autofluorescence of the eukaryotic cells.

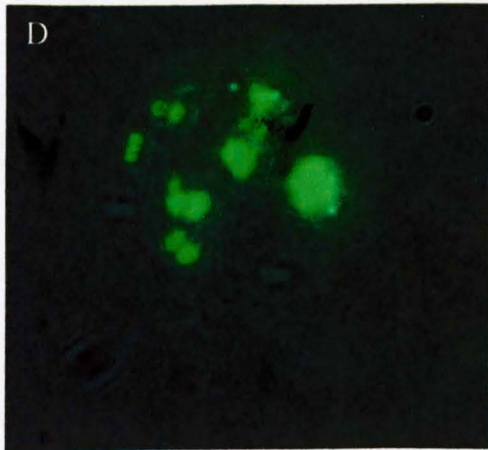
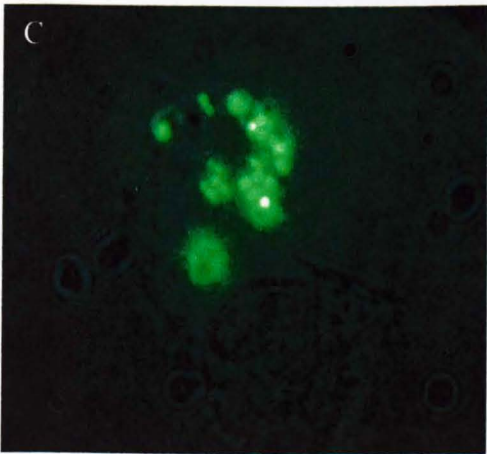
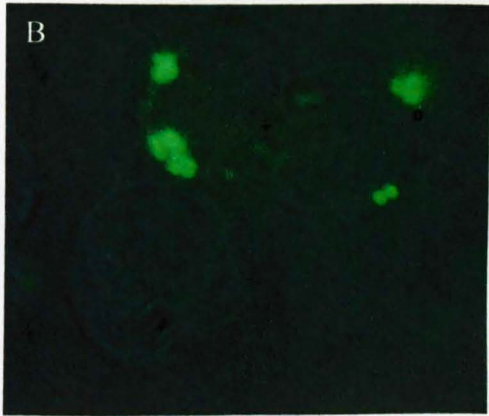
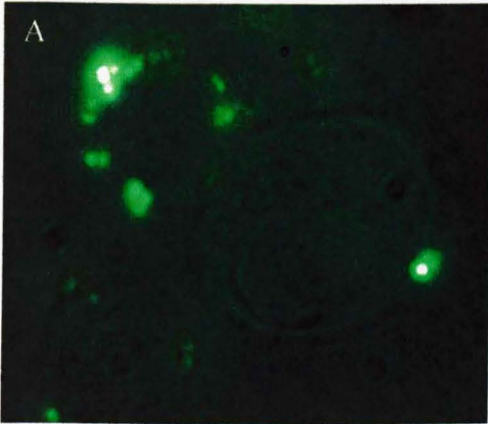
Although the proteins appear to be unstable, the results suggest that the proteases degrading tagged proteins in *L. monocytogenes* may differ in specificity from those in *E. coli*, hence the altered half-lives. It appears as though the protease reactions resulting in degradation of GFP may be dependent on a number of factors, for example strain, growth conditions, competing targets within the cell etc. Nevertheless, what is known is that a protein that is known to be very stable has been converted to an unstable variant through the use of a natural protease activity, which is found in many different bacteria. The unstable characteristics of these C-terminal changed proteins have been observed in *E. coli*, *P. putida* (Anderson *et al.*, 1998) and also in *L. monocytogenes*.

4.5. Tagging bacterial cells with GFP to monitor bacterial movement in an intracellular environment

Although primarily known as an extracellular pathogen, *S. aureus* has been shown to internalise and survive within a wide range of mammalian cells, especially endothelial cells (Vann and Proctor, 1987, Almeida, 1996). Menzies and Kourteva (1998) proved that, in addition to their presence within vacuoles (Hamill, 1986), they could exist free within the cytoplasm. This pilot experiment was performed in order to determine whether *S. aureus* RN4220 could become internalised in a tissue culture cell line and whether the bacteria appeared to grow and divide in an intracellular environment and also to determine whether the GFP protein could generate a fluorescent signal in an intracellular environment.. This was achieved through using *S. aureus* (pSB2018) and a human umbilical veined endothelial cell line (HUVEC).

HUVEC cells were seeded onto glass coverslips, these were grown until the cells were approximately 80-90% confluent. *S. aureus* RN4220 (pSB2018) were grown overnight in BM Cm7. This was centrifuged and the pellet washed twice in fresh medium. This was then diluted 1:20 and grown for a further 1 hour period. Following this, the bacterial culture was diluted again 1:20 and grown for 3 hours at 37°C. In the meantime, the medium on the HUVEC cells was replaced with un-supplemented RPMI (no antibiotics). 1ml samples of the bacterial culture were centrifuged and resuspended in 10ml RPMI, this was then added to the HUVEC cells which were then incubated for a further two hour period as described in Section 2.12. After incubation, HUVEC cells were washed in PBS and fixed with 3% formalin as described in the Materials and Methods, Section 2.12. The mounted coverslips were then observed by fluorescence microscopy in order to locate intracellular bacteria. The resulting images are illustrated in Figures 4.5.1a, b, c, d.

Figure 4.5.1: Intracellular GFP tagged *S. aureus* expressing *gfp3* from pSB2018 (P_{xylA} -*xylR*-*gfp3opt*)



It can be clearly seen from the images (Figure 4.5.1) that *S. aureus* RN4220 cells have become intracellular following contact with the cell surfaces of HUVEC cells. Bayles *et al.* (1998) showed that *S. aureus* that had been introduced to a MAC-T cell line were associated with the cell surface through a pseudopod-like structure. These structures were assumed to be involved with engulfing the bacteria, leading to the formation of membrane bound endosomes. Although not very clear from these illustrations, it appeared as though some of these intracellular bacteria were surrounded by a membrane whilst some were free in the cytoplasm. A better representation of the cellular structures could be obtained from confocal microscopy, this would also give unquestionable data concerning the location of the tagged bacteria.

Having shown that GFP can be used to follow the movement of bacteria in an intracellular environment, then it may be possible, through the use of the unstable GFP variants, to build expression vectors that could report on gene expression within the cell.

4.6. Discussion

L. monocytogenes (pSB2018) were grown in BHI both with and without the addition of 0.5% xylose. During the course of the experiment growth and fluorescence characteristics of the cells were examined. It was determined that the promoter was well regulated by xylose although expression was not completely repressed when the inducer was not present. When xylose was absent from the culture media, production of GFP3opt was reduced ten-fold to about 4000 units, but these levels of fluorescence were higher than the background fluorescence shown by non-recombinant *L. monocytogenes* cells, suggesting that this was GFP fluorescence and not just auto-fluorescence of the bacterial cells. The low-level fluorescence of the bacterial population when cells were grown without inducer has been confirmed by fluorescence microscopy, which showed that a few fluorescent cells were present within the population. These data indicated that some GFP3 production was occurring within the cells harbouring pSB2018, even when xylose was absent, which implied that P_{xyIA} was not fully repressed. When *L. monocytogenes* (pSB2018) were grown with 0.5% xylose, production of GFP3 increased 10-fold. This showed that the xylose dependent regulator, *xylR*, present on this plasmid, bound xylose which was added to the culture, thus de-repressing P_{xyIA}. Although the promoter had been induced by xylose, it took a period of around five hours before an increase in GFP3 fluorescence was seen within the bacterial culture. This initial delay in fluorescence was expected, as once *gfp3opt* has been translated, post-translational modification has to occur in order for the chromophore to fold resulting in fluorescent protein. Due to this delay in forming fluorescent protein and its resultant stability within the cell, it is impossible to determine the promoter kinetics within the bacteria in real time. If the promoter is repressed or down regulated late in the growth cycle, no difference in the fluorescence characteristics of the cells would be seen due to the stability of GFP3opt. However, if the promoter was repressed early on, a decrease in RFU may be observed, due to dilution of the signal as the cells divide.

When *L. monocytogenes* (pSB2019) were grown in medium without xylose a high level of GFP3 fluorescence was seen from the cells. This was approximately the

same or higher than that observed when *L. monocytogenes* (pSB2018) was induced by xylose. This indicated that although both the P_{xyIR} and P_{xyIA} promoters are present on pSB2019, *xyIR* has been successfully removed from the plasmid, as when no xylose was present in the media high expression of *gfp3opt* was seen from the bacterial cells. This is unlike *L. monocytogenes* expressing *gfp3opt* from pSB2018, which showed only low levels of GFP3 production when grown without xylose.

A major drawback of GFP is its stability once formed (Tombolini *et al.*, 1997), this makes the protein less valuable for real time gene expression studies. The stable GFP is unable to reflect bi-directional changes in gene expression within the cell. The expression of *gfp3opt* from both pSB2018 and pSB2019 gives no reflection on the promoter dynamics within the cell due to the stability of the protein produced, neither of the expression vectors could be used to reflect any bi-directional changes in gene expression.

Keiler *et al.* (1996) showed that specific C-terminal oligopeptide extension caused an otherwise stable protein to degradation by certain intracellular tail-specific proteases. The construction of the unstable *gfp3* variants was based on this natural protein degradation system, which is based on SsrA mediated tagging of prematurely terminated polypeptides at the COOH end. The *ssrA* transcript is a stable 362 nucleotide RNA molecule that exhibits some tRNA properties and can be charged with alanine (Komine *et al.*, 1994). Genes homologous to *ssrA* have been identified in Gram positive (Ushida *et al.*, 1994) and Gram negative bacteria, (Brown *et al.*, 1990, Tyagi and Klinger, 1992) implying this peptide tagging system mediated by *ssrA* is conserved in bacteria. The COOH terminal tail sequence of the *ssrA* encoded peptide tag (YALAA) are similar to a COOH terminal tail sequence (WVAAA) recognised by Tsp (Silber and Sauer, 1994), a periplasmic endonuclease and by a cytoplasmic protease that degrades proteins in a tail dependent manner (Silber and Sauer, 1994). Thus it was reasoned that tagging with the *ssrA* encoded peptide might target proteins for degradation by COOH terminal specific proteases.

Keiler *et al.*, (1996) proposed that in *E. coli*, the *ssrA* transcript targets peptides translated from mRNA lacking a termination codon. Subsequently, a peptide tag with the sequence AANDENYALAA is attached to the COOH terminus of the nascent polypeptide chain by cotranslational switching of the ribosome from the damaged DNA to the *ssrA* transcript. The resulting protein carries the C-terminal tag, is recognised and rapidly degraded by intracellular tail-specific proteases (Keiler *et al.*, 1996). In the periplasm, the degradation of this C-terminal modified protein is executed by the tail specific protease Tsp, whereas tagged proteins located in the cytoplasm are thought to be broken down by Clp proteases.

gfp3 mutants were made by constructing variants with minor alterations in the Tsp consensus sequence (Anderson *et al.*, 1998). As GFP accumulates within the cytoplasm, it thought that the degradation process of the C-terminally tagged proteins occurs through the action of Clp proteases, which are ATP dependant enzymes whose mode of action has been previously described in the introduction.

In order to create *gfp* vectors that could be used in gene expression studies, two unstable *gfp3* variants were studied; these encode proteins that have a much shorter half-life compared to GFP3. *L. monocytogenes* cells harbouring pSB2020 and pSB2021, encode translationally optimised *gfp3* AGA and *gfp3* ASV respectively, and were seen to show lower levels of fluorescence compared to cells expressing *gfp3opt* from pSB2018. There is also a difference in fluorescence levels between cells that are expressing the two unstable GFP proteins. Cells harbouring pSB2021 showed much lower levels of fluorescence, about four-fold lower, compared to cells containing pSB2020. Cells harbouring pSB2020 showed approximately a three-fold reduction in fluorescence compared to cells expressing *gfp3opt* from pSB2018; this is increased to a seven-fold reduction when *gfp3opt* ASV is expressed from pSB2021. These data are not surprising and support the observation made by Anderson *et al.* (1998) who showed that in *E. coli* the unstable *gfp3* variant used in the construction of pSB2021 has a shorter half-life (60 minutes) than the equivalent unstable *gfp3* in pSB2020 (300 minutes).

In all cases, when cells were grown without added xylose, levels of fluorescence decreased by approximately 10 fold. Again this showed that the P_{xyIA} promoter is not completely repressed and some read-through of the downstream gene occurs. One other point that was observed was that when cells expressed *gfp3opt* ASV, the most unstable *gfp3* variant, the initial growth rate of the bacteria was decreased, indicating that some energy drain or metabolic load was being placed upon the cells early in the growth experiment. This may be due to the high ATP requirement necessary for degradation of the protein by Clp proteases. Another possible explanation for the decreased growth rates shown by *L. monocytogenes* expressing the different *gfp3* variants in the actual plasmid. Gruss and Ehrlich (1988) showed that pC194, which makes up part of the expression vectors, generated large quantities of high molecular weight (HMW) DNA upon insertion of heterologous DNA fragments, the quantity of the HMW DNA depended on the nature of the inserted fragment. If this was true then this may be reflected in the overall growth rates of bacteria harbouring the *gfp3* expression vectors, this will be discussed in greater detail in Chapter 8.

The data gained from observing fluorescence of the unstable *gfp3* variants suggested that P_{xyIA} is constitutive, as fluorescence from the unstable *gfp3* expression vectors does not decrease, but is seen to plateau suggesting equilibrium has been attained between synthesis and degradation of the protein. If the promoter had been downregulated the level of fluorescence from *L. monocytogenes* harbouring the unstable *gfp3* vectors may be expected to decrease, due to the degradation of the protein and also due to dilution of the signal by dividing bacteria.

Experiments have shown that the fluorescence of *L. monocytogenes* (pSB2018) did not decrease and in fact levels of fluorescence were seen to increase slightly probably due to incomplete repression of the P_{xyIA} promoter, suggesting the GFP3 protein was stable. This was as expected as this *gfp3* variant contains no C-terminal modification, and therefore contains no protease recognition sequences. The fluorescence of *L. monocytogenes* containing pSB2020 and pSB2021 was seen to decrease significantly after repression of P_{xyIA} . As the action of the P_{xyIA} promoter has been repressed, little new GFP is made and hence the degradation of existing protein could be observed

and the half-lives of the proteins resolved using the method of Anderson *et al.* (1998). The *in vivo* half-lives were determined to be approximately 54 minutes for mature GFP3 ASV and greater than 3 hours GFP3 AGA. Anderson *et al.* (1998) reported half-lives of approximately 60 and 300 minutes respectively for GFP3 ASV and GFP3 AGA in *E. coli*, and in *P. putida* the *in vivo* half-life of GFP3 ASV was reported to be approximately 190 minutes. So it does appear as though in *L. monocytogenes* these unstable GFP3 proteins are turned over within the cell and have a shorter half-life compared to GFP3opt. The observed degradation of rates of GFP3 ASV in *E. coli* and *L. monocytogenes* compare well, however a much longer degradation rate was observed in *P. putida* (Anderson *et al.*, 1998). The observed degradation rate appears to depend on the species expressing the protein. This suggests that the proteases degrading the tagged proteins in *L. monocytogenes* may differ in specificity from those in other bacteria, hence the altered degradation rates. Due to their unstable nature, these *gfp3* expression vectors could be used to determine more accurately the promoter kinetics within bacterial cells or used as an indicator of gene expression. However, they still do not provide a real time indication of events occurring within the cell, as time is still needed for fluorescent protein to fold after its initial translation. Nevertheless, the unstable *gfp3* variant with the shortest half-life should be able to report any down regulation of gene expression, as such events would be marked by a decrease in fluorescent output.

Experiments utilising *S. aureus* RN4220 (pSB2018) showed that a signal from the *gfp3opt* could be observed in an intracellular environment when the bacteria were grown with xylose to induced P_{xylA} . Thus it is hoped that similar experiments may be performed using other *gfp3* expression vectors to investigate gene expression within the bacteria. However, in order to observe gene expression in real time, the unstable *gfp3* variants would have to be utilised, but there is some doubt as to whether the signal from these would be able to be seen above the background fluorescence observed from the HUVEC cells.

CHAPTER 5

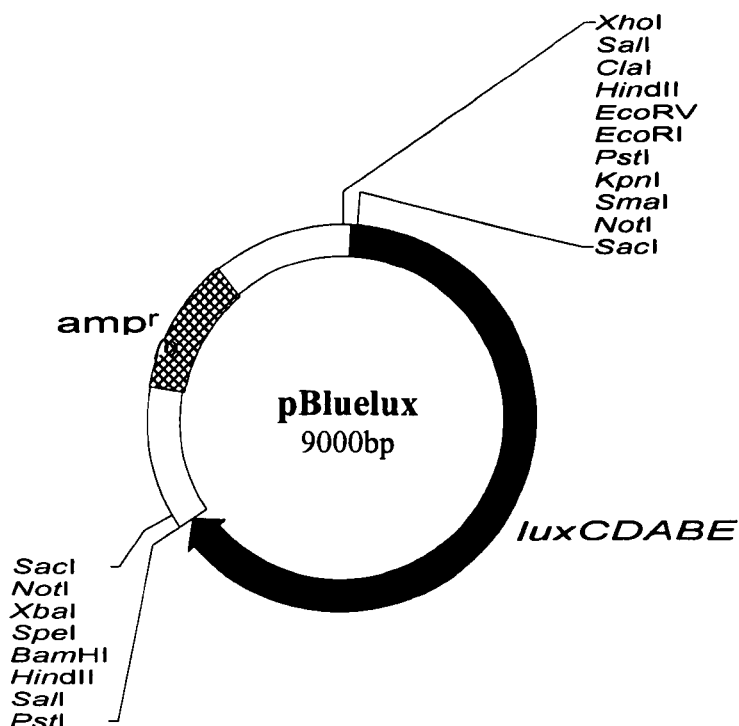
CONSTRUCTION AND EVALUATION OF A *LUX* BASED REPORTER FOR EXPRESSION IN GRAM POSITIVE BACTERIA

CHAPTER 5: CONSTRUCTION AND EVALUATION OF A *LUX* BASED REPORTER FOR EXPRESSION IN GRAM POSITIVE BACTERIA

5.1. Expression of the *Photobacterium luminescens lux* operon from the P_{xyn} Promoter

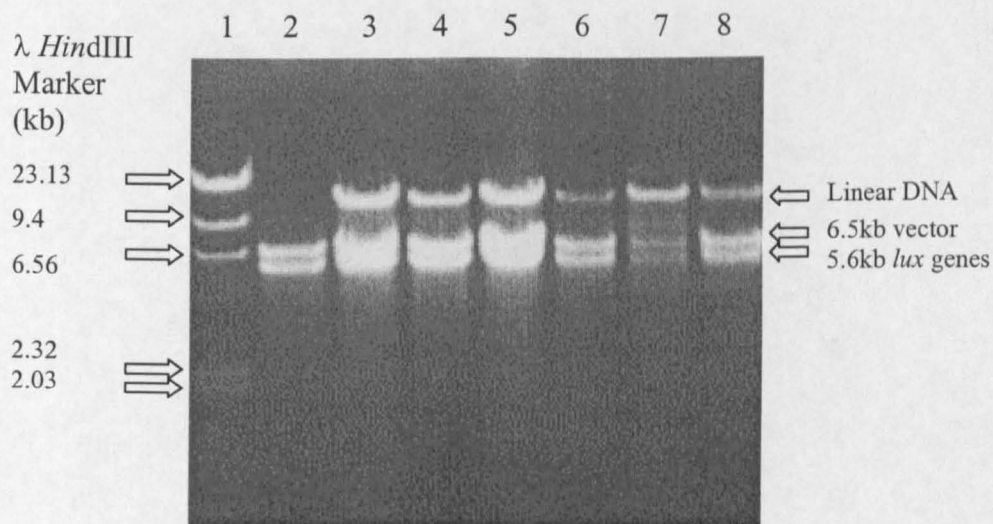
The *luxCDABE* operon from *P. luminescens* ATCC29999 had previously been inserted into the *Sma*I restriction site of pBluescript II KS (unpublished, J. Throup), this resulted in the construction of pBluelux which is illustrated in Figure 5.1.1. This plasmid contained the *luxCDABE* operon in the opposite orientation to the *lacZ* promoter, and thus *E. coli* JM109 cells harbouring this construct showed only low levels of bioluminescence.

Figure 5.1.1: Restriction map of pBluelux



The *lux* operon was excised from pBluelux upon restriction with *Sna*BI and *Sal*I. The purified DNA was then ligated with pGC4 which had previously been digested with *Sma*I / *Sal*I in order to excise the *luxAB* fusion from the plasmid. Following ligation of the two DNA fragments the DNA was introduced into *E. coli* JM109 cells by electroporation. Colonies that contained recombinant DNA were isolated on ampicillin selective agar and then observed under a Hamamatsu VIM3 camera to ascertain the bioluminescent properties of the cells. DNA was prepared by plasmid miniprep from those colonies that were seen to be highly bioluminescent and the resulting DNA investigated by restriction analysis with *Eco*RI and *Sal*I. Analysis of restricted DNA by agarose gel electrophoresis showed that all the colonies contained the 5.8kb *lux* insert into the plasmid, restriction analysis of the DNA and a resulting restriction map of the new plasmid construct, named pSB2022, are shown in Figures 5.1.2a and Figures 5.1.2b

Figure 5.1.2a: Restriction Analysis of DNA thought to contain the *lux* operon

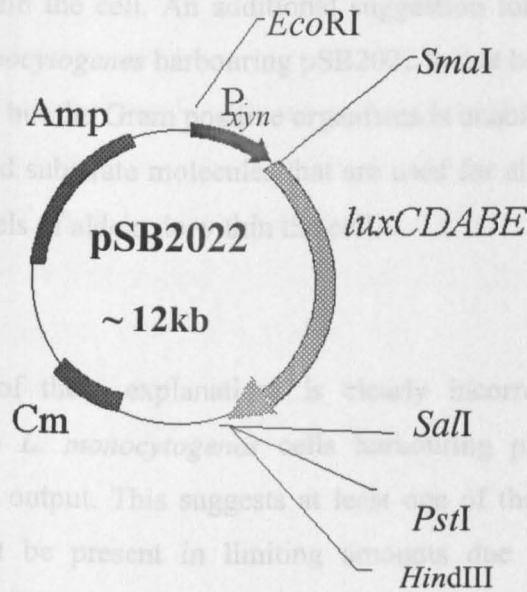


Layout of gel:

Lane1: λ HindIII

Lane2-8: Putative DNA thought to contain the *lux* operon restricted with *Eco*RI and *Sal*I

Figure 5.1.2b: Restriction map of pSB2022



L. monocytogenes were transformed with pSB2022 by electroporation. After incubation on BHI agar containing chloramphenicol at $7\mu\text{gml}^{-1}$ some recombinant colonies were isolated. When these were examined under a Hamamatsu VIM3 camera, the bioluminescent emission from the recombinant organisms was found to be extremely faint. It was unclear why when pSB2022 was introduced into *L. monocytogenes* the cells were not as bioluminescent as *E. coli* cells harbouring the same construct. It is known that the P_{xyn} promoter is strongly expressed in Gram positives as high bioluminescent levels are observed from *L. monocytogenes* cells harbouring pGC4, due to the expression of *luxAB*, which is downstream of P_{xyn}. The low luminescence levels could be attributed to a lack of FMNH₂ or molecular oxygen within the cells, but this too appears unlikely, again due to the fact that expression of *luxAB* can be observed in *L. monocytogenes* cells.

There are several issues that could be responsible for the poor luminescence emission observed from *L. monocytogenes*. It is possible that transcription of the *lux* operon is being terminated prematurely resulting in the production of a partial transcript, this

would lead to an incomplete set of Lux proteins being synthesised. Another possible explanation is that translation of one or more of the *lux* genes is poorly initiated or prematurely terminated which would again lead to an incomplete set of Lux proteins present within the cell. An additional suggestion for the low light levels produced from *L. monocytogenes* harbouring pSB2022 is that both transcription and translation are efficient but the Gram positive organism is unable to produce sufficient amounts of the fatty acid substrate molecules that are used for aldehyde production, resulting in limiting levels of aldehyde within the cell.

The latter of these explanations is clearly incorrect as addition of exogenous aldehyde to *L. monocytogenes* cells harbouring pSB2022 did not increase the luminescent output. This suggests at least one of the luciferase subunits (LuxA or LuxB) must be present in limiting amounts due to inefficient transcription or translation within the cells.

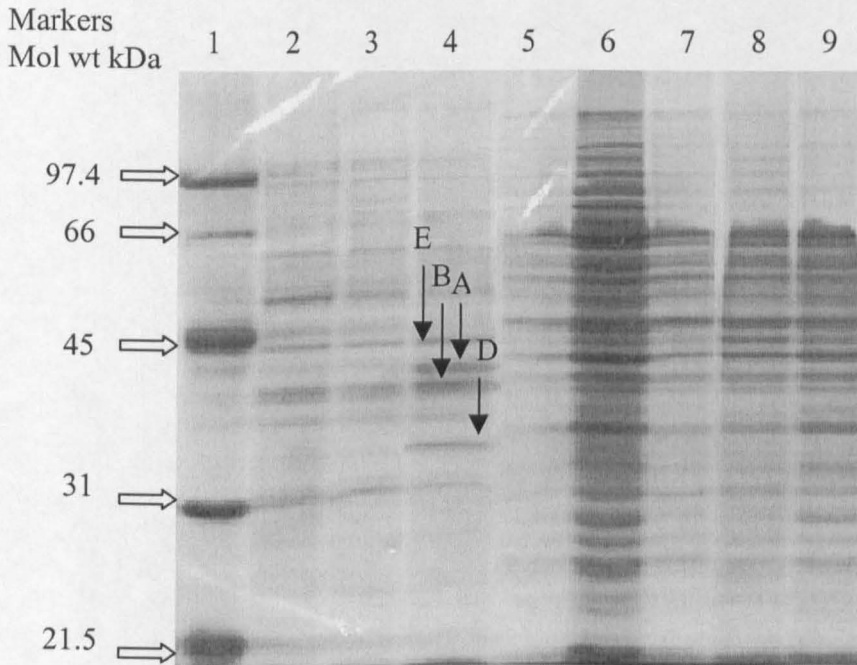
In order to determine whether the problem was one of inefficient translation, it was decided to try and identify the different protein products of the 5 genes of the *lux* operon using SDS PAGE. In order to isolate proteins from *L. monocytogenes*, cells were subjected to sonication as described in Section 2.9.2. As a control *E. coli* cells expressing *lux* from pSB2022 were also run on the same gel. The resulting gel is depicted in Figure 5.1.3.

Upon examination of the gel it could be seen that some of the 5 polypeptides of the *lux* operon could be seen in *E. coli* (pSB2022). The *lux* operon produces individual peptides of the following molecular weights, LuxC, 54kDa; LuxD, 34kDa; LuxA, 40kDa; LuxB, 37kDa; LuxE, 44kDa. In the *E. coli* cells containing pSB2022 there appeared to be at least 3, possibly 4, novel peptides, these are indicated on the gel which is represented in Figure 5.1.3. It is thought that these bands correspond to the peptides LuxA, B, D and E. However, it is clear from examination of the gel that none of the genes of the *lux* operon were being highly expressed in *L. monocytogenes* cells carrying the plasmid borne *lux* operon, pSB2022, as no bands could be

identified that correspond to the size of the gene products expected. This data suggests that the limiting factor to *lux* operon expression in Gram positive bacteria is either limited transcription of the *lux* genes or limited translation of the *lux* genes. If transcription was prematurely terminated it would lead to the formation of a partial transcript and subsequently to the production of an incomplete set of Lux proteins. If the low luminescent levels were attributed to translation of one or more of the *lux* genes being prematurely terminated or poorly initiated, this too would lead to the production of an incomplete set of Lux proteins. Previous experience of gene expression in such organisms (Jacobs *et al.*, 1991; Hill *et al.*, 1994; Qazi *et al.*, 1998) led to the surmise that the problem was most likely to be that of inefficient translational initiation within the cell.

Figure 5.1.3: SDS PAGE gel of *E. coli* (pSB2022) and *L. monocytogenes* (pSB2022)

Unique bands seen in the whole cell extracts of cells expressing Lux proteins are indicated with an arrow



Layout of gel:

Lane1: Low range SDS PAGE Makers

Lane2: *E. coli* JM109

Lane3: *E. coli* JM109 (pGC4)

Lane4: *E. coli* JM109 (pSB2022), bands corresponding to Lux proteins marked with arrows

Lane 5: *L. monocytogenes* 7973 (pSB2022)

Lane6: *L. monocytogenes* 7973

Lane7: *L. monocytogenes* 7973 (pSB2022)

Lane 8: *L. monocytogenes* 7973 (pGC4)

Lane 9: *L. monocytogenes* 7973

5.2. Reconstruction of the *P. luminescens lux* operon

Analysis of the *lux* operon DNA sequence suggested that *luxA*, *luxC* and *luxE* were poorly translated within Gram positive bacteria. In order to circumvent this problem PCR primers were designed that incorporated enhanced translational initiation signals for the genes which DNA sequence analysis suggested might be poorly translated, as described by Vellanoweth (1993). So that the individual genes of the *lux* operon could be cloned, the PCR primers also incorporated restriction sites at both the 5' and 3' ends of the coding sequence. The restriction sites on each primer are indicated in Table 5.2.1.

Table 5.2.1: Restriction sites incorporated into the primers for amplification of the *lux* operon

The sequences of the primers are given in Appendix 1.

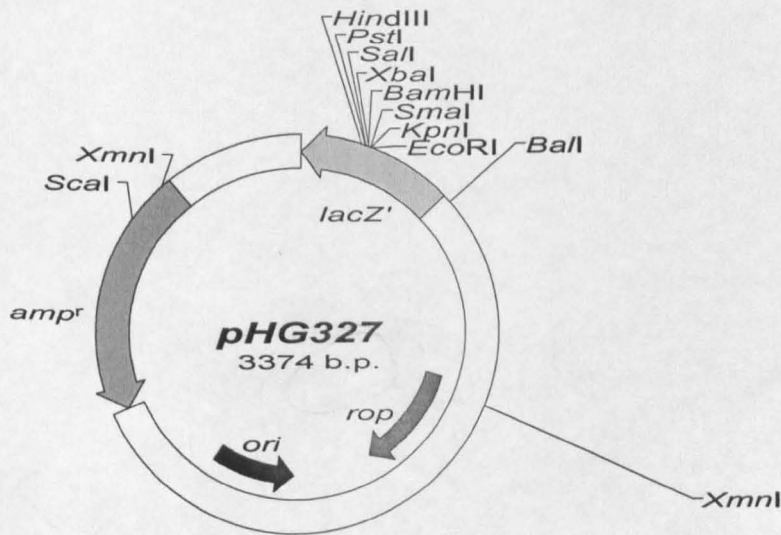
Primer	Restriction Site
5' <i>luxA</i> (forward) primer 12	<i>EcoRI</i> / <i>SalI</i>
3' <i>luxB</i> (reverse) primer 13	<i>KpnI</i>
5' <i>luxC</i> (forward) primer 14	<i>KpnI</i>
3' <i>luxD</i> (reverse) primer 15	<i>BamHI</i>
5' <i>luxE</i> (forward) primer 16	<i>BamHI</i>
3' <i>luxE</i> (reverse) primer 17	<i>PstI</i> / <i>EcoRV</i>

The primer pairs were used in PCR reactions in which *luxAB*, *luxCD* and *luxE* were amplified from pBluelux, the details of which have previously been described in Section 5.1. The plasmid pBluelux was used in the reaction at a concentration of $1\text{ng}\mu\text{l}^{-1}$, this provided a source of template DNA for all the *lux* genes. The PCR reaction was set up essentially as described in Section 2.5.3, primers used were 12 and 13, 14 and 15, and 16 and 17. As all the primer pairs were used separately in one reaction to amplify their specific genes, this was reflected in the

annealing temperature and DNA extension time that was used. The reaction parameters incorporated an annealing temperature of 60°C for 3 minutes and an extension period for 3 minutes at 72°C. The resulting PCR products were examined by agarose gel electrophoresis, which confirmed the presence of DNA bands of 2.2, 2.4, and 1.1kb, which corresponded to *luxAB*, *luxCD* and *luxE* respectively.

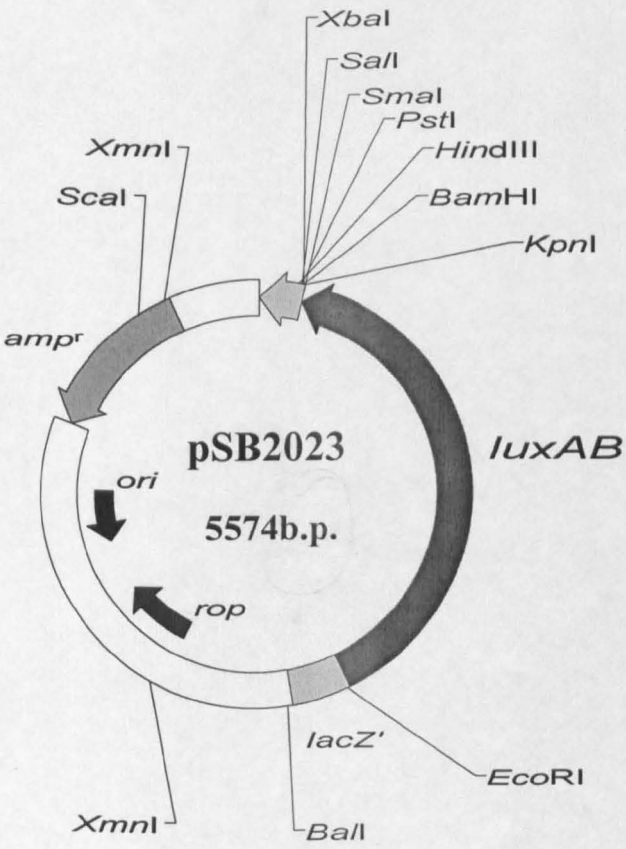
The PCR product that encodes the *luxAB* genes was purified from a low melting point agarose gel by freeze thaw. The purified DNA was then restricted with *KpnI* and *EcoRI*. After inactivation of the restriction enzymes using phenol chloroform extraction, the digested PCR product was ligated with pHG327, previously restricted with the same enzymes. The plasmid pHG327 is based on pHG165 (Stewart *et al.*, 1986) and has the pUC18 multi-cloning site within the *lacZ α* peptide gene and is illustrated in Figure 5.2.1.

Figure 5.2.1: Restriction Map of pHG327



The ligated DNA was then used to transform *E. coli* JM109 competent cells by electroporation. Cells containing recombinant DNA were isolated following selection on ampicillin agar plates. Those colonies that grew on the antibiotic plates were then screened under a Hamamatsu VIM3 camera in the presence of exogenous aldehyde in order to detect any bioluminescence from the cells. DNA was prepared by plasmid miniprep of the one colony that did show a luminescent phenotype along with a dark colony as a control. These were then analysed by restriction analysis with *EcoRI* and also by using *SaII* / *EcoRI*. After the restriction digests were electrophoresed on an agarose gel it could be seen that the plasmid DNA from the colony that exhibited a luminescent phenotype contained a 2.2kb insert, this being the *luxAB* genes, this construct was named pSB2023 and is pictured in Figure 5.2.2.

Figure 5.2.2: Restriction Map of pSB2023

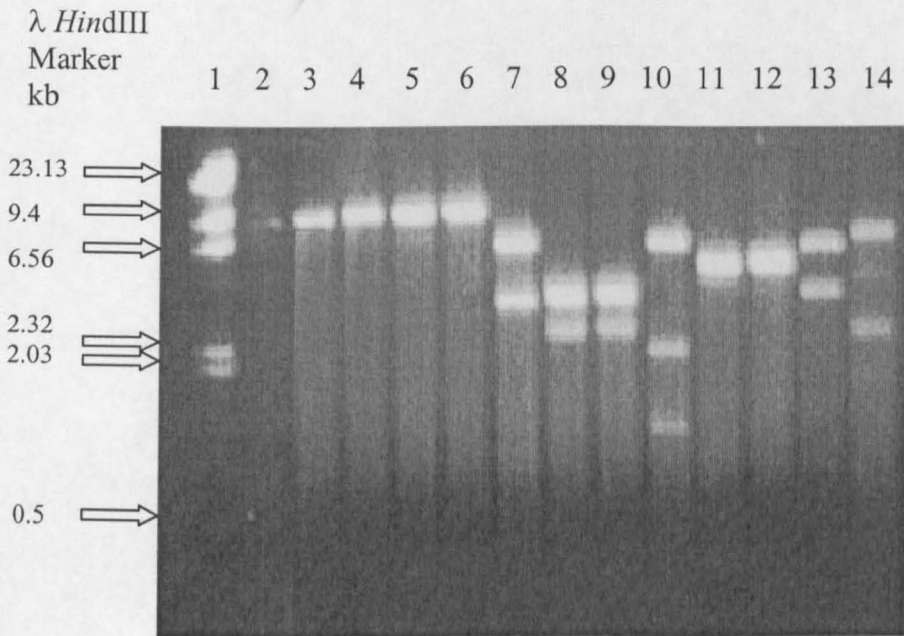


In order to create a construct where no additional substrates need to be added for bioluminescence to occur it was necessary to clone the *luxCD* and *luxE* genes downstream of *luxAB*. It was decided to reorganise the *lux* operon such that the luciferase was separate, but adjacent to the aldehyde genes on the plasmid. This would mean that either the aldehyde or the luciferase genes could be excised independently from the expression vector.

Both *luxCD* and *luxE* had previously been amplified by PCR, using primers 14 and 15, and 16 and 17 respectively which are detailed in Appendix 1, in order to incorporate an enhanced translational signal at the 5' coding region of *luxC* and *luxE*. The PCR products were electrophoresed on a low melting point agarose gel and each band excised. The DNA was then purified from the gel slice by freeze thaw purification. Purified *luxCD* was then restricted with *KpnI/BamHI*, and *luxE* was digested with *BamHI/PstI*. All the restriction enzymes were inactivated using phenol chloroform extraction. Following re-precipitation of the restricted DNA, both *luxCD* and *luxE* were ligated with pSB2023, which had previously been restricted with *KpnI/PstI* and then purified from a low melting point agarose gel by freeze thaw. The ligated DNA was then used to transform *E. coli* JM109 competent cells by electroporation, recombinant colonies were then isolated by selection on agar plates containing ampicillin and IPTG. Colonies that grew following subsequent incubation on these plates were then screened using a Hamamatsu VIM3 camera to determine if any of the transformants were bioluminescent. A few colonies were seen to be highly bioluminescent without the addition of exogenous aldehyde, indicating that both *luxCD* and *luxE* had inserted downstream of *luxAB* in pSB2023. DNA isolated from the bioluminescent colonies was subsequently restricted with *EcoRI/EcoRV* to excise the cloned *lux* operon from the plasmid backbone of pHG327. Agarose gel electrophoresis indeed showed that these digests resulted in the formation of two products of approximately 5.6kb and 3.4kb, corresponding to the *lux* operon and pHG327 respectively. Having confirmed that some of the transformants contained the new *lux* operon construct, named pSB2024, a large-scale DNA preparation was performed by plasmid maxiprep. This DNA was then investigated further by restriction analysis in order to verify the new construct. The DNA was restricted with a variety of restriction enzymes, which were then analysed by agarose gel

electrophoresis. The resulting gel from the restriction analysis of pSB2024 and the determined restriction map are illustrated in Figures 5.2.3 and 5.2.4 respectively.

Figure 5.2.3: Restriction Analysis of pSB2024



Layout of gel:

Lane1: λ HindIII Marker

Lane3: *Pst*I

Lane4: *Sal*II

Lane5: *Kpn*I

Lane6: *Bam*HI

Lane7: *Eco*RV

Lane8: *Eco*RI / *Eco*RV

Lane2: *Eco*RI

Lane9: *Sal*II / *Eco*RV

Lane10: *Bam*HI / *Eco*RV

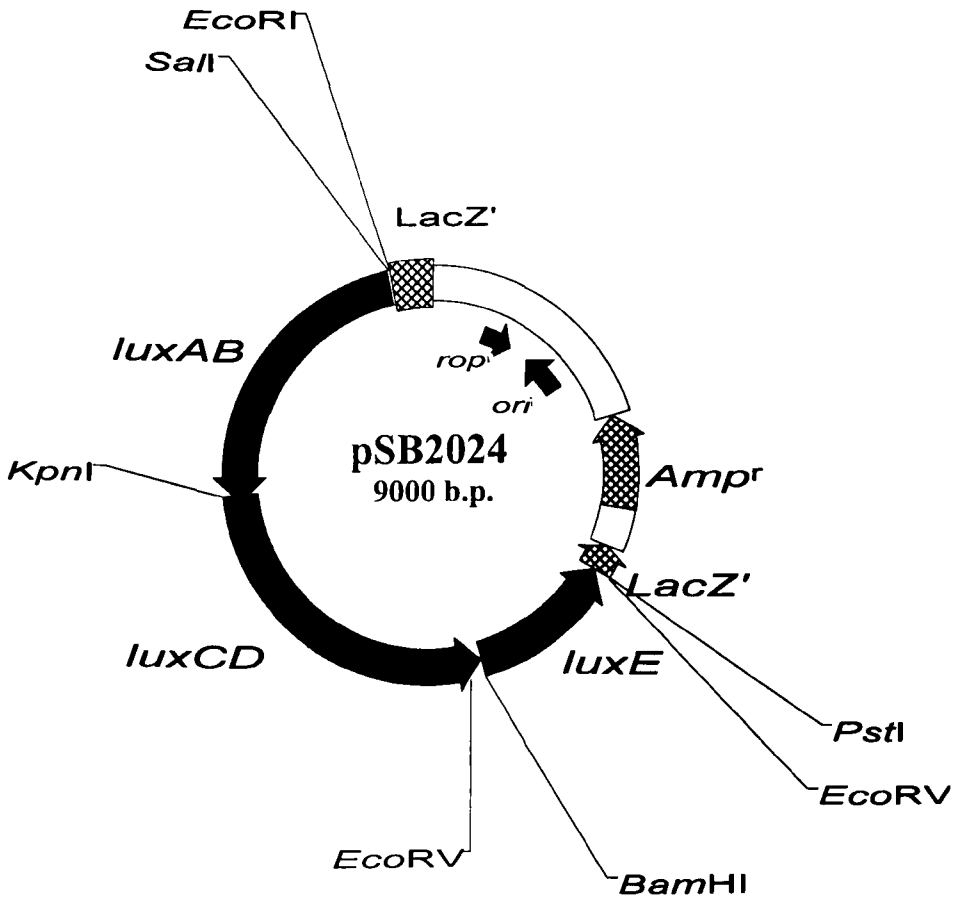
Lane11: *Eco*RI / *Bam*HI

Lane12: *Sal*II / *Bam*HI

Lane13: *Sal*II / *Pst*I

Lane14: *Bam*HI / *Kpn*I

Figure 5.2.4: Restriction Map of pSB2024



The restriction analysis showed that *luxCD* was downstream of *luxAB* and that *luxE* was downstream of both these sets of genes. Reconstruction of the *lux* operon appeared to have been achieved, with the aldehyde genes now separated from the luciferase genes, but both were adjacent on the plasmid.

The activity of pSB2024 cannot be observed in Gram positive bacteria due to the fact that it doesn't have a Gram positive origin of replication, or an antibiotic resistance gene that is suitable for use in Gram positive organisms. In order to look at expression of the *luxABCDE* operon in Gram positives it was necessary to excise the

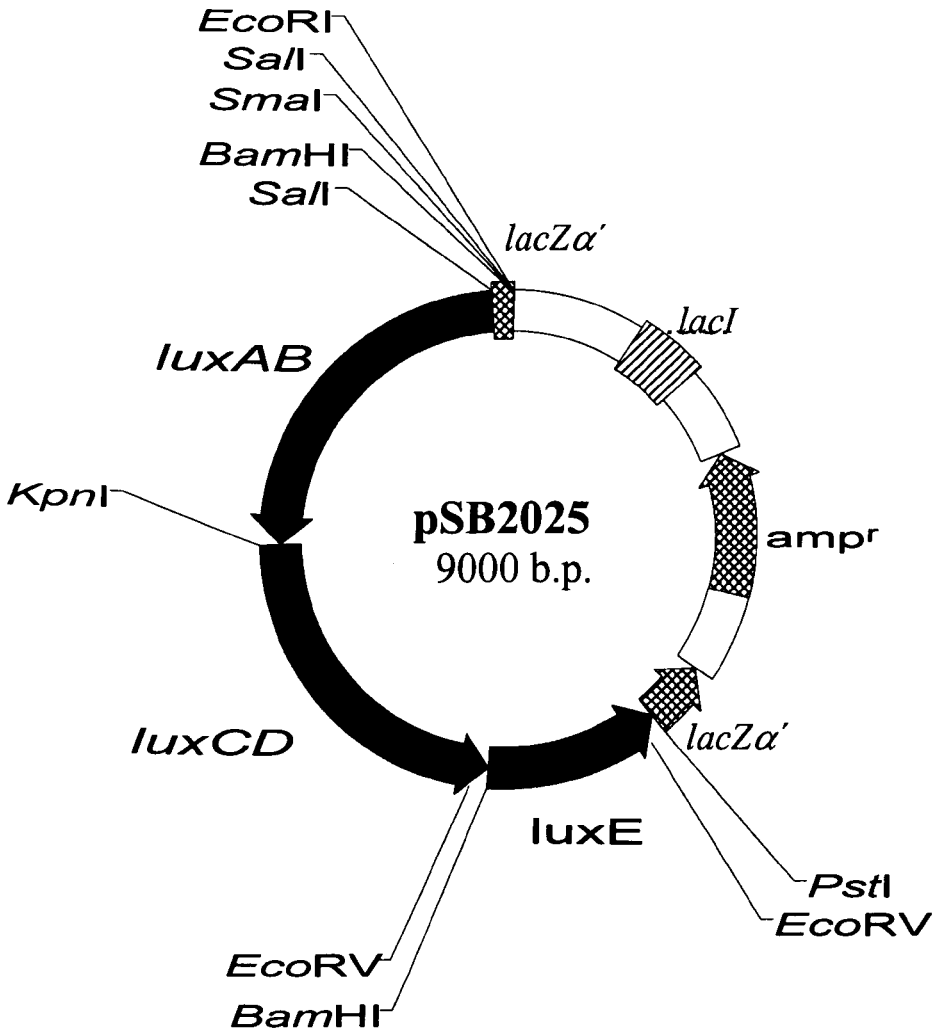
lux genes from pSB2024 and insert them into a Gram positive shuttle vector. However, there were no convenient restriction sites in the shuttle vectors that were available, into which the excised *luxABCDE* cassette could be inserted, so it was decided to first insert the *lux* operon into the super linker plasmid pSL1190 (Pharmacia) to create new restriction sites around the operon. This plasmid contains all 64 hexamer recognition sequences and is hence useful in vector construction.

5.3. Cloning the *luxABCDE* operon into the superlinker Plasmid pSL1190

pSL1190, supplied by Pharmacia, was restricted with *MunI* / *PstI*, this was then electrophoresed on a low melting point agarose gel and purified by freeze thaw purification. The *luxABCDE* operon was excised from pSB2024 upon restriction with *EcoRI* / *PstI*, after electrophoresis on a low melting point agarose gel the band corresponding to the *lux* operon was excised and purified by freeze thaw. Following ligation of these two DNA fragments the ligated DNA was used to transform *E. coli* JM109 competent cells by electroporation. Colonies containing recombinant DNA were selected by plating the transformation mix onto agar plates containing ampicillin. Although the *luxABCDE* operon had been inserted into pSL1190, the recombinant colonies were not expected bioluminesce due to the fact that the reporter fragment had been inserted in the opposite orientation to the promoter. Nevertheless, colonies obtained were screened under a Hamamatsu VIM3 camera to look for any luminescence produced from the cells and a few colonies showed a very faint bioluminescent phenotype.

These weakly bioluminescent colonies were isolated and DNA prepared from the recombinant cells by plasmid miniprep. The resulting DNA was subsequently restricted with *PvuII*, which confirmed the *luxABCDE* operon was present within these recombinant colonies. As this recombinant DNA, named pSB2025, was required for further manipulation, pure DNA was prepared by maxiprep and was then subjected to further investigations by restriction analysis. The restriction map of pSB2025 is shown in Figure 5.3.1. Having now successfully integrated the *luxABCDE* operon into pSL1190, due to the number of unique restriction sites at both ends of the coding sequence, the operon could now be excised and inserted into the Gram positive shuttle vector of choice.

Figure 5.3.1: Restriction map of pSB2025



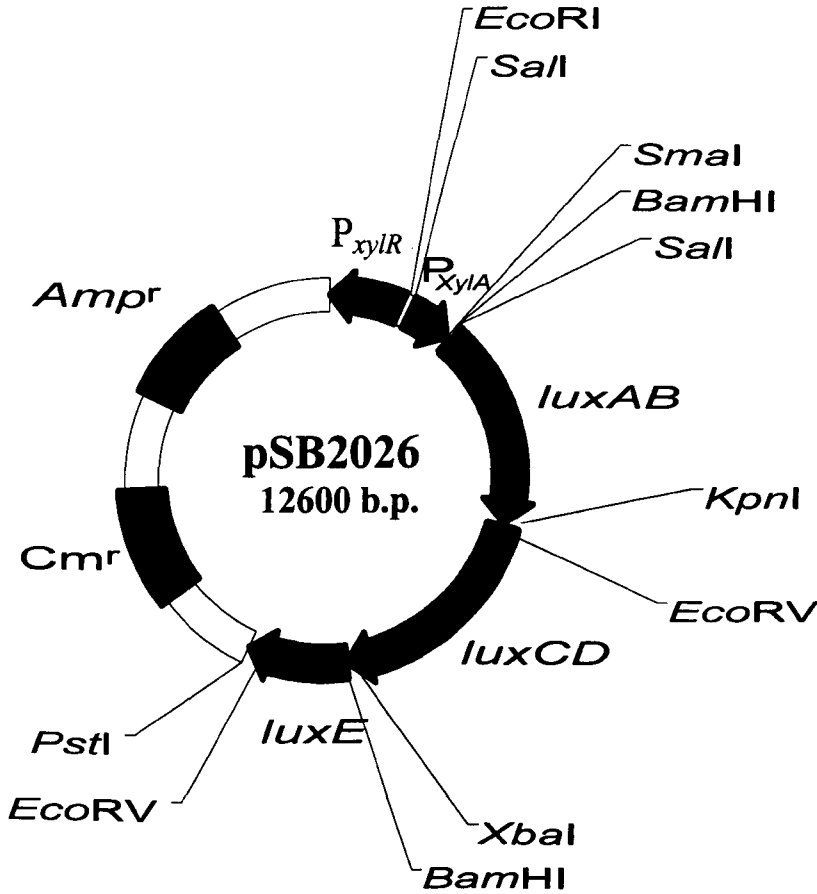
5.4. Cloning the *luxABCDE* operon into a Gram positive shuttle vector

It was decided to clone the *luxABCDE* operon downstream of *xyIR* P_{*xyIA*}. This would result in a reporter plasmid whose promoter could be induced by the addition of 0.5% xylose to the bacterial culture medium resulting in bioluminescent expression of cells containing the plasmid. The most effortless to achieve this was to clone the *lux* operon into an existing construct, in this case the *gfp* expression vector pSB2018 was

chosen. This plasmid is based on the Gram positive shuttle vector pMK4 (Sullivan *et al.*, 1984) and the construction of which has been described earlier in Chapter 3, Section 3.12.

The *gfp3opt* gene was excised from the reporter plasmid pSB2018 after restriction with *SmaI* / *PstI*. The digested vector was then purified from a low melting point agarose gel and ligated with the *lux* operon, which had been excised from pSB2025 and purified from a low melting point agarose gel following digestion of the DNA with *SmaI* / *PstI*. The ligated DNA was subsequently transformed into *E. coli* by electroporation of JM109 competent cells, recombinant colonies were then isolated after incubation on ampicillin selective agar. Any resulting transformants were also screened under a Hamamatsu VIM3 camera. With the recombinant colonies, some were seen to be more luminescent than others, it was thought that the ones that were less luminescent were colonies containing pSB2025 and were present due to carry through of the original *lux* cloning vector. To check if these bioluminescent colonies contained the new *lux* shuttle vector or whether they contained pSB2025, those colonies that exhibited a luminescent phenotype were isolated onto agar plates containing chloramphenicol. This would allow for selection of the new *lux* plasmid as pSB2025 does not contain a chloramphenicol resistance gene, so cells harbouring this plasmid would not grow. A number of colonies grew under chloramphenicol selection, these were also shown to be highly bioluminescent. To verify that these cells contained the correct construct, DNA was prepared from the cells by plasmid miniprep, this was subsequently checked by restriction analysis, which showed that all the bioluminescent chloramphenicol resistant cells contained the Gram positive *lux* plasmid, designated pSB2026. After amplification of the DNA by plasmid maxiprep, the DNA was investigated further by restriction analysis, which resulted in the production of the restriction map depicted in Figure 5.4.1

Figure 5.4.1: Restriction map of pSB2026

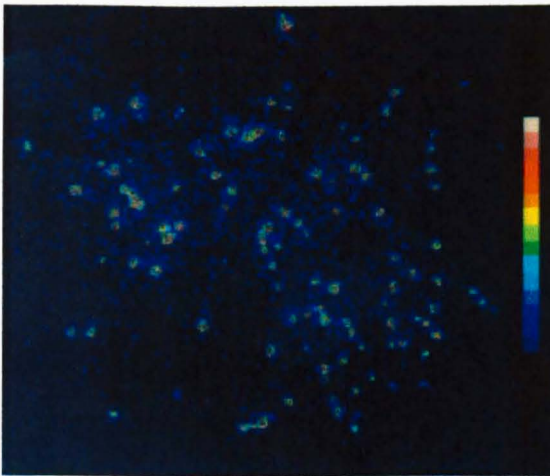


The *lux* reporter pSB2026 was introduced into *L. monocytogenes* by electroporation of competent cells, recombinant colonies were obtained after selection on BHI agar plates containing xylose and chloramphenicol. These were then screened under a Hamamatsu VIM3 camera and the luminescent output from the cells noticed. Although the bioluminescence generated from the Gram positive bacteria did not appear to be at parity with *E. coli* cells expressing *lux* from the same plasmid, the observed light levels were much greater than anything previously observed in *L. monocytogenes*. When cells had been plated onto medium that did not contain added xylose, only very low levels of luminescence were observed from the cells, compared to cells that when grown with added xylose which were highly luminescent, this is illustrated in Figure 5.4.2. It is already known that this promoter appears to be well regulated in *L. monocytogenes*, as investigations performed on *L.*

monocytogenes cells expressing *gfp* from pSB2018 showed that P_{xylR} could be repressed by the addition of xylose to the culture media allowing expression of *gfp3opt* from P_{xylA} .

Figure 5.4.2: *L. monocytogenes* (pSB2026) recombinant colonies when grown on media with and without added xylose.

Images gained after a 1 minute acquisition



L. monocytogenes (pSB2026).
Cells grown on BHI Cm7 agar
at 37°C with xylose added at a
concentration of 0.5%



L. monocytogenes (pSB2026).
Cells grown on BHI Cm7 agar
at 37°C

To determine whether a bioluminescent phenotype could be obtained from other Gram positive bacteria harbouring pSB2026, the plasmid was introduced into *S. aureus* RN4220 by electroporation according to the method of Augustin and Gotz (1990). The resulting transformants, obtained following selection on chloramphenicol selective agar plates containing 0.5% xylose, showed a bioluminescent phenotype when examined under a Hamamatsu VIM3 camera, indicating the plasmid containing the *lux* operon, pSB2026, had been successfully introduced into the *S. aureus* cells.

In addition to expressing *lux* genes from pSB2026 in *S. aureus* RN4220, it was also decided to express the *lux* genes in another laboratory strain, namely *S. aureus* 8325-4. However, attempts to introduce DNA isolated from *E. coli* by electroporation were unsuccessful. Subsequently, DNA was isolated from *S. aureus* RN4220 (pSB2026) by plasmid miniprep, this was then used to transform *S. aureus* 8325-4 by electroporation of competent cells. The recombinant colonies that were isolated following selection on chloramphenicol agar plates with 0.5% added xylose, were seen to be highly bioluminescent.

So, it has been shown that this reconstructed *lux* operon can be efficiently expressed in Gram positive bacteria. It is planned to apply these bioluminescent organisms to *in vivo* imaging experiments to look at gene expression of the organisms during pathogenesis. As expression of the *lux* operon is dependent on the presence of added xylose, it was decided to make a constitutive *lux* reporter by excision of the *xylR* gene from the promoter region. This would give bacteria that were light without the added need for xylose.

5.5. Construction of a Constitutive *lux* Reporter for Expression Studies in Gram positive bacteria

To create a constitutive *lux*-cloning vector, the P_{xylA} -*luxABCDE* fragment was excised from pSB2025 following enzymatic restriction with *EcoRI* and *PstI*. This was then ligated with pCG4, which had had the P_{xyn} promoter, and *luxAB* fusion genes excised after the DNA had been digested with both *EcoRI* and *PstI*. After transformation of *E. coli* JM109 competent cells with the ligated DNA, recombinant colonies were selected on their ability to grow on antibiotic media and produce light without the addition of exogenous aldehyde or added xylose. In order to confirm that the *xylR* regulator gene had been excised from the DNA, colonies that showed a light phenotype were grown in antibiotic selective media and DNA prepared from the cells by plasmid miniprep. Studies of the *xylR* DNA sequence revealed a unique *XhoI* restriction site upstream of the *EcoRI* site, which had been used to excise P_{xylA} . Thus if the *xylR* gene had been successfully removed from the promoter-*lux* fragment, the plasmid DNA from the new recombinant colonies should not contain a *XhoI* site, therefore upon restriction with *XhoI* and *PstI* the DNA should only be linearised. This is illustrated in Figure 5.5.1. Some recombinants were identified which produced only one band upon restriction with *XhoI* and *PstI*, indicating that the *xylR* gene had been excised. This constitutive plasmid was referred to as pSB2027 and subsequent restriction analysis with a variety of endonucleases confirmed the positions of enzymes on the restriction map depicted in Figure 5.5.2.

Figure 5.5.1: Linear restriction map of the *xylR-luxABCDE* fragment from pSB2026

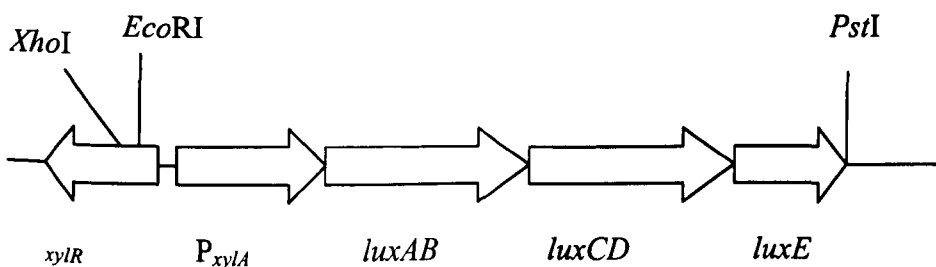
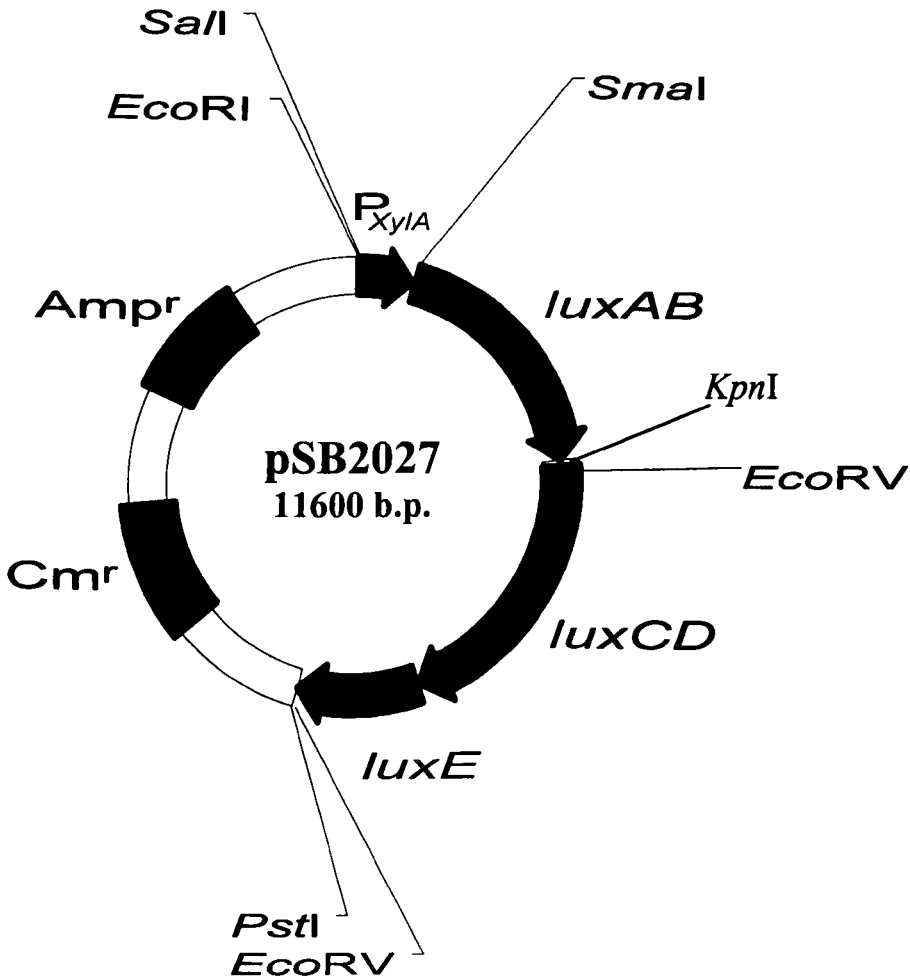


Figure 5.5.2: Restriction Map of pSB2027



Restriction mapping confirmed the validity of pSB2027 and showed that *xylR* had been successfully removed from the DNA. The cloning vector pSB2027 was then introduced into two different Gram positive species by electroporation, these being *L. monocytogenes* 7973 and *S. aureus* RN4220. Recombinant colonies of each bacterial strain were obtained following selection on chloramphenicol agar plates, all of which were seen to have a highly bioluminescent phenotype when examined under a Hamamatsu VIM3 camera. As DNA prepared from *E. coli* JM109 cells could not be directly introduced into *S. aureus* 8325-4, DNA was prepared from *S. aureus* RN4220 (pSB2027) by plasmid miniprep and subsequently introduced into *S. aureus*

8325-4 by electroporation. In this case all the resulting transformants showed a highly luminescent phenotype indicating that the *lux* genes were efficiently translated within the cell.

All Gram positive bacteria showed a luminescent phenotype on medium that did not contain xylose, showing xylose was not required for P_{xyIA} to be active, thus it appears as though expression of the *lux* genes is constitutive.

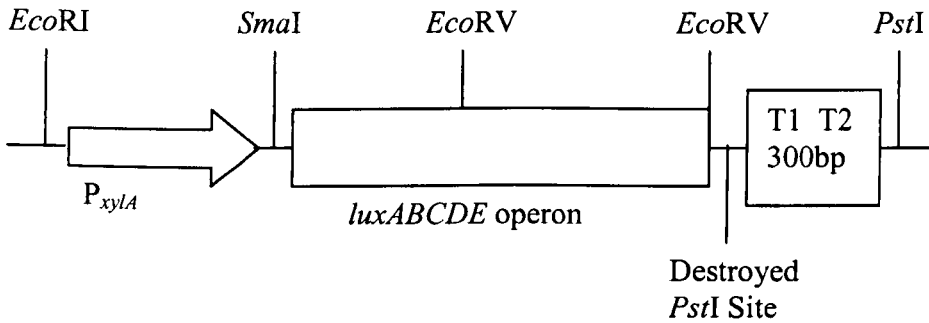
5.6. Cloning a transcriptional terminator downstream of the *lux* operon

As no transcriptional terminator was cloned downstream of the *lux* genes, it was decided to clone the *rnnB* terminator from *E. coli* downstream of the *lux* expression vector pSB2027, to see if this had any apparent effect on reporter activity and stability within cells expressing *lux*. The termination region of the *rnnB* gene is large and complex and the whole region can be employed as an efficient terminator of transcription.

In this study, PCR primers were designed to the DNA sequence of the *rnnB* gene such that the inverted repeats forming the T1 and T2 terminators and the two smaller repeats, IR1 and IR2 would be amplified by the ensuing PCR reaction. It was decided to amplify this whole region as Orosz *et al.* (1991) showed that this fragment containing both terminators and both inverted repeats gave high termination efficiency when cloned in either orientation. Details of the primers used, primers 18 and 19 are given in Appendix 1.

In order to clone this terminator fragment, restriction sites were incorporated into the PCR primers, a *NsiI* site at the 5' end of the coding sequence and a *PstI* restriction site at the 3' end. As *NsiI* is compatible with *PstI* this would enable the orientation of the inserted fragment to be determined as illustrated in Figure 5.6.1.

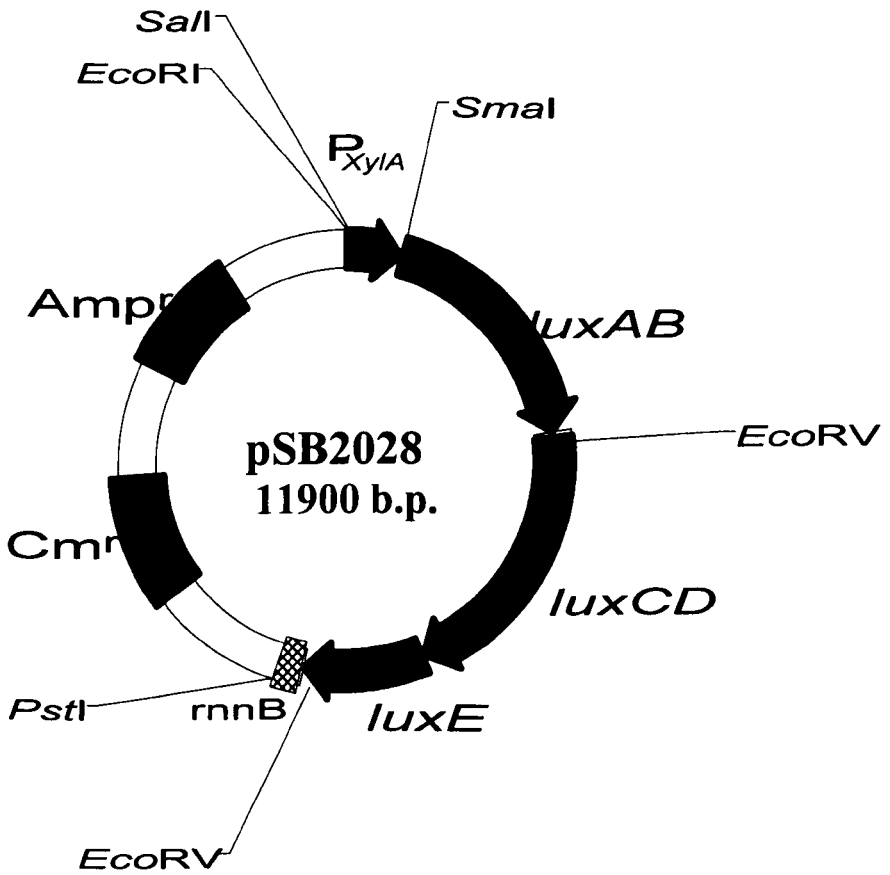
Figure 5.6.1: Strategy used for cloning the *rnnB* terminator downstream of the *luxABCDE* operon



Using primers 18 and 19, PCR was used to amplify the *rnnB* terminator fragment from the genome of *E. coli* JM109. The reaction was performed essentially as described in the Materials and Methods, Section 2.5.3, using an annealing temperature of 50°C for 1 minute followed by an equivalent period of DNA extension at 72°C. The ensuing PCR product was restricted with *NsiI* and *PstI* and subsequently ligated with pSB2027 which had been linearised upon restriction with *PstI*. The ligated DNA was introduced into *E. coli* JM109 competent cells by electroporation and recombinant colonies acquired following selection on agar plates containing ampicillin. These colonies were then screened under a Hamamatsu VIM3 camera to determine those colonies that exhibited a bioluminescent phenotype. Some light colonies were picked into fresh broth and DNA isolated from them by plasmid miniprep. This DNA was then restricted with *EcoRV* / *PstI* to determine whether the recombinant DNA contained the *rnnB* terminator downstream of the *lux* operon, and if so, the orientation of the cloned insert. As shown in Figure 5.6.1, if the terminator had inserted in the correct orientation, upon restriction with *EcoRV* and *PstI*, a small band of around 300bp would be excised along with bands of approximately 3kb and 9kb. One of those colonies isolated did indeed show the presence of this 300bp insert indicating that the *rnnB* terminator fragment had been inserted downstream of the

luxABCDE operon, this new construct was designated pSB2028, and is depicted in Figure 5.6.2:

Figure 5.6.2: Restriction Analysis of *lux* recombinant colonies thought to contain the *rnnB* terminator



This new expression vector pSB2028, was introduced into *L. monocytogenes* by electroporation of competent cells. The resulting recombinant colonies were seen to be bioluminescent under a Hamamatsu VIM3 camera, but by eye it appeared as though colonies containing pSB2028 were not as light as the equivalent colonies expressing *lux* from pSB2027.

In order to determine the reporter activity of each of these *lux* plasmids and to also determine whether expression of these 5 proteins affects growth of cells harbouring them, growth curves were carried out with *L. monocytogenes* harbouring each of these new expression vectors.

5.7. Growth of *L. monocytogenes* harbouring the xylose inducible *lux* plasmid pSB2026

L. monocytogenes containing the xylose inducible *lux* plasmid (pSB2026), were grown overnight in BHI containing chloramphenicol both with and without 0.5% xylose. Overnight cultures were then diluted 1/100 to approximately the same starting OD into fresh pre-warmed broth containing the same supplements and grown at 37°C in a shaking water-bath. As a control, *L. monocytogenes* (pMK4) were grown and subcultured in the same way, but in this case *lacZ* expression was induced by the addition of 0.5mM IPTG to the culture medium. Both optical density (OD) and bioluminescence readings were taken at hourly intervals with bioluminescence being measured as soon as the sample was taken from the flask. The bioluminescence was represented as relative light units (RLU).

To take into account the effect of growth on the bioluminescence readings, the RLU values obtained were divided by the appropriate OD values to give RLU/OD. The RLU/OD values were plotted against time on an arithmetic graph, also the OD values were plotted against time, this showed both the bioluminescent and growth properties of cells expressing different plasmids, a representation of the data is shown in Figures 5.7.1 and 5.7.2.

From the data illustrated in Figures 5.7.1 and 5.7.2 it could be seen that expression of P_{xyIA} was well regulated by xylose, as when no xylose was added to the culture medium little luminescence was seen from the cells expressing *lux* from pSB2026. This data also shows that when cells harbouring pSB2026 were grown in the presence of 0.5% xylose a bioluminescent phenotype was exhibited. The light was seen to peak after approximately 5 hours, which corresponded to cells in mid exponential phase. As cells approached stationary phase, the luminescence had decreased rapidly, indicating that no new or only low levels of Lux proteins were being generated. These data suggest that P_{xyIA} is not acting in a constitutive manner, as the light levels do not remain high throughout the whole growth cycle. The

promoter only appears to be active up to mid exponential phase, and then it seems to be downregulated, as shown by the rapid decrease in luminescent output.

When the same growth curves were performed with the equivalent GFP3 reporter, pSB2018, levels of GFP did not reach a high level until early stationary phase, levels of GFP also remained high and were not seen to decrease. This is probably due to the time needed for the GFP chromophore to form fluorescent protein, the time needed for enough GFP to be formed to produce a fluorescent signal and also due to the fact that once formed GFP is an extremely stable protein and has a long half-life (Tombolini *et al.*, 1997). That GFP fluorescence was observed shows that the promoter was active, but as fluorescence levels remain high due to the stability of the protein (Tombolini *et al.*, 1997) it cannot be determined whether or not the promoter was active during the whole growth cycle or whether at some point activity of the promoter was reduced. When *lux* is used, due to the fact that the light levels peak and then decrease to a low output, this indicates that the promoter is downregulated during late exponential growth. However, the decrease in bioluminescence may be attributed to a lack of energy in the cells. In order for the bioluminescent process to occur energy is required, this is derived from the bacterium's electron transport chain. Thus if the metabolic activity of the cells has been downregulated then this may explain the decrease in bioluminescence. However, this appears unlikely, as when the bioluminescence decreases the cells are in exponential phase, therefore energy requirement should not be an issue. Nevertheless, by using *lux*, promoter kinetics and dynamics can be studied in real time as when the promoter is downregulated a corresponding decrease in light output is observed. Thus *lux* would appear to be a better real time reporter and would readily reflect any bi-directional changes in gene expression within the cell.

One phenomenon that can be noticed from the data illustrated in Figures 5.7.1 and 5.7.2 is the slower initial growth rate of cells harbouring pSB2026. It may be thought that this was due to expression of the *lux* genes, but this phenomenon was observed when cells were grown both with and without xylose. When cells were grown without xylose the initial slower growth rate was not as marked as when xylose was

added to the bacterial culture, but growth was still decreased initially. This suggests that whilst expression of the *lux* genes does appear to slow down the initial growth rate, bioluminescence cannot be entirely responsible, as when *L. monocytogenes* (pSB2026) were grown without xylose very little luminescence was observed. This suggests that some other factor may be responsible for this initial slower growth rate. Gruss and Ehrlich (1988) suggested that pC194, from which pMK4 is derived produced HMW DNA upon the insertion of heterologous DNA fragments. The amount of HMW DNA appeared to depend on the size and nature of the inserted DNA fragment. This may explain why cells harbouring pSB2016 show an initial slower growth rate even when P_{xylA} has not been activated., as if the cells contain large amounts of HMW DNA it will take longer for the plasmid DNA to replicate. This appears to be backed up further from experiments where *L. monocytogenes* (pMK4) were grown with and without the inducer IPTG, here no differences were observed in the initial growth rate. This will be discussed in greater detail in Chapter 8.

Another possible explanation for the initial slower growth rate could be the initial inoculum size used to set up the experiments. Although it was thought that all cultures were inoculated to the same level, at this low optical density only an estimate can be made by the spectrophotometer and so values obtained at this low level cannot be deemed accurate. This however seems unlikely as the same general trends were seen each time that the experiment was performed.

The decreased initial growth rate suggests an increased metabolic load upon cells expressing *lux*. If expression of *lux* was placing a significant energy drain upon the cells then this would be reflected in the exponential growth rates of the bacteria. The exponential growth rates are given in Table 5.7.1.

Table 5.7.1: Mean Exponential Growth Rates of *L. monocytogenes* harbouring pSB2026 with pMK4 as a control culture

Growth rate is shown as increase in optical density per hour

t-test performed using *L. monocytogenes* (pMK4) grown without inducer as a control

Plasmid	Growth rate - inducer	Growth rate + inducer	Standard Deviation - inducer	Standard Deviation + inducer
pSB2026	0.159	0.161	9.19×10^{-3} P > 0.05	2.12×10^{-3} P > 0.05
pMK4	0.238	0.219	9.90×10^{-3} control	0.024 P > 0.05

From the exponential growth rates of all the bacterial cultures shown in Table 5.7.1, it can be seen that there is no difference in the growth rates between *L. monocytogenes* (pSB2026) that are bioluminescent and those that are not. This suggests that expression of *lux* does not affect the growth rate of exponentially growing cultures. Whilst the bacteria are not luminescent throughout exponential growth, some light is produced, so if expression of *lux* did place an extra energy drain upon the cells this might be expected to be reflected in the bacterial growth rates. The exponential growth rates of bacteria harbouring pSB2026 are lower than equivalent cells harbouring pMK4. As pSB2026 is approximately 7kb bigger than pMK4, plasmid size may have an effect on the bacterial growth rate, as it takes longer to transcribe, translate and replicate a bigger plasmid.

From this experiment it was determined that P_{xyIA} was not constitutive as previously thought, but is only expressed up to late exponential phase before it is down-regulated within the cell. Expression of the *lux* genes appears to place some metabolic load upon the cell, demonstrated by the decreased initial growth rate, however, some of this load could be attributed to the plasmid size and the nature of the plasmid, this will be discussed further in Chapter 8.

Figure 5.7.1: Growth and Bioluminescence of *L. monocytogenes* (pSB2026)

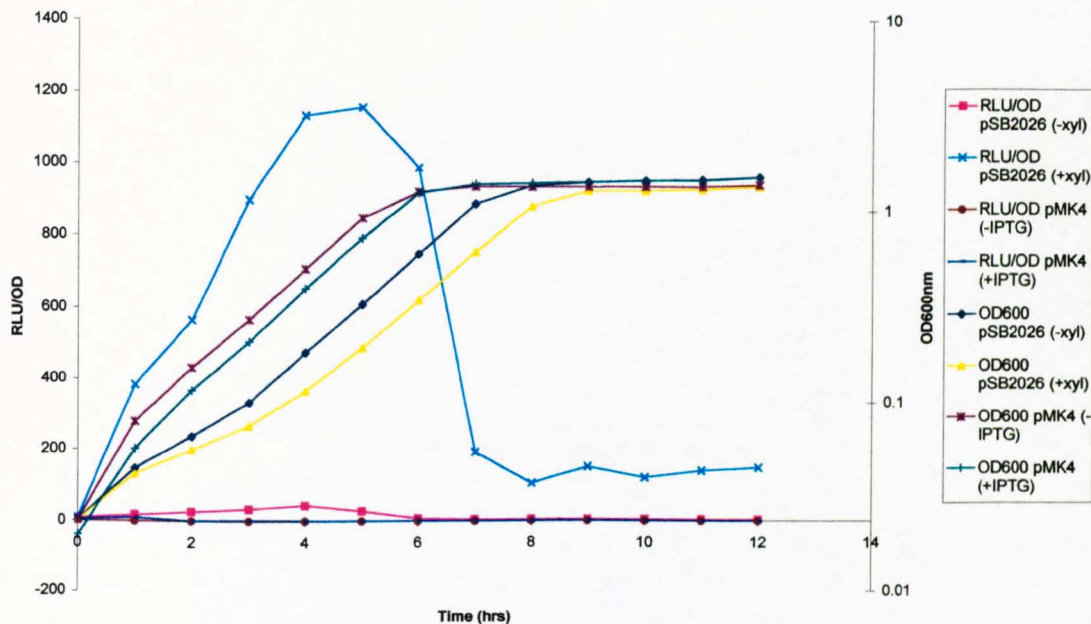
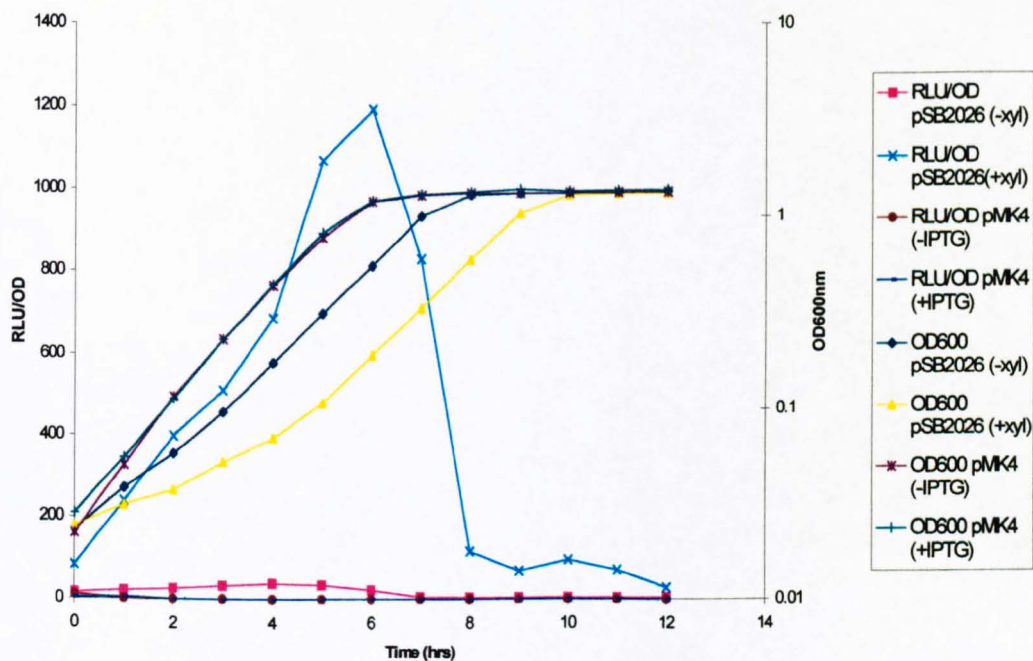


Figure 5.7.2: Growth and Bioluminescence of *L. monocytogenes* (pSB2026)



5.8. Comparison of Growth and bioluminescence of *L. monocytogenes* (pSB2026) and *L. monocytogenes* (pSB2027)

These experiments were performed to observe any differences in light output between an inducible *lux* plasmid, pSB2026, and one where the promoter was thought to be constitutive in its action, pSB2027. The experiment was carried out as before, *L. monocytogenes* harbouring pSB2026 were induced to express *lux* by adding 0.5% xylose to the culture medium, but cells harbouring pSB2027 were grown only in antibiotic selective broth. *L. monocytogenes* (pMK4) were grown with and without the inducer IPTG so it could be sure that expression of genes from, and maintenance of the plasmid within the bacteria had no adverse effect on the growth of the cells. Optical density and relative bioluminescence (RLU) were measured as before, and once again the RLU values obtained were divided by OD to take into account the effect of cell number on the bioluminescence values. The RLU/OD values were then plotted against time on an arithmetic graph; in order to compare growth of the bacteria to the luminescent output the OD values were also plotted on the same graph on a log scale, a representation of the data obtained is shown in Figures 5.8.1 and 5.8.2.

Upon examination of these data, the most striking observation is the difference in light output between the *L. monocytogenes* cells containing the two *lux* plasmids. Expression of the *lux* genes from *L. monocytogenes* (pSB2027) was seen to be approximately 10-fold higher, as shown by a ten-fold increase in luminescent output, than *L. monocytogenes* expressing *lux* from pSB2026. It is not really understood why this occurs, as essentially the two plasmids are the same except for the absence of *xylR* from pSB2027. It may be that when *xylR* is present, even when xylose is added to the culture medium, P_{xylA} is not fully de-repressed, hence levels of luminescence are lower, a higher concentration of xylose in the media may give rise to a higher luminescent output. When the repressor is not present, as in the *lux* reporter pSB2027, *lux* expression occurs without the need for any inducers, indicating the constitutive nature of the promoter. As expected due to the absence of *lux* genes in the plasmid, no bioluminescence was observed from the cells harbouring pMK4.

It can be seen from the data that the luminescence peaks when the bacteria are in mid exponential phase and then decreases fairly rapidly. There are two possible explanations for this. It is possible that P_{xylA} is a growth phase dependent promoter and is downregulated at a specific point in the growth cycle, in this case mid exponential phase. Another explanation is that the cells cannot produce enough energy to drive the bioluminescent reaction. This appears unlikely as when bioluminescence is downregulated within the cells, the bacteria are still growing exponentially, thus there should still be sufficient energy available to drive the bioluminescent reaction.

One other factor that can be seen from Figure 5.8.1 and 5.8.2 is the slower initial growth rate of bacteria that express *lux* from both pSB2026 and pSB2027, the longest being from cells containing pSB2026. It seems feasible to suggest that luminescent output is not responsible for this slower initial growth rate, as *L. monocytogenes* (pSB2026) when grown with xylose are approximately 10 fold less luminescent than *L. monocytogenes* (pSB2027). The only difference between these two plasmids is the presence of *xylR* on pSB2026. It is possible that the observed initial slower growth rate of *L. monocytogenes* (pSB2026) is due to the size of the plasmid, which is approximately 500bp bigger than pSB2027. Gruss and Ehrlich (1988) suggested that insertion of DNA fragment into pC194, from which these expression vectors are comprised, lead to the production of HMW DNA. If *L. monocytogenes* (pSB2026) are producing more HMW DNA compared to *L. monocytogenes* (pSB2027) then this may explain the observed initial slower growth rate. If *L. monocytogenes* (pSB2026) do contain large amounts of HMW DNA then this may also explain the lower luminescence levels observed. This will be discussed further in Chapter 8.

Although the initial growth period varies between cells harbouring the different expression vectors, the actual exponential growth rate does not appear to vary significantly; this is illustrated in Table 5.8.1.

Table 5.8.1: Mean exponential growth rates of *L. monocytogenes* (pSB2026) and *L. monocytogenes* (pSB2027)

Growth rate is shown as an increase in optical density per hour

t-test performed using *L. monocytogenes* (pMK4) grown without inducer as a control

Plasmid	Mean Growth rate	Standard Deviation	P
pSB2026	0.164	2.12×10^{-3}	> 0.05
pSB2027	0.174	0.021	> 0.05
pMK4 (+ve)	0.219	0.024	> 0.05
pMK4 (-ve)	0.238	9.90×10^{-3}	control

It can be seen from the above data that expression of the *lux* genes does appear to slightly lower the exponential growth rate. However, it is not clear whether this decreased growth rate is due to the production of Lux proteins or whether the actual presence of the plasmid slows down growth. *L. monocytogenes* (pSB2027) are approximately 10-fold more luminescent than *L. monocytogenes* (pSB2026) and yet the exponential growth rates are not significantly different. This suggests that expression of *lux* does not place a significant energy drain upon the bacteria, but the reduced growth rates are due to some other factor, possibly the size of the plasmid that the cells contain.

Figure 5.8.1: Growth and bioluminescence of *L. monocytogenes* harbouring constitutive and inducible lux plasmids

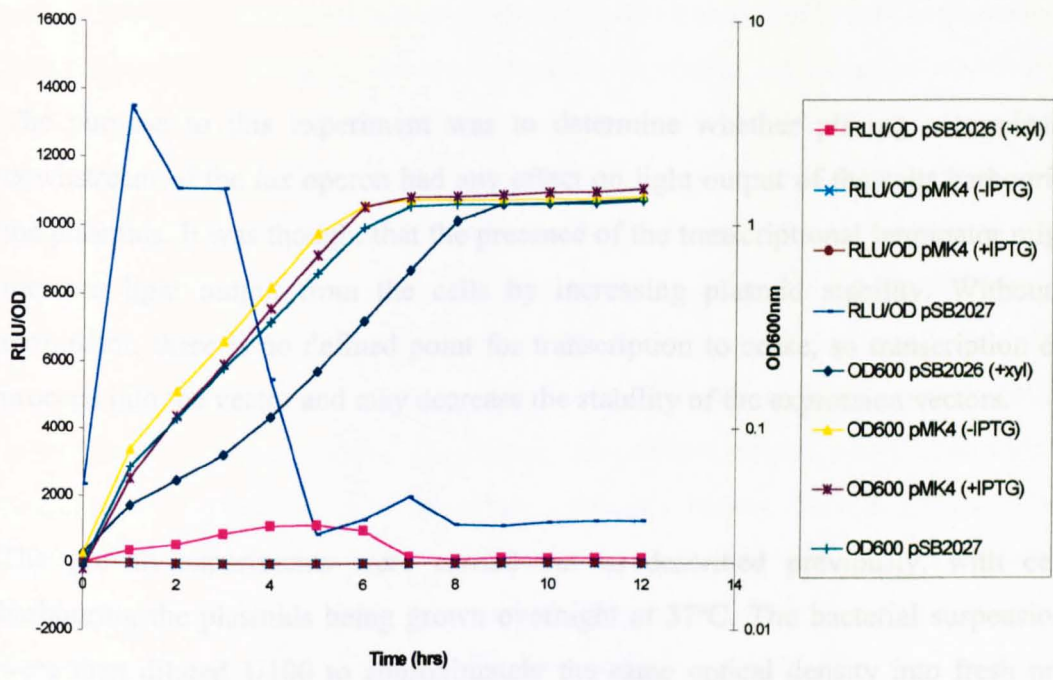
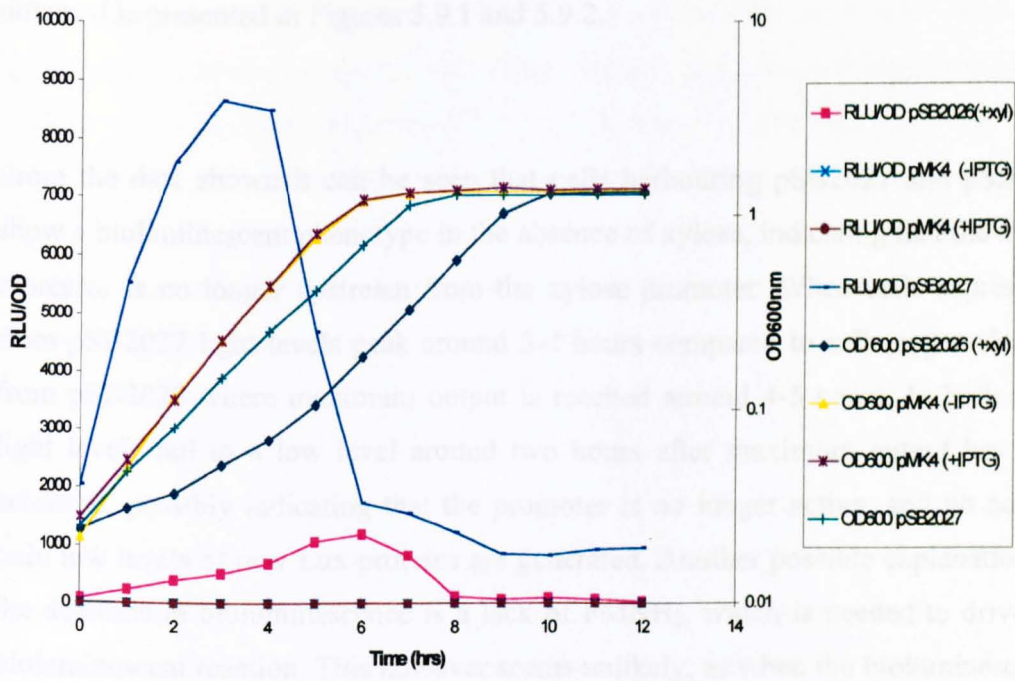


Figure 5.8.2: Growth and bioluminescence of *L. monocytogenes* harbouring constitutive and inducible lux plasmids



5.9. Comparison of growth and bioluminescence of *L. monocytogenes* (pSB2028) and *L. monocytogenes* (pSB2027)

The purpose to this experiment was to determine whether placing a terminator downstream of the *lux* operon had any effect on light output of the cells harbouring the plasmids. It was thought that the presence of the transcriptional terminator might increase light output from the cells by increasing plasmid stability. Without a terminator, there is no defined point for transcription to cease, so transcription can proceed into the vector and may decrease the stability of the expression vectors.

The growth experiments were carried out as described previously, with cells harbouring the plasmids being grown overnight at 37°C. The bacterial suspensions were then diluted 1/100 to approximately the same optical density into fresh pre-warmed medium. At hourly intervals both the optical density and bioluminescence were measured with the RLU/OD being calculated for each time point. The RLU/OD and the OD values were then plotted with respect to time, a representation of the data obtained is presented in Figures 5.9.1 and 5.9.2.

From the data shown it can be seen that cells harbouring pSB2027 and pSB2028 show a bioluminescent phenotype in the absence of xylose, indicating that the xylose repressor is no longer upstream from the xylose promoter. When cells express *lux* from pSB2027 light levels peak around 3-4 hours compared to cells expressing *lux* from pSB2028 where maximum output is reached around 4-5 hours. In both cases light levels fall to a low level around two hours after maximum output has been achieved, possibly indicating that the promoter is no longer active, and no new or only low levels of new Lux proteins are generated. Another possible explanation for the decrease in bioluminescence is a lack of FMNH₂, which is needed to drive the bioluminescent reaction. This however seems unlikely, as when the bioluminescence decreases the cells are still growing exponentially, so energy requirement should not be an issue.

When the *rnnB* terminator was placed downstream of the *lux* operon light levels were much lower, approximately five-fold, than the equivalent construct pSB2027, without the terminator. Two possible reasons could be responsible for the decrease in light output demonstrated by *L. monocytogenes* expressing the *lux* genes encoded by pSB2028. It may be that the overall transcript levels within the cell have been reduced, but this is unlikely as the promoter is the same as that in pSB2027. A more plausible explanation is that mRNA is transcribed at the same rate but degraded more rapidly when the *rnnB* terminator is present. Bacterial mRNA is unstable and is constantly degraded by ribonucleases. In bacteria both endonucleases and exonucleases are involved in the degradation of mRNA. Susceptibility to degradation is conferred by sequences that are targets for endonucleolytic attack. The overall direction of degradation is 5'-3', which probably results from a succession of endonucleolytic cleavages following the last ribosome. Degradation of the released fragments of mRNA proceeds by exonucleolytic attack from the free 3'-OH end towards the 5' terminus (i.e. the opposite direction to transcription).

It is possible that by placing a terminator downstream of the *lux* genes a sequence has caused structural rearrangements that determine a cleavage site. Once the endonuclease has cleaved the mRNA, exonucleolytic degradation starts at the new 3' end and degrades the 5' fragment. If the mRNA transcript was degraded, this would reduce the overall levels of Lux proteins transcribed within the cell, depending on the extent of the degradation luminescent output would decrease accordingly. If the stability of the mRNA has been decreased, i.e. the mRNA has a shorter half-life, then it can only be translated a limited number of times before it is functionally inactivated.

~~It can be noticed that~~ *L. monocytogenes* expressing the Lux proteins appear to have a slower initial growth rate than *L. monocytogenes* expressing *lacZ*, i.e. cells harbouring pMK4 whose growth rate does not appear to be affected upon induction with IPTG. This slower initial growth rate is much greater for *L. monocytogenes* (pSB2028) than *L. monocytogenes* (pSB2027), this is reflected by the increased time taken for the bacteria to enter stationary phase. It may be that these differences in

growth rate at the start of the growth cycle may be due to the initial inoculum size, as at such low levels an accurate reading from the spectrophotometer cannot be obtained. However, it seems unlikely that this is the case as each time the experiment was repeated the same trends were seen.

It seems unlikely that these differences in the initial growth rate are due to expression of *lux* placing an energy drain upon the cells, as *L. monocytogenes* (pSB2028) that have the slowest initial growth rate are approximately 6 times less luminescent than *L. monocytogenes* (pSB2027). Some other factor, maybe in combination with *lux* expression is responsible for this decreased initial growth rate observed from *L. monocytogenes* harbouring the *lux* expression vectors.

It is clear that the differences at the start of the growth period are not due to expression of the *lux* genes as both the *lux* plasmids are the same, except for the presence of the terminator on pSB2028. It may be that the instability of the *lux* transcript places a metabolic load upon the cell, with energy being used to degrade the transcript and also to make more RNA to replace that being degraded. As the transcript is unstable, more has to be made overall in order to have sufficient transcript available from which protein can be translated, hence the extended lag phase. This however seems unlikely as initially levels of luminescence within the cell are not that high.

Another possible explanation for the decreased initial growth rate could be due to the size of the plasmid that the cells contain. The expression vector pSB2028 is only ~300bp larger than pSB2027. It is possible that a limit has been reached whereby cells can efficiently transcribe, translate and replicate plasmid DNA. It is also possible that this extra 300bp causes a significant increase in the levels of HMW DNA that are produced within the cell (Gruss and Ehrlich, 1988). If HMW DNA production has been increased then this too may explain the longer initial growth period as it would take longer for cells to replicate the plasmid. This will be discussed further in Chapter 8.

Although the initial growth period appears to vary between cells harbouring the different *lux* plasmids, the exponential phase of growth does not appear to differ significantly. The exponential growth rates are given in Table 5.9.1.

Table 5.9.1: Exponential growth rates of *L. monocytogenes* cells harbouring pSB2027 and pSB2028.

Growth rate is shown as an increase in optical density per hour

t-test performed using *L. monocytogenes* (pMK4) grown without inducer as a control

Plasmid	Mean Growth rate	Standard Deviation	P
pMK4 (-ve)	0.238	9.90×10^{-3}	Control
pMK4 (+ve)	0.219	0.024	> 0.05
pSB2027	0.174	0.021	> 0.05
pSB2028	0.164	0.041	< 0.05

L. monocytogenes (pSB2027) and *L. monocytogenes* (pSB2028) have lower exponential growth rates compared to *L. monocytogenes* (pMK4). It is thought that this is not entirely due to expression of *lux*, as luminescence observed from cells harbouring pSB2027 is much greater than cells harbouring pSB2028. It does appear as though the size of the plasmid that the cells contain does affect the bacterial growth rate as growth rate is significantly decreased from cells with pSB2027 and pSB2028 compared with cells harbouring pMK4.

Figure 5.9.1: Growth and bioluminescence of *L. monocytogenes* harbouring constitutive *lux* plasmids with and without a transcriptional terminator

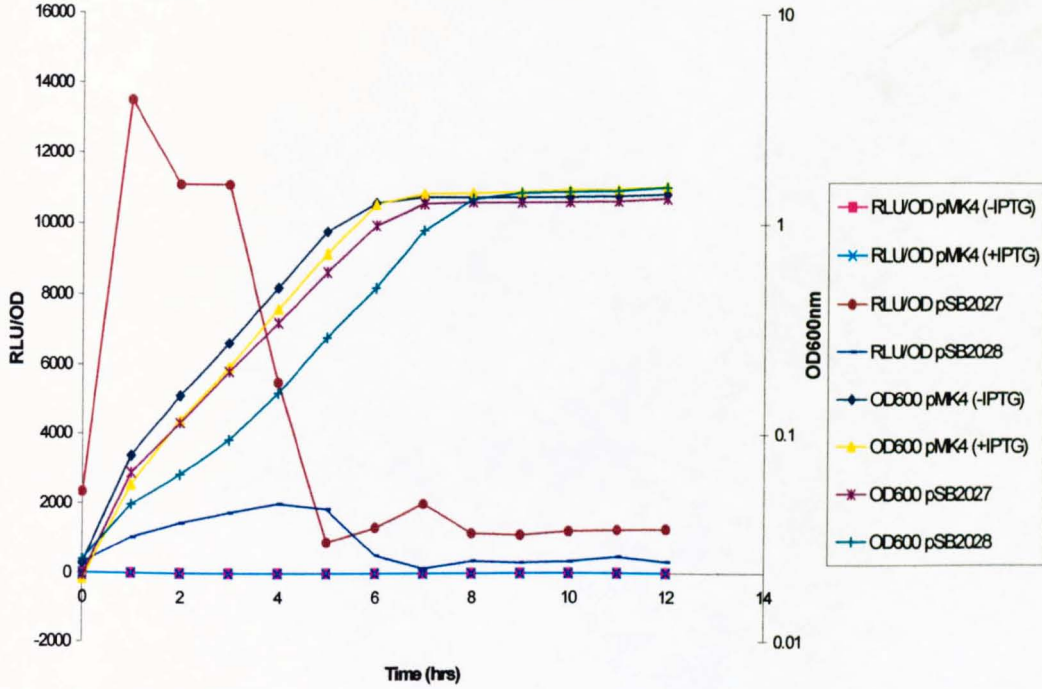
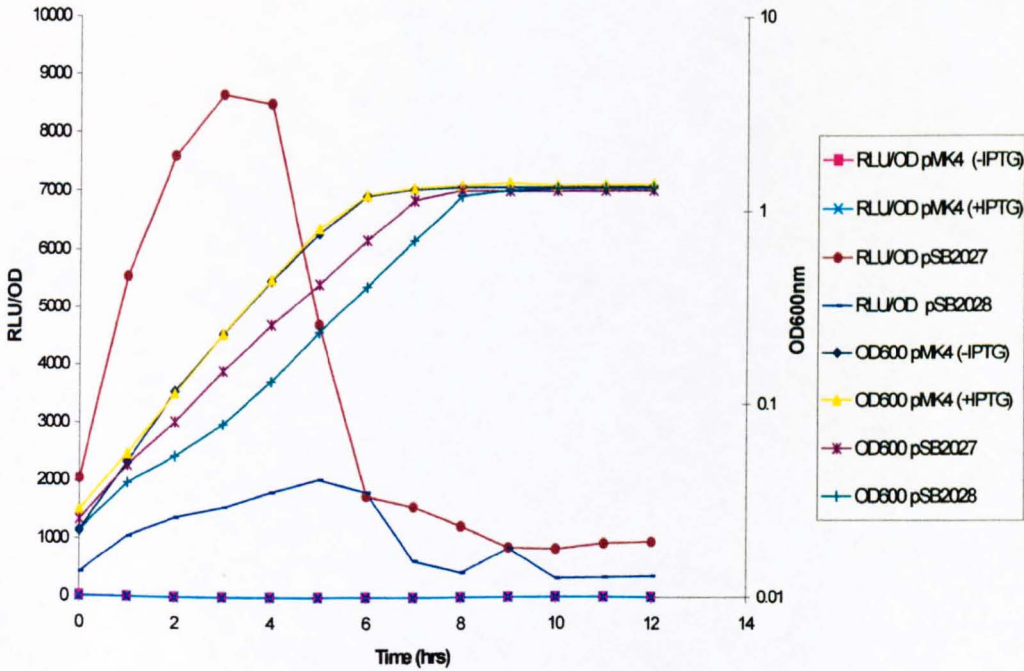


Figure 5.9.2: Growth and bioluminescence of *L. monocytogenes* harbouring *lux* plasmids both with and without a transcriptional terminator



5.10. Two-dimensional gel Electrophoresis (2-D PAGE) of *L. monocytogenes* (pSB2026)

A *lux* operon has been constructed that can be expressed effectively in Gram positive organisms, however as light emission is still not at parity with Gram negative equivalents it is believed that expression can be further enhanced. The design of the reconstructed *lux* operon was based upon independent assessment of translation initiation of the separate genes in the *lux* operon and subsequent enhancement of the translation initiation regions of *luxA*, *luxC* and *luxE*, no modifications were made to the start of *luxB* or *luxD*.

In order to determine whether the 5-*lux* genes were being translated with the same efficiency it was decided to assess the relative amounts of the separate Lux proteins produced using 2-D PAGE. This was achieved by making whole cells protein from *L. monocytogenes* cells containing pSB2027 (*lux* operon downstream of P_{xyIA} promoter). As a control, whole cell extracts of *L. monocytogenes* expressing GFP from pSB2019 were also prepared, this plasmid contained the same promoter, the only difference was the reporter gene, which in this case was *gfp3opt*. Overnight cultures of *L. monocytogenes* cells harbouring the two plasmids were grown overnight, these were then used to inoculate fresh broth at a 1/100 dilution. Cells expressing the *lux* genes were harvested when the light reached a maximum level, at this point *lux* proteins would also be present at a high concentration within the cell, and this corresponded with an optical density of around 0.3-0.4. Cells harbouring the GFP plasmid were also harvested at approximately the same OD₆₀₀ as cells expressing the bioluminescent plasmid pSB2027. Cells were washed in an equal volume of PBS, concentrated 10-fold in sonication buffer and then disrupted using a mini-bead beater (Biospec Products). A total protein assay (Bio-rad) was then performed in order to calculate the concentration of protein in the samples so that the same concentration of protein could then be loaded onto the gel.

The horizontal 2-D gel electrophoresis was performed using the Immobiline DryStrip kit according to the instructions provided by Pharmacia. The first dimension was performed with the Multiphore II electrophoresis unit using Immobiline DryStrips of pH4-7 as the isoelectric points of the individual Lux proteins were already known. Following separation of proteins according to isoelectric point, they were then separated by molecular weight by horizontal SDS electrophoresis using ExcelGel SDS polyacrylamide gradient gels. The gel consisted of a stacking gel followed a polyacrylamide gradient of 12-14%, these were run on the Multiphore II electrophoresis unit. 2-D gels were then stained with Coomassie blue and separated proteins subsequently visualised following destaining of the gel. The gels obtained are illustrated in Figures 5.10.1 and 5.10.2, this shows the 2-D protein profile from *L. monocytogenes* cells harbouring pSB2019 and pSB2027 respectively. Using the protein profile from *L. monocytogenes* cells expressing GFP from pSB2019 as a reference gel, the two gels were compared using the ImageMaster software version 1.1 (Pharmacia), which allows protein spots to be detected and quantified, and any novel spots to be identified. Dr Sara Movahedi kindly performed the gel analysis.

On comparison of the whole cell extracts of *L. monocytogenes* (pSB2027) to *L. monocytogenes* (pSB2019), several additional spots were detected. It was hoped that only 5 new spots would be present, each one representing one of the Lux proteins. However a total of 15 unique spots were present. This was far more than predicted and it is thought that this is either due to loss of the sample when being loaded onto the first dimension, or it is due to the fact that the control protein samples were not as concentrated as the sample containing the Lux proteins and hence some of the cellular proteins have not been detected on the reference gel.

Those bands that have been isolated as being unique are shown on Figure 5.10.2 with those thought to be the Lux proteins labelled A-E. The known details of these Lux proteins are compared to values obtained from the 2-D analysis in Table 5.10.1. Also represented in this table are the relative volumes of each spot, i.e. the relative concentration of each protein spot.

Table 5.10.1: Comparison of known and calculated properties of the individual Lux proteins

Protein	Known Mwt kDa	Measured Mwt kDa	Known Isoelectric point (IEP)	Measured Isoelectric point (IEP)	Volume of Spot
LuxA (1)	40.99	42.98	6.1	6.58	10.18
(2)		43.85		6.55	5.96
LuxB	37.59	39.52	4.76	5.15	3.22
LuxC	54.95	55.02	6.2	6.6	4.84
LuxD	34.65	34.56	5.2	5.58	1.83
LuxE	45.47	46.2	5.8	6.15	6.39

Although the protein analysis does not clearly show the 5 unique Lux proteins, other spots have been eliminated from either their molecular weight data or their position on the gel. There are two possible spots, both approximately the same molecular weight and IEP on the gel that could correspond to LuxA, the only real difference is between the intensities of the spots, with one being much bigger. As LuxA is part of the luciferase complex and a large amount of light is seen from cells harbouring this plasmid, it is thought that spot A1 is correct. Nevertheless, which ever spot is correct both are of a greater intensity than the spot thought to correspond to LuxB, suggesting that translation of the *luxB* gene is less efficient that that of *luxA*. The spots thought to correspond to LuxC and LuxE are marked on the gel, both these are more concentrated than LuxB. This may be expected however as the start of *luxA*, *luxC* and *luxE* were all translationally enhanced, therefore more protein may be expected. The one band that was not easily identifiable was that corresponding to LuxB. The gel analysis equipment did isolate one possible spot, but this one spot was very faint on the gel. It may just be that translation of the *luxD* gene is poor due to poor initiation of translation, as this had not been enhanced for *luxD*.

Data obtained from the 2-D PAGE is not clear-cut. It appears as though *luxB* and *luxD* are not being translated with such efficiency as the other *lux* genes, but this may be expected as translation of these genes has not been enhanced for expression in Gram positive bacteria. In order to properly assess the relative amounts of Lux proteins produced by *L. monocytogenes* cells, more concentrated cell extracts need to be obtained. This could be achieved by freeze drying the protein samples and then reconstituting them in a smaller volume. Another way to obtain a more concentrated sample would be to lyse the cells by sonication instead of using the bead beater. This has been done for protein samples used in one-dimensional gels and resulted in concentrated samples that actually had to be diluted in order to resolve individual bands.

Also, it would be better to observe expression of the *lux* genes from the plasmid that contains *xyIR* P_{*xyIA*} (pSB2026). As it is known that expression of the *lux* genes is almost completely inhibited in the absence of xylose it would be better to compare expression of the genes from cells grown with and without xylose. However, this may not be as good as using the constitutive *lux* plasmid (pSB2027), as section 5.8 showed light levels from pSB2026 were significantly lower than cells expressing *lux* from pSB2027.

Once the separate amounts of Lux proteins have been analysed it can then be determined whether the *lux* operon needs to be engineered further. Any genes that are found to be poorly translated, indicated by low levels of protein, will be engineered via PCR to translationally enhance the 5' coding region of the gene for expression in Gram positive bacteria.

Figure 5.10.1: 2-D analysis of whole cell extracts of *L. monocytogenes* harbouring pSB2019

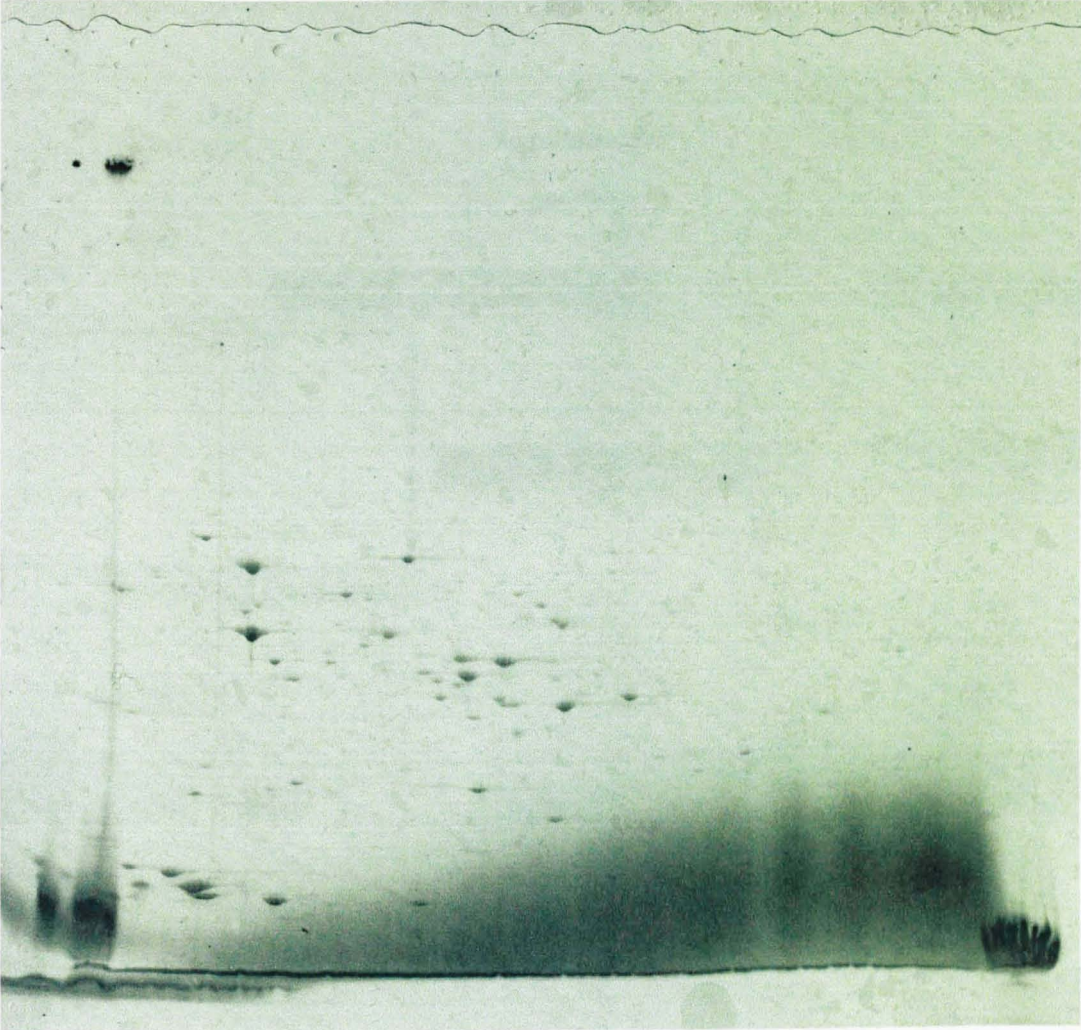
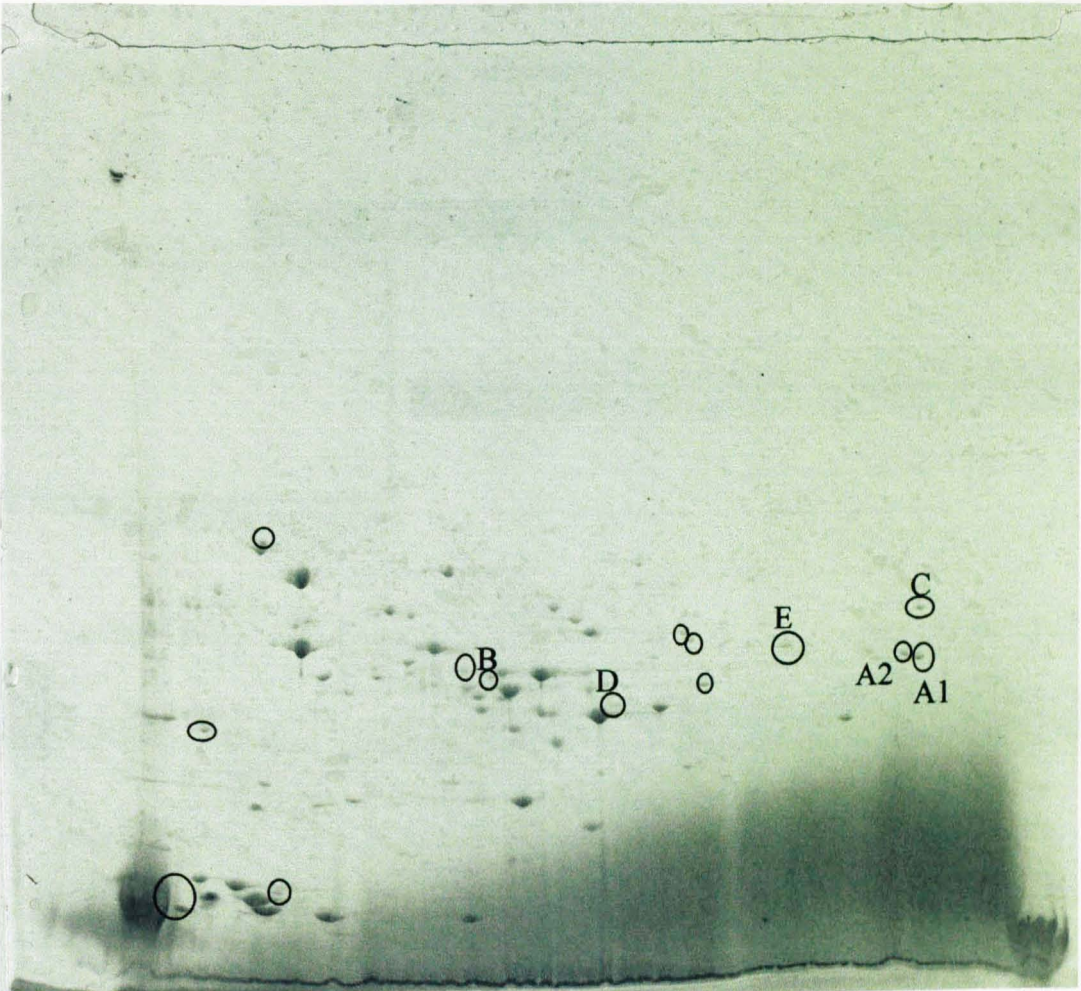


Figure 5.10.2: 2-D gel analysis of whole cell extracts of *L. monocytogenes* harbouring pSB2027

Circles indicate possible novel proteins in the sample



5.11. Discussion

The *lux* operon of *P. luminescens* was placed on a plasmid under the control of a strong promoter, in this case P_{xym} . When this reporter plasmid was used to transform Gram positive bacteria the light emission from the recombinant organism was extremely faint. Upon addition of exogenous aldehyde to cells expressing this plasmid the light levels did not increase, this showed that it was not an inability of the cell to synthesis substrate. Analysis of whole cell extracts of *L. monocytogenes* harbouring this plasmid by SDS PAGE suggested that only very low levels of Lux proteins were being generated. Previous experience of gene expression in such organisms (Jacobs *et al.*, 1991; Hill *et al.*, 1994; Qazi *et al.*, 1998) led to the supposition that the problem was one of inefficient translation initiation.

The *P. luminescens lux* operon was therefore reconstructed by incorporating enhanced translational signals for those genes that the DNA sequence suggested may be poorly translated, in this case *luxA*, *luxC* and *luxE*. The 5' region of these genes were engineered *via* PCR to enhance translational initiation in Gram positive bacteria. The reconstructed *lux* operon was placed downstream of P_{xylA} , both in the presence and absence of the *xylR* regulator gene upstream of this. These constructs were introduced into *L. monocytogenes* and two strains of *S. aureus*, RN4220 and 8325-4, with the result that the bioluminescence was significantly increased. Growth experiments using *L. monocytogenes* harbouring these plasmids showed that higher levels of luminescence were obtained when *xylR* was not present on the plasmid, i.e. with pSB2027, suggesting that P_{xylA} has not been fully de-repressed, however in each case the cells were not bioluminescent throughout the period of growth. The bioluminescence peaked as cells were in mid exponential phase and then dropped, suggesting that this promoter was not constitutive and was only active in the early stages of growth, or that energy was limiting in the bacteria. This seems unlikely as the bacteria are still growing exponentially, therefore there should be enough FMNH₂ that the bacteria can used to drive the bioluminescent reaction. For bacterial tracking studies etc, an alternative promoter that is both strong and constitutive in its action, but also regulatable, is desirable to give high luminescence levels throughout

growth. One approach to identify such promoters is to use the reconstructed *lux* operon on promoter probe vectors. However, a high bacterial transformation efficiency is required, and as this cannot be attained with *L. monocytogenes*, *S. aureus* and *S. epidermidis* the studies would possibly be performed in *B. subtilis* due to its relatively high transformation efficiency. Analysis of the separate Lux proteins by 2-D gel electrophoresis suggested that *luxB* and *luxD* are translated with less efficiency than the other *lux* genes. However, due to the fact that the cell samples did not appear to be of an equal concentration and also that the samples were not concentrated enough, no definite results could be obtained. Ideally the experiment needs to be repeated using more concentrated cell samples. On the basis of the information gained the 5' coding sequence region of any genes that appear to be poorly translated will be engineered by PCR to enhance translation initiation in Gram positive organisms. However, if all the *lux* genes are found to be translated equally well, this would suggest that the lower levels of light seen from the organisms is due to sub-optimal transcription within the cell.

In order to advance our understanding of host-pathogen interactions and gene regulation, non-invasive assays for monitoring the progression of infectious agents and other biological processes in the living animal are required. Although tissue culture models do provide important information on host pathogen interaction, the *in vitro* model system is deficient in reproducing most if not all the host immune system and can never replicate the complex dynamic interaction that occur *in vivo*. The experiments of Contag *et al.* (1995) allowed bacterial movement to be viewed non-invasively within the living animal. However, the reporter constructs available gave very poor luminescent output when expressed in Gram positive organisms thus making such *in-vivo* experiments impossible, and to this end it was decided to optimise expression of individual *lux* genes for expression studies in Gram positive organisms.

The *lux* reporters constructed during the course of this project have resulted in much greater luminescent output from cells harbouring the expression vectors. However, it appears as though the *lux* genes are only expressed throughout early exponential

phase. Once a *lux* reporter has been constructed that is constitutive when induced, the construct can be used to track Gram positive pathogens during pathogenesis by using animal models, e.g. the erythema / subcutaneous abscess model (Kinsman, 1986) in mice to study staphylococcal infection. Photonic imaging during the course of infection should provide data on the growth and spread of constitutively bioluminescent bacteria (Contag *et al.*, 1995). The use of the reconstructed *lux* operon in reporter constructs should also provide information about the temporal and spatial induction of specific genes.

These newly constructed reporters have many other potential uses, for example they could be of value in studies that concern the spread and survival of genetically modified micro-organisms in soil environments, and to gain a better understanding of how the engineered organisms move through the soil and interact with the indigenous microbial community. One specific example for utilising the *lux* genes is to follow bioremediation of contaminated areas within the environment. When observing the performance of an introduced degrader, it is important that the spread of the bacteria can be monitored and also that information can be obtained concerning their metabolic activity. By using *lux*, these issues are addressed, as bioluminescence is only observed in metabolically active cells. The *lux* reporter system also allows single cell detection and its activity can be monitored non-destructively and *in situ*.

CHAPTER 6

CONSTRUCTION OF A DUAL REPORTER FOR EXPRESSION STUDIES IN GRAM POSITIVE BACTERIA

CHAPTER 6: CONSTRUCTION OF A DUAL REPORTER FOR EXPRESSION STUDIES IN GRAM POSITIVE BACTERIA

6.1. Creating a dual reporter

So far reporter plasmids have been constructed that encode either the *gfp3* gene or the engineered *luxABCDE* operon from *P. luminescens*. As each reporter has its own advantages and disadvantages it was decided to construct a plasmid that would confer both a green fluorescent and bioluminescent phenotype upon cells harbouring the expression vector. Such a construct would reveal a greater amount of information when performing any *in situ* studies. For example, during an infection process the bioluminescent marker would provide data on the growth and spread of constitutively luminescent bacteria as well as providing information about the temporal and spatial induction of particular genes at the macro level. The *gfp3* reporter cannot give a real time representation of gene induction and expression due to the time taken for the chromophore to fold and generate fluorescent protein. Nevertheless, *gfp3* does provide an excellent positional marker on those cells expressing the gene, even on fixed samples, and thus individual bacteria could be located within an animal following sectioning. This would provide data on how individual bacteria contribute to the infection process and how infection proceeds.

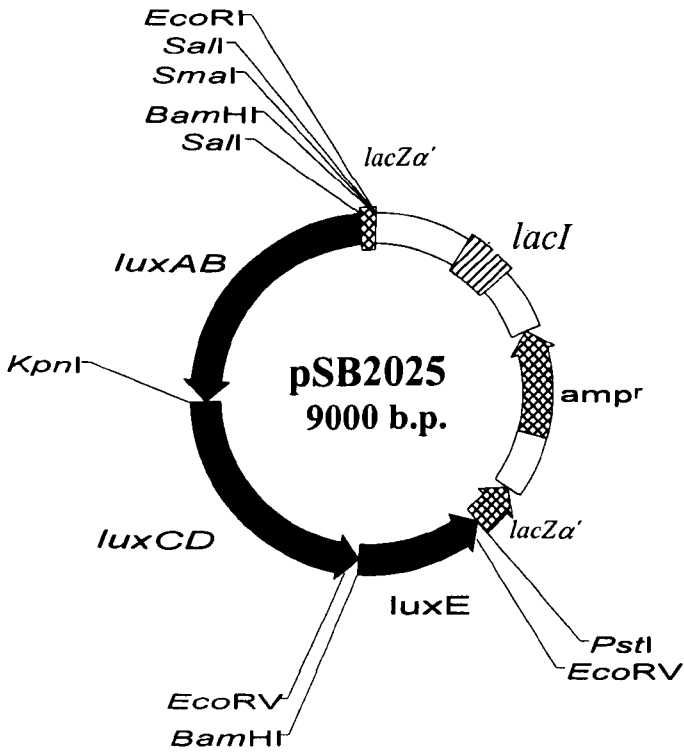
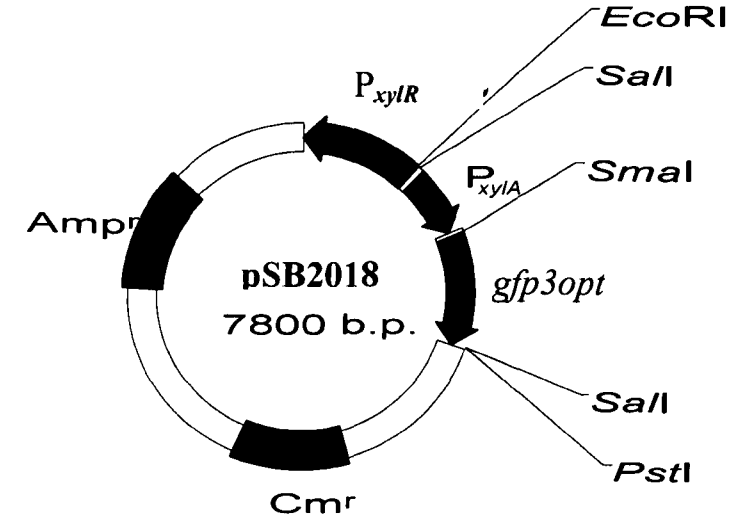
As microorganisms are exploited in many areas of environmental biotechnology, including bioremediation and biocontrol, genetically engineered microorganisms are being constructed for these environmental applications. A dual reporter system has previously been developed by Unge *et al.* (1999) by utilisation of the *luxAB* and *gfp* genes. The bioluminescence phenotype of the *luxAB* reporter is directly related to the metabolic activity of the cell. Bacterial luciferase catalyses the following reaction:

$RCHO + O_2 + FMNH_2 \rightarrow RCOOH + H_2O + FMN + \text{light (490nm)}$, where R is a long chain fatty aldehyde. Due to the requirement of reducing equivalent (FMNH₂),

the bioluminescence phenotype of the *luxAB* marker is dependent on the cellular energy status. Thus the bioluminescence is directly related to the metabolic activity of the cells, and as such can be used to assess the relative metabolic activity of specific bacterial populations upon the addition of exogenous aldehyde to the sample. In contrast GFP fluorescence has no requirement for energy and does not require additional substrates to fluoresce (Chalfie *et al.*, 1994). The expression of *gfp* in this dual reporter system allows fluorescent cells to be rapidly enumerated by flow cytometry ((Ropp *et al.*, 1995). However, in this system only the *luxAB* genes have been utilised which requires the addition of exogenous aldehyde to the samples before luminescence is observed. Whilst this does give a good representation of the metabolic activity of the cells, it would be more advantageous to use cells expressing the whole operon, so the metabolic activity can be measured immediately upon sampling and also continuously. Such a reporter whilst being valuable in the enumeration and evaluation of the active proportion of a bacterial population in environmental studies could also be used for gene expression studies and localisation studies *in vivo*.

In order to build a dual reporter plasmid, two existing expression vectors were used. These were pSB2018 (the Gram positive *gfp3* vector) and pSB2025 (*luxABCDE* in a superlinker plasmid). These starting plasmids are shown in Figure 6.1.1.

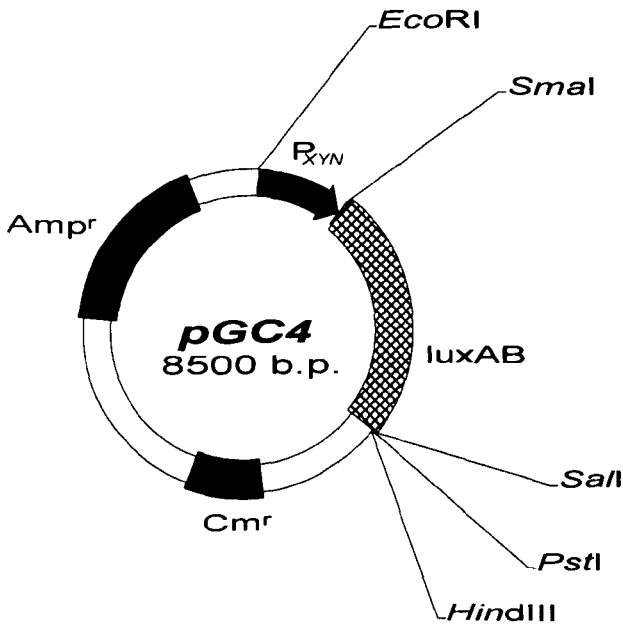
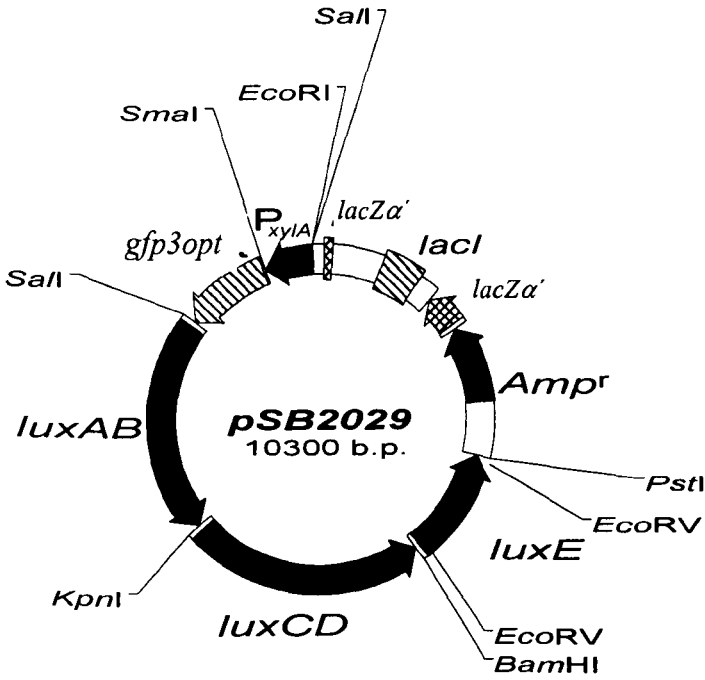
Figure 6.1.1: Expression vectors pSB2018 and pSB2025



Both pSB2018 and pSB2025 were restricted with *SalI*. With pSB2018 a band of approximately 1.3kb was generated upon restriction, this contained the P_{xylA} promoter and the translationally optimised *gfp3* gene. The fragment excised from pSB2025 following restriction with *SalI* was too small to see on an agarose gel, however the plasmid DNA (approximately 9kb) was still purified to prevent re-ligation of this small fragment into the rest of the vector. Purification of the appropriate DNA was achieved by freeze thaw purification of excised DNA bands following electrophoresis of the DNA on a low melting point agarose gel. The purified DNA fragments were then ligated together and subsequently used to transform *E. coli* JM109 competent cells by electroporation. Cells containing recombinant DNA were isolated following selection on ampicillin LB agar plates. Recombinant colonies that contained the dual expression vector were observed to fluoresce green under excitation conditions and were also seen to have a bioluminescent phenotype following examination under a Hamamatsu VIM3 camera. Although the phenotype of the recombinant colonies suggested that the new expression vector was correct, DNA was prepared from some of the colonies by plasmid miniprep. The resulting DNA was restricted with *EcoRI* and *PstI*, which produced bands of approximately 7kb and 3.4kb which were presumed to be the P_{xylA} -*gfp3opt-lux* fragment and the plasmid backbone respectively. This new construct was named pSB2029.

The dual expression vector pSB2029 only contains a Gram negative origin of replication. Due to this it will not replicate in Gram positive bacteria. In order to express both reporter genes in Gram positive organisms they were placed onto a Gram positive shuttle vector, in this case pGC4 was chosen. Both pGC4 and pSB2029, illustrated in Figure 6.1.2, were restricted with *EcoRI* / *PstI* in order to excise the P_{xyn} -*luxAB* fragment and the P_{xylA} -*gfp3opt-lux* fragments respectively. All DNA was purified by freeze thaw following electrophoresis on a low melting point agarose gel.

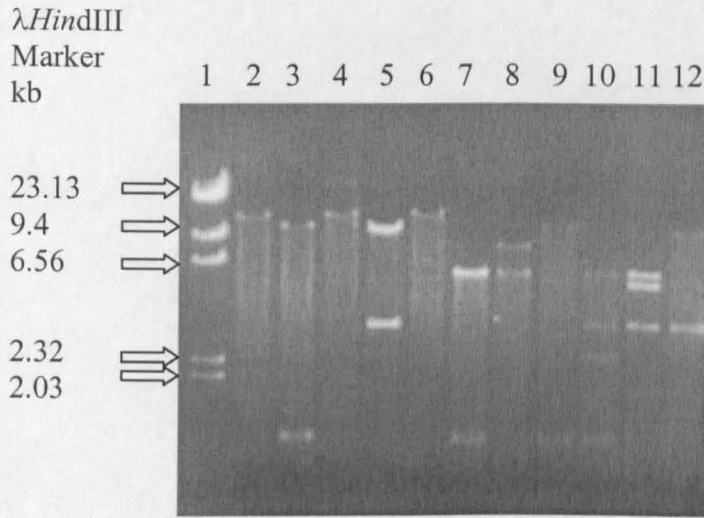
Figure 6.1.2: Restriction maps of pSB2029 and pGC4



Following purification, the two fragments of DNA were ligated together. Recombinant colonies were isolated following selection on ampicillin agar plates. When examined, some of these were observed to fluoresce under blue light excitation and were also seen to be bioluminescent following examination under a Hamamatsu VIM3 camera. In order to check that these cells contained the new plasmid, and not the starting plasmid pSB2029, colonies exhibiting the two phenotypes were picked onto agar plates containing chloramphenicol. Only derivatives of pGC4 were able to grow on this due to the presence of a chloramphenicol resistance marker on the plasmid. DNA was isolated from those colonies that grew on chloramphenicol by plasmid miniprep, this was subsequently restricted with both *EcoRI* / *PstI* and *EcoRI* / *SaII* which proved that the constructs were correct, the new plasmid was designated pSB2030.

One recombinant colony was chosen and DNA prepared by plasmid maxiprep. As a final check of pSB2030 the DNA was examined by restriction analysis, and the resulting agarose gel analysis is illustrated in Figures 6.1.3. All the enzymes digested the plasmid as predicted apart from *SmaI*, which did not appear to be restricting the DNA efficiently, shown by the presence of a large amount of uncut DNA from this single digest. However, as all the other digested appeared to map correctly, it was presumed that the construct was correct. The restriction map of pBS2030 is illustrated in Figure 6.1.4.

Figure 6.1.3: Restriction Analysis of pSB2030



Layout of Gel:

Lane1: λ *HindIII*

Lane2: *EcoRI*

Lane3: *SalI*

Lane4: *SmaI*

Lane5: *EcoRV*

Lane6: *PstI*

Lane7: *PstI* / *SalI*

Lane8: *PstI* / *EcoRI*

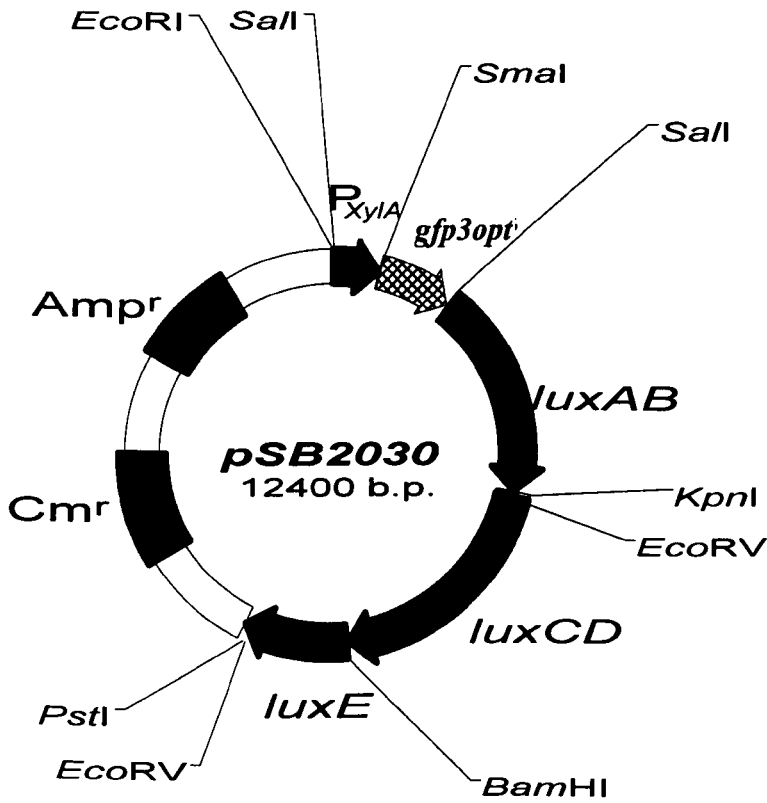
Lane9: *SmaI* / *SalI*

Lane10: *EcoRV* / *SalI*

Lane11: *EcoRI* / *EcoRV*

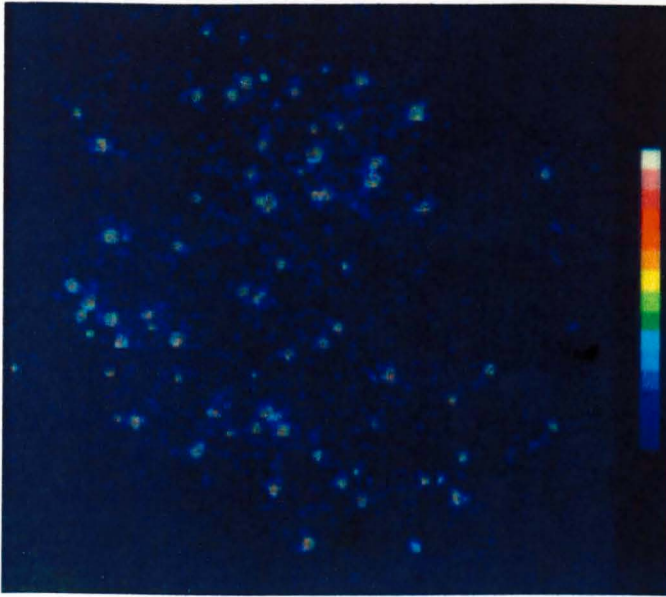
Lane12 : *EcoRV* / *SmaI*

Figure 6.1.4: Restriction Map of pSB2030



The plasmid pSB2030 was introduced into *L. monocytogenes* by electroporation of competent cells, and recombinant colonies were isolated following selection on chloramphenicol agar plates. These colonies were then screened under a Hamamatsu VIM3 camera to examine the bioluminescence. All colonies were seen to be constitutively bioluminescent as illustrated in Figure 6.1.5. However, it appeared as though cells harbouring pSB2030 were not as luminescent as the equivalent *lux* reporter, pSB2027. Individual colonies that were seen to be bioluminescent were mounted on a glass slide in PBS and examined under a fluorescence microscope. All individual cells were seen to fluoresce green with relatively high intensity indicating that the *gfp3opt* had been translated efficiently.

Figure 6.1.5: Recombinant Colonies of *L. monocytogenes* (pSB2030)



Having successfully introduced pSB2030 into *L. monocytogenes*, it was decided to introduce the plasmid into *S. aureus*. *S. aureus* RN4220 was transformed with pSB2030 by electroporation of competent cells following the method of Augustin and Gotz (1990). Recombinant colonies were isolated following growth, for 2 days at 37°C, on chloramphenicol selective agar plates. Resulting transformants were then screened under a Hamamatsu VIM3 camera to observe bioluminescence. All recombinant colonies were observed to be luminescent, and the luminescent properties of a single colony are illustrated in Figure 6.1.6. DNA from *S. aureus* RN4220 harbouring pSB2030 was prepared by plasmid miniprep. This was then used to transform *S. aureus* 8325-4 by electroporation of competent cells. Following selection on chloramphenicol selective agar plates, recombinant colonies were screened under a Hamamatsu VIM3 camera in order to observe the bioluminescence. The bioluminescence characteristics of a single recombinant colony are shown in Figure 6.1.7. A single light colony of *S. aureus* RN4220 (pSB2030) and *S. aureus* 8325-4 (pSB2030) were also resuspended in PBS on a glass cover slip and observed by fluorescence microscopy under blue light excitation, all individual cells were seen to fluoresce green under these excitation conditions. This indicated that both reporter genes were being translated efficiently within the Gram positive bacteria.

Figure 6.1.6: Colonies of *S. aureus* RN4220 (pSB2030)

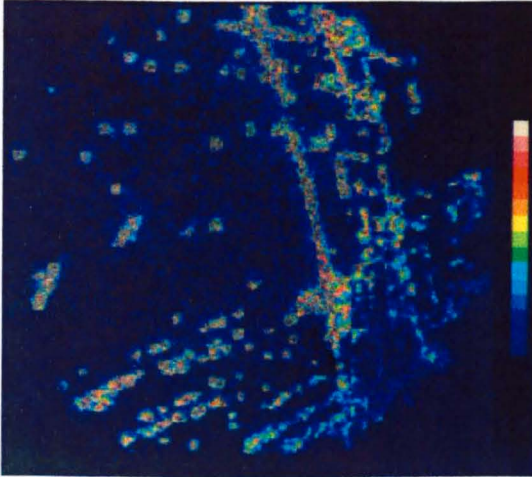
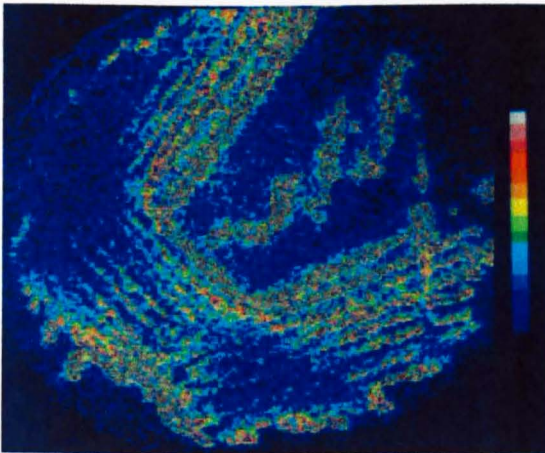
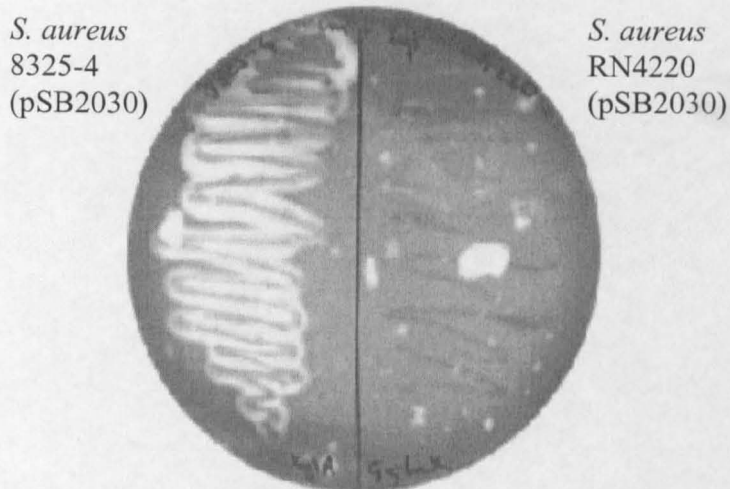


Figure 6.1.7: Colonies of *S. aureus* 8325-4 (pSB2030)



In order to verify that these two strains of staphylococci harbouring pSB2030 were different, a single colony of each was streaked onto a chloramphenicol selective blood agar plate. The results of this are illustrated in Figure 6.1.8.

Figure 6.1.8: Haemolytic activity of two different strains of *S. aureus*



From Figure 6.1.8 it can be seen that the two colonies exhibit different haemolytic properties indicating that these are two different strains of staphylococci. *S. aureus* 8325-4 is haemolytic whereas *S. aureus* RN4220 is not, and shows no signs of blood haemolysis. Both colonies were shown to be bioluminescent and also fluoresced green under blue light excitation due to the expression of *lux* and *gfp3opt* from pSB2030.

6.2. Comparison of growth and fluorescence of *L. monocytogenes* (pSB2019) and *L. monocytogenes* (pSB2030)

These experiments were performed to observe the fluorescence of *L. monocytogenes* containing both pSB2019 and pSB2030, these plasmids express *gfp3opt* or *gfp3opt-luxABCDE* respectively from P_{xylA} . *L. monocytogenes* (pSB2019) and *L. monocytogenes* (pSB2030) were grown overnight in antibiotic selective BHI broth. All cultures were diluted 100-fold into fresh culture medium and optical density and relative fluorescence measured at hourly intervals. In order to observe whether expression of *gfp3* affected bacterial growth rate, a culture of non-recombinant *L. monocytogenes* 7973 cells were grown overnight and measurements made in the same way. The measured values of green fluorescence on *L. monocytogenes* (pSB2019) and *L. monocytogenes* (pSB2030) were corrected for background fluorescence by subtracting the corresponding measured values from the control culture of *L. monocytogenes*. This gave the relative fluorescence (RFU) for each test culture. To take into account the effect of dilution on bacterial fluorescence, the RFU values were divided by the corresponding OD values (RFU/OD). The RFU/OD were plotted as a function of time on an arithmetic plot, in addition to this, the OD values were also plotted on the same graph on a log scale as a function of time. This was done so the level of fluorescence relative to the bacterial growth rate could be compared. A representation of the data is illustrated in Figure 6.2.1 and 6.2.2.

From the data shown in Figures 6.2.1 and 6.2.2 it can be seen that the fluorescence between *L. monocytogenes* harbouring the two-*gfp3opt* expression vectors varies markedly. Nevertheless, in both cases high levels of GFP fluorescence is observed in the absence of xylose, indicating that P_{xylA} is derepressed as the *xylR* regulator gene is no longer present on the plasmid. *L. monocytogenes* (pSB2019) show a much greater level of fluorescence than *L. monocytogenes* (pSB2030). When cells express *gfp3opt* from pSB2019, the levels of fluorescence observed are approximately five times greater than *L. monocytogenes* cells expressing both *gfp3opt* and *lux* genes from pSB2030. In both cases fluorescence begins to increase once cells have entered stationary phase. This delay in observing a fluorescent signal is probably due to two

independent factors, the rate of synthesis of functional protein, and the dilution of the fluorescent signal as cells divide. The post-translational formation of a functional chromophore occurs approximately 2 hours after synthesis of GFP (Heim *et al.*, 1995) in *E. coli*, however as GFP is not an enzyme there is no signal amplification derived from multiple substrate cleavage by one molecule of reporter protein. So although the *gfp* gene is transcribed and subsequently translated from exponentially growing cells, the signal does not start to increase until approximately six hours later due to the post-translational modification that occurs and the effect of dilution on the signal by rapidly growing and dividing cells.

The fact that the fluorescence seen from *L. monocytogenes* expressing the dual reporter gene was much lower than that from *gfp3opt* alone, suggests that a greater metabolic load is placed upon the cells with pSB2030, resulting in lower translation of the genes downstream of P_{*xyIA*}. This possible extra energy drain on the cells may be due to the fact that *L. monocytogenes* (pSB2030) express six recombinant proteins compared to just the one GFP protein expressed by equivalent cells bearing pSB2019. Also, cells harbouring pSB2030 have an extra 5.8kb segment of DNA compared to those harbouring the single *gfp3* expression vector, thus cells may require more energy to transcribe, translate and replicate the plasmid DNA. It appears unlikely that the levels of transcript from *L. monocytogenes* (pSB2030) have decreased compared to *L. monocytogenes* (pSB2019), as the same promoter is present upstream of the reporter genes in each plasmid.

Observations made from Figures 6.2.1 and 6.2.2 indicate that the exponential growth rate of the fluorescent cultures is changed from that of the non-recombinant *L. monocytogenes*. The gradient of the non-recombinant cells appears to be slightly steeper compared to cells expressing either the single or dual *gfp3* reporter, indicating that the non-fluorescent *L. monocytogenes* have a faster growth rate. GFP3 levels in the cell tend to plateau in stationary phase, due to the delay between the initial translation and formation of functional protein, this suggests that *gfp3opt* is actively being transcribed and translated within the cell during exponential phase. Thus if expression of *gfp3opt* and the dual reporter does place an energy drain upon

the cells it should be reflected in the exponential growth rate. The exponential growth rates are illustrated in Table 6.2.1.

Table 6.2.1: Mean exponential growth rates of *L. monocytogenes* (pSB2019) and *L. monocytogenes* (pSB2030)

Growth rate is shown as an increase in optical density per hour

t-test performed using *L. monocytogenes* 7973 as a control

Plasmid	Mean Growth Rate	Standard Deviation	P
Non-recombinant <i>L. monocytogenes</i> 7973	0.332	0.0184	Control
<i>L. monocytogenes</i> (pSB2019)	0.281	2.83×10^{-3}	> 0.05
<i>L. monocytogenes</i> (pSB2030)	0.198	8.49×10^{-3}	< 0.05

From the data given in Table 6.2.1 it can be seen that non-recombinant *L. monocytogenes* cells have a faster exponential growth rate than either population of fluorescent bacteria. *L. monocytogenes* with the dual expression vector have the slowest rate of growth, compared to both non-fluorescent bacteria and cells containing pSB2019, supporting the theory that production of both GFP3 and Lux proteins places a significant energy drain on the bacterial cell, much greater than production of GFP3 alone.

One other feature that lends support to the thought that the dual reporter places a metabolic load upon the cells is the slower initial growth rate shown by *L. monocytogenes* expressing the dual reporter plasmid.

This initial slower growth rate could be attributed to differences in the amounts of the initial inoculum used in the experiments, due to the limitations of the

spectrophotometer, which is unable to give an accurate representation of bacterial populations at low dilutions. This may be true, but it seems unlikely that the same trends would be seen each time that the experiment was performed.

One possible explanation for the initial slower growth rate that was observed by *L. monocytogenes* (pSB2030) could be plasmid size. This plasmid is quite large at approximately 12kb, this may be beyond the limits that the bacterial cell can efficiently transcribe, translate and replicate. As mentioned previously pC194, a derivative of pMK4, tends to form high molecular weight (HMW) DNA following insertion of heterologous DNA fragments. It has been shown (Gruss and Ehrlich, 1988) that pC194, which replicates by a rolling circle type replication with ssDNA intermediates generates HMW DNA upon insertion of DNA fragments. It also appeared that as the size of the DNA insert increased the amount of HMW DNA also increased. The size difference between pSB2019 and pSB2030 is approximately 5.8kb. It is possible that insertion of such a large DNA fragment causes the production of large amounts of HMW DNA within the bacteria and this slows down the initial growth rate as cells start to divide and replicate, hence the extended lag phase and decreased rate of exponential growth. This will be discussed further in Chapter 8.

Figure 6.2.1: Growth and Fluorescence of *L. monocytogenes* (pSB2019) c.f. *L. monocytogenes* (pSB2030)

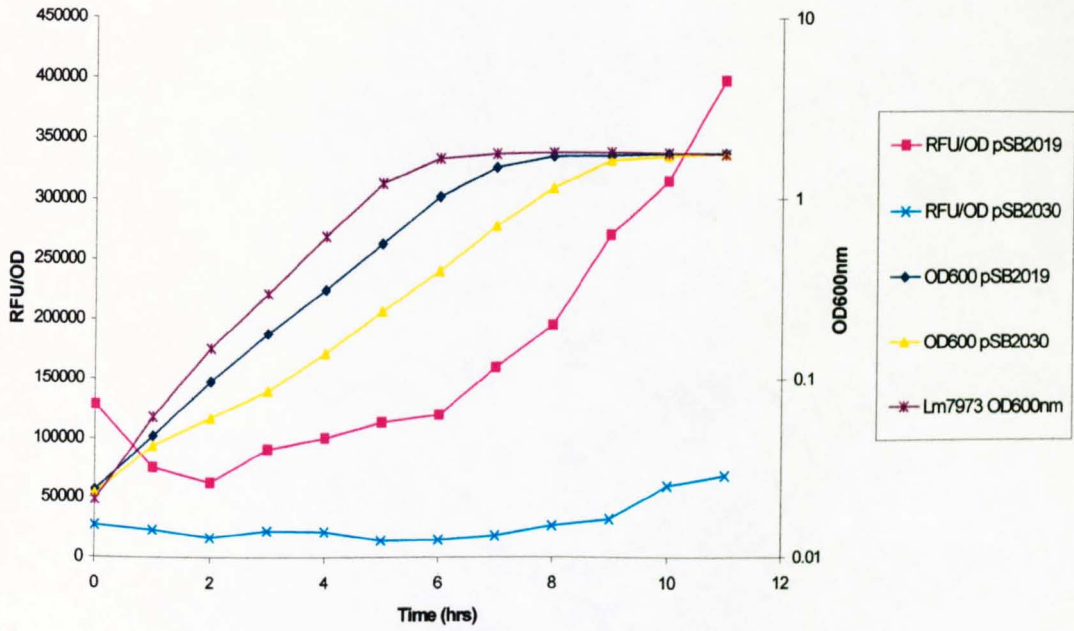
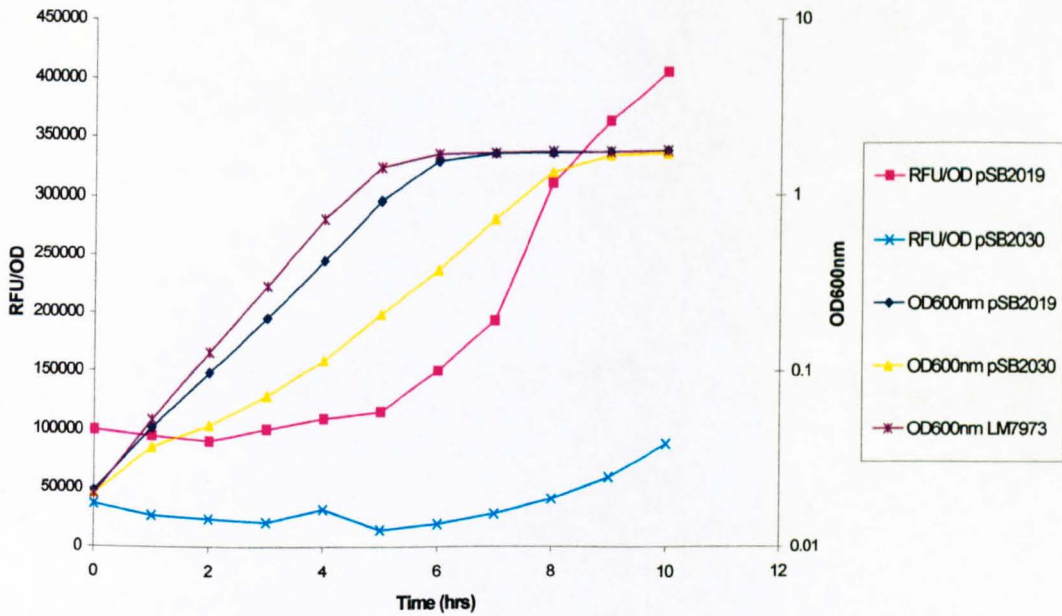


Figure 6.2.2: Growth and fluorescence of *L. monocytogenes* (pSB2019) c.f. *L. monocytogenes* (pSB2030)



6.3. Growth and bioluminescence of *L. monocytogenes* (pSB2027) and *L. monocytogenes* (pSB2030)

These experiments were carried out as previously described in order to observe the growth and luminescent properties of *L. monocytogenes* harbouring the dual reporter plasmid compared to cells containing the *lux* expression vector (pSB2027). As a control, *L. monocytogenes* (pMK4) were grown in the presence of IPTG to induce expression of *lacZ*. Previous experiments had shown that induction of pMK4 did not alter the growth characteristics of cells expressing the gene. With all cultures, both optical density and bioluminescence were measured at hourly intervals. In order to account for the effect of OD on the bioluminescence measurements (RLU), RLU values were divided by the corresponding optical density readings. The generated RLU/OD values were plotted on an arithmetic plot with respect to time, in order to compare the luminescent output to growth, OD values were also plotted on the same graph on a log scale. A representation of the data gained is illustrated in Figure 6.3.1 and 6.3.2.

From the illustrated data it can be seen that xylose is not needed for expression of the *lux* genes, this indicates that the *xylR* regulator gene has been excised from the promoter fragment so that P_{xylA} is not dependent on xylose for its induction. The levels of luminescence generated from the strains bearing the expression vectors were very different. With *L. monocytogenes* (pSB2027), the *lux* expression vector, cells were approximately five times more luminescent than *L. monocytogenes* containing the dual reporter. This corresponds with fluorescence data gathered from observing *gfp3opt* expression, with the dual reporter generating around five times less fluorescent protein than observed with a single *gfp3opt* reporter. The fact that when cells express both reporter genes, expression levels of both are reduced five-fold, indicates that either an energy drain is placed upon the cells or the cells cannot transcribe, translate and replicate the 6.5kb fragment of reporter DNA efficiently, hence the lower fluorescence and luminescence signals. As a high luminescent output is generated from cells harbouring the *lux* plasmid, it does appear as though a size threshold has been surpassed whereby DNA is efficiently transcribed and

translated within the cell. It is possible that the extra 800bp when *gfp3opt* is placed upstream of *luxABCDE* places a significant metabolic load upon the cell due to the size of the plasmid which needs to be replicated within *L. monocytogenes* and the possible production of HMW DNA within the cells. The formation of HMW DNA within the cell depends on the size and nature of the inserted DNA and also the plasmid size (Gruss and Ehrlich, 1988).

If the lower output from the reporter genes was due to an increased energy drain being placed upon the bacterial cells, this may be manifested by a decrease in the exponential growth rate. The average exponential growth rates of the cultures used in the experiment are given in Table 6.3.1.

Table 6.3.1: Mean growth rates of *L. monocytogenes* harbouring *lux* expression vectors.

Growth rate is shown as an increase in OD per hour

t-test performed using *L. monocytogenes* (pMK4) grown without inducer as a control

Plasmid	Mean Growth Rate	Standard Deviation	P
<i>L. monocytogenes</i> (pMK4)	0.185	0.023	Control
<i>L. monocytogenes</i> (pSB2027)	0.174	0.021	> 0.05
<i>L. monocytogenes</i> (pSB2030)	0.175	9.90×10^{-3}	< 0.05

It can be noticed that *L. monocytogenes* (pMK4) have the highest growth rate, indicating that expression of *LacZ* places less of an energy drain upon the cells than expression of the *lux* genes or the dual reporter. There is no significant difference between the exponential growth rates of *L. monocytogenes* (pSB2027) or *L. monocytogenes* (pSB2030) which again supports the theory that expression of *gfp3opt* places no significant energy drain upon the bacteria. When the exponential growth rates of *L. monocytogenes* harbouring the dual reporter were compared to

those of *L. monocytogenes* harbouring a *gfp* expression vector, growth rates were seen to be significantly reduced when cells expressed the dual reporter. These data suggests that of the two reporter genes it is *lux* that places the increased energy drain upon cells expressing the proteins. This is not unexpected as one of the substrates for bioluminescence is reduced flavin mononucleotide (FMNH₂) which is provided from the bacterium's electron transport chain.

The Lux proteins are not expressed throughout exponential phase, Lux proteins are expressed to approximately mid-exponential phase and then rapidly decrease. It can be noticed from the data that the larger the plasmid that the cells contain, the slower the initial growth of the bacteria, thus the longer the delay until Lux proteins are expressed within the cells. Although bioluminescence does place a significant energy drain upon bacteria expressing *lux* due to the requirement for FMNH₂, this alone cannot be responsible for the initial observed decrease in bacterial growth rate, as at this point only low levels of bioluminescence are perceived. It is apparent that some other factor contributes to this noticeable decrease in the initial growth rate of cells expressing both reporter genes.

As previously stated, the size of DNA inserted into the original cloning vector can cause the production of HMW DNA within the cells. This in turn appears to affect the initial growth rate of the bacteria, when they are actively dividing and replicating DNA within them. As the decrease in the initial growth rate is much more apparent from *L. monocytogenes* expressing both reporter genes, this suggests that a limit has been reached whereby DNA can be effectively replicated within the cells without placing a significant metabolic load upon cells harbouring them. This will be discussed further in Chapter 8.

Figure 6.3.1: Growth and bioluminescence of *L. monocytogenes* (pSE2027) c.f. *L. monocytogenes* (pSE2030)

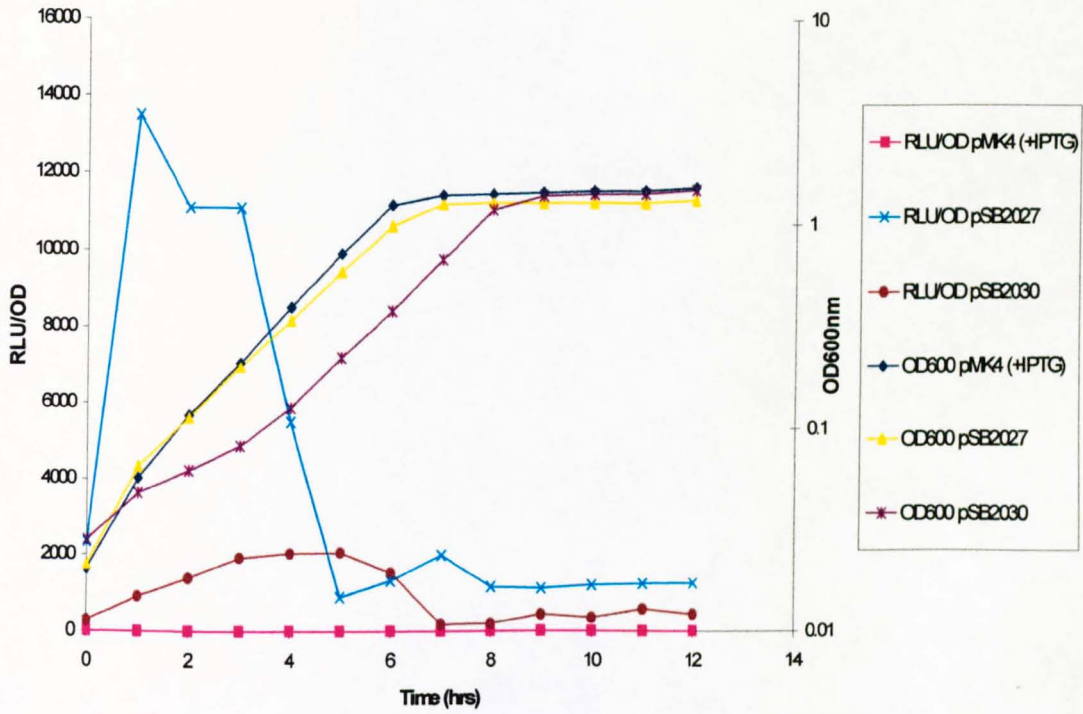
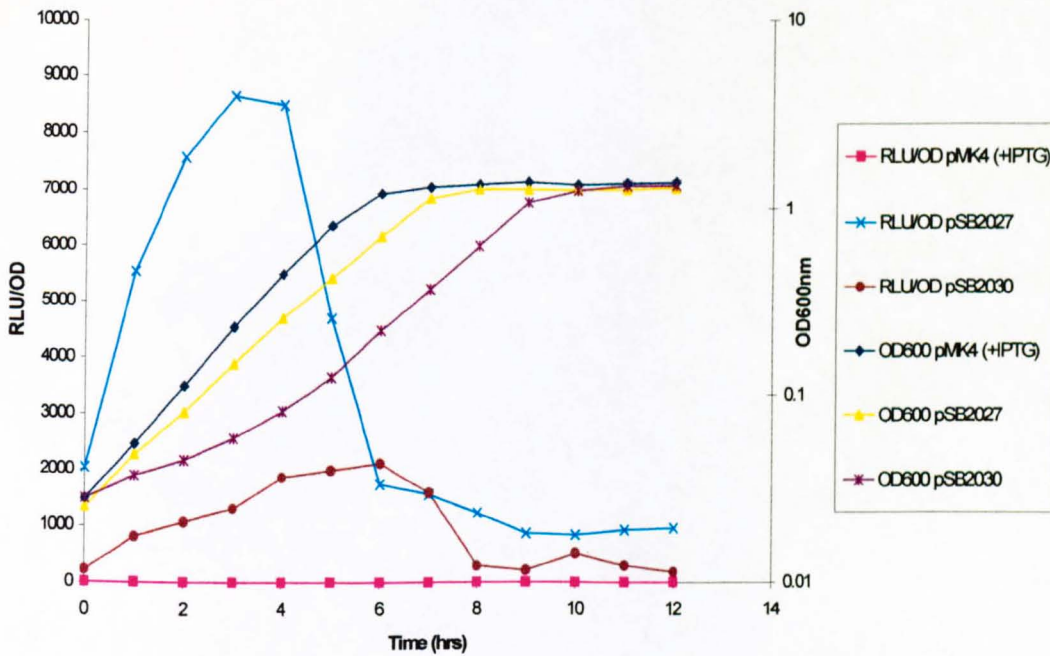


Figure 6.3.2: Growth and bioluminescence of *L. monocytogenes* (pSE2027) c.f. *L. monocytogenes* (pSE2030)



6.4. Discussion

A dual *gfp3-luxABCDE* reporter has been constructed and placed on a shuttle vector downstream of P_{xylA} . The promoter had been cloned in such a way as to remove the *xylR* repressor gene, thus removing the need for xylose to be present to de-repress the promoter in order to obtain gene expression.

The dual expression vector (pSB2030) has been shown to confer both luminescence and fluorescence on different Gram positive bacteria, these being *L. monocytogenes* and *S. aureus*. All recombinant colonies were highly bioluminescent, although levels obtained did not appear to be as high as when the reconstructed *lux* operon was expressed from a similar plasmid (pSB2027) without *gfp*. Upon examination by fluorescence microscopy, individual cells from recombinant bioluminescent colonies were also seen to fluoresce under blue light excitation due to the expression of *gfp3opt*. All individual cells were seen to have a fluorescent phenotype.

Experiments examining the growth and fluorescence of *L. monocytogenes* (pSB2030) compared with *L. monocytogenes* (pSB2019) showed that the dual reporter appeared to have a lower rate of exponential growth and was also approximately five times less fluorescent than cells expressing *gfp3opt* on its own. This suggests that *L. monocytogenes* producing GFP have less energy drain placed upon them than cells expressing the five Lux proteins along with GFP. When the growth rate of *L. monocytogenes* (pSB2030) was compared with *L. monocytogenes* (pSB2027) the difference in the rate of exponential growth was not significantly different, however in this case the cells are producing around the same number of different proteins (five and six respectively). When bioluminescence was examined, cells harbouring the dual reporter construct showed lower luminescence levels (about five-fold) than cells expressing Lux proteins from pSB2027.

As well as the lower output generated by *L. monocytogenes* (pSB2030), cells harbouring the dual reporter had a slower initial growth rate compared to that of the single reporters. This decrease in growth rate cannot be entirely attributed to bioluminescence, as at this point cells do not show a highly luminescent phenotype, bioluminescence does not peak until mid-exponential phase, therefore there is no large demand placed upon the cells for FMNH₂ early in the growth cycle. One factor suggested to be responsible for this initial decreased growth rate is plasmid size, which places an increased metabolic load upon cells harbouring the expression vectors. It appears as though the larger the plasmid, the slower the growth of the bacteria initially, this may be due to the production of HMW DNA which can form when heterologous DNA inserts into the plasmid (Gruss and Ehrlich, 1988). As previously mentioned this will be discussed at greater length in Chapter 8

To assess the merits of each reporter gene the RFU/OD and RLU/OD, obtained when both *lux* and *gfp3opt* were expressed in *L. monocytogenes* from pSB2030, were plotted arithmetically as a function of time. A representation of the data obtained is illustrated in Figure 6.4.1 and 6.4.2.

From this data it can be seen that Lux proteins reach a peak level within the cell approximately 5 hours into the growth period, whereas GFP levels do not begin to plateau until a further 6 hours after this, approximately 11 hours into growth. This suggests that the generation of functional Lux proteins is much quicker than formation of fluorescent GFP. Lux is also amplified enzymatically within the cell, whereas GFP is not and the fluorescence signal in a particular cell, therefore, depends largely on two broad parameters: the rate of synthesis of functional protein and, because GFP is very stable, the rate of dilution as the cells divide. So, although it takes around 11 hours for a significant fluorescent signal to be generated, this is not all due to the time taken for the chromophore to fold, rather a combination of factors including growth rates of the bacterium and dilution rates of the protein.

This data confirms that GFP cannot be used to monitor rapid changes in gene expression due to the time needed for a fluorescent signal of sufficient intensity to be generated. In order to monitor gene induction and expression *lux* would appear to be the reporter of choice, as the signal is generated much more rapidly within the cell compared to that of *gfp3opt*. Due to their apparent instability within the cell, the Lux proteins would also reflect down-regulation of the gene of interest was occurring, as shown by a decrease in luminescent output. However, due to the stability of GFP, this makes it the reporter of choice for monitoring bacterial progression and accumulation within cells, for example during infection (Kinsman, 1986). It also enables the precise location of individual bacterial cells to be established.

The data gathered shows that although these two reporters are very different in their action, both have their own merits which makes this dual expression vector a powerful tool for gene expression studies *in vivo* and bacterial localisation experiments. These reporters as they stand could be used for *in vivo* tracking experiments. The experiments of Contag *et al.* (1995) allowed bacterial movement to be viewed non-invasively within the living animal during the course of infection. *Lux* reporters permit the monitoring of gene expression over time, as the short half-life of the luciferases guarantees that the photon emission observed represents the gene of interest. These points suggest that in theory the activity of any gene fusion to *lux* could be examined in live animal tissues. During an infection process the bioluminescent marker of the dual reporter would provide data on the growth and spread of constitutively luminescent bacteria as well as providing about the temporal and spatial induction of particular genes, whereas expression of *gfp3* provides an excellent positional marker, allowing the precise location of the organism to be determined.

Figure 6.4.1: Comparison of bioluminescence and fluorescence of *L. monocytogenes* (pSB2030)

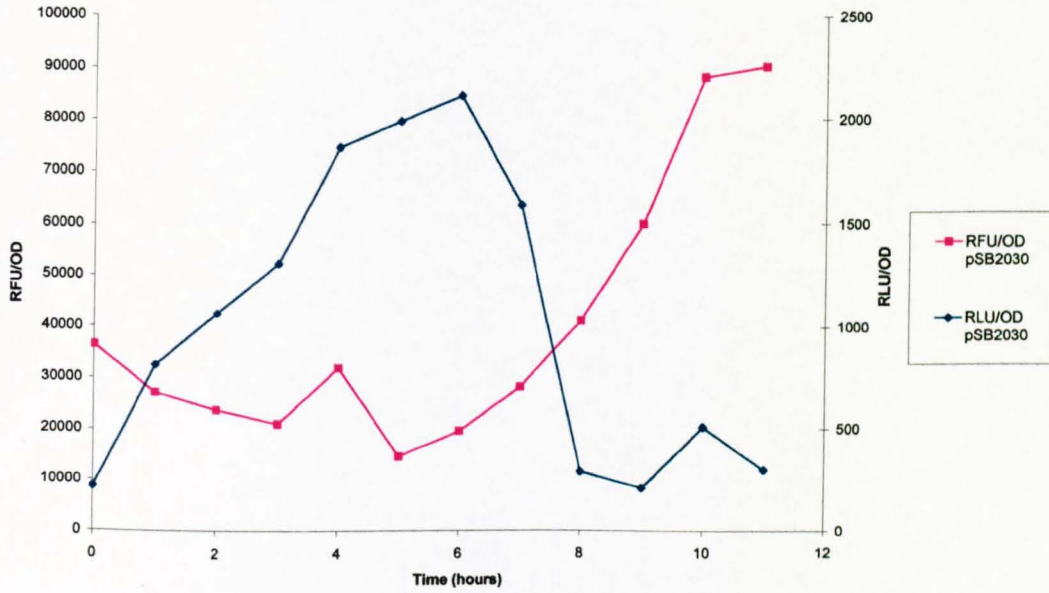
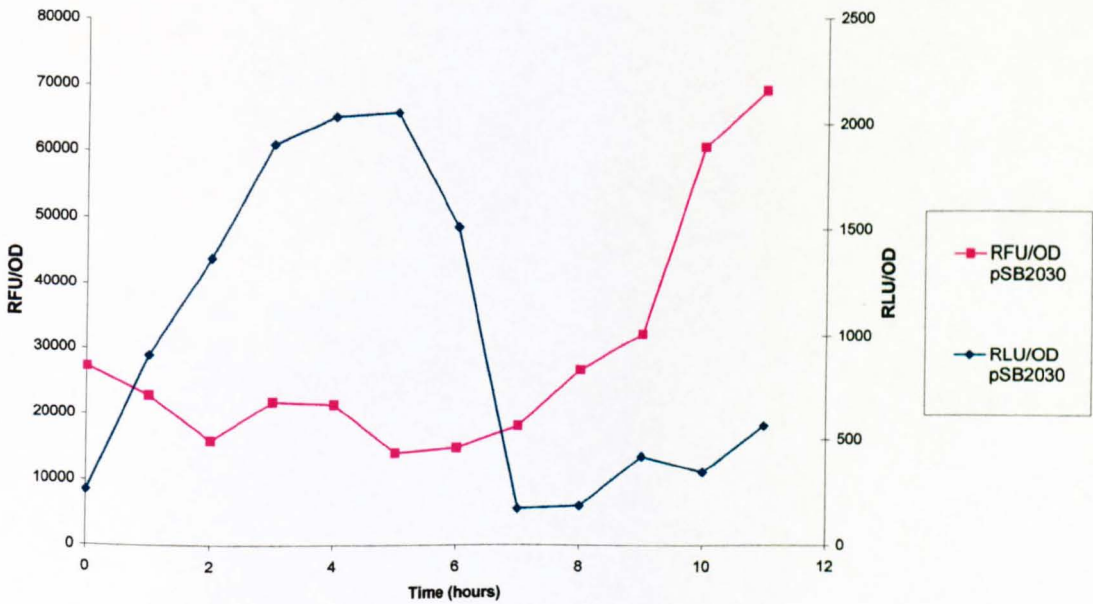


Figure 6.4.2: Comparison of bioluminescence and fluorescence of *L. monocytogenes* (pSB2030)



CHAPTER 7

CONSTRUCTION, EVALUATION AND USE OF REPORTER SYSTEMS FOR THE *AGR* P3 PROMOTER SYSTEM OF *STAPHYLOCOCCUS AUREUS*

CHAPTER 7: CONSTRUCTION, EVALUATION AND USE OF REPORTER SYSTEMS FOR THE *AGR* P3 PROMOTER SYSTEM OF *STAPHYLOCOCCUS AUREUS*

This work was carried out with the technical assistance of Mr Neil Dickinson and Miss Emillie Council.

The *agr* regulatory locus controls a range of *S. aureus* extracellular virulence factors. In order to derive a better understanding of the *agr* virulence system of *S. aureus*, a variety of reporter systems for the *agr* P3 promoter were constructed. The *agr* locus is composed of two divergent transcripts, RNAII and RNAIII, controlled by the P2 and P3 promoters respectively. RNAIII is the effector molecule of the *agr* regulon, and it is this that is responsible for the virulence phenotype exhibited by *S. aureus*. The regulation of the virulence phenotype is controlled in a cell-density dependent manner and has been previously discussed in the Introduction, Section 1.4.

7.1. Construction of a *gfp* reporter for the *agr* P3 promoter of *S. aureus*

Previous work led to the surmise that the native *gfp3* gene was transcribed efficiently in Gram positive bacteria, but translation within the cells was limited, illustrated by the fact that only a small proportion of the bacteria were seen to fluoresce when examined by fluorescence microscopy. In order to enhance translation, a strong Shine-Dalgarno sequence was incorporated upstream of the initiation codon *via* PCR as described by Vellanoweth (1993). This led to recombinant *S. aureus* and *L. monocytogenes* cells where the majority of the population exhibited a fluorescent phenotype upon examination by fluorescence microscopy.

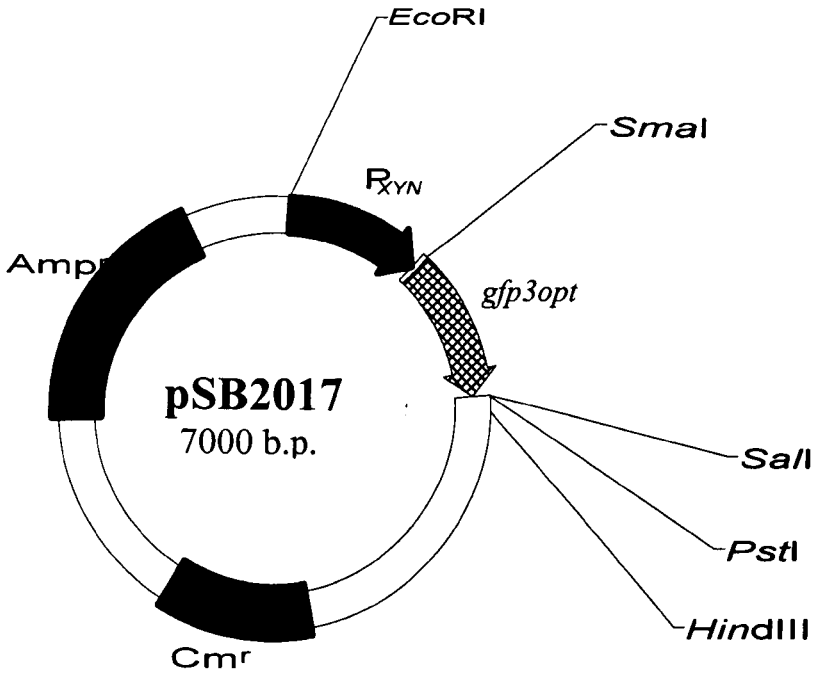
In order to clone the P3 promoter, PCR primers were used to amplify the promoter and generate restriction sites at both the 5' and 3' ends of the sequence in order to

allow directional cloning. At the 5' end an *EcoRI* site was introduced, with a *SmaI* site being incorporated at the 3' end, these were designated primers 20 and 21 respectively. Details of the primers are given in Appendix 1.

These PCR primers were used in a 30-cycle PCR to amplify the nucleotide sequence of the intergenic regulatory region between the two-*agr* promoters. The PCR reaction was performed essentially as described in the Material and Methods, Section 2.5.3 using *S. aureus* 8325-4 cells as template DNA. Incorporated into the reaction was an annealing period of 1 minute at 52°C and a 1 minute period of DNA extension at 72°C. The resulting PCR products were analysed by agarose gel electrophoresis, which confirmed the presence of a band of approximately 200bp which was assumed to be P3. This P3 promoter fragment was purified by freeze thaw purification from a low melting point agarose gel, subsequently restricted with *EcoRI* and *SmaI* in order to generate cohesive ends on each end of the fragment, following restriction the DNA was purified further by phenol chloroform extraction. In order to clone this promoter fragment, it was decided to use an existing *gfp* expression vector, the one that was chosen was pSB2017, which contains *gfp3opt* downstream of P_{*xyn*}; this is illustrated in Figure 7.1.1. This plasmid pSB2017 was also restricted with *EcoRI* and *SmaI* to excise P_{*xyn*}, the restricted DNA then purified from a low melting point agarose gel. The two purified DNA fragments were ligated together, and used to transform *E. coli* JM109 competent cells by electroporation. Recombinant colonies were isolated following selection on ampicillin selective agar.

As one promoter had been exchanged for another, it was impossible to determine from phenotypic analysis if any of the recombinant colonies contained the new clone. DNA was prepared from the recombinant colonies by plasmid miniprep, this was then restricted with *EcoRI* and *SmaI*. The restricted DNA was analysed by agarose gel electrophoresis and some of the samples showed the presence of a band of approximately 200bp in length, this was assumed to be the P3 promoter as P_{*xyn*} is much bigger at 800bp. However, examination of recombinant colonies containing this putative new *gfp* expression vector by fluorescence microscopy revealed that the bacterial population was non-fluorescent.

Figure 7.1.1: Restriction Map of pSB2017



In order to confirm that these cells did contain P3 upstream of *gfp3opt*, PCR analysis was performed. The reaction was carried out as described earlier, using the 5' forward primer to P3 and the *gfp* reverse sequencing primer, these are primers 20 and 7 respectively and are given in Appendix 1. The PCR products were electrophoresed on an agarose gel, in some cases a band of approximately 200bp was observed. The only way that a band of this size can be generated is if P3 has inserted into the cloning vector upstream of *gfp3opt*. The basis behind the reaction is illustrated in Figure 7.1.2. These data suggested that some of the recombinant colonies did contain the correct construct. The recombinant DNA was prepared on a large scale by plasmid maxiprep and further restriction analysis confirmed the nature of the DNA. This new *gfp* reporter of *agr* expression was designated pSB2031 and is illustrated in Figure 7.1.3.

Figure 7.1.2: Basis behind the PCR used to amplify putative DNA thought the contain the P3 promoter

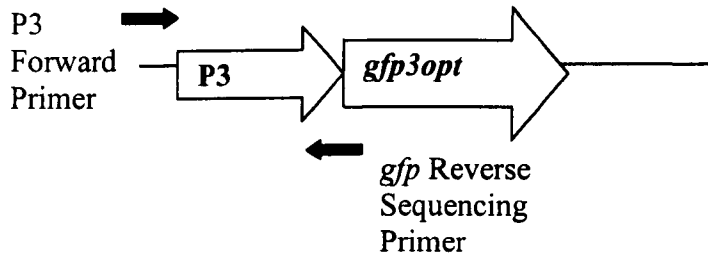
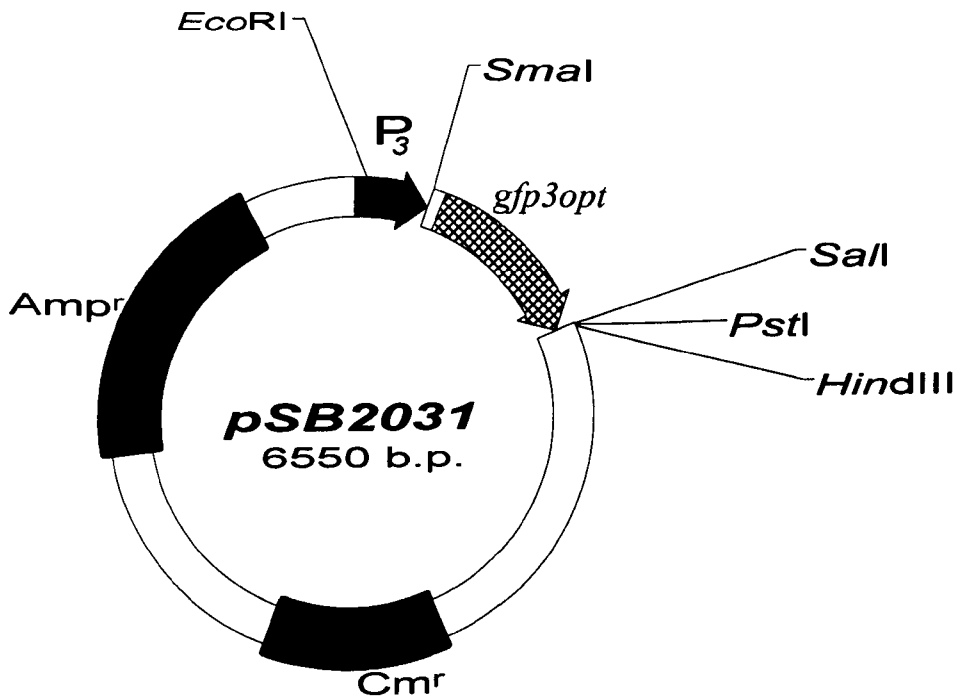


Figure 7.1.3: Restriction Map of pSB2031



It was decided to transform *S. aureus* 8325-4 with pSB2031 by electroporation of competent cells. However, attempts to introduce DNA isolated from *E. coli* were unsuccessful and no recombinant colonies were obtained. In order to overcome the restrictions of DNA methylation, pSB2031 was introduced into *S. aureus* RN4220 by electroporation of competent cells. *S. aureus* RN4220 is a transformable mutant of *S. aureus* 8325-4, this is due to the fact that it is restriction deficient. Colonies containing recombinant DNA were isolated following selection on chloramphenicol agar plates, all individual cells from a recombinant colony were seen to fluoresce following examination by fluorescence microscopy. However *S. aureus* RN4220, would be little use as a reporter of *agr* expression as it itself is an *agr* mutant, but from the recombinant cells DNA was prepared by plasmid miniprep. This DNA was then used to transform *S. aureus* 8325-4 as previously described. Cells from the resulting recombinant colonies were also shown to be fluorescent following examination by fluorescence microscopy.

7.2. *In vitro* evaluation of pSB2031 as a reporter of *agr* expression

To evaluate this system, it was first necessary to determine that P3 could be induced *in vitro* resulting in expression of *gfp3opt*. This was achieved by adding spent supernatant from *S. aureus* grown overnight to the fresh bacterial cultures and observing the expression of *gfp3opt*. It was thought that if P3 was induced through peptide signalling molecules present in the supernatant then the reporter activity would be induced earlier within the experiment and also that a greater level of fluorescence may be observed from the cells.

S. aureus 8325-4 (pSB2031) was grown overnight at 37°C in BHI broth containing chloramphenicol (BHI Cm7), following centrifugation, the spent supernatant was transferred into sterile flasks and the cells were washed twice in fresh medium to remove any autoinducer molecules present, this was then used to inoculate fresh BHI Cm7 at 1:100 dilution. The bacteria were grown for a further 1 hour period, this was then diluted 1:25 into fresh BHI Cm7 and BHI Cm7 containing supernatant at 10%

and 50%. Both optical density and fluorescence were measured at intervals throughout the experiment as described in Section 2.4 and 2.14 respectively. In order to take into account the effect of bacterial growth on the fluorescence values, the measured relative fluorescence was divided by the corresponding optical density (OD) measurements for each time period (RFU/OD). The RFU/OD values were plotted arithmetically as a function of time, in order to assess how the fluorescence changed relative to the growth of the bacteria the OD values were also plotted on the same graph as a function of time. Although the assay was performed when 50% of the culture supernatant was added to the bacterial cells, the bacteria in this flask flocculated. Due to this the optical density and fluorescence could not be measured accurately and the data obtained was anomalous, due to this the data is not shown on the graph. It is possible that the observed clumping was due to the production of an extracellular polysaccharide adhesin that *S. aureus* is known to produce. A representation of the data obtained is illustrated in Figure 7.2.1.

From the data several salient points can be determined. It was noticed that the optical densities from the two bacterial cultures were approximately identical although the fluorescence characteristics were markedly different, with that obtained from the culture grown in the presence of 10% supernatant being significantly higher than cells grown in unsupplemented medium. Expression of *gfp3opt* does not produce an energy drain upon the bacteria, shown by the fact that exponential rate of growth is unchanged, suggesting that increased expression of *gfp3opt* does not slow down the rate of bacterial growth.

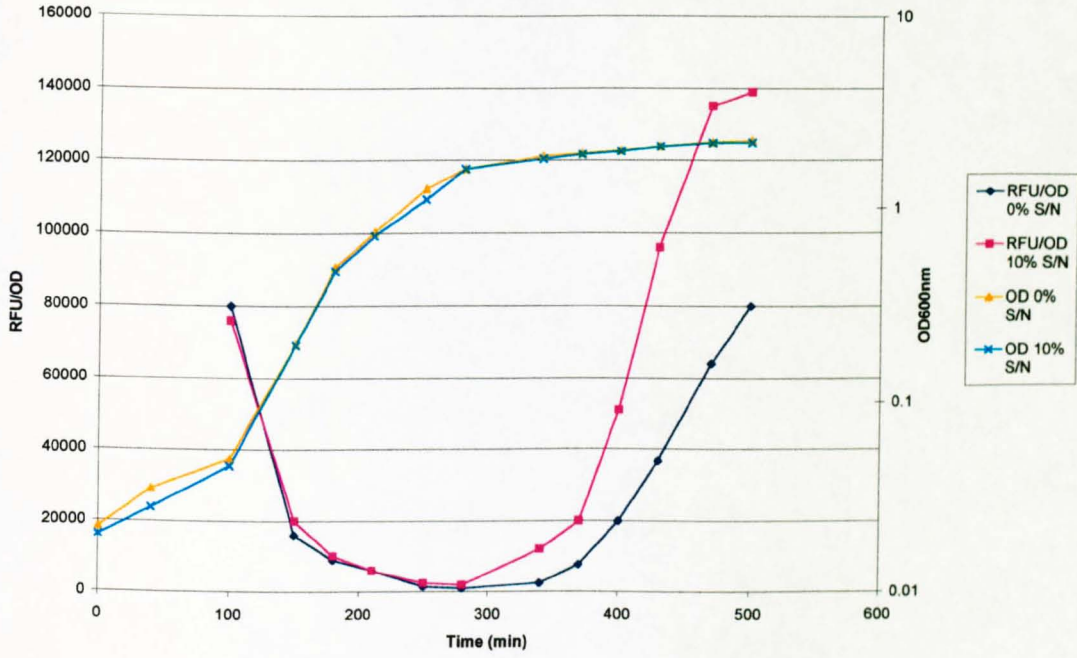
Both bacterial cultures show an initial decrease in fluorescence at the start of the experiment. This is most likely due to a combination of factors, these being a fall in residual P3 activity due to dilution of the autoinducing peptide when the cells were cycled, the rate of synthesis of functional protein, and the effect of dilution of fluorescent GFP protein as the cells divide. If only low levels of new protein are synthesised as the cells are growing and dividing, then the amount of fluorescent protein per cell will decrease. It is suggested that only low levels of GFP3 will be produced early in the growth cycle due to the fact that the autoinducer peptide

(encoded by *agrD*) is secreted at low levels due to constitutive expression of *agr*. As production of this protein is regulated in a cell density dependent manner, this means that the more cells present the more peptide is produced. As the peptide positively regulates its own production, it is not surprising that levels of GFP protein do not start to increase until cell reach the end of exponential phase.

When *S. aureus* 8325-4 (pSB2031) were grown with no added bacterial culture supernatant, levels of fluorescence were seen to increase slowly after approximately 300 minutes. The same phenomenon was seen when *S. aureus* 8325-4 (pSB2031) were grown with 10% supernatant, although the rate of increase in the fluorescence with respect to time observed (shown by a steeper gradient on the fluorescence curve) was greater than that seen when cells were grown in the absence of supernatant. This suggested that P3 was being activated to a greater extent when cells were grown with 10% supernatant, the greater the activity of the promoter the greater the increase in fluorescence output. Also when cells were grown with 10% supernatant, the overall fluorescence was around twice the level seen when cells were grown in unsupplemented BHI Cm7. This again demonstrates that the promoter was more active in these cells, shown by the increased reporter activity.

That a higher level of fluorescence was observed when cells were grown with 10% supernatant was not unexpected. It is known that *S. aureus* produced autoinducer peptide in a cell density dependent manner, thus the bacterial supernatant would contain the Group1 *agrD*-derived octapeptide-signalling molecule, thus it may be expected that GFP fluorescence would be observed earlier when cells were grown with 10% supernatant compared to the control culture, due to a more rapid activation of P3. From Figure 7.2.1 it can be seen that this is the case, with cell grown in 10% supernatant starting to show an increase in fluorescence approximately 60 minutes before the equivalent culture grown in 0% supernatant. These data together tend to confirm the hypothesis that *agr* P3 activation is under temporal control as well as being control in a density dependent manner (Chan and Foster, 1998; Cheung *et al.*, 1998; Chien *et al.*, 1998; Manna *et al.*, 1998)

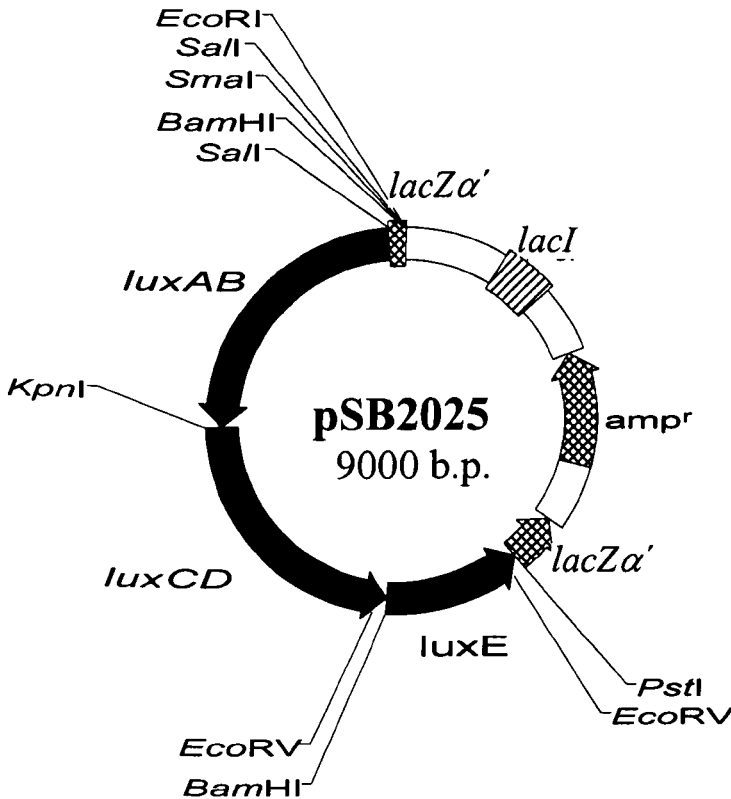
Figure 7.2.1: *In vitro* induction of the P3 promoter from *S. aureus* 8325-4 (pSB2031) through the addition of spent bacterial supernatant to the culture media



7.3. Construction of a *luxABCDE* reporter for the *agr* P3 promoter of *S. aureus*

In order to build a *lux* reporter of *agr* expression existing reporter constructs were used. These were pSB2031 (*gfp3opt* reporter of *agr* expression) which is illustrated in Section 7.1, and pSB2025 (*luxABCDE* in the superlinker plasmid pSL1190) the restriction map of which is illustrated in Figure 7.3.1.

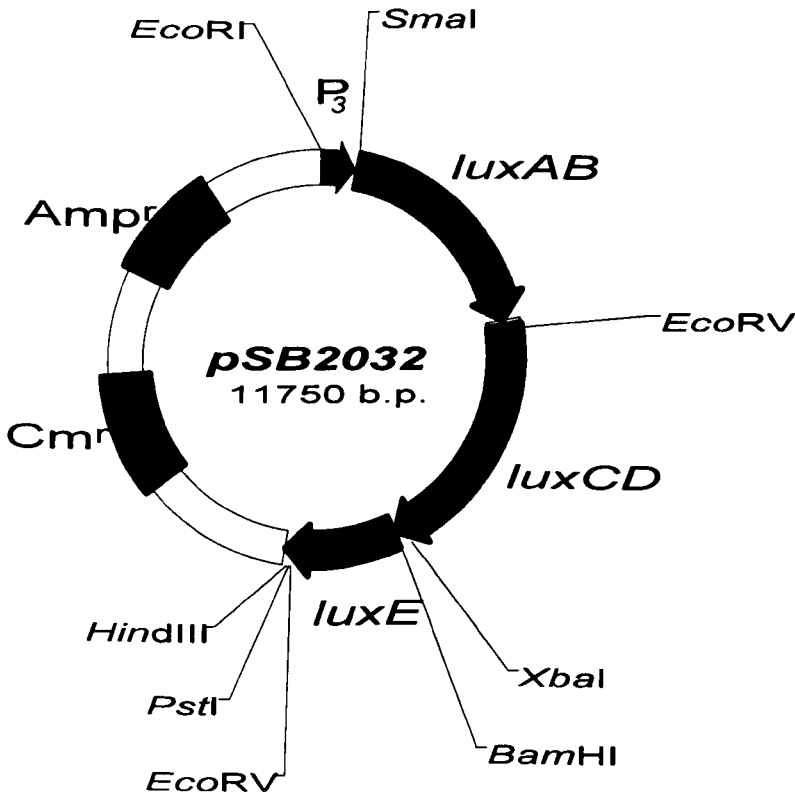
Figure 7.3.1: Restriction map of pSB2025



To perform the cloning pSB2025 was restricted with *SalI* / *PstI*, the excised *lux* fragment was then purified from a low melting point agarose gel by freeze thaw purification. The vector pSB2031 was restricted with the same enzymes to excise

gfp3opt, this DNA fragment was also purified from a low melting point agarose gel. The two DNA fragments were ligated, this was then used to transform *E. coli* JM109 competent cells. Recombinant colonies were isolated following selection on ampicillin selective agar plates, which were then screened under a Hamamatsu VIM3 camera, any recombinants that presented a bioluminescent phenotype were isolated and selected onto media containing chloramphenicol. This would confirm whether the cells contained the new *lux* expression vector as pSB2025 does not contain a chloramphenicol resistance gene, so cells harbouring this plasmid would not grow. A number of the bioluminescent recombinants were resistant to chloramphenicol. To verify that these cells contained the correct construct, PCR was performed using the recombinant cells as template DNA. The reaction was performed using the 5' forward primer designed to the P3 nucleotide sequence and the reverse primer designed to the 3' coding region of *luxB*, these were primers 20 and 13 respectively, details of which can be found in Appendix 1. So, if *luxABCDE* had been inserted downstream of P3 then a band of approximately 2.2kb should be amplified by the reaction. The 30 cycle PCR was performed essentially as described in the Materials and Methods, Section 2.5.3, it incorporated an annealing temperature of 52° for 3 minutes followed by a 3.5 minute period of DNA extension at 72°C. The products of the reaction were electrophoresed on an agarose gel which showed the presence of a band approximately 2.2kb in size, this confirmed that the recombinant DNA was correct and a new *lux* expression system had been constructed. This new plasmid, illustrated in Figure 7.3.2, was designated pSB2032 and was prepared on a large scale by plasmid maxiprep.

Figure 7.3.2: Restriction Map of pSB2032



In order to observe the *agr* expression system, this plasmid was introduced into *S. aureus* 8325-4. However, previous work had shown that DNA derived from *E. coli* could not be directly introduced into *S. aureus* 8325-4, but had to undergo DNA modification through the use of an intermediate staphylococcal species. Therefore pSB2032 was introduced into *S. aureus* RN4220 by electroporation of competent cells. Recombinant colonies were isolated by selection on agar plates containing chloramphenicol and then screened using a Hamamatsu VIM3 camera to observe the bioluminescent phenotype. DNA was prepared from bioluminescent colonies by plasmid miniprep, this was then used to transform *S. aureus* 8325-4 electrocompetent cells. Again, agar plates containing chloramphenicol were used to isolate recombinant colonies, these were screened under a Hamamatsu VIM3 camera which showed all the recombinant were bioluminescent, indicating that pSB2032 had been

introduced into the bacteria and the *lux* genes were being efficiently expressed from the plasmid.

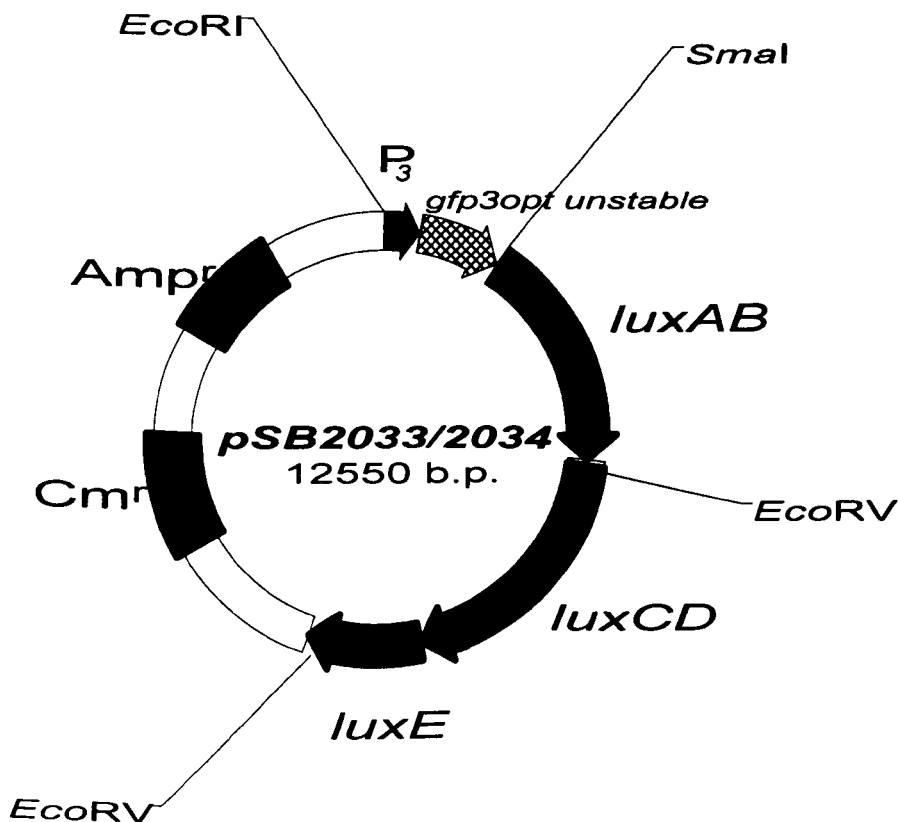
7.4. Construction of a dual reporter for the *agr* P3 promoter of *S. aureus*

In order to create a dual reporter to observe *agr* expression in *S. aureus*, rather than using the stable *gfp3* variant, it was decided to use the unstable *gfp3* variants of Anderson *et al.* (1998). It was thought that these *gfp3* variants would provide a better representation of real time gene expression within the cell, due to their unstable nature. Two unstable *gfp3* variants were chosen for this cloning, these were *gfp3* (LAA) and *gfp3* (ASV), kindly provided as pJBA41 and pJBA46 by J. Anderson. These were amplified in a 30-cycle PCR using the translationally enhanced primer designed to the 5' region of *gfp* (primer 11) and a reverse primer that was designed to a homologous area of the unstable *gfp3* variants downstream of the protease recognition sequence (primer 3), both primers incorporated restriction endonuclease recognition sequences to facilitate the cloning process, details of these primers are given in Appendix 1. The PCR reaction incorporated a 1-minute annealing period at 50°C followed by a 1-minute period of DNA extension at 72°C.

Following the amplification of the unstable *gfp3* genes by PCR, the resulting PCR products were analysed by agarose gel electrophoresis. This confirmed the presence of a band of approximately 800bp, which corresponded to the known size of *gfp3*, therefore the reaction appeared to have been successful. Following purification from a low melting point agarose gel, the DNA was restricted with *Sma*I / *Sal*I, the restriction enzymes were then removed from the DNA by phenol chloroform extraction. The restricted unstable *gfp3opt* genes were then ligated with pSB2032, which had previously been restricted with the same endonucleases and subsequently purified from a low melting point agarose gel. The ligated DNA was used to transform *E. coli* JM109 competent cells by electroporation and recombinant colonies were isolated by selection on ampicillin agar plates. The resulting recombinants were screened under blue light excitation and also under a Hamamatsu

VIM3 camera to identify positive clones, some colonies were found to be luminescent, but colonies were not observed to be fluorescent. However, this was expected as when the stable *gfp3* variant was placed downstream of P3 recombinant *E. coli* colonies did not fluoresce, this is probably due to poor activation of this promoter in *E. coli* and also due to the fact that there is no signal amplification from *gfp* as there is with *lux*. DNA was prepared from these luminescent colonies by plasmid miniprep and subsequently restricted with *EcoRI* and *SmaI*. The restricted DNA was analysed by agarose gel electrophoresis and in some cases a band of around 1.1kb was isolated, which corresponds to the P3- *gfp3opt* unstable fragment, the validity of the constructs was confirmed by further restriction mapping. The resulting constructs were designated pSB2033 (*gfp3opt* LAA) and pSB2034 (*gfp3opt* ASV) and are illustrated in Figure 7.4.1.

Figure 7.4.1: Restriction map of pSB2033 and pSB2034



Having verified that pSB2033 and pSB2034 were correct by restriction mapping, DNA was prepared on a larger scale by plasmid maxiprep. This was then introduced into *S. aureus* RN4220 by electroporation of competent cells. The resulting recombinant colonies were screened under a Hamamatsu VIM3 camera to determine whether the cells contained the recombinant DNA. Having isolated bioluminescent colonies, DNA was prepared from these by plasmid miniprep, this was then used to transform electrocompetent *S. aureus* 8325-4. Once more recombinant colonies were screened under a Hamamatsu VIM3 camera to establish whether cells contained the recombinant DNA. Those colonies found to be bioluminescent were also examined by fluorescence microscopy. *S. aureus* 8325-4 (pSB2033) were noticeably less fluorescent than *S. aureus* 8325-4 (pSB2034), this was not unexpected as Anderson *et al.* (1998) reported *gfp3* LAA to have a shorter half-life than *gfp3* ASV, 30 and 60 minutes respectively.

7.5. *In vitro* Evaluation of pSB2033 and pSB2034 as a reporter of *agr* expression through the use of bacterial supernatant and *lux* expression

7.5.1. Monitoring *luxABCDE* expression upon induction of P3

In order to confirm that the *agr* system could be induced by exogenous peptide signalling molecules, similar experiments were performed as previously described in Section 7.2. *S. aureus* 8325-4 (pSB2033) and *S. aureus* 8325-4 (pSB2034) were grown overnight in BM Cm7 and the supernatant harvested following centrifugation. The cells were washed twice, diluted 1:100 into BM Cm7, grown for a further 1 hour at 37°C and then subcultured at a 1:100 dilution into fresh BM Cm7 containing the spent supernatant at a final concentration of 0%, 10% or 50%. The diluted bacterial cultures were then loaded into a 96-well microtitre plate (200µl per well) and bioluminescence and optical density measurements taken over a 24-hour period at 37°C in an Anthos Lucy-1 photoluminometer. As a control, equivalent measurements were made on un-inoculated media, but the luminescence output was found to be negligible.

In order to take into account the effect of bacterial growth upon the bioluminescence readings, the RLU values obtained were divided by the corresponding relative OD values, to generate RLU/OD. The RLU/OD was then plotted arithmetically as a function of time in order to compare the bioluminescent output from each culture. Also, to compare luminescent output to the growth of the bacteria, the RLU/OD and relative OD values were plotted on the same graph as a function of time. The data obtained from *S. aureus* 8325-4 (pSB2033) and *S. aureus* 8325-4 (pSB2034) is illustrated in Figures 7.5.1.1 and 7.5.1.2 and Figures 7.5.1.3 and 7.5.1.4 respectively.

Measurements made in this experiment provide data on the levels of luminescence and thus the level of activation of P3 and generation of RNAIII transcript at any one time within the growth experiment. With both plasmid-containing cultures the same

general trends were seen, the most evident being that when 10% supernatant was added to the bacterial culture the cells showed a much higher level of bioluminescence compared to cells that were grown in the absence of added culture supernatant. The luminescence was seen to be induced and reach a maximal level when the bacteria were in stationary phase, this reflects the cell-density dependent activation of P3 through the expression of *agr*. Having peaked, the levels of luminescence decrease fairly rapidly. This is most likely due to a lack of energy within the *S. aureus* which are now reaching the end of their growth cycle, as the cells are no longer dividing and actively respiring. This lack of energy means the bacteria cannot obtain FMNH₂ from their own electron transport chain to drive the bioluminescence reaction. When no supernatant was added to the bacterial cultures, although levels attained were much lower than when 10% supernatant was added to the bacterial cultures, luminescence was increased during stationary phase of growth, this corresponds with the auto-induced action of the *agr* locus and thus induction of P3. Upon the addition of 10% supernatant it appears as though P3 has been induced by the spent supernatant, illustrated by the fact that a 3-fold increase in luminescence is observed. The rate of increase in fluorescence with respect to time is also greater than that seen when no supernatant was added. These results can be explained by the presence of the autoinducing peptide-signalling molecule in the culture supernatant encoded by *agrD*. Due to the fact that the peptides are at a higher concentration when the bacteria are grown with 50% supernatant, it is somewhat surprising that the bacteria only showed a low luminescent output. This may be explained by a lack of nutrients in the media, therefore if the bacteria were not actively growing and respiring there will be less FMNH₂ from which energy can be derived to drive the bioluminescence reaction. This, coupled with the fact that the experiment was performed in a very small volume to surface ratio (low O₂ concentration) may explain why the luminescence was low.

Figure 7.5.1.1: *S. aureus* 8325-4 (pSB2033) grown in the presence of different concentration of spent bacterial supernatant (data represents RFU/OD vs time)

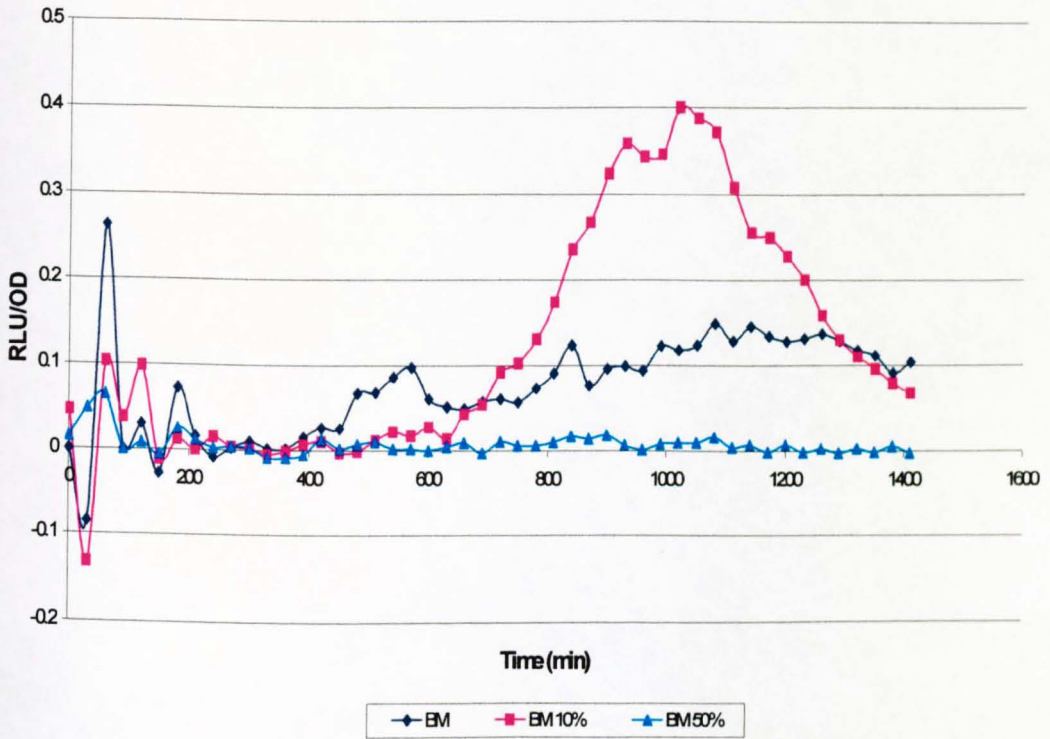


Figure 7.5.1.2: *S. aureus* 8325-4 (pSB2033) grown in the presence of different concentration of spent bacterial supernatant (data represents RFU/OD and OD vs time)

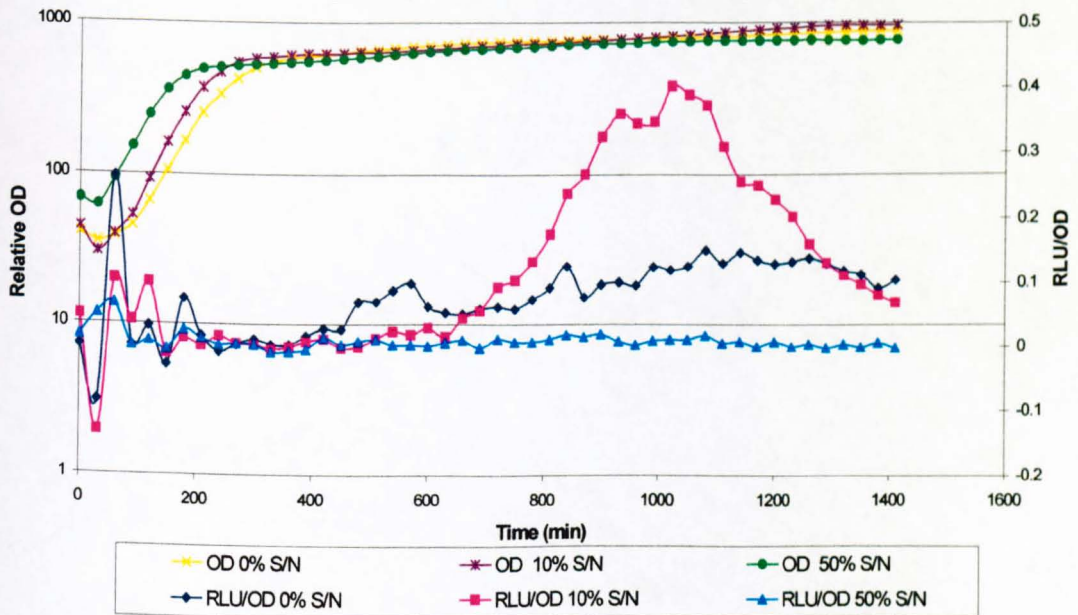


Figure 7.5.1.3: *S. aureus* 8325-4 (pSB2034) grown in the presence of different concentrations of spent bacterial supernatant (data represents RLU/OD vs time)

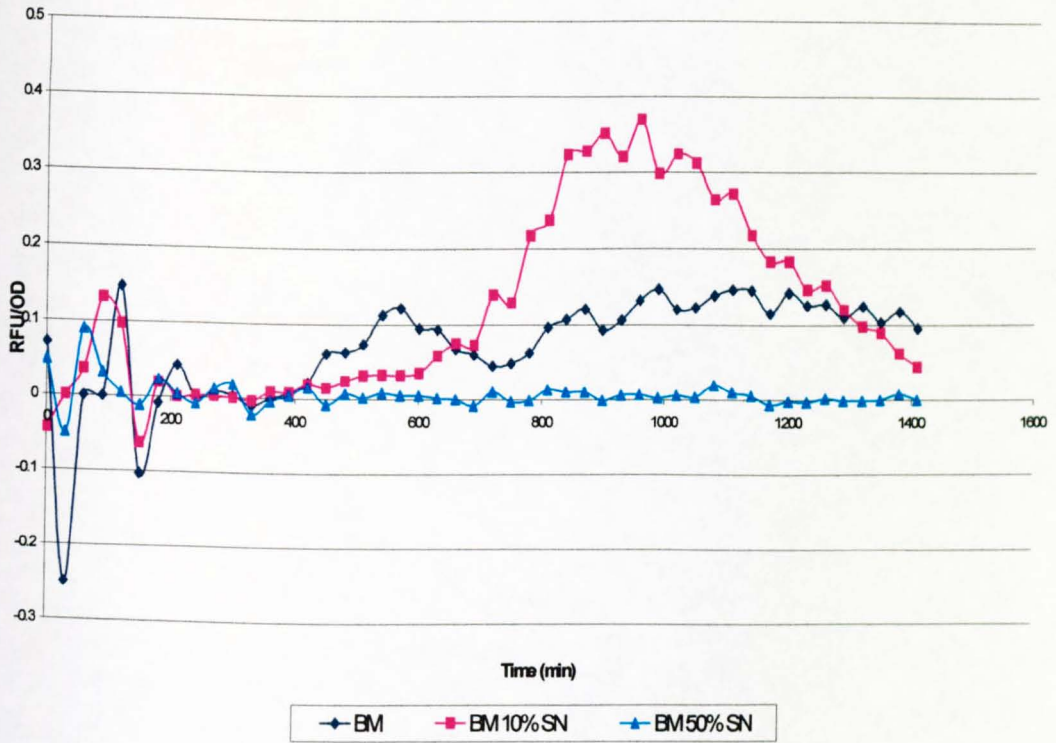
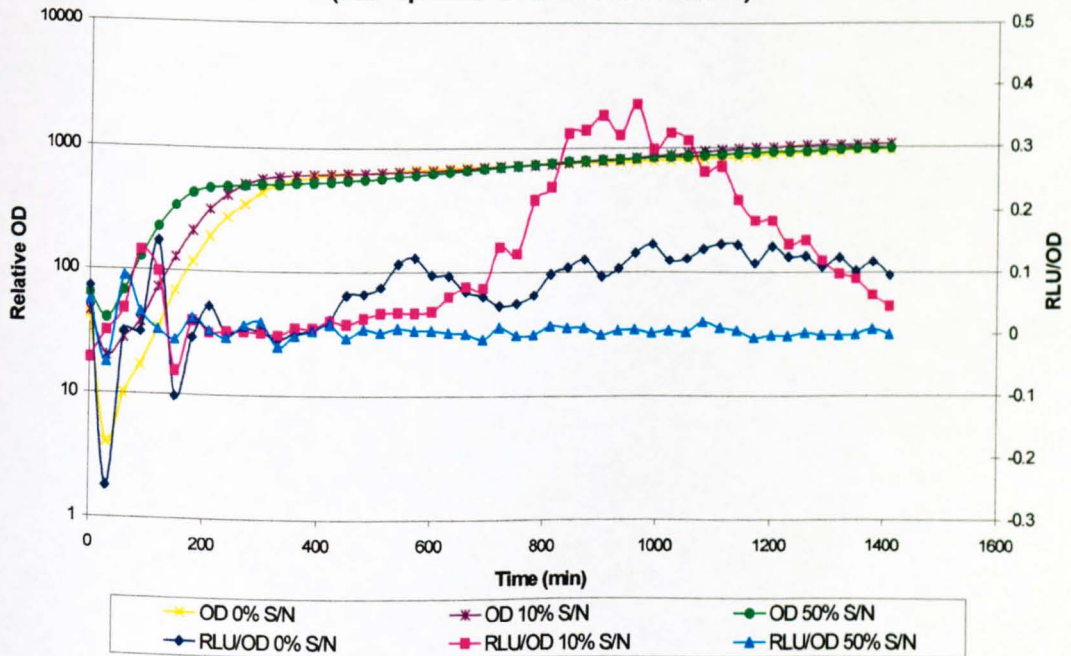


Figure 7.5.1.4: *S. aureus* 8325-4 (pSB2034) grown in the presence of different concentrations of spent bacterial supernatant (data represents RLU/OD and OD vs time)



7.5.2. Monitoring *luxABCDE* and *gfp3opt* expression upon induction of P3

When *S. aureus* 8325-4 (pSB2033) were examined by fluorescence microscopy, the cells were seen to fluoresce with a very weak intensity compared to *S. aureus* 8325-4 (pSB2034). This is most likely due to the fact the *gfp3opt* LAA which is expressed from pSB2033 has been reported to have a shorter half-life than cells expressing *gfp3opt* ASV from pSB2034 (Anderson *et al.*, 1998). For this reason it was determined that this *gfp3* variant (*gfp3opt* LAA) would be a better reporter of gene expression, thus the fluorescent and luminescent properties of *S. aureus* 8325-4 (pSB2033) were investigated upon addition of spent bacterial supernatant.

An overnight culture of *S. aureus* 8325-4 (pSB2033) was washed and subcultured into fresh BM Cm7 at a 1:20 dilution. Following a further 1 hour period of growth at 37°C, this was diluted 1:25 into BM Cm7 containing 0%, 10% or 50% of the spent supernatant from the original overnight culture. At measured intervals three sets of data were gathered as described in Section 2.4, 2.13 and 2.14 which correspond to optical density (OD), relative luminescence (RLU) and relative fluorescence (RFU) respectively. Both the RLU and RFU were divided by OD to take into account the effect of bacterial growth on reporter activity. The RLU/OD and RFU/OD were plotted arithmetically on separate graphs as a function of time, and is illustrated in Figures 7.5.2.1 and 7.5.2.2, additionally to compare the output from the two different reporter genes, both sets of data have been plotted on one graph again as a function of time and this is represented in Figure 7.5.2.3.

From the data represented, the two reporters appear to show the same pattern of induction of P3, although that observed from monitoring *gfp3opt* LAA expression is delayed by approximately 100 minutes compared to expression of *lux*. This delay in the production of fluorescent GFP is most likely due to the period required for the chromophore to fold and form fluorescent protein.

One notable point derived from the data is that 50% added supernatant generates the highest output from the reporter genes and thus indicates the highest level of P3 activation. This is not surprising as in 50% supernatant there is more autoinducing peptide, thus more signal with which P3 can be activated. In all cases the maximum reporter activity is reached when cells are in stationary phase, this reflects the cell density dependent activation of P3 through the accumulation of autoinducing peptide. However, the fact that the greatest signal was generated when 50% supernatant was added to the culture medium is different to that observed in Section 7.5.1 when the luminescence from cells harbouring these expression vectors was determined in the Anthos Lucy-1 photoluminometer, and 50% supernatant was found to give poor induction of *lux*. This is most likely due to the different culture conditions used in this experiment, with cells being grown in a larger surface area to volume ratio and also with constant aeration.

When the luminescent output is examined it can be seen that when cells are grown with 50% supernatant the maximum output is attained when cells have stopped exponential growth at approximately 475 minutes and after this levels of luminescence rapidly decrease. This decrease in bioluminescence may be energy related. As cells are no longer growing exponentially, they may not be generating large amounts of FMNH₂, which is one of the substrates necessary for the bioluminescent process. Another possibility for the decrease in the luminescent output may be due to deactivation of the P3 promoter, this in turn would result in no new Lux proteins being generated and therefore this decrease in luminescence could be attributed to degradation of the existing mRNA and proteins within the bacteria. The hypothesis of promoter repression is backed by the signal generated from the unstable *gfp3opt*, which is also seen to decrease after maximum expression. As this *gfp3* is an unstable *gfp3* variant, this data suggests that the level of degradation is significantly greater than that of production. This tends to suggest that P3 is no longer active, thus resulting in a lower expression of the downstream genes, hence the lower signal generated from the reporters. If the promoter activity was maintained at a constant level, previous experiments performed with a constitutive promoter suggest that the level of GFP within the cell would remain at a constant level, with the rate of synthesis being equal to or greater than that of degradation.

Figure 7.5.2.1: Luminescence data obtained from *S. aureus* 8325-4 (pSB2033) grown in the presence of different concentrations of spent bacterial supernatant (data represents RLU/OD vs Time)

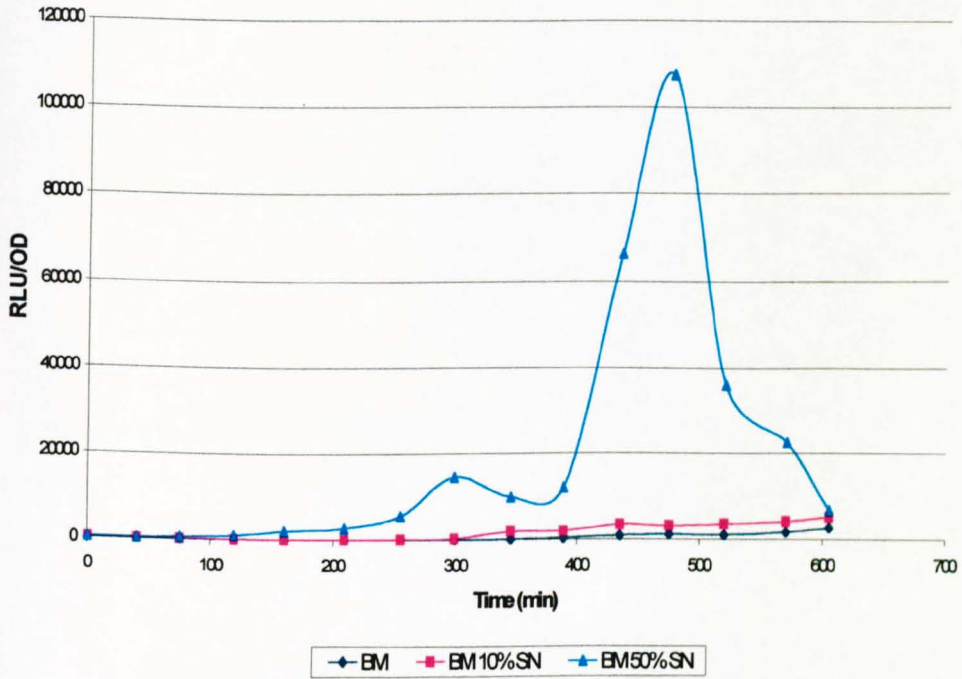


Figure 7.5.2.2: Fluorescence data obtained from *S. aureus* 8325-4 (pSB2033) grown in the presence of different concentrations of spent bacterial supernatant (data represents RFU/OD vs Time)

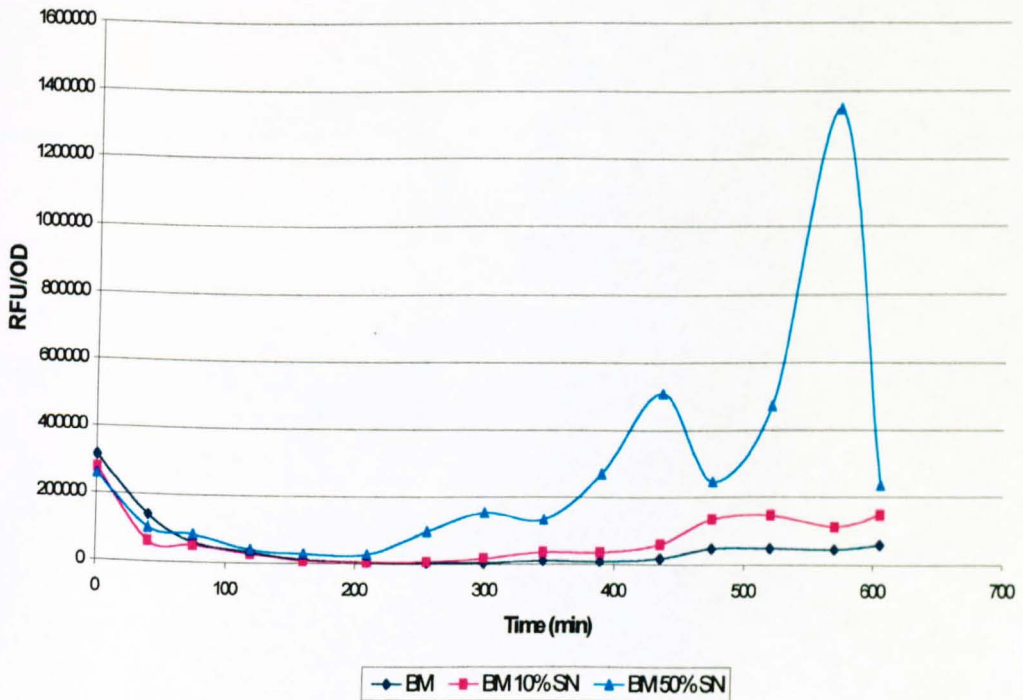
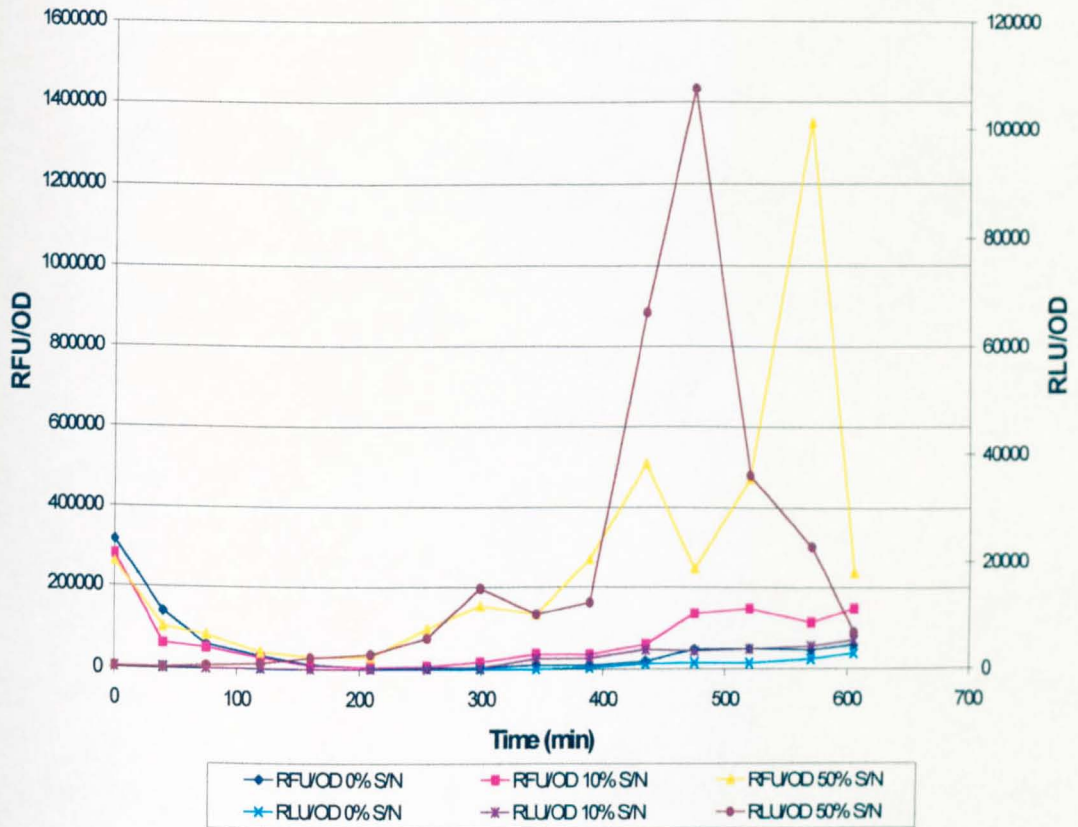


Figure 7.5.2.3: Fluorescence and luminescence data obtained from *S. aureus* 8325-4 (pSB2033) grown in the presence of different concentrations of spent bacterial supernatant (data represents RFU/OD and RLU/OD vs Time)



7.6. Use of the dual reporter of *agr* expression to evaluate potential activators and inhibitors of P3 activity

7.6.1. Determining the minimum concentration of a synthetic group-1 activator molecule required to induce P3

In order to determine that the observed induction of reporter activity was due to autoinducing peptide, the assay was repeated using a synthetic activator molecule. The synthetic P3 activator (GP1) specific to Group 1 staphylococci, was kindly provided by the department of Pharmaceutical Sciences, Nottingham. The induction of P3 by this synthetic molecule (GP1) was assayed utilising *S. aureus* 8325-4 (pSB2033) and *S. aureus* 8325-4 (pSB2034) using bioluminescence as a reporter of P3 activity.

S. aureus 8325-4 harbouring the 2 expression vectors were grown overnight at 37°C. These were washed, resuspended in 1 volume of fresh medium and diluted 1:100 into fresh BM Cm7. The cultures were grown for a further 3 hours then diluted 1:10 into fresh BM Cm7. The GP1 was then added to the diluted cells at varying concentrations and the samples loaded into a 96-well microtitre plate. The concentrations of the activator molecule used in the experiments are shown in Table 7.6.1.1. The plate was incubated for 24 hours at 37°C, shaking, in an Anthos Lucy-1 photoluminometer, with OD and bioluminescence measurements being measured every 30 minutes.

Table 7.6.1.1: Concentrations of the GP1 used to induce P3 activity from *S. aureus* 8325-4 (pSB2033) and *S. aureus* 8325-4 (pSB2034)

GP1 concentration (μM)	100	75	50	25	15	5	control
Diluted culture (μl)	181	186	190	195	197	199	200
GP1 (μl)	19	14	10	5	3	1	0

To take the effect of optical density (OD) on the bioluminescence readings (RLU), the RLU were divided by the corresponding relative OD values, which generated RLU/OD. To see how bioluminescence was altered with time, the RLU/OD were plotted arithmetically as a function of time. Also, to compare how the luminescence values changed through the growth curve with respect to time, the RLU/OD and relative OD values were plotted on the same graph as a function of time. The results of testing the efficacy of the activator molecule with *S. aureus* 8325-4 (pSB2033) and *S. aureus* 8325-4 (pSB2034) are illustrated in Figures 7.6.1.1 and 7.6.1.2 and Figures 7.6.1.3 and 7.6.1.4 respectively.

The results of the experiment shown that this synthetic activator molecule, GP1, could induce luminescence, hence P3 activation, even at concentrations as low as 5 μ M. When the plasmid containing *S. aureus* 8325-4 were grown in the presence of the activator molecule, luminescence was seen to induce after the bacteria has entered stationary phase. The luminescent signal; was observed to peak and then signal intensity was rapidly lost. It is thought that at this point, as the cells are no longer exponentially growing, little free energy would be available, thus the cell would not be able to obtain enough energy from its electron transport chain to drive the bioluminescent reaction.

The bacteria appear to show a dose response curve to the activator molecule, lower levels of the activator molecule may lead to a lower luminescent output. When no activator was added to the bacterial culture the levels of luminescence observed were comparatively low, approximately 10-fold lower than equivalent cultures where *agr* expression had been induced by the addition of activator molecule to the bacterial culture medium. These data indicated that both constructs were good reporters of autoinducer dependent P3 expression.

Figure 7.6.1.1: *S. aureus* 8325-4 (pSB2033) grown with different concentrations of a synthetic activator (data represents RLU/OD vs Time)

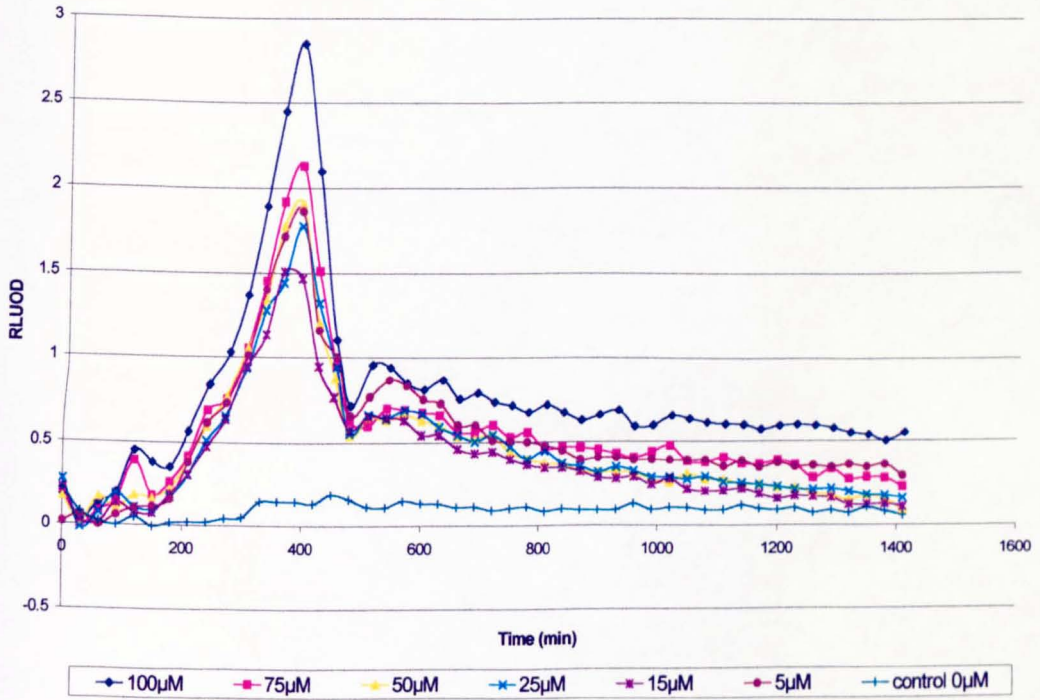


Figure 7.6.1.2: *S. aureus* 8325-4 (pSB2033) grown with different concentrations of a synthetic activator (data represents RLU/OD and OD vs Time)

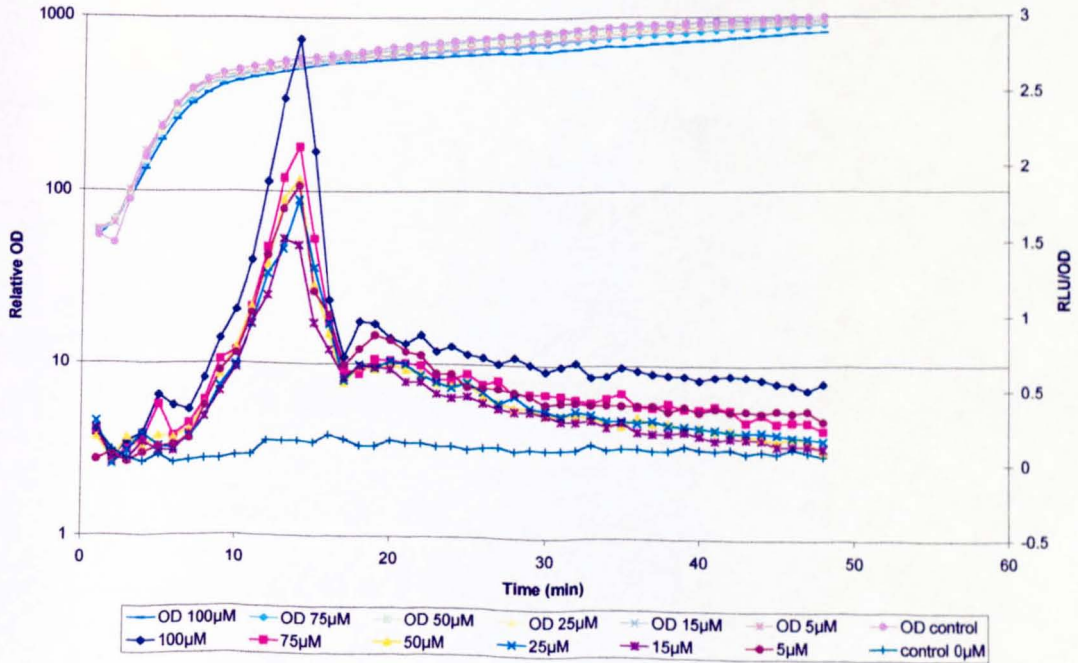


Figure 7.6.1.3: *S. aureus* 8325-4 (pSB2034) grown with different concentrations of a synthetic activator (data represents RLU/OD vs Time)

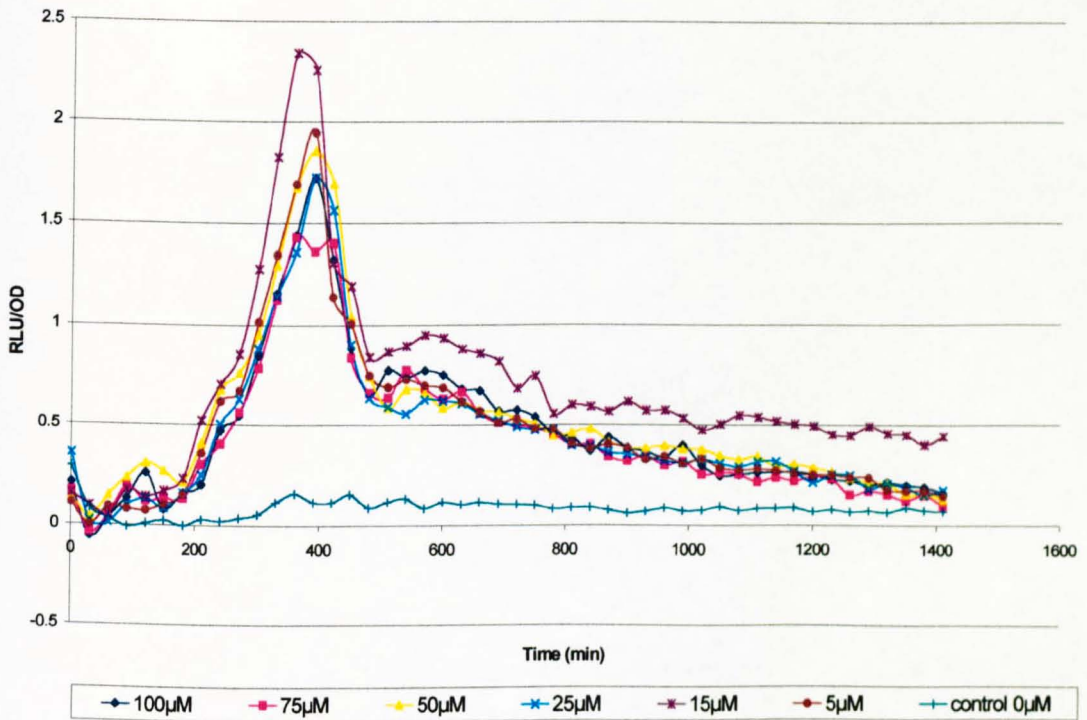
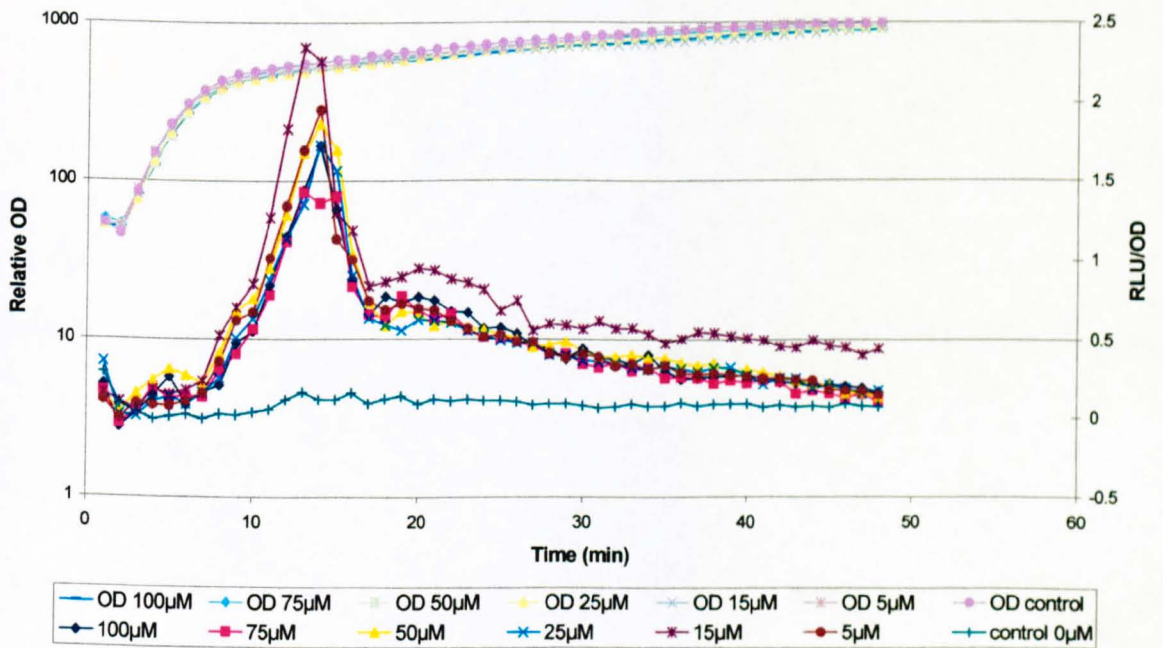


Figure 7.6.1.4: *S. aureus* 8325-4 (pSB2034) grown with different concentrations of a synthetic activator (data represents RLU/OD and OD vs Time)



7.6.2. Determining the minimum concentration of a synthetic *agr* inhibitor from *S. lugdunensis* required for inhibition of P3

Having proved that the P3 promoter could be activated, as shown by an increase in bioluminescent output from *S. aureus* 8325-4 cells harbouring either pSB2033 or pSB2034, it was decided to see if *agr* expression could be repressed through the addition of a synthetic inhibitor, kindly provided by the Department of Pharmaceutical Sciences.

S. aureus 8325-4 (pSB2033) and *S. aureus* 8325-4 (pSB3034) were grown overnight at 37°C. The bacterial cells were washed in BM and resuspended in fresh media, this was then used to inoculate fresh BM Cm7 at 1:100 dilution. After a further 3-hour period of growth, the bacterial cells were diluted 1:10 into BM Cm7 containing 10% of the overnight spent supernatant. The inhibitor was then added to the bacterial cultures at various concentrations as illustrated in Table 7.6.2.1, samples were then loaded into a microtitre plate and optical density and luminescence measured at 30 minute intervals in an Anthos Lucy-1 photoluminometer. The relative luminescence values (RLU) were divided by the corresponding relative optical density measurements (OD) to take into account the effect of bacterial growth. The RLU/OD values were then plotted arithmetically as a function of time. To determine when the reporter was expressed with respect to bacterial growth, the RLU/OD and relative OD values were also plotted on the same graph as a function of time. The data obtained from the experiments with *S. aureus* (pSB2033) and *S. aureus* (pSB2034) is illustrated in Figures 7.6.2.1 and 7.6.2.2 and Figures 7.6.2.3 and 7.6.2.4 respectively.

Table 7.6.2.1: Concentrations of the inhibitor used to repress P3 activity from *S. aureus* 8325-4 (pSB2033) and *S. aureus* 8325-4 (pSB2034)

Inhibitor concentration (μM)	100	50	10	5	1	0
Diluted culture (μl)	137.6	143.8	238	75	135	150
Inhibitor (μl)	12.4	6.2	2	75 μl of the 10 μM dilution	15 μl of the 10 μM dilution	0

The assay was performed in the presence of the natural autoinducing peptide, as previous experiments had shown that higher levels of bioluminescence were attained when the peptide was present within the supernatant. The results of these experiments showed that the synthetic inhibitor from *S. lugdunensis* was efficient *in vitro* against the natural autoinduced *agr* P3 activity. This was illustrated by the fact that when *S. aureus* 8325-4 (pSB2033) and *S. aureus* 8325-4 (pSB2034) were grown in the presence of the inhibitor molecule the level of luminescence was observed to be much lower than when no inhibitor was added to the culture medium. Levels as low as 1 μM were seen to significantly decrease the luminescent output suggesting a decrease in P3 activity. Concentrations between 5-10 μM completely inhibited the action of P3 demonstrated by the absence of a luminescent phenotype of cells harbouring the expression vectors. The response of the luminescent signal is seen to mimic that observed in a dose response experiment, with a greater dosage appearing to have a greater effect on the signal generated from the bacteria.

Figure 7.6.2.1: Utilising *S. aureus* 8325-4 (pSB2033) to determine the effective concentration of a synthetic *agr* inhibitor (data represents RLU/OD vs Time)

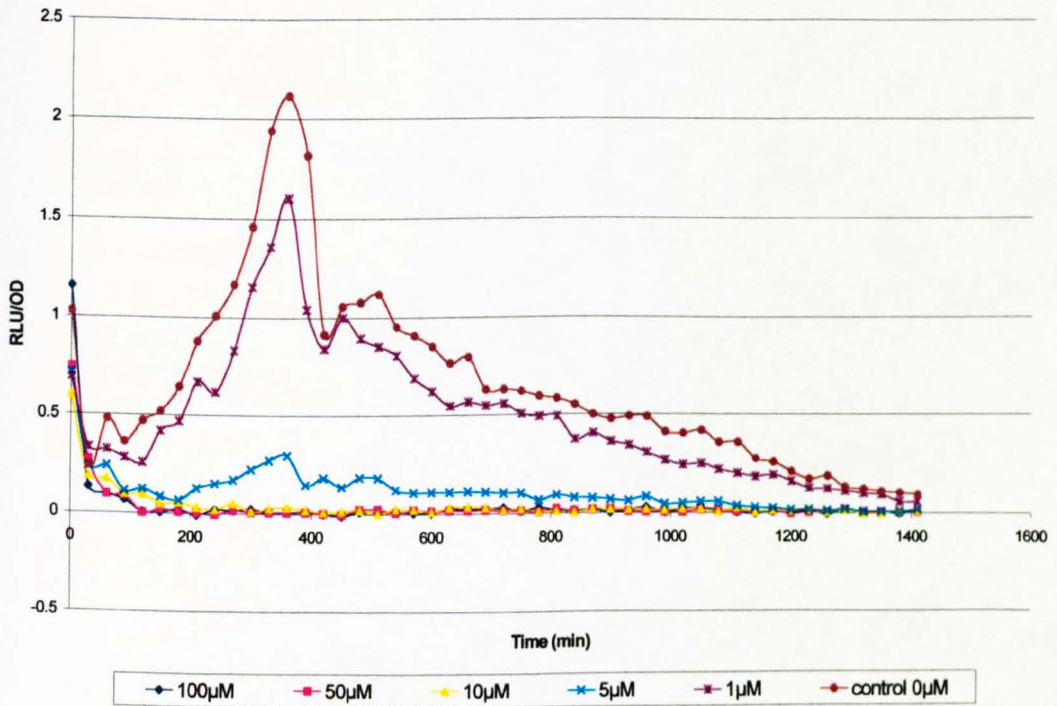


Figure 7.6.2.2: Utilising *S. aureus* 8325-4 (pSB2033) to determine the effective concentration of a synthetic *agr* inhibitor (data represents RLU/OD and OD vs Time)

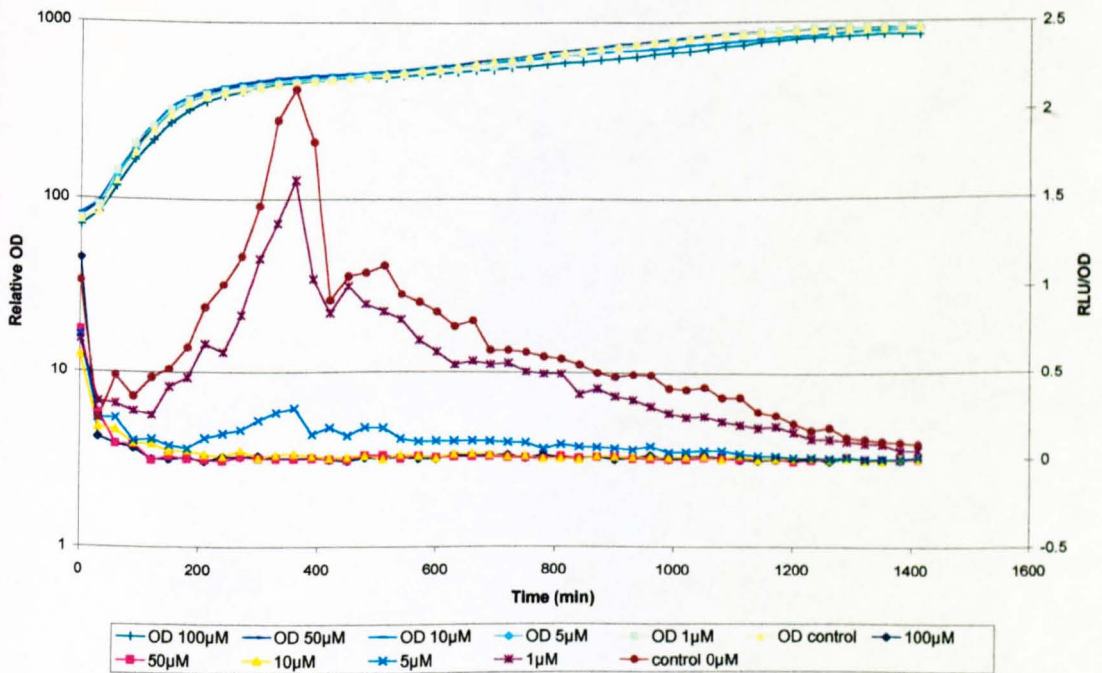


Figure 7.6.2.3: Utilising *S. aureus* 8325-4 (pSB2034) to determine the effective concentration of a synthetic agr inhibitor (data represents RLU/OD vs Time)

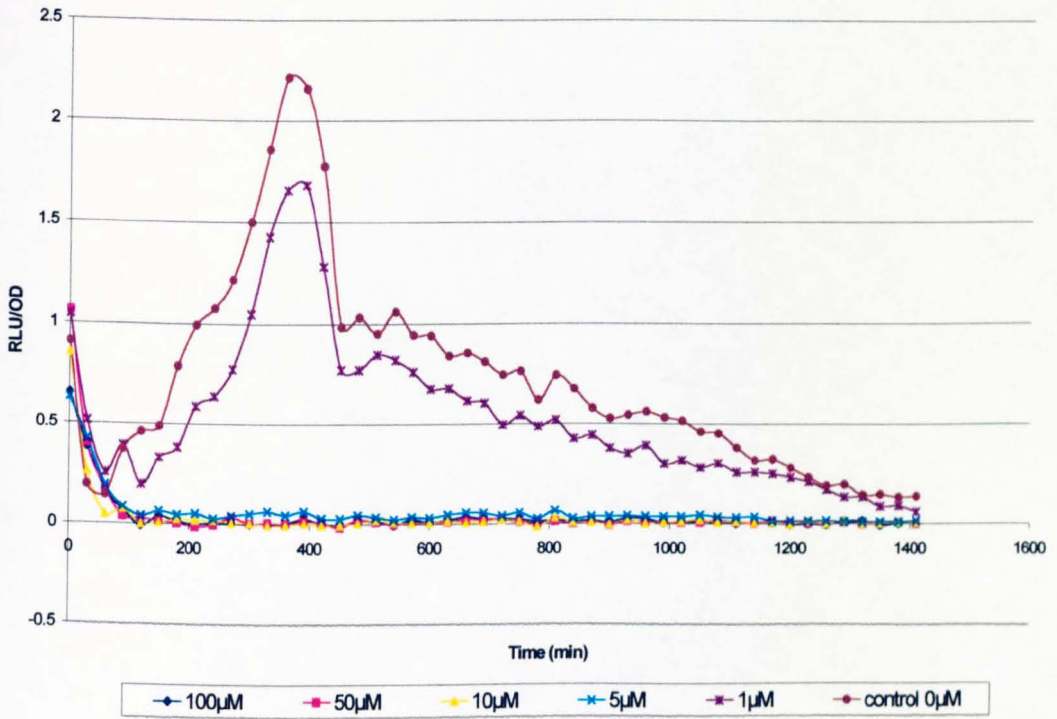
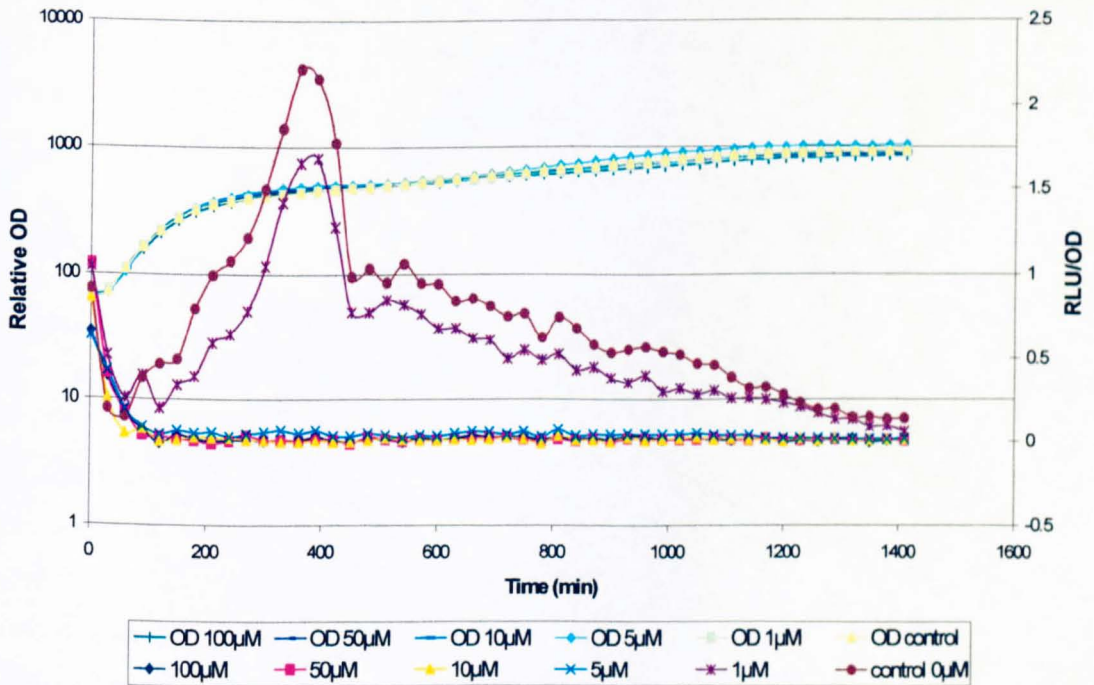


Figure 7.6.2.4: Utilising *S. aureus* 8325-4 (pSB2034) to determine the effective concentration of a synthetic agr inhibitor (data represents RLU/OD and OD vs Time)



7.7. Discussion

Having successfully expressed *lux* and *gfp* in Gram positive bacteria, the reporter genes have been used to create a series of reporter plasmids to study expression of the P3 promoter of the *agr* operon of *S. aureus*. This has led to the construction of four new expression vectors, pSB2031 (*gfp3opt*), pSB2032 (*luxABCDE*), pSB2033 (*gfp3opt* LAA-*luxABCDE*) and pSB2034 (*gfp3opt* ASV-*luxABCDE*). All these plasmids have been introduced into *S. aureus* RN4220 and *S. aureus* 8325-4, although it should be noted when cells harbouring pSB2033 were examined by fluorescence microscopy very few cells showed a fluorescent phenotype. This is most likely due to the fact that this unstable *gfp3* has the shortest half-life of all the unstable *gfp3* variants, approximately 30 minutes in *E. coli* (Anderson *et al.*, 1998). Therefore due to the nature of the protein it is not unexpected that bacteria expressing *gfp3opt* LAA were noticeably less fluorescent than bacteria expressing *gfp3opt* ASV.

Upon the addition of spent bacterial supernatant the *S. aureus* harbouring these *agr* reporter plasmids, the activity of P3 was seen to be induced to a higher level. This was illustrated by the fact that when bacterial supernatant was added to the culture media the output from the reporter gene increased. This indicated that the P3 promoter had been activated thus increasing the expression of genes downstream from it.

Having proved that these reporter plasmids could be induced using culture supernatants, the activity of the P3 promoter was investigated through the use of specific synthetic activator and inhibitor molecules. It was seen that only low concentrations of this synthetic activator molecule were necessary to induce the activation of P3, which showed a dose response to the molecule and that luminescence could not be increased past a certain threshold level. The action of the P3 promoter could also be inhibited through the use of an inhibitor synthesised on the basis of the *S. lugdunensis agr* activator molecule. This molecule was observed to

block the cell density dependent regulation of *agr* expression, represented by the fact that *S. aureus* harbouring the expression vectors when grown in the presence of this inhibitor were non-luminescent, reflecting inhibition of P3.

S. aureus is a pathogen with a broad host range and is a leading cause of infection in humans and domestic animals world-wide. Infections associated with this organism are very common and often life threatening. The emerging resistance of antibiotics, such as methicillin (MRSA) and vancomycin (VRSA) resistant isolates by this organism has caused considerable alarm within the medical community. Although new antibiotics have been discovered that are potentially able to cure such infections with a reduced selective pressure, there is an obvious need for developing alternative therapies and thus avoiding the overuse of antibiotics which is one factor that hastens the development of drug resistant bacteria. It is thought that if inhibitor molecules to the promoter that induces expression of extracellular virulence factors could be developed then this may lead to alternative therapies for staphylococcal infections, hence reducing the need for antibiotics.

CHAPTER 8

DISCUSSION

CHAPTER 8: DISCUSSION

Listeria monocytogenes and *Staphylococcus aureus* are Gram positive pathogens that are significantly important within the medical community and in the case of *L. monocytogenes* within the food industry. In order to advance our understanding of host-pathogen interactions and gene regulation, non-invasive assays for monitoring the progression of infectious agents and other biochemical processes in the living animal are needed.

Both gene expression and bacterial movement can be monitored through the use of reporter genes. Several factors must be considered when choosing the reporter gene, the most important of which is that the reporter must code for a phenotype not already displayed by the host. The phenotype of the reporter must be fairly easy to detect and ideally it should be possible to assay the phenotype quantitatively. In this study two reporter systems were chosen, these being bacterial bioluminescence (*lux*) and green fluorescent protein (*gfp*).

GFP3 is a red shifted *gfp* variant which is an extremely stable protein, and whilst it cannot be used for real time gene expression studies *per se* it can be used to tag bacterial cells and follow their progression in an intracellular environment, thus gaining knowledge on how individual bacteria contribute towards the infection process. Many *gfp* variants are now available, some of these contain a short peptide sequence at the C-terminal end of the protein which renders it susceptible to indigenous housekeeping proteases (Anderson *et al.*, 1998). This degradation of C-terminally modified proteins was first demonstrated by Keiler *et al.* (1996), who showed that specific C-terminal oligopeptide extensions could render otherwise stable proteins to degradation by certain intracellular tail-specific proteases. This system was exploited by Anderson *et al.* (1998) who created variants of *gfp3* which were degraded at different rates within the cell, the protein variants had half-lives ranging from 30 minutes to a few hours when synthesised in *E. coli* and

Pseudomonas putida (Anderson *et al.*, 1998). As these unstable GFP proteins do not accumulate within the cell then they should provide data on promoter kinetics and gene expression within bacteria as well as providing a visual tag by which bacterial movement and localisation can be studied.

gfp has been expressed in a wide range of Gram negative bacteria, including *E. coli* (Chalfie *et al.*, 1994) and *P. fluorescens* (Tombolini *et al.*, 1996) and a number of Gram positive bacteria, including *Bacillus subtilis* (for example Arigonin *et al.*, 1995) and *Enterococcus faecalis*, *Streptococcus gordonii* and *Streptococcus bovis* (Scott *et al.*, 1998). This study required the efficient expression of *gfp* in *L. monocytogenes* and *S. aureus* for the use as a transcriptional reporter gene. However, when *gfp* was placed downstream of a promoter that had been determined to be strongly activated in *L. monocytogenes*, P_{xyn} , the level of GFP produced within the cells was very small compared to *E. coli* expressing *gfp* from the same promoter. Analysis of mRNA by Northern blot indicated that the problem was that of translation and different molecular techniques were employed to obtain homogeneously fluorescent Gram positive bacterial populations. The problem was resolved through a combination of factors, the use of a different promoter (P_{xyIA}) which was observed to give high, well regulated, expression of genes downstream of the promoter in *L. monocytogenes*, and through translational enhancement of the 5' coding region of *gfp*. Vellanoweth (1993) postulated that in *B. subtilis* a strong Shine-Dalgarno sequence was necessary for efficient translation, this was determined to be AAGGAGG. The spacing between the Shine-Dalgarno sequence and the initiation codon was also found to be critical, with the optimum being between 7-9 base spacings. The combination of a well regulated promoter and a translationally optimised *gfp3* gene resulted in a high level of *gfp3* expression in Gram positive bacteria, will all individual cells exhibiting a fluorescent phenotype upon excitation, demonstrated by fluorescence microscopy.

The other reporter that was utilised within the course of this study was bacterial luminescence, *luxCDABE* from *P. luminescens*. Luciferase activity offers several advantages over alternative systems (Carmi *et al.*, 1989); superior sensitivity and

ease of assay recommend luciferase as a real time, non-destructive reporter. Previously it has been shown that a high level of bioluminescence can be achieved from *Bacillus subtilis*, provided that the luciferase genes are efficiently expressed (Jacobs *et al.*, 1991). This was made possible by transcription from a strong Gram positive promoter, and engineering of the *luxA* together with the use of a *luxAB* fusion gene (Hill *et al.*, 1991). Such constructs have been shown to be active in a wide range of Gram positive organisms, including *S. aureus*, *S. epidermidis*, *Listeria monocytogenes* and *Streptococcus pneumoniae*. These constructs are useful for *in vitro* studies, but the need for exogenous substrate for the luciferase makes them problematic for *in vivo* bacterial pathogenicity studies in animals, hence the desire to engineer the whole *lux* operon for efficient expression in Gram positive bacteria.

When expression of the *luxCDABE* operon from P_{xyn} (pSB2022) was observed in *L. monocytogenes* the level of luminescence observed was much lower than *E. coli* harbouring the same expression vector. It was unclear why when pSB2022 was introduced into *L. monocytogenes* the cells were not as bioluminescent as *E. coli* cells harbouring the same construct. It is known that the P_{xyn} promoter is strongly expressed in Gram positives as high bioluminescent levels are observed from *L. monocytogenes* cells harbouring pGC4, due to the expression of a *luxAB* fusion, which is downstream of P_{xyn} . The low luminescence levels could be attributed to a lack of FMNH₂ or molecular oxygen within the cells, but this too appears unlikely, again due to the fact that high expression of *luxAB* can be observed in *L. monocytogenes* cells. Additionally, when exogenous aldehyde was added to *L. monocytogenes* harbouring this *luxCDABE* expression vector, no increase in luminescent output was observed, indicating that either *luxA* or *luxB* or both were limiting in the reaction.

Previous experience of gene expression in such organisms (Jacobs *et al.*, 1991; Hill *et al.*, 1994; Qazi *et al.*, 1998) led to the surmise that the problem was most likely to be that of inefficient translational initiation within the cell. From experience derived from expression of *gfp* in Gram positive organisms, through PCR the 5' coding regions of *luxA*, *luxC* and *luxE* were translationally enhanced for expression in Gram

positive bacteria as described by Vellanoweth (1993). The *lux* operon was then engineered such that *luxAB* were adjacent to *luxCDE* on a plasmid downstream of the strong, regulatable promoter P_{xylA} . This led to highly luminescent *L. monocytogenes* and *S. aureus* cells, and whilst the luminescence is still not yet at parity with expression in *E. coli*, levels of luminescence are higher than anything observed previously in Gram positive bacteria. It has still to be determined whether expression of *luxABCDE* could be increased further in Gram positive bacteria by further translational enhancements. Analysis of total cellular proteins from bacteria harbouring the *lux* expression vectors was not conclusive, but it may be that either *luxB* or *luxD* is being translated with lower efficiency than the other *lux* genes in the Gram positive organisms.

Having constructed these expression vectors, experiments were performed to observe the output from cells harbouring the reporter genes. It was noticed that when cells expressed *gfp3*, an increase in the fluorescent output was not noticed until approximately 5 hours into the growth experiment. This corresponded to bacteria that were in late exponential phase. Unlike *lux*, *gfp3* is not an enzyme and so there is no signal amplification derived from multiple cleavage by one molecule of reporter protein. The fluorescence signal in one cell depends on two factors, the rate of synthesis of functional protein following post-translational formation of a functional chromophore, and the dilution of fluorescent protein as the bacteria divide.

The data gathered from the fluorescence experiments while providing information of the levels of fluorescent protein, it does not give an accurate representation of promoter dynamics within the cell. Another problem with using *gfp3* for gene expression studies and studies of promoter dynamics is the stability of GFP3 which was estimated to have a half-life greater than one day (Anderson *et al.*, 1998). This can be overcome to a certain degree through the use of the unstable *gfp3* variants, which have been translationally enhanced for expression in Gram positive bacteria and which were shown to degrade in *L. monocytogenes* at different rates depending on the C-terminal extension.

A more accurate representation of the promoter dynamics was obtained from *L. monocytogenes* expressing *luxABCDE*. Here luminescence was seen to peak as cells were in mid-exponential phase and then decrease. This suggests that the promoter is not constitutive as first thought from the experiments with *gfp3* but is in fact only active during early exponential growth. It might be argued that the decrease in luminescence is due to a lack of FMNH₂ from the bacteria, that is necessary to the bioluminescent reaction and is derived from the bacterium's electron transport chain. However, this appears unlikely as when luminescence was seen to decrease the bacteria are still growing exponentially and so obtaining energy in the form of FMNH₂ should not be an issue, as the bacteria are actively growing and respiring.

This issue is backed up by data obtained from observing luminescent output from *S. aureus* 8325-4 expressing *lux* from pSB2033 and pSB2034, dual reporters of P3 expression. These bacteria were seen to express *lux* in late exponential phase / stationary phase. This is due to the fact that *agr* expression is cell density dependent, therefore in later stages of growth more autoinducing peptide is present, thus a greater activation of P3 is observed resulting in higher output from the reporter, in this case *lux*. The luminescence was observed to peak in stationary phase and levels then decreased. This may be due to repression of the promoter, or possibly it could be attributed to a lack of energy in the cells as they are no longer actively growing, therefore there will be limited levels of FMNH₂ available for the bioluminescent reaction.

The fact that bioluminescence can be observed from cells in stationary phase illustrates the fact that P_{*xyIA*} is only active in the early stages of growth. The decrease in bioluminescence from *L. monocytogenes* expressing *lux* in exponential phase is more likely to be due to repression of the promoter and not due to a lack of FMNH₂ in the bacteria. When observing *gfp3* expression this down-regulation of promoter activity is not observed, probably due to the stability of the protein and the delay observed between expressing *gfp3* and forming functional protein.

One other factor was that was observed from expression of *lux* and *gfp3* in *L. monocytogenes*, was the slower initial growth rate when cells contained one of the expression vectors. It appeared that expression of the genes was not responsible for this initial slower growth rate, as in lag phase only a low level of reporter activity was observed, so no significant energy drain would be placed upon the cells. This decrease in the initial growth rate was also seen when *L. monocytogenes* harboured the vector but expression of the genes was not induced, i.e. xylose was not added to the bacterial culture medium. It appeared that the actual presence of the expression vectors within *L. monocytogenes* contributed to the initial slower growth rate observed by the bacteria.

All the expression vectors constructed during the course of this study are based on pMK4, this was generated from the fusion of pUC9 and pC194, and hence contains both a Gram negative and Gram positive origin of replication (Sullivan *et al.*, 1984)). However, pC194 shows several properties unfavourable for cloning and stability. It generates considerable amounts of ssDNA in *B. subtilis*, approximately 20% of the total plasmid DNA (te Riele *et al.*, 1986) and it may also generate large amounts of high-molecular DNA when carrying heterologous inserts (Gruss and Ehrlich, 1988).

The plasmid pC194 was originally isolated from *S. aureus*. Evidence exists that this plasmid replicates by a rolling-circle mechanism similar to that described for ssDNA *E. coli* bacteriophages (Baas and Jansz, 1988). The presence of ssDNA is an important criterion for rolling circle replication plasmids. However, ssDNA is generally only detectable with small plasmid derivatives, less than approximately 4-7 kb. With larger derivatives or with plasmids carrying inserts, the relative amount of ssDNA decreases, whereas the level of HMW DNA increases (Gruss and Ehrlich, 1988).

Gruss and Ehrlich (1988) reported that if foreign DNA is inserted into pC194, the plasmid generates aberrant replication products of high molecular weight (HMW DNA). They estimated that as much as 90% of the plasmid DNA might be present as

HMW. HMW DNA consists of linear head to tail multimers in which five or more copies are tandemly arranged. However, Gruss and Ehrlich (1988) observed that only those plasmids that replicate by a rolling-circle type replication with ssDNA intermediates generate HMW DNA, HMW DNA was not produced from a plasmid with no ssDNA replicative intermediate.

The production of HMW DNA depends upon a number of factors, one of these being the nature of the DNA fragment inserted. The experiments of Gruss and Ehrlich (1988) suggested that inserts of a particular origin could cause production of HMW whereas other inserts of approximately the same size did not. For example it was found that inserts of several types of *E. coli* origin (e.g. pBR322 or pUC plasmids) stimulated HMW DNA production whereas other types of DNA had little effect. Their experiments showed that DNA inserts as small as 500 base pairs could result in HMW DNA formation. In general the level of HMW DNA is related to plasmid size, with small plasmids derivatives yielding low amounts of this product, i.e. the greater the insert the greater the amount of HMW DNA produced in the cell.

From the experiments that observed growth of *L. monocytogenes* harbouring the expression vectors it appears that the bigger the plasmid slower the initial growth rate. As none of the reporters are expressed at high levels in lag phase or early exponential phase, it seem unlikely that it is expression of the reporters that is responsible for the slower initial growth rates that were observed.

It is possible that if the reporter plasmids form large quantities of HMW DNA then this may be the limiting factor to growth in the early stages of the experiment. Production of HMW DNA is a result of the termination sequence not being recognised at the ori^+ sequence. If this is not recognised the DNA is not circularised to form a dsDNA molecule, instead more linear copies of the plasmid are generated and these products accumulate in the cell and possibly slow down the initial growth rate. If the replicating leading strand is not closed through the action of Rep, then the molecule of DNA gets longer in length. If this were the case then it takes longer for

the cells to replicate the plasmid, this combined with the added factor of having to make new cellular proteins in order to divide may result in the observed extended lag period. Gruss and Ehrlich (1988) also suggested that the formation of HMW DNA was dependent of the size of the heterologous insert, this would explain why the plasmids with the bigger cloned insert had the slowest initial growth rate.

The production of HMW DNA may also be reflected in the plasmid instability of these expression vectors. It was found that cells expressing *lacZ* from pMK4 were stable, but when DNA fragments were cloned into pMK4 the stability of the plasmid decreased. This again appeared to be related to size with the bigger plasmids being much more unstable than ones where smaller DNA fragments had been inserted.

Having built these reporter constructs and showed that they can be expressed at high levels in Gram positive bacteria, it is hoped that they can be used for bacterial tagging experiments to observe how bacteria are able to invade cells and in the case of *L. monocytogenes* to follow the progression of the bacteria as they move intracellularly. They can also be utilised in gene expression studies and also for studying pathogenicity *in vivo*. Through the use of mini-transposons it is hoped to identify genes involved in pathogenicity of specific bacteria and observe expression of these genes throughout the infective process to investigate how the bacteria causes disease.

Whilst *gfp3* provides an excellent positional marker, it is not the ideal reporter when monitoring gene expression in real time. It is possible that the unstable *gfp3* variants may be more use as a real time reporter, especially in marking the downregulation of genes as this would be accompanied by a decrease in fluorescent output. However, the unstable *gfp3* variants do still not provide a real time indication of events occurring in the cell as time is needed for the chromophore to fold and generated fluorescent protein. This delay between promoter induction and expression of the reporter was reflected with *S. aureus* 8325-4 harbouring the dual reporter of *agr*

expression. Here the luminescent output was seen to peak approximately two hours prior to that from observing *gfp3* expression from the same plasmid.

The data gathered during the course of this study shows that although these two reporters are very different in their action, both have their own merits which makes the dual expression vector a powerful tool for gene expression studies *in vivo* and bacterial localisation experiments. These reporters as they stand could be used for *in vivo* tracking experiments. The experiments of Contag *et al.* (1995) allowed bacterial movement to be viewed non-invasively within the living animal during the course of infection. *Lux* reporters permit the monitoring of gene expression over time, as the short half-life of the luciferase guarantees that the photon emission observed represents the gene of interest. These points suggest that in theory the activity of any gene fusion to *lux* could be examined in live animal tissues. During an infection process the bioluminescent marker would provide data on the growth and spread of constitutively luminescent bacteria as well as providing about the temporal and spatial induction of particular genes. Although the *gfp3* cannot be used to give an accurate representation of gene expression due to the stability of the protein formed, it does provide an excellent marker on those cells expressing the gene even on fixed samples. These two markers in combination would provide data on how individual bacteria contribute to the infection process and how infection proceeds. This may have a significant impact upon the development of novel drugs, understanding gene regulation during development and during infectious processes, as well as many other biological events such as monitoring bacteria within the environment in processes such as bioremediation and biocontrol. Here the dual reporter would allow simultaneous monitoring of the metabolic activity and cell number of a specific bacterial population, and would allow monitoring of specific bacteria *in situ* in environmental samples.

Whilst much of our understanding of the virulence factors of pathogenic bacteria has come from experiments performed with the bacteria grown in culture, the culture conditions are different from those *in vivo*. The *in vitro* model systems available, whilst providing information on host pathogen interactions, they can never replicate

the complex and dynamic interactions that occur *in vivo*. It is hoped that through the use of these reporters a better understanding of how infection proceeds can be determined and how genes involved in pathogenicity are regulated.

REFERENCES

REFERENCES

- ABDELINOUR, A., ARVIDSON, S., BREMELL, T., RYDED, C. and TARKOWSKI, A. (1993) The accessory gene regulator (*agr*) controls *Staphylococcus aureus* virulence in a murine arthritis model. *Infection and Immunity* 61, 3879-3885.
- ALMEIDA, R. A., MATTHEWS, K. R., CIFRIAN, E., GUIDRY, A. J. and OLIVER, S. P. (1996) *Staphylococcus aureus* invasion of bovine mammary epithelial cells. *Journal of Dairy Science* 79, 1021-1026.
- ANDERSON, J. B., STERNBERG, C., POULSEN, L. K., BJØRN, S. P., GIVSKOV, M. and MOLIN, S. (1998) New unstable variants of Green Fluorescent Protein for studies of transient gene expression in bacteria. *Applied and Environmental Microbiology* 64, 2240-2246.
- ANDERSON, M. T., TJIOE, I. M., LORINCZ, M. C., PARKS, D. R., HERZENBERG, L. A., NOLAN, G. P. and HERZENBERG, L. A. (1996) Simultaneous fluorescence-activated cell sorter analysis of two distinct transcriptional elements within a single cell using engineered green fluorescent proteins. *Proceedings of the National Academy of Science* 93, 8508-8511.
- APPLEGATE, B. M., KEHRMEYER, S. R. and SAYLER, G. S. (1998) A chromosomally based tol-luxCDABE whole cell reporter for benzene, toluene, ethylbenzene and xylene (BTEX) sensing. *Applied and Environmental Microbiology* 64, 2730-2735.
- ARIGONI, F., POGLIANI, K., WEBB, C. D., STRAGIER, P. and LOSICK, R. (1995) Localisation of protein implicated in establishment of cell type to sites of asymmetric division. *Science* 270, 637-640.
- ARVIDSON, S., JANZON, L., LOFDAHL, S. and MORFELDT, E. (1989) In *Genetic transformation and expression*, P. 511-518. Eds. L. O. Butler and B. E. B. Moseley. Intercept Ltd. Wimborne, Dorset, UK.
- AUGUSTIN, J and GOTZ, F. (1990) Transformation of *Staphylococcus epidermidis* and other staphylococcal species with plasmid DNA by electroporation. *FEMS Microbiology Letters* 66, 203-208.

- AUSUBEL, F. M., BRENT, R., KINGSTON, R. E., MOORE, D. D., SEIDMAN, J. G., SMITH, J. A., and STRUHL, K. (1994) *Current Protocols in Molecular Biology*. John Wiley and Sons, Chichester, UK.
- BAAS, P. D. and JANSZ, H. S. (1988) Single-stranded DNA phage origins. *Current Topics in Microbiology and Immunology* 136, 31-70.
- BALBAN, N. and NOVICK, P. (1995) Autocrine regulation of toxin synthesis by *Staphylococcus aureus*. *Proceedings of the National Academy of Science USA* 92, 1619-1623.
- BALDWIN, T. O., ZIEGLER, M. M. and POWERS, D. A. (1979) Covalent structure of subunits of bacterial luciferase: NH₂-terminal sequence demonstrates subunit homology. *Proceedings of the National Academy of Science USA* 76, 488-4889.
- BARG, N., BUNCE, C., WHEELER, L., REED, G. and MUSSER, J. (1992) Murine model of cutaneous infection with Gram positive cocci. *Infection and Immunity* 60, 2636-2640.
- BAUMANN, P., BAUMANN, M., WOOLKALIS, M. and BANG, S. (1983) Evolutionary relationships in *Vibrio* and *Photobacterium*. A basis for a natural classification. *Annual Review in Microbiology* 37, 369-398.
- BAYER, M. G., HEINRICH, J. H. and CHEUNG, A. L. (1996) The molecular structure of the *sar* locus in *Staphylococcus aureus*. *Journal of Bacteriology* 178, 4563-4570.
- BAYLES, K. W., WESSON, C. A., LIU, L. E., FOX, L. K., BOHACH, G. A. and TRUMBLE, W. R. (1998) Intracellular *Staphylococcus aureus* escapes the endosome and induces apoptosis in epithelial cells. *Infection and Immunity* 66, 336-342.
- BEHARI, J. and YOUNGMAN, P. (1998) A homolog of CcpA mediates catabolite control in *Listeria monocytogenes* but not carbon source regulation of virulence genes. *Journal of Bacteriology* 180, 6316-6324.

- BERNADINI, M. L., MOUNIER, J., D'HAUTEVILLE, H., COQUIS-RONDON, M. and SANSONETTI, P. J. (1989) Identification of *icsA*, a plasmid locus of *Shigella flexneri* that governs bacterial intra- and intercellular spread through interactions with F-actin. *Proceedings of the National Academy of Science USA* 86, 3867-3871.
- BLOSSER, T. (1979) Economic losses from and the national research program on mastitis in the United States. *Journal of Dairy Science* 345, 175-176.
- BOHNE, J., SOKOLOVIC, Z. and GOEBEL, W. (1994) Transcriptional regulation of *prfA* and PrfA-regulated virulence genes in *Listeria monocytogenes*. *Molecular Microbiology* 11, 1141-1150.
- BOKMAN, S. H. and WARD, W. W. (1981) Renaturation of *Aequorea* green fluorescent protein. *Biochemical and Biophysical Research Communication* 101, 1372-1380.
- BOYLAN, R. J., MENDELSON, N. H., BROOKS, D. and YOUNG, F. E. (1972) Regulation of the bacterial cell wall: Analysis of a mutant *B. subtilis* defective in biosynthesis of teichoic acid. *Journal of Bacteriology*, 110, 281-290.
- BRAUN, L., DRAMSI, S., DEHOUX, P., BIERNE, H., LINDAHL, G. and COSSART, P. (1997) InlB: an invasion protein of *Listeria monocytogenes* with a novel type surface association. *Molecular Microbiology* 25, 285-294.
- BRAUN, L., OHAYON, H. and COSSART, P. (1998) The InlB protein of *Listeria monocytogenes* is sufficient to promote entry into mammalian cells. *Molecular Microbiology* 27, 1077-1087.
- BRON, S. and VENEMA, G. (1972) Ultraviolet inactivation and excision repair in *Bacillus subtilis*. Construction and characterisation of a transformable eightfold auxotrophic strain and two ultraviolet sensitive derivatives. *Mutat. Res.* 15, 1-10.
- BROWN, J. W., HUNT, D. K. and PACE, N. R. (1990) Nucleotide sequence of the 10Sa RNA gene of the beta-purple eubacterium *Alcaligenes eutrophus*. *Nucleic Acid research* 18, 2820.

- BUBERT, A., SOKOLOVIC, Z., CHUN, S. K., PAPTAEODOROU, L., SIMM, A. and GOEBEL, W. (1999) Differential expression of *Listeria monocytogenes* virulence genes in mammalian host cells. *Molecular General Genetics* 261, 323-336.
- CAMILL, A. (1996) Non-invasive techniques for studying pathogenic bacteria in the whole animal. *Trends in Microbiology* 4, 295-296.
- CAMILLI, A., PORTNOY, D. A. and YOUNGMAN, P. (1990) Insertional mutagenesis of *Listeria monocytogenes* with a novel Tn917 derivative that allows direct cloning of DNA flanking transposon insertions. *Journal of Bacteriology* 172, 3738-3744.
- CAMILLI, A., TILNEY, L. and PORTNOY, D. (1993) Dual roles of *plcA* in *Listeria monocytogenes* pathogenesis. *Molecular Microbiology* 8, 143-157.
- CAMPBELL, A. K. (1989) Living light: biochemistry, function and biomedical applications. *Essays Biochem* 24, 41-76.
- CARMI, O. A., STEWART, G. S. A. B., ULITZYR, S. and KUHN, J. (1987) Use of bacterial luciferase to establish a promoter probe vehicle capable of non-destructive real-time analysis of gene expression in *Bacillus* spp. *Journal of Bacteriology* 169, 2165-2170.
- CHAKRABORTY, T., LEIMEISTER-WÄCHTER, M., DOMAN, E., HARTL, M., GOEBEL, W., NICHTERLEIN, T and NOTERMANS, S. (1992) Coordinate regulation of virulence genes in *Listeria monocytogenes* requires the product of the *prfA* gene. *Journal of Bacteriology* 174, 568-574.
- CHALFIE, M., TU, Y., EUSKIRCHEN, G., WARD, W. W. and PRASHER, D. C. (1994) Green fluorescent protein as a marker of gene expression. *Science* 263, 802-805.
- CHAN, P. F. and FOSTER, S. J. (1998) Role of SarA in virulence determinant production and environmental signal transduction in *Staphylococcus aureus*. *Journal of Bacteriology* 180, 6232-6241.
- CHAN, P. F. and FOSTER, S. J. (1998) The role of environmental factors in the regulation of virulence-determinant expression in *Staphylococcus aureus* 8325-4. *Microbiology* 144, 2469-2479.

- CHARBONNEAU, H., WALSH, K. A., McCANN, R. O., PRENERGAST, F. G., CORMIER, M. J and VANAMAN, T. C. (1985) Amino acid sequence of the calcium-dependent photoprotein aequorin. *Biochemistry* 24, 6762-6771.
- CHEUNG, A. L., BAYER, M. G. and HEINRICHS, J. H. (1997) *sar* genetic determinants necessary for transcription of RNA II and RNA III in the *agr* locus of *Staphylococcus aureus*. *Journal of Bacteriology* 179, 3963-3971.
- CHEUNG, A. L., COOMEY, J. M., BUTLER, C. A., PROJAN, S. J. and FISCHETTI, V. A. (1992) Regulation of exoprotein expression in *Staphylococcus aureus* by a locus (*sar*) distinct from *agr*. *Proceedings of the National Academy of Science USA* 89, 6462-6466.
- CHEUNG, A. L., EBERHARDT, K. J., CHUNG, E., YEAMAN, M. R., SULLAM, P. M., RAMOS, M. and BAYER, A. S. (1994) Diminished virulence of *sar*⁻/*agr*⁻ mutant of *Staphylococcus aureus* in the rabbit model of endocarditis. *Journal of Clinical Investigation* 94, 1815-1822.
- CHEUNG, A. L., NAST, C. C. and BAYER, A. S. (1998) Selective activation of *sar* promoters with the use of green fluorescent protein transcriptional fusions as the detection system in the rabbit endocarditis model. *Infection and Immunity* 66, 5988-5993.
- CHIEN, Y. T. and CHEUNG, A. L. (1998) Molecular interactions between two global regulators, *sar* and *agr*, in *Staphylococcus aureus*. *Journal of Biological Chemistry* 273, 2645-2652.
- CHIEN, Y. T., MANNA, A. C. and CHEUNG, A. L. (1998) SarA is a determinant of *agr* activation in *Staphylococcus aureus*. *Molecular Microbiology* 30, 991-1001.
- CODY, C. W., PRASHER, D. C., WESTLET, W. M., PRENDERGAST, F. G. and WARD, W. W. (1993) Chemical structure of the hexapeptide chromophore of the *Aequorea* green fluorescent protein. *Biochemistry* 32, 1212-1218.
- COLEPICOLO, P., CHO, K., POINAR, G. O. and HASTINGS, J. W. (1989) Growth and luminescence of the bacterium *Xenorhabdus luminescens* from a human wound. *Applied and Environmental Microbiology* 55, 2601-2606.

- CONTAG, C. H., CONTAG, P. R., MULLINS, J. I., SPILMAN, S. D., STEVENSON, D. K. and BENARON, D. A. (1995) Photonic detection of bacterial pathogens in living host. *Molecular Microbiology* 18, 593-603.
- COOK, N., SOLCOCK, D. J., WATERHOUSE, R. N., PROSSER, J. I., GLOVER, L. A. and KILLHAM, K. (1993) Construction and detection of bioluminescent strains of *Bacillus subtilis*. *Journal of Applied Bacteriology* 75, 350-359.
- CORMACK, B. P and STRUHL, K. (1993) Regional codon randomisation: defining a TATA-binding protein surface required for RNA polymerase III transcription. *Science* 262, 244-248.
- CORMACK, B. P., VALDIVIA, R. H. and FALKOW, S. (1996) FACS optimised mutants of the green fluorescent protein (GFP). *Gene*, 173, 33-38.
- COSSART, P. and KOCKS, C. (1994) The actin based motility of the facultative intracellular pathogen *Listeria monocytogenes*. *Molecular Microbiology* 13, 395-402.
- COSSART, P. and MENGAUD, J. (1989) *Listeria monocytogenes*: a model system for the molecular study of intracellular parasitism. *Mol. Biol. Med.* 6, 463-474.
- COSTERTON, J. W. (1984) The formation of biocide resistant biofilms in industrial, natural and medical settings. *Developm. Industr. Microbiology* 25, 363-372.
- CUBBIT, A. B., HEIM, R., ADAMS, S. R., BOYD, A. E., GROSS, L. A. and TSIEN, R. Y. (1995) Understanding, improving and using green fluorescent proteins. *Trends in Biochemical Sciences* 20, 448-455.
- DABIRI, G. A., SANGER, J. M., PORTNOY, D. A. and SOUTHWICK, F. S. (1990) *Listeria monocytogenes* moves rapidly through the host-cell cytoplasm by inducing directional actin assembly. *Proceedings of the National Academy of Science USA* 87, 6068-6072.
- DAHL, M. K., DEGENKOLB, J. and HILLEN, W. (1994) Transcription of the *xyl* operon is controlled in *Bacillus subtilis* by tandem overlapping operators spaced by four base pairs. *Journal of Molecular Biology* 243, 413-424.

- DAHL, M. K., SCHMIEDEL, D. and HILLEN, W. (1995) Glucose and glucose-6-phosphate interaction with xyl repressor proteins from *Bacillus* ssp. may contribute to regulation of xylose utilisation. *Journal of Bacteriology* 177, 5467-5472.
- DELAGRAVE, S., HAWTIN, R. E., SILVA, C. M., YANG, M. M. and YOUVAN, D. C. (1995) Red shifted excitation mutants of the green fluorescent protein *Bio Technology* 13, 151-154.
- DICKNEITE, C., BÖCKMANN, R., SPORY, A., GOEBEL, W and SOKOLOVIC, Z. (1998) Differential interaction of the transcription factor PrfA and the PrfA-activating factor (Paf) of *Listeria monocytogenes* with target sequences. *Molecular Microbiology* 27, 915-928.
- DOMANN, E., WEHLAND, J., ROHDE, M., PISTOR, S., HARTI, M., GOEBEL, W., LEIMEISTER-WÄCHTER, M., WUENSCHER, M. and CHAKRABORTY, T. (1992) A novel bacterial gene in *Listeria monocytogenes* required for host cell microfilament interaction with homology to the proline-rich region of vivculin. *EMBO Journal* 11, 1981-1990.
- DOMANN, E., LEIMEISTER-WÄCHTER, M., GOEBEL, W. and CHAKRABORTY, T. (1991) Molecular cloning, sequencing and identification of a metalloprotease gene from *Listeria monocytogenes* that is species specific and physically linked to the listeriolysin gene. *Infection and Immunity* 59, 65-72.
- DONG, H. J., NILSSON, L. and KURLAND, C. G. (1996) Co-variation of tRNA abundance and codon usage in *Escherichia coli* at different growth rates. *Journal Molecular Biology* 43, 28-31.
- DRAMSI, S., BISWAS, I., MAGUIN, E., BRAUN, L., MASTROENI, P. and COSSART, P. (1995) Entry of *Listeria monocytogenes* into hepatocytes requires expression of InlB, a surface protein of the internalin multigene family. *Molecular Microbiology* 16, 251-261.
- DRAMSI, S., KOCKS, C., FORESTIER, C. and COSSART, P. (1993) Internalin-mediated invasion of epithelial cells by *Listeria monocytogenes* is regulated by the bacterial growth state, temperature, and the pleiotropic regulator *prfA*. *Molecular Microbiology* 9, 931-941.

- DREVETS, D. A. (1998) *Listeria monocytogenes* virulence factors that stimulate endothelial cells. *Infection and Immunity* 66, 232-238.
- DUNLAP, P. (1991) Organisation and regulation of bacterial luminescence genes. *Photochemistry and Photobiology* 54, 1157-1170.
- DURAN, S. P., KAYSER, F. H. and BERGER-BACHI, B. (1996) Impact of *sar* and *agr* on methicillin resistance in *Staphylococcus aureus*. *FEMS Microbiology Letters* 141, 255-260.
- EHRIG, T., O'KANE, D. J. and PRENDERGAST, F. G. (1995) Green fluorescent protein with altered fluorescence excitation spectra. *FEBS Letters* 367, 163-166.
- ENGBRECHT, J. and SILVERMAN, M. (1984) Identification of genes and gene products necessary for bacterial bioluminescence. *Proceedings of the National Academy of Science USA* 81, 4154-4158.
- ENGBRECHT, J., NEALSON, K. H. and SILVERMAN, M. (1983) Bacterial bioluminescence: isolation and genetic analysis of functions from *Vibrio fishcheri*. *Cell* 32, 773-781.
- ENGBRECHT, J., SIMON, M. and SILVERMAN, M. (1985) Measuring gene expression with light. *Science* 227, 1345-1347.
- ENGELBRECHT, F., CHUN, S. K., OCHS, C., HESS, J., LOTTSPEICH, F., GOEBEL, W. and SOKOLOVIC, Z. (1996) A new PrfA-regulated gene of *Listeria monocytogenes* encoding a small secreted protein which belongs to the family of internalins. *Molecular Microbiology* 21, 823-837.
- FARMER, J. J., JORGENSEN, J. H., GRIMONT, P. A. D., AKHURST, R. J., POINAR, G. O., AGERON, E., PIERCE, G. V., SMITH, J. A., CARTER, G. P., WILSON, K. L. and HICKMAN-BRENNER, F. W. (1989) *Xenorhabdus luminescens* (DNA hybridisation group 5) from human clinical specimens. *Journal of Clinical Microbiology* 27, 1594-1600.
- FELDEN, B., HIMENO, H., MUTO, A., ATKINS, J. F. and GESTELAND, R. F. (1996) Structural organisation of *Escherichia coli* tmRNA. *Biochimie*. 78, 979-983.

FELDEN, B., HIMENO, H., MUTO, A., McCUTCHEON, J. P., ATKINS, J. F. and GESTELAND, R. F. (1997) Probing the structure of the *Escherichia coli* 10Sa RNA (tmRNA). *RNA* 3, 89-103.

FERROW, J. P. (1980) Subclinical mastitis: biology and economics. *Compend. Contin. Educ. Pract. Vet.* 2, 5223-5234.

FORAN, D. R. and BROWN, W. M. (1988) Nucleotide sequence of the *luxA* and *luxB* genes of the bioluminescent marine bacterium *Vibrio fischeri*. *Nucleic Acid Research* 16, 777.

FOSTER, T. J., O'Reilly, M., PHONIMDAENG, P., COONEY, J., PATEL, A. H. and BRAMLEY, A. J. (1990) Genetic studies of virulence factors of *Staphylococcus aureus*. Properties of coagulase and gamma toxin, alpha-toxin, beta-toxin and protein A in the pathogenesis of *S. aureus* infections. In *Molecular Biology of the Staphylococci*. (Ed) R. P. Novick. UCH Publishers, New York.

FRACKMAN, S., ANHALT, M. and NEALSON, K. H. (1990) Cloning, organisation, and expression of the bioluminescence genes of *Xenorhabdus luminescens*. *Journal of Bacteriology* 172, 5767-5773.

FREITAG, N. E. and JACOBS, K. E. (1999) Examination of *Listeria monocytogenes* intracellular gene expression by using the green fluorescent protein of *Aequorea victoria*. *Infection and Immunity* 67, 1844-1852.

FREITAG, N. E., RON, L. and PORTNOY, D. A. (1993) Regulation of the PrfA transcriptional activator of *Listeria monocytogenes*: multiple promoter elements contribute to intracellular growth and cell-to-cell spread. *Infection and Immunity* 61, 2537-2544.

GAILLARD, J. L., BERCHE, P., FREHEL, C., GOUIN, E. and COSSART, P. (1991) Entry of *Listeria monocytogenes* into cells is mediated by internalin, a repeat protein reminiscent of surface antigens from Gram positive cocci. *Cell* 65, 1127-1141.

GAILLARD, J. L., BERCHE, P., MOUNIER, J., RICHARD, S. and SANSONETTI, P. (1987) In vitro model of penetration and intracellular growth of *L. monocytogenes* in human enterocyte-like cell line Caco-2. *Infection and Immunity* 55, 2822-2829.

- GAILLARD, J. L., JAUBERT, F. and BERCHE, P. (1996) The *inlAB* locus mediates the entry of *Listeria monocytogenes* into hepatocytes *in vivo*. *Journal of Experimental Medicine* 183, 359-369.
- GERDES, H. H. and KAETHER, C. (1996) Green fluorescent protein: applications in cell biology. *FEBS Letters* 389, 44-47.
- GLASER, S. M., YELTON, D. E. and HUSE, W. D. (1992) Antibody engineering by codon-based mutagenesis in a filamentous phage vector system. *Journal of Immunology* 149, 3903-3913.
- GOTTESMAN, S., CLARK, W. P., de CRECY-LAGARD, V. and MAURIZI, R. (1993) ClpX, an alternative subunit for the ATP-dependent Clp protease of *Escherichia coli*. *Journal of Biological Chemistry* 268, 22618-22626.
- GOTTESMAN, S., ROCHE, E., ZHOU, Y and SAUER, R. T. (1998) The ClpXP and ClpAP proteases degrade proteins with carboxy-terminal peptide tails added by the SsrA tagging system. *Genes Dev.* 12, 1338-1347.
- GOTTESMAN, S., WICKNER, S. and MAURIZI, M. R. (1997) Protein quality control: triage by chaperones and proteases. *Genes Dev.* 11, 815-823.
- GOUIN, E., MENGAUD, J., and COSSART, P. (1994) The virulence gene cluster of *Listeria monocytogenes* is also present in *Listeria ivanovii*, an animal pathogen; and *Listeria seeligeri*, a nonpathogenic species. *Infection and Immunity* 62, 3550-3553.
- GRAY, M. L. and KILLINGER, A. H. (1966) *Listeria monocytogenes* and listeric infections. *Bacteriol. Rev.* 30, 309-382.
- GREGORY, S. H., SAGNIMENI, A. J. and WING, E. J. (1996) Expression of the *inlAB* operon by *Listeria monocytogenes* is not required for entry into hepatic cells *in vivo*. *Infection and Immunity* 64, 3983-3986.
- GREIFFENBERG, L., SOKOLOVIC, Z., SCHNITTLER, H. J., SPORY, A., BÖCKMANN, R., GOEBEL, W. and KUHN, M. (1997) *Listeria monocytogenes* infected human umbilical vein endothelial cells: internalin-independent invasion, intracellular growth, movement, and host cell responses. *FEMS Microbiology Letters* 157, 163-170.

- GRIMAUD, R., KESSEL, M., BEURON, F., STEVENS, A. C. and MAURIZI, M. R. (1998) Enzymatic and structural similarities between the *Escherichia coli* ATP-dependent proteases, ClpXP and ClpAP. *Journal of Biological Chemistry* 273, 12476-12481.
- GRUSS, A. and EHRLICH, S. D. (1988) Insertion of foreign DNA into plasmids from Gram positive bacteria induces formation of high-molecular weight multimers. *Journal of Bacteriology* 170, 1183-1190.
- GRUSS, A., ROSS, H. and NOVICK, R. (1987) Functional analysis of a palindromic sequence required for normal replication of several staphylococcal species. *Proceedings of the National Academy of Science USA* 84, 2165-2169.
- HAMILL, R. J., VANN, J. M. and PROCTOR, R. A. (1986) Phagocytosis of *Staphylococcus aureus* by cultured bovine aortic endothelial cells: model for post-adherence events in endovascular infections. *Infection and Immunity* 54, 833-836.
- HASS, J., PARK, E. C and SEED, B. (1996) Codon usage limitations in the expression of HIV-1 envelope glycoprotein. *Current Biology* 6, 315-324.
- HASSLER, S. (1995) Green fluorescent protein: the next generation. *Bio Technology* 13, 103-104.
- HASTINGS, J. W., POTRIKAS, C. J., GUPTA, S. C., KURFURST, M. and MAKEMSON, J. C. (1985) Biochemistry and physiology of bioluminescent bacteria. *Advances in Microbiology and Physiology* 26, 235-291.
- HEIM, R. and TSIEN, R. Y. (1996) Engineering the green fluorescent protein for improved brightness, longer wavelengths and fluorescence resonance energy transfer. *Current Biology* 6, 178-182.
- HEIM, R., CUBITT, A. B. and TSIEN, R. Y. (1995) Improved green fluorescence. *Nature (London)*, 373, 663-664.
- HEIM, R., PRASHER, D. C. and TSIEN, R. Y. (1994) Wavelength mutations and posttranslational autoxidation of green fluorescent protein. *Proceedings of the National Academy of Science USA* 91, 12501-12504.

- HEINRICHS, J. H., BAYER, M. G. and CHEUNG, A. L. (1996) Characterisation of the *sar* locus and its interactions with *agr* in *Staphylococcus aureus*. *Journal of Bacteriology* 179, 418-423.
- HERMAN, C., THEVENET, D., BOULOC, P., WALKER, G. C. and D'ARI, R. (1998) Degradation of carboxy-terminal-tagged cytoplasmic proteins by the *Escherichia coli* protease HflB (FtsH) *Genes and Development* 12, 1348-1355.
- HILL, P. J. and STEWART, G. S. A. B. (1994) Use of *lux* genes in applied biochemistry. *Journal of Bioluminescence and Chemiluminescence* 9, 211-215.
- HILL, P. J., REES, C. E. D., WINSON, M. K. and STEWART, G. S. A. B. (1993) The application of *lux* genes. *Biotechnology and Applied Biochemistry* 17, 3-14.
- HILL, P. J., VINICOMBE, D. A., SOPER, C. J., SETLOW, P., WAITES, W. M., DENYER, S. and STEWART, G. S. A. B. (1994) Bioluminescence and spores as biological indicators or inimical processes. *Journal of Applied Bacteriology Symposium supplement* 76 129S-134S.
- HUDSON, M. C., RAMP, W. K., NICHOLSON, N. C., WILLIAMS, A. S. and NOUSIAINEN, M. T. (1995) Internalisation of *S. aureus* by cultured osteoblasts. *Microbial Pathogenicity* 19, 409-419.
- HUECK, C. J. and HILLEN, W. (1995) Catabolite repression in *Bacillus subtilis*: a global regulatory mechanism for the Gram positive bacteria. *Molecular Microbiology* 15, 395-401.
- HUECK, C. J., HILLEN, W. and SAIER, Jr, M. H. (1994) Analysis of a cis-active sequence mediating catabolite repression in Gram positive bacteria. *Research in Microbiology* 145, 503-518.
- HUECK, C. J., KRAUS, A., SCHMIEDEL, D. and HILLEN, W., (1995) Cloning, expression and functional analysis of the catabolite control protein CcpA from *Bacillus megaterium*. *Molecular Microbiology* 16, 855-864.
- IKEMYRA, I. (1981) Correlation between the abundance of *Escherichia coli* transfer RNAs and the occurrence of the respective codons in its protein sequence. *Journal Molecular Biology* 146, 1-21.

- INOUE, S. and TSUJI, F. I. (1994) *Aequorea* green fluorescent protein: Expression of the gene and fluorescence characteristics of the recombinant protein. *FEBS Letters* 341, 277-280.
- INOUE, S., NOGUCHI, M., SAKAKI, Y., TAKAGI, Y., MIYATA, T., IWANAGA, S., MIYATA, T. and TSUJI, F. I. (1985). Cloning and sequence analysis of cDNA for the luminescent protein aequorin. *Proceedings of the National Academy of Science USA* 82, 3154-3158.
- JACOBS, M., HILL, P. J. and STEWART, G. S. A. B. (1991) Highly bioluminescent *Bacillus subtilis* obtained through high-level expression of a *luxAB* fusion gene. *Molecular General Genetics* 230, 251-256.
- JANZON, L. and ARVIDSON, S. (1990) The role of the delta-lysin gene (*hld*) in the regulation of virulence genes by the accessory gene regulator (*agr*) in *Staphylococcus aureus*. *EMBO Journal* 9, 1391-1399.
- JANZON, L., LOFDAHL, S. and ARVIDSON, S. (1989) Identification of the delta-lysin gene, *hld*, adjacent to the accessory regulator (*agr*) of *Staphylococcus aureus*. *Molecular General Genetics* 219, 480-485.
- Ji, G., BEAVIS, R. and NOVICK, R. P. (1997) Bacterial interference caused by autoinducing peptide variants. *Science* 276, 2027-2030.
- Ji, G., BEAVIS, R. C. and Novick, R. P. (1995) Cell density control of staphylococcal virulence mediated by an octapeptide pheromone. *Proceedings of the National Academy of Science USA* 92, 12055-12059.
- JOHNSON, F. H. and SHIMOMURA, O. (1978) *Methods in Enzymology* 57, 271-291.
- KAIN, S. R., ADAMS, M., KONDEPUDI, A., YANG, T. T., WARD, W. W. and KITTS, P. (1995) Green fluorescent protein as a reporter of gene expression and protein localisation. *Bio Techniques* 19, 650-655.
- KARZAI, A. W., SUSSKIND, M. M. and SAUER, R. T. (1999) SmpB, a unique RNA-binding protein essential for the peptide-tagging activity of SsrA (tmRNA). *The EMBO Journal* 18, 3793-3799.

- KATAYAMA, Y., GOTTESMAN, S., PUMPHREY, J., RUDIKOFF, S., CLARK, W. P. and MAURIZI, M. R. (1988) The two component, ATP dependent Clp protease of *Escherichia coli*. Purification, cloning and mutational analysis of the ATP binding component. *Journal of Biological Chemistry* 263, 15226-15236.
- KEILER, K. C., WALLER, P. R. H. and SAUER, R. T. (1996) Role of a peptide tagging system in degradation of proteins synthesised from damaged messenger RNA. *Science* 271, 990-993.
- KINSMAN, O. S. (1986) Models for staphylococci colonisation and skin infections. In *Experimental Models in Antimicrobial Chemotherapy*. Vol 2, p. 135-146. Eds. Zak and Sande
- KLEEREBEZEM, M., QUADRI, L. E. N., KUIPERS, O. P. and de VOS, W. M. (1997) Quorum sensing by peptide pheromones and two-component signal-transduction systems in Gram positive bacteria. *Molecular Microbiology* 24, 895-904.
- KLOOS, W. E., ORBAN, B. S. and WALKER, D. D. (1981) Plasmid composition of *Staphylococcus* species. *Can. J. Microbiol.* 27, 271-278.
- KNUTTON, S., BALDWIN, T., WILLIAMS, P. H. and McNEISH, A. S. (1989) Actin accumulation at sites of bacterial adhesion to tissue culture cells: Basis of a new diagnostic test for enteropathogenic and enterohemorrhagic *Escherichia coli*. *Infection and Immunity* 57, 1290-1298.
- KOCKS, C., GOUIN, E., TABOURET, M., BERCHE, P., OHAYON, H. and COSSART, P. (1992) *Listeria monocytogenes* induced actin assembly requires the *actA* gene product, a surface protein. *Cell* 68, 521-531.
- KOMINE, Y., KITABATAKE, M., YOKOGAWA, T., NISHIKAWA, K. and INIKUCHI, H. (1994) A tRNA like structure is present in 10Sa RNA, a small stable RNA from *Escherichia coli*. *Proceedings of the National Academy of Science USA* 91, 9223-9227.
- KORNBLUM, J., KREISWIRTH, B., PROJAN, S., ROSS, H. and NOVICK, R. P. (1990) *Agr*: a polycistronic locus regulating exoprotein synthesis in *Staphylococcus aureus*, p.373-402. In *Molecular Biology of the staphylococci*. VCY Publishers, New York.

- KUHN, M. and GOEBEL, W. (1995) Molecular studies on the virulence of *Listeria monocytogenes*. *Genetic Engineering* 17, 31-51.
- KUHN, M. and GOEBEL, W. (1998) Host cell signalling during *Listeria monocytogenes* infection. *Trends in Microbiology* 6, 11-15.
- KUHN, M., KATHARIOU, and Goebel, W. (1988) Hemolysis supports survival but not entry of the intracellular bacterium *Listeria monocytogenes*. *Infection and Immunity* 56, 3477-3486.
- KURLAND, C. and GALLANT, J. (1996) Errors of heterologous protein expression. *Current Opinion in Biotechnology* 7, 489-493.
- LAMPIDIS, R., GROSS, R., SOKOLOVIC, Z., GOEBEL, W. and KREFT, J. (1994) The virulence regulator protein of *Listeria ivanovii* is highly homologous to PrfA from *Listeria monocytogenes* and both belong to the Crp-Fnr family of transcription regulators. *Molecular Microbiology* 13, 141-151.
- LAWLIS, B., DENNIS, M., CHEN, E., SMITH, D. and HENNER, D. (1984) Cloning and sequencing of the xylose isomerase and xylulose kinase genes of *Escherichia coli*. *Applied Environmental Microbiology* 47, 5-21.
- LEBRUN, M., MENGAUD, J., OHAYON, H., NATO, F. and COSSART, P. (1996) Internalin must be on the bacterial cell surface to mediate entry of *Listeria monocytogenes* into epithelial cells. *Molecular Microbiology* 21, 579-592.
- LECUIT, M., OHAYON, H., BRAUN, L., MENGAUD, J. and COSSART, P. (1997) Internalin of *Listeria monocytogenes* with an intact leucine-rich repeat region is sufficient to promote internalisation. *Infection and Immunity* 65, 5309-5319.
- LEE, C. Y., SZITTNER, R. and MEIGHEN, E. A. (1991) The *lux* genes of the luminous bacterial symbiont, *Photobacterium leiognathi*, of the ponyfish. *European Journal of Biochemistry* 201, 161-167.
- LEIMEISTER-WÄCHTER, M., HAFFNER, C., DOMANN, E., GOEBEL, W. and CHAKRABORTY, T. (1990) Identification of a gene that positively regulates expression of listeriolysin, the major virulence factor of *Listeria monocytogenes*. *Proceedings of the National Academy of Science USA* 87, 8336-8340.

- LINA, G., JARRAUD, S., Ji, G., GREENLAND, T., PEDRAZA, A., ETIENNE, J., NOVICK, R. P. and VANDENESCH, F. (1998) Transmembrane topology and histidine protien kinase activity of AgrC, the *agr* signal receptor in *Staphylococcus aureus*. *Molecular Microbiology* 28, 655-662.
- LOFDAHL, S., MORFELDT, E., JANZON, L. and ARVIDSON, S. (1988) Cloning of a chromosomal locus (*exp*) which regulates the expression of several exoprotein genes in *Staphylococcus aureus*. *Molecular General Genetics* 211, 435-440.
- LYBARGER, L., DEMPSEY, D., PATTERSON, G. H., PISTON, D. W., KAIN, S. R. and CHERVENAK, R. (1998) Dual colour flow cytometric detection of fluorescent proteins using single laser (488nm) excitation. *Cytometry* 31, 147-152.
- MANCICI, J. A., BOYLAN, M., SOLY, R. R., GRAHAM, A. F. and MEIGHEN, E. A. (1988) Cloning and expression of the *Photobacterium phosphoreum* luminescence system demonstrates a unique *lux* organisation. *Journal of Biological Chemistry* 263, 14308-14314.
- MANNA, A. C., BAYER, M. G. and CHEUNG, A. L. (1998) Transcriptional analysis of different promoters in the *sar* locus in *Staphylococcus aureus*. *Journal of Bacteriology* 180, 3828-3836.
- MARGOLIN, W. (1998) A green light for the bacterial cytoskeleton. *Trends in Microbiology* 6, 233-238.
- MAURIZI, M. R., CLARK, W., KIM, S. H., and GOTTESMAN, S. (1990) ClpP represent a unique family of serine proteases. *Journal of Biological Chemistry* 265, 12546-12552.
- MAYVILLE, P., JI, G., BEAVIS, R., YANG, H., GOGER, M., NOVICK, R. P. and MUIR, T. W. (1999) Structure and analysis of synthetic autoinducing thiolactone peptides from *Staphylococcus aureus* responsible for virulence. *Proceedings of the National Academy of Science USA* 96, 1218-1223.
- MEIGHEN, E. A. (1988) Enzymes and genes from the *lux* operons of bioluminescent bacteria. *Annual Review of Microbiology* 42, 151-176.
- MEIGHEN, E. A. (1991) Molecular biology of bacterial bioluminescence. *Microbiological Reviews* 55, 123-142.

- MEIGHEN, E. a. (1993) Bacterial bioluminescence: organisation, regulation, and application of the *lux* genes. *FASEB Journal* 7, 1016-1022.
- MEIGHEN, E. A. (1994) Genetics of bacterial bioluminescence. *Annual Review of Genetics* 28, 117-139.
- MENGAUD, J., DRAMSI, S., GOUIN, E., VAZQUEZ-BOLAND, J. A., MILON, G. and COSSART, P. (1991) Pleiotropic control of *Listeria monocytogenes* virulence factors by a gene that is autoregulated. *Molecular Microbiology* 5, 2273-2283.
- MENGAUD, J., OHAYON, H., GOUNON, P., MÈGE, R. M. and COSSART, P. (1996) E-cadherin is the receptor for internalin, a surface protein required for entry of *Listeria monocytogenes* into epithelial cells. *Cell* 84, 923-932.
- MENZIES, B. E. and KOURTEVA, I. (1998) Internalisation of *Staphylococcus aureus* by endothelial cells induces apoptosis. *Infection and Immunity* 66, 5994-5998
- MILENBACHS, A. A., BROWN, D. P., MOORS, M. and YOUNGMAN, P. (1997) Carbon-source regulation of virulence gene expression in *Listeria monocytogenes*. *Molecular Microbiology* 23, 1075-1085.
- MISTELI, T. and SPECTOR, D. L. (1997) Applications of the green fluorescent protein in cell biology and biotechnology. *Nature Biotechnology* 15, 961-964.
- MITRA, R. D., SILVA, C. M. and YOUNG, D. C. (1996) Fluorescence resonance energy transfer between blue-emitting and red shifted excitation derivatives of the green fluorescent protein. *Gene* 173, 13-17.
- MORFEDLT, E., JANZON, L., ARVIDSON, S. and LÖFDAHL, S. (1988) Cloning of a chromosomal locus (*exp*) which regulates the expression of several exoprotein genes in *Staphylococcus aureus*. *Molecular General Genetics* 211, 435-440.
- MORFELDT, E., PANOVA-SAPUNDJIEVA, I., GUSTAFSSON, B. and ARVIDSON, S. (1996) Detection of the response regulator AgrA in the cytosolic fraction of *Staphylococcus aureus* by monoclonal antibodies. *FEMS Microbiology Letters* 143, 195-201.

- MORFELDT, E., TEGMARK, K. and ARVIDSON, S. (1996) Transcriptional control of the *agr*-dependent virulence gene regulator, RNAIII, in *Staphylococcus aureus*. *Molecular Microbiology* 21, 1227-1237.
- MORIN, J. G. and HASTINGS, J. W. (1971) Energy transfer in a bioluminescent system. *Journal of Cell Physiology* 77, 313-318.
- MORISE, H., SHIMOMURA, O., JOHNSON, F. H. and MINANT, J. (1974) Intermolecular energy transfer in the bioluminescent system of *Aequorea*. *Biochemistry* 13, 2656-2662.
- MOUNIER, J., RYTER, A., COQUIS-RONDON, M. and SANSONETTI, P. J. (1990) Intracellular and cell to cell spread of *Listeria monocytogenes* involves interaction with F-actin in the enterocyte-like cell line Caco-2. *Infection and Immunity* 58, 1048-1058.
- MUTO, A., SATO, S., TADAKI, T., FUFUSHIMA, M., USHIDA, C. and HIMENO, H. (1996) Structure and function of 10Sa RNA: trans-translation system. *Biochimie* 78, 985-991.
- MUTO, A., USHIDA, C. and HIMENO, H. (1988) A bacterial RNA that functions as both a tRNA and a mRNA. *Trends in Biochemical Sciences* 23, 25-29.
- NEALSON G. M. and ESCHER, A. (1998) Visualising the chaperonin-mediated folding of a luciferase-GFP fusion. , p.425-428. In A. Roda, Pazzagli, M, L. J. Kricka, and P. E. Stanley (ed) *Bioluminescence and chemiluminescence perspectives for the 21st century*, Proceeding of the 10th International symposium, John Wiley and Sons, Inc.
- NIXON, B. T., RONSON, C. W. and AUSUBEL, R. M. (1986) Two-component regulatory systems responsive to environmental stimuli share strongly conserved domains with the nitrogen assimilation regulatory genes *ntrB* and *ntrC*. *Proceedings of the National Academy of Science USA* 83, 7850-7854.
- NOVICK, R. P. (1999) Regulation of pathogenicity in *Staphylococcus aureus* by a peptide based density sensing system. In *Cell-Cell Signalling in Bacteria*, p. 129-146. Eds. G. M. Dunny and S. C. Winans. American Society for Microbiology, Washington, D. C.

- NOVICK, R. P. and MUIR, T. W. (1999) Virulence gene regulation by peptides in staphylococci and other Gram positive bacteria. *Current Opinion in Microbiology* 2, 40-45.
- NOVICK, R. P., PROJAN, S., KORNBLUM, J., ROSS, H., KREISWIRTH, B. and MOGHAZEH, S. (1995) The *agr* P-2 operon: an autocatalytic sensory transduction system in *Staphylococcus aureus*. *Molecular General Genetics* 248, 446-458.
- NOVICK, R. P., ROSS, H. F., PROJAN, S. J., KORNBLUM, J., KREISWIRTH, B. and MOGHAZEH, S. (1993) Synthesis of staphylococcal virulence factors in controlled by a regulatory RNA molecule, *EMBO Journal* 12, 3967-3975.
- O'FARRELL, P. H. (1975) High-resolution two-dimensional electrophoresis of proteins. *Journal of Biological Chemistry* 250, 4007-4021.
- O'KANE, D. J. and PRASHER, D. C. (1992) Evolutionary origins of bacteriology bioluminescence. *Molecular Microbiology* 6, 443-449.
- O'KANE, D. J., LINGLE, W. L., WAMPLER, J. E., LEGOCKI, M., LEGOCKI, R. P. and STALAY, A. A. (1988) Visualisation of bioluminescence as a marker of gene expression in *rhizobium* infected soybean root nodules. *Plant Molecular Biology* 10, 387-399.
- OGAWA, H., INOUE, S., TSUJI, F. I., YASUDA, K. and UMESONO, K. (1995) Localisation, trafficking, and temperature dependence of the *Aequorea* green fluorescent protein in cultured vertebrate cells. *Proceedings of the National Academy of Science USA* 92, 11899-11903.
- ORMÖ, M., CUBITT, A. B., KALLIO, K., GROSS, L. A., TSIEN, R. Y. and REMINGTON, S. J. (1996) Crystal structure of the *Aequorea victoria* green fluorescent protein. *Science* 273, 1392-1395.
- OROSZ, A., BOROS, I. And VENETIANER, P. (1991) Analysis of the complex transcription termination region of the *Escherichia coli rrnB* gene. *European Journal of Biochemistry* 201, 653-659.
- PARK, S. F. AND STEWART, G. S. A. B. (1990) High-efficiency transformation of *Listeria monocytogenes* by electroporation of penicillin treated cells. *Gene*, 94, 129-132.

- PATON, G. I., PALMER, G., BURTON, M., RATTRAY, E. A. S., McGRATH, S. P., GLOVER, L. A. and KILLHAM, K. (1997) Development of an acute and chronic ecotoxicity assay using *lux*-marker *Rhizobium leguminosarum* biovar *trifolii*. *Letters in Applied Microbiology* 24, 296-300.
- PENG, H. L., NOVICK, R. P., KREISWIRTH, B., KORNBLUM, J. and SCHLIEVERT, P. (1988) Cloning, characterisation and sequencing of an accessory gene regulator (*agr*) in *Staphylococcus aureus*. *Journal of Bacteriology* 179, 4365-4372.
- PINES, J. (1995) GFP in mammalian cell. *Trends in Genetics* 11, 326-327.
- PORANKIEWICZ, J., WANG, J. and CLARKE, A. K. (1999) New insights into the ATP-dependent Clp protease: *Escherichia coli* and beyond. *Molecular Microbiology* 32, 449-458.
- PORTNOY, D. A. T., CHAKRABORTY, W., GOEBEL, W. and COSSART, P. (1992) Molecular determinants of *Listeria monocytogenes* pathogenesis. *Infection and Immunity* 60, 1263-1267.
- POYART, C., ABACHIN, E., RAZAFIMANANTSOA, I. and BERCHE, P. (1993) The zinc metalloprotease of *L. monocytogenes* is required for maturation of phosphatidylcholin phospholipase C: direct evidence obtained by gene complementation. *Infection and Immunity* 61, 1576-1580.
- PRASHER, D. (1995) Using GFP to see the light. *Trends in Genetics* 11, 320-323.
- PRASHER, D. C., ECKENRODE, V. K., WARD, W. W., PRENDERGAST, F. G. and CORMIER, M. J. (1992) Primary structure of the *Aequorea victoria* green fluorescent protein. *Gene* 111, 229-233.
- PROCTOR, R. A., BALWIT, J. M. and VESGA, O. (1994) Variant subpopulations of *Staphylococcus aureus* as cause of persistent and recurrent infections. *Infect. Agents Dis.* 3, 302-312.
- PROJAN, S. and NOVICK, R. (1997) The molecular basis of virulence, p.55-81. In G. Archer and K. CROSSLEY (ed) *staphylococci in human disease*. Churchill Livingstone, New York.

- QAZI, S. N. A., HILL, P. J. and REES, C. E. D. (1998) Expression of green fluorescent protein (GFP) in Gram positive bacteria, p.463-466. In A. Roda, Pazzagli, M, L. J. Kricka, and P. E. Stanley (ed) *Bioluminescence and chemiluminescence perspectives for the 21st century*, Proceeding of the 10th International symposium, John Wiley and Sons, Inc.
- QIAN, L. and WILKINSON, M. (1989) DNA fragment purification: Removal of agarose 10 minutes after electrophoresis. *Bio Techniques* 10, 736-738.
- RECHTIN, T. M., GILLASPY, A. F., SCHUMACHER, M. A., BRENNAN, R. G., SMELTZER, M. S. and HURLBURT, B. K. (1999) Characterisation of the SarA virulence gene regulation of *Staphylococcus aureus*. *Molecular Microbiology* 33, 307-316.
- RECSEI, P., KREISWIRTH, B., O'REILLY, M., SCHLIEVERT, P., GRUSS, A. and NOVICK, R. (1986) Regulation of exoprotein gene expression by *agr*. *Molecular General Genetics* 202, 58-61.
- RENZONI, A., KLARSFELD, A., DRAMSI, S. and COSSART, P. (1997) Evidence that PrfA, the pleiotropic activator of virulence genes in *Listeria monocytogenes*, can be present but inactive. *Infection and Immunity* 65, 1515-1518.
- RIENDEAU, D. A., RODRIGUEZ, A. and MEIGHEN, E. A. (1982) Resolution of the fatty acid reductase from *Photobacterium phosphoreum* into acyl-protein synthetase and acyl-CoA reductase activities. Evidence for an enzyme complex. *Journal of Biological Chemistry* 257, 6908-6915.
- RIPIO, M. T., VAZQUEZ-BOLAND, J. A., VEGA, Y., NAIR, S. and BERCHE, P. (1998) Evidence for expressional crosstalk between the central virulence regulator PrfA and the stress response mediator ClpC in *Listeria monocytogenes*. *FEMS Microbiology Letters* 158, 45-50.
- RIZZUTO, R., BRINI, M., DE GIORGI, F., ROSSI, R., HEIM, R., TSIEN, R. Y. and POZZAN, T. (1996) Double labelling of subcellular structures with organelle-targeted GFP mutants *in vivo*. *Current Biology* 6, 183-188.
- RIZZUTO, R., BRINI, M., PIZZO, P., MURGIA, M. and POZZAN, T. (1995) Chimeric green fluorescent protein as a tool for visualising subcellular organelles in living cells. *Current Biology* 5, 635-642.

- ROBART, F. D. and WARD, W. W. (1990) Solvent perturbations of *Aequorea* green fluorescent protein. *Photochemistry and Photobiology* 51, 92s.
- RODRIGUEZ, A., RIENDEAU, D. and MEIGHEN, E. (1983a) Purification of the acyl-CoA reductase component from a complex responsible for the reduction of fatty acids in bioluminescent bacteria. Properties and acyl-transferase activity. *Journal of Biological Chemistry* 258, 5233-5238.
- RODRIGUEZ, A., WALL, L., RIENDEAU, D. and MEIGHEN, E. A. (1983b) Fatty acid acylation of proteins in bioluminescent bacteria. *Biochemistry* 22, 5604-5611.
- ROPP, J. D., DONAHUE, C. J., WOLFGANG-KIMBALL, D., HOOLEY, J. J., CHIN, J. Y. W., HOFFMAN, R. A., CUTHBERTSON, R. A. and BAUER, K. D. (1995) *Aequorea* green fluorescent protein analysis by flow cytometry. *Cytometry* 21, 309-317.
- ROTH, A. (1985) Purification and protease susceptibility of the green fluorescent protein of *Aequorea victoria* with a note on *Halistra ura*. Ph.D. Thesis, Rutgers University, New Brunswick, NJ.
- RYGUS, T. and HILLEN, W. (1991) Inducible high-level expression of heterologous genes in *Bacillus megaterium* using the regulatory elements of the xylose utilisation operon. *Applied Microbiology and Biotechnology* 35, 594-599.
- RYGUS, T. and HILLEN, W. (1992) Catabolite repression of the *xyl* operon in *Bacillus megaterium*. *Journal of Bacteriology* 174, 3049-3055.
- SAIKI, R., GELFANO, D. H., STOFFEL, S., SCHARF, S. J., HIGUCHI, R., HORN, G. J., MULLIS, K. B. and ERLICH, A. H. (1988) Primer directed enzymatic amplification of DNA with a thermostable DNA polymerase. *Science* 239, 487-491.
- SAMBROOK, J., FRITSCH, E. F. and MANIATIS, T. (1989). *Molecular cloning: a laboratory manual* 2nd Ed. Cold Spring harbour Press, Cold Spring Harbour, New York.
- SCHIRMER, E. C., CLOVER, J. R., SINGER, M. A. and LINDQUIST, S. (1996) Hsp100 / Clp proteins: a common mechanism explains diverse functions. *Trends in Biochemical Sciences* 21, 289-296.

- SCHMIEDEL, D., KINTRUP, M., KÜSTER, E. and HILLEN, W. (1997) Regulation of expression, genetic organisation and substrate specificity of xylose uptake in *Bacillus megaterium*. *Molecular Microbiology* 23, 1053-1062.
- SCHNEEWIND, O., MODEL, P. and FISCHETTI, V. A. (1992) Sorting of protein-A to the staphylococcal cell wall. *Cell* 70, 267-281.
- SCOTT, K. P., MERCER, D. K., GLOVER, L. A. and FLINT, H. J. (1998) The green fluorescent protein as a visible marker for lactic acid bacteria in complex ecosystems. *FEMS Microbiology Ecology* 23, 219-230.
- SEELIGER, H. P. R. (1988) Listeriosis-history and actual development. *Infection and Immunity* 16, 81-85.
- SEOL, J. H., BAEK, S. H., KANG, M. S., HA, D. B. and CHUNG, C. H. (1995) Distinctive roles of the two ATP-binding sites in ClpA, the ATPase component of Ti in *Escherichia coli*. *Journal of Biological Chemistry* 270, 8087-8092.
- SHAW, J. J. and KADO, C. (1985) Development of a *Vibrio* bioluminescence gene-set to monitor phytopathogenic bacteria during the ongoing disease process in a non-disruptive manner. *Bio Technology* 4, 560-564.
- SHEEHAN, B., KLARSFELD, T., EBRIGHT, R. and COSSART, P. (1996) A single substitution in the putative helix-turn-helix motif of the pleiotropic activator PrfA attenuates *Listeria monocytogenes* virulence. *Molecular Microbiology* 20, 785-797.
- SHEEHAN, B., KOCKS, C., DRAMSI, S., GOUIN, S., KLARSFELD, A. D., MENGAUD, J. and COSSART, P. (1994) Molecular and genetic determinants of the *Listeria monocytogenes* infectious process. *Current Topics in Microbiology and Immunology* 192, 187-216.
- SHIMOMURA, O., JOHNSON, F. H. and SAIGA, Y. (1962) Extraction, purification and properties of aequorin, a bioluminescent protein from the luminous hydromedusan, *Aequorea*. *J. Cell Comp. Physiol.* 59, 223-239.
- SILBER, K.R. and SAUER, R.T. (1994) Deletion of the *prc* (*tsp*) gene provides evidence for additional tail-specific proteolytic activity in *Escherichia coli* K-12. *Molecular General Genetics* 242, 237-240.

- SILVERMAN, M., MARTIN, M. and ENGEBRECHT, J. (1989) Regulation of luminescence in marine bacteria. In *Genetics of Bacterial Diversity*, p 71-86. Eds. Hopwood., D. A. and Chater, K. F. Academic Press, London.
- SINGH, S. K. and MAURIZI, M. R. (1994) Mutational analysis demonstrates different functional roles for the two ATP-binding sites in ClpAP protease from *Escherichia coli*. *Journal of Biological Chemistry* 269, 29537-29545.
- SMITH, C. K., BAKER, T. A. and SAUER, R. T. (1999) Lon and Clp family proteases and chaperones share homologous substrate-recognition domains. *Proceedings on the National Academy of Science USA* 96, 6678-6682.
- SMITH, G. S., MARQUIS, H., JONES, S., JOHNSTON, N. C., PORTNOY, D. A. and GOLDFINE, H. (1995) The two distinct phospholipases C of *Listeria monocytogenes* have overlapping roles in escape from a vacuole and cell-to-cell spread. *Infection and Immunity* 63, 4231-4237.
- SOLY, R. R., MANCINI, J. A., FERRI, S. R., BOYLAN, M. and MEIGHEN, E. A. (1988) A new *lux* gene in bioluminescent bacteria codes for a protein homologous to the bacterial luciferase subunits. *Biochemical and Biophysical Research Communications* 155, 351-358.
- SPANJAARD, R. A. and VAN DUIN, J. (1988) Translation of the sequence AGG-AGG yields 50% ribosomal frameshift. *Proceedings of the National Academy of Science USA* 85, 7967-7971.
- SQUIRES, C. and SQUIRES, C. L. (1992) The Clp proteins: proteolysis regulators or molecular chaperones. *Journal of Bacteriology* 174, 1081-1085.
- STEARNS, T. (1995) The green revolution. *Current Biology* 5, 262-264.
- STEWART, G. S. A. B. and WILLIAMS, P. (1992) *lux* genes and the applications of bacterial bioluminescence. *Journal of General Microbiology* 138, 1289-1300.
- STEWART, G. S. A. B., LUBINSKY-MINK, S., JACKSON, C. G., CASSEL, A. and KUHN, J. (1986) Phg165: a pRB322 copy number derivative of pUC8 for cloning and expression. *Plasmid* 15, 172-181.

- STEWART, G. S. A. B., SMITH, A. T. and DENYER, S. P. (1989) Genetic engineering of bioluminescent bacteria. *Food Science and Technology Today* 2, 7-10.
- SULLIVAN, M. A., YABABIN, R. E. and YOUNG, F. E. (1984) New shuttle vectors for *Bacillus subtilis* and *Escherichia coli* which allow rapid detection of inserted fragments. *Gene* 29, 21-26.
- SURPIN, M. A. and WARD, W. W. (1989) Reversible denaturation of *Aequorea* green fluorescent protein – thiol requirement. *Photochemistry and Photobiology* 49, WPM-B2.
- TADAKI, T., FUKUSHIMA, M., USHIDA, C., HIMENO, H. and MUTO, A. (1995) Interaction of 10Sa RNA with ribosomes in *Escherichia coli*. *FEBS Letters* 399, 223-226.
- TANNAHILL, D., BRAY, S. and HARRIS, W. A. (1995) A drosophila (spl) gene is neurogenic in *Xenopus*-a green fluorescent protein study. *Developmental Biology* 168, 694-697.
- TE RIELE, H., MICHEL, B., and EHRLICH, S. D. (1986) Single stranded DNA in *Bacillus subtilis* and *Staphylococcus aureus*. *Proceedings of the National Academy of Science USA* 83, 2541-2545.
- TEGMARK, K., MORFELDT, E. and ARVIDSON, S. (1998) Regulation of *agr*-dependent virulence genes in *Staphylococcus aureus* by RNA III from coagulase-negative staphylococci. *Journal of Bacteriology* 180, 3181-3186.
- THERIOT, J. A., MITCHISON, T. J., TILNEY, L. G. and PORTNOY, D. A. (1992) The rate of actin-based motility of intracellular *Listeria monocytogenes* equals the rate of actin polymerisation. *Nature* 357, 257-260.
- THOMPSON, M. W. and MAURIZI, M. R. (1994) Activity and specificity of *Escherichia coli* ClpAP protease in cleaving model peptide substrates. *Journal of Biological Chemistry* 269, 18201-18208.
- THOMPSON, M. W., SINGH, S. K. and MAURIZI, M. R. (1994) Processive degradation of proteins by the ATP-dependent Clp protease from *Escherichia coli*: requirement for the multiple array of active sites in ClpP but not ATP hydrolysis. *Journal of Biological Chemistry* 269, 18209-18215.

- TILNEY, L. G. and PORTNOY, D. A. (1989) Actin filaments and the growth and movement, and the spread of the intracellular bacterial parasite, *Listeria monocytogenes*. *Journal of Cell Biology* 109, 1597-1608.
- TILNEY, L. G. and TILNEY, M. S. (1993) The wily ways of a parasite: induction of actin assembly by *Listeria*. *Molecular Microbiology* 1, 25-31.
- TOMBOLINI, R., UNGE, A., DAVEY, M. E., de BRUIJN, F. J. and JANSSON, J. K. (1997) Flow cytometric and microscopic analysis of GFP-tagged *Pseudomonas fluorescens* bacteria. *FEMS Microbiology Ecology* 22, 17-28.
- TU, G. F., REIS, G. E., ZHANG, J. G., MORITZ, R. L. and SIMPSON, R. J. (1995) C-terminal expression of truncated recombinant proteins in *Escherichia coli* with a 10Sa RNA decapeptide. *Journal of Biological Chemistry* 270, 9322-9326.
- TYAGI, J. S. and KLINGER, A. K. (1992) Identification of the 10Sa RNA structural gene of *Mycobacterium tuberculosis*. *Nucleic Acid Research* 20, 138.
- UNGE, A., TOMBOLINI, R., MØLBAK, L. and JANSSON, J. (1999) Simultaneous monitoring of cell number and metabolic activity of specific bacterial populations with a dual *gfp-luxAB* marker system. *Applied and Environmental Microbiology* 65, 813-821.
- USHIDA, C., HIMENO, T., WATANABE, T. and MUTO, A. (1994) tRNA like structures in 10Sa RNAs of *Mycoplasma capricolum* and *Bacillus subtilis*. *Nucleic Acid Research* 22, 3392-3396.
- VANN, J. M. and PROCTOR, R. A. (1987) Ingestion of *Staphylococcus aureus* by bovine endothelial cells results in real time and dose dependent damage to endothelial cell monolayers. *Infection and Immunity* 55, 2155-2163.
- VAZQUEZ-BOLAND, J. A., KOCKS, C., DRAMSI, S., OHAYON, H., GEFOFFROY, C., MENGAUD, J. and COSSART, P. (1992) Nucleotide sequence of the lecithinase operon of *Listeria monocytogenes* and possible role of lecithinase in cell-to-cell spread. *Infection and Immunity* 60, 219-230.
- VELLANOWETH, R. L. Translation and its regulation. In: Sonenshein AL, Hoch JA, Losick R, editors. *Bacillus subtilis and Other Gram Positive Bacteria, Biochemistry, Physiology and Molecular Genetics*. Washington, D.C: American Society for Microbiology, 1993: 699-711.

- WANG, J., HARTLING, J. A. and FLANAGAN, J. M. (1997) The structure of ClpP at 2.3Å resolution suggests a model for ATP-dependent proteolysis. *Cell* 91, 447-465.
- WANG, S. and HAZELRIGG, T. (1994) Implications for *bcd* mRNA localisation from spatial distribution of exu protein in *Drosophila* oogenesis. *Nature* 369, 400-403.
- WARD, W. W. (1979) In *Photochemical and Photobiological Reviews*, 4, 1-57, e.d. K. C. Smith, Plenum, New York.
- WARD, W. W. (1981) Properties of the Coelenterate green fluorescent protein, p235-242. In *Bioluminescence and Chemiluminescence: Basic Chemistry and Analytical application*. Eds. DeLuca, M and McElroy, W. D. Academic Press, NY.
- WARD, W. W. and BOKMAN, S. H. (1982) Reversible denaturation of *Aequorea* green fluorescent protein: physical separation and characterisation of the renatured protein. *Biochemistry* 21, 4535-4550.
- WARD, W. W., CODY, C. W. and HART, R. C. (1980) Spectrophotometric identity of the energy transfer chromophores in *Renilla* and *Aequorea* green fluorescent proteins. *Photochemistry and Photobiology Review* 31, 611-615.
- WAWRZYNOW, A., BANECKI, B. and ZYLICZ, M. (1996) The Clp ATPase define a novel class of molecular chaperones. *Molecular Microbiology* 21, 895-899.
- WEISS, B., JACQUEMIN-SABLON, A., LINE, T. R., FAREED, G. C. and RICHARDSON, C. C. (1968) Enzymatic breakage and rejoining of deoxyribonucleic acid. *Journal of Biological Chemistry* 243, 4543-4555.
- WESSON, C. A., LIU, L. E., TODD, K. M., BOHACH, G. A., TRUMBLE, W. R. and BAYLES, K. W. (1998) *Staphylococcus aureus* *Agr* and *Sar* global regulators influence internalisation and induction of apoptosis. *Infection and Immunity* 66, 5238-5243.
- WILLIAMS, K. P. and BARTEL, D. P. (1996) Phylogenetic analysis of tmRNA secondary structure. *RNA* 2, 1306-1310.

- WILLIAMS, K. P. and BARTEL, D. P. (1998) The tmRNA website. *Nucleic Acids Research* 26, 163-165.
- YANG, F., MOSS, L. G. and PHILLIPS, G. N. Jr. (1996) The molecular structure of green fluorescent protein. *Nature Biotechnology* 14, 1246-1251.
- YANG, T. T., SINAI, P., GREEN, G., KITTS, P. A., CHEN, Y. T., LYBARGER, L., CHERVENAK, R., PATTERSON, G. H., PISTON, D. W. and KAIN, S. R. (1998) Improved green fluorescence and dual colour detection with enhanced blue and green variants of the green fluorescent protein. *Journal of Biological Chemistry* 273, 8212-8216
- YANISH-PERRON, C., VIERA, J. and MESSING, J. (1985) Improved M13 phage cloning vectors and host strains: nucleotide sequences of the M13amp18 and pUC vectors. *Gene* 33, 103-119.
- YAO, L., BENGUALID, V., LOWY, F. D., GIBBONS, J. J., HATCHER, V. B. and BERMAN, J. W. (1995) Internalisation of *Staphylococcus aureus* by endothelial cells induces cytokine gene expression. *Infection and Immunity* 63, 1835-1839.
- YOUVAN, D. C. and MICHEL-BEYERLE. (1996) Structure and fluorescence mechanism of GFP. *Nature Biotechnology* 14, 1219-1221.

APPENDICES

APPENDIX 1: PCR PRIMERS USED IN THE COURSE OF THE PROJECT

All primer sequences are given in a 5' to 3' direction

Restriction endonuclease sites are indicated in bold

Primer Reference number	Forward or Reverse Primer	Incorporated Restriction Site	Primer Sequence
Primer 1 <i>gfp</i>	Forward	<i>Sma</i> I	CCG GAT CCC GGG AGG AGG AAC AAA GAT GAG TAA AGG AG
Primer 2 <i>gfp</i>	Reverse	<i>Sal</i> I	TTA CGC GTC GAC ACA TTT ATT TGT ATA GTT C
Primer 3 Unstable <i>gfp</i>	Reverse	<i>Sal</i> I	CTG GAT GTC GAC ACA GGA GTC CAA GCT CAG C
Primer 4 <i>gfp p/t</i>	Forward	<i>Sma</i> I	CCG GAT CCC GGG AGC AAC AAA GAT GAG TAA AGG AG
Primer 5 <i>xyIR</i>	Forward	<i>Mun</i> I	GGC TAA CAA TTG CGT TGA CTT AAC TAA CTT ATA G
Primer 6 <i>xyIR</i>	Reverse	<i>Sma</i> I	GTC ATT TCC CGG GTT GAT TTA AGT GAA CAA GTT TAT C
Primer 7	Reverse <i>gfp</i> sequencing primer	None	CAA CAA GAA TTG GGA CAA C

APPENDIX 1: cont

Primer Reference number	Forward or Reverse Primer	Incorporated Restriction Site	Primer Sequence
Primer 8 <i>gfp r/s</i>	Forward	<i>SmaI</i>	CCG GAT CCC GGG AGG AGG AAC AAA GAT GAG TAA CAA GGG CGA ACT TTT CAC TGG AGT TG
Primer 9 <i>egfp</i>	Forward	<i>SmaI</i>	CCG GAT CCC GGG AAG GAG GGG TCG CCA CCA TGG TGA G
Primer 10 <i>egfp</i>	Reverse	<i>SalI</i>	GCT AGA GTC GAC GCC GCT TTA CTT GTA CAG
Primer 11 <i>gfp opt</i>	Forward	<i>SmaI</i>	CCG GAT CCC GGG TTA ACA AGG AGG AAT AAA AAA TGA GTA AAG GCG AAG AAC TTT TCA CTG GAG
Primer 12 <i>luxA</i>	Forward	<i>EcoRI / SalI</i>	GCA CGA ATT CGT CGA CAG GAG GAC TCT CTA TGA AAT TTG GAA AC
Primer 13 <i>luxB</i>	Reverse	<i>KpnI</i>	CAA CTC GGT ACC TAT TAG GTA TAT TTC ATG TGG
Primer 14 <i>luxC</i>	Forward	<i>KpnI</i>	CCC CGG TAC CAG GAG GAA GGC AAA TAT GAC TAA AAA AAT TTC
Primer 15 <i>luxD</i>	Reverse	<i>BamHI</i>	CTC AGG ATC CTT TAA GAC AGA GAA ATT GC

APPENDIX 1: cont

Primer Reference number	Forward or Reverse Primer	Incorporated Restriction Site	Primer Sequence
Primer 16 <i>luxE</i>	Forward	<i>Bam</i> HI	CCC GGA TCC TGA GGA GGA AAA CAG GTA TGA CTT CAT ATG
Primer 17 <i>luxE</i>	Reverse	<i>Pst</i> I / <i>Eco</i> RV	GGG TTA GCT GCA GGA TAT CAA CTA TCA AAC GC
Primer 18 terminator	Forward	<i>Nsi</i> I	GGA CCA GGC ATG CAT CGT AGC GCC GAT GGT AG
Primer 19 terminator	Reverse	<i>Pst</i> I	GCG GCC GAT CTG CAG GAG TTT GTA GAA ACG CAA AAA G
Primer 20 P3	Forward	<i>Eco</i> RI	CAC CGA ATT CCT CAC TGT CAT TAT ACG
Primer 21 P3	Reverse	<i>Sma</i> I	CAT CAA CCC CGG GCC ATC ACA TCT CTG TCA TCT AG

APPENDIX 2

Plasmid stability assays of *L. monocytogenes* harbouring vectors based on pMK4: overnight cultures grown overnight without antibiotic and then plated onto selective and none selective agar plates

plasmid	Plates used	Dilution 10 ⁻⁸	Dilution 10 ⁻⁷	Dilution 10 ⁻⁶	Dilution 10 ⁻⁵	Mean Count	Percentage loss
pMK4	BHI	0	30	231	Not done	237	25%
		0	27	243			
	Cm7	2	15	160	Not done	177	
		2	12	193			
pGC4	BHI	TFTC	TFTC	103	TNTC	119	49%
		TFTC	TFTC	134	TNTC		
	Cm7	TFTC	TFTC	53	TNTC	61	
		TFTC	TFTC	68	TNTC		
pSB2002 (<i>gfpwt</i>)	BHI	TFTC	TFTC	193	TNTC	194	92%
		TFTC	TFTC	194	TNTC		
	Cm7	TFTC	TFTC	TFTC	165	152.	
		TFTC	TFTC	TFTC	138		
pSB2003 (<i>gfp3</i>)	BHI	TFTC	TFTC	141	TNTC	159	47%
		TFTC	TFTC	177	TNTC		
	Cm7	TFTC	TFTC	79	TNTC	79	
		TFTC	TFTC	78	TNTC		

Plasmid stability assays of *L. monocytogenes* harbouring vectors based on pMK4: overnight cultures grown overnight with antibiotic and then plated onto selective and none selective agar plates

plasmid	Plates used	Dilution 10 ⁻⁸	Dilution 10 ⁻⁷	Dilution 10 ⁻⁶	Dilution 10 ⁻⁵	Mean Count	Percentage loss
pMK4	BHI	7	44	TNTC	TNTC	51	None i.e. Stable
		8	58	TNTC	TNTC		
	Cm7	2	67	TNTC	TNTC	53	
		3	39	TNTC	TNTC		
pGC4	BHI	TFTC	8	110	TNTC	107	19%
		TFTC	15	104	TNTC		
	Cm7	TFTC	9	101	TNTC	89	
		TFTC	10	76	TNTC		
pSB2002 (<i>gfpwt</i>)	BHI	TFTC	22	229	TNTC	258	67%
		TFTC	25	286	TNTC		
	Cm7	TFTC	6	97	TNTC	87	
		TFTC	9	77	TNTC		
pSB2003 (<i>gfp3</i>)	BHI	TFTC	9	177	TNTC	171	29%
		TFTC	16	165	TNTC		
	Cm7	TFTC	14	116	TNTC	123	
		TFTC	14	130	TNTC		

TFTC: too few to count to give an accurate representation of viable count

TNTC: too many to count to give an accurate representation of viable count

To determine an accurate measure of viable count, numbers of colonies present should be between 30-300.

APPENDIX 3: Genetic Markers

<i>ara</i>	Inability to utilise arabinose
<i>dam</i>	Cytosine methylation at GATC sequences abolished
<i>dcm</i>	Cytosine methylation at CC(x)GG sequences abolished
<i>endA</i>	DNA-specific endonuclease I activity abolished
<i>F</i>	Self transmissible, low copy number plasmid
<i>galK</i>	Inability to utilise galactose
<i>gyrA</i>	subunit A, resistant to nalidixic acid
<i>hsdR</i>	host specific restriction and/or modification of endonuclease R
<i>lacI^q</i>	repressor protein, overproduces <i>lac</i> repressor, turning off expression from P _{lac}
<i>lacZAM15</i>	Expresses carboxyterminal fragment that complements the <i>lacZα</i> fragment on many vectors, gives blue colour on Xgal
<i>Lac-proAB</i>	Deletion of whole <i>lac</i> operon and <i>proAB</i> , so cell requires proline unless it carries F' <i>proAB</i>
<i>lacY</i>	Galactosidase permease activity abolished
<i>leu</i>	Requirement for leucine in minimal media
<i>pro</i>	Requirement for proline in minimal media
<i>recA1</i>	major recombination gene, also involved in λ induction
<i>recBCD</i>	Exonuclease V activity abolished (has exonuclease activity on double stranded DNA, also cleaves single stranded DNA both exo- and endonucleolytically)
<i>relA</i>	permits RNA synthesis in absence of protein synthesis
<i>rpsL</i>	Streptomycin resistance
<i>supE</i>	suppressor of amber (UAG) mutations, inserts glutamine
<i>thi</i>	Requirement for thiamine in minimal media
<i>thr</i>	Requirement for threonine in minimal media
<i>traD36</i>	Inactivation of conjugal transfer of F'